Performance Assessment of Wastewater Treatment Plants

Multi-objective analysis using plant-wide models

MAGNUS ARNELL
FACULTY OF ENGINEERING | LUND UNIVERSITY

Performance Assessment of Wastewater Treatment Plants

Performance Assessment of Wastewater Treatment Plants

Multi-Objective Analysis Using Plant-Wide Models

by Magnus Arnell

LUND
UNIVERSITY

Thesis for the degree of Doctor of Philosophy in Engineering

Thesis supervisors: Associate Professor Ulf Jeppsson,
Associate Professor Hans Bertil Wittgren and Professor Bengt Carlsson

Faculty opponent: Associate Professor Diego Rosso, University of California, Irvine, USA

To be presented, with the permission of the Faculty of Engineering of Lund University, for public criticism in the M:B lecture hall, Mechanical Engineering building, Ole Römers väg 1, Lund, on Friday the 16th of December 2016 at 10:15 a.m.

Organization	Document name
LUND UNIVERSITY Division of Industrial Electrical Engineering and Automation Box 118 SE–221 00 LUND, Sweden	**DOCTORAL DISSERTATION** Date of disputation 2016-12-16 Sponsoring organization The Swedish Research Council Formas, The Swedish Water and Wastewater Association, SP Technical Research Institute of Sweden and Lund University.
Author(s) Magnus Arnell	

Title and subtitle

Performance Assessment of Wastewater Treatment Plants – Multi-Objective Analysis Using Plant-Wide Models

Abstract

As the knowledge about anthropogenic impacts of climate change has grown, the awareness of the contributions from treatment of wastewater has widened the scope for wastewater treatment plants (WWTPs). Not only shall ever stricter effluent constraints be met, but also energy efficiency be increased, greenhouse gases mitigated and resources recovered. All under a constant pressure on costs. The main objective of this research has been to develop a plant-wide modelling tool to evaluate the performance of operational strategies for multiple objectives at the plant and for off-site environmental impact.

The plant-wide model platform Benchmark Simulation Model no. 2 (BSM2) has been modified to improve the evaluation of energy efficiency and include greenhouse gas emissions. Furthermore, the plant-wide process model has been coupled to a life cycle analysis (LCA) model for evaluation of global environmental impact. For energy evaluation, a dynamic aeration system model has been adapted and implemented. The aeration model includes oxygen transfer efficiency, dynamic pressure in the distribution system and non-linear behaviour of blower performance. To allow for modelling of energy recovery via anaerobic co-digestion the digestion model of BSM2 was updated with a flexible co-digestion model allowing for dynamic co-substrate feeds. A feasible procedure for substrate characterisation was proposed. Emissions of the greenhouse gases CO_2, CH_4 and N_2O were considered. The bioprocess model in BSM2 was updated with two-step nitrification, four-step denitrification and nitrifier denitrification to capture N_2O production. Fugitive emissions of the three gases were included from digestion, co-generation and sludge storage. The models were tested in case studies for the three areas of development: aeration, co-digestion and greenhouse gas production. They failed to reject the hypothesis that dynamic process models are required to assess the highly variable operations of wastewater treatment plants. All parts were combined in a case study of the Käppala WWTP in Lidingö, Sweden, for comparison of operational strategies and evaluation of stricter effluent constraints. The averaged model outputs were exported to an LCA model to include off-site production of input goods and impact of discharged residues and wastes. The results reveal trade-offs between water quality, energy efficiency, greenhouse gas emissions and abiotic depletion of elemental and fossil resources.

The developed tool is generally applicable for WWTPs and the simulation results from this type of combined models create a good basis for decision support.

Key words

benchmarking, BSM, codigestion, energy efficiency, greenhouse gases, life cycle assessment, mathematical modelling, wastewater treatment

Classification system and/or index terms (if any)

Supplementary bibliographical information	Language
	English
ISSN and key title	ISBN
	978-91-88934-72-7 (print) 978-91-88934-73-4 (pdf)
Recipient's notes	Number of pages: 232 / Price
	Security classification

I, the undersigned, being the copyright owner of the abstract of the above-mentioned dissertation, hereby grant to all reference sources the permission to publish and disseminate the abstract of the above-mentioned dissertation.

Signature _____ Date 2016-11-09

DOKUMENTDATABLAD enl SIS 61 41 21

Performance Assessment of Wastewater Treatment Plants

Multi-Objective Analysis Using Plant-Wide Models

by Magnus Arnell

Lund University

Cover illustration front: Ink drawing. Artist: Ninnie Svensson.

Cover illustration back: Portrait illustrating the biography of the author. Photo: Magnus Arnell.

Funding information: The thesis work was financially supported by The Swedish Research Council Formas (211-2010-141), The Swedish Water and Wastewater Association (10-106, 12-108), The Swedish Association of Graduate Engineers (Scholarship for Environmental Research), SP Technical Research Institute of Sweden and Lund University. Case studies have been funded through contracts by Tekniska Verken in Linköping, Eskilstuna Strängnäs Energi och Miljö, IVL Swedish Environmental Institute and Käppalaförbundet. Furthermore, the Swedish WWT research and education consortium VA-cluster Mälardalen was instrumental for realising this funding.

© Magnus Arnell 2016

Division of Industrial Electrical Engineering and Automation,
Department of Biomedical Engineering,
Faculty of Engineering, Lund University, Sweden

ISBN: 978-91-88934-72-7 (print)
ISBN: 978-91-88934-73-4 (pdf)
CODEN: LUTEDX/(TEIE-1080)/1-232/(2016)

Printed in Sweden by Media-Tryck, Lund University, Lund 2016

Dedicated to my beloved family
Cecilia – Alva – Carl

Contents

Acknowledgements . . . iii
List of Publications and Author's Contributions . . . v
Popular Summary . . . xi
Populärvetenskaplig sammanfattning . . . xiii

1 Introduction **1**
1.1 Aim and Purpose of Research . . . 2
1.2 Delimitations . . . 2
1.3 Hypothesis . . . 3
1.4 Key Contributions . . . 3
1.5 Outline of Thesis . . . 5

2 Background **7**
2.1 Scope of Wastewater Treatment . . . 7
2.2 Energy Use and Recovery in Wastewater Treatment . . . 9
2.3 Greenhouse Gas Emissions from Wastewater Treatment . . . 12
2.4 Performance Assessment of Wastewater Treatment Plants . . . 17
2.5 History of Process Modelling . . . 18
2.6 Benchmark Simulation Model Platform . . . 20

3 Modelling Greenhouse Gas Emissions **23**
3.1 Modelling N_2O Production . . . 23
3.2 Description of BSM2G . . . 25
3.3 Integrated Evaluation of Greenhouse Gas Emissions, Effluent Water Quality and Costs . . . 30
3.4 Modelling N_2O Production in Side-Stream Treatment . . . 33
3.5 Calibration of N_2O Production in a Full-Scale Activated Sludge Unit . . . 37
3.6 Summary of Key Findings . . . 39

4 Aeration System Modelling **41**
4.1 Introduction to Aeration System Modelling . . . 41
4.2 Including an Aeration Model in BSM . . . 43
4.3 Case Studies on Aeration Modelling . . . 48
4.4 Summary of Key Findings . . . 56

5 Modelling Anaerobic Co-Digestion in Plant-Wide Models **59**
5.1 Energy Recovery Through Anaerobic Digestion 59
5.2 Substrate Characterisation 62
5.3 Sensitivity Analysis 67
5.4 Implementing Anaerobic Co-Digestion in BSM2 69
5.5 Summary of Key Findings 75

6 Multi-Objective Performance Assessment Using Coupled Process Models and Life Cycle Assessment **77**
6.1 Combining Process Modelling and Life Cycle Assessment 77
6.2 Life Cycle Analysis Model 79
6.3 Case Study on Käppala Wastewater Treatment Plant 79
6.4 Using Results for Decision Support 89
6.5 Summary of Key Findings 90

7 Conclusions and Future Research Needs **93**
7.1 General Conclusions 93
7.2 Future Research 96

References **99**

Scientific publications **117**
Paper I: Balancing effluent quality, economic cost and greenhouse gas emissions during the evaluation of (plant-wide) control/operational strategies in WWTPs 119
Paper II: Dynamic modelling of nitrous oxide emissions from three Swedish sludge liquor treatment systems 131
Paper III: Aeration system modelling – case studies from three full-scale wastewater treatment plants 143
Paper IV: Parameter estimation for modelling of anaerobic co-digestion 149
Paper V: Modelling anaerobic co-digestion in Benchmark Simulation Model no. 2: Parameter estimation, substrate characterisation and plant-wide integration 161
Paper VI: Multi-objective performance assessment of wastewater treatment plants combining process models and life cycle assessment 179

Acknowledgements

Firstly, I would like to express my sincere gratitude to my supervisor Associate Professor Ulf Jeppsson for giving me the opportunity to do a Ph.D. and for his committed support during the last five years. His immense knowledge, continuous strive to keep me at course and sense of quality in research have been of inestimable help through the time of research and for writing this thesis. I could not imagine having a better advisor and mentor for my Ph.D study.

Besides my main supervisor, I would like to thank my co-supervisors Dr. Hans Bertil Wittgren, and Prof. Bengt Carlsson for their guidance in the academic world, insightful comments and encouragement, but also for their tough questions, which gave me incentives to widen my research from various perspectives.

I would also like to thank my academic colleagues at the division of Industrial Electrical Engineering and Automation at Lund University: Prof. em. Gustaf Olsson, Dr. Xavier Flores-Alsina, Dr. Erik Lindblom, M.Sc. Kimberly Solon and M.Sc. Ramesh Saagi, for the open collaboration, fruitful discussions and all the hands on help in coding and writing.

As an industrial Ph.D. student, the support from my managers Dr. Erik Kärrman and Charlotta Möller at SP Urban Water Management has been essential. I am for ever grateful for their trust, understanding of the conditions for research studies and, not least, for providing time and resources necessary for finalising my thesis. My development as researcher has also benefited greatly from all the fun, inspiring and intellectual discussions we have had among all the colleagues at SP Urban Water Management. Thank you!

This research has been conducted in several projects including valuable industrial partners. I would like to thank the partners for their time and commitment to supply all necessary information for the research. Malin Asplund and Robert Sehlén at Tekniska Verken in Linköping; Roland Alsbro, Pernilla Norwald and Lina Falk at Eskilstuna Strängnäs Energi och Miljö; and Andreas Thunberg and Catharina Grundestam at Käppalaförbundet. Much of the success of these projects are thanks to them and their colleagues' dedication.

The research in the field of wastewater treatment modelling is truly collaborative and the extended research family I have been working and publishing together with has been essential for the success and provided great joy along the way. I would like to acknowledge all my co-authors and especially the collaboration with Linda Åmand, Magnus Rahmberg, Sofia Andersson, Christian Junestedt and Felipe Oliveira on the plant-wide modelling; Peter Vanrolleghem, Lisha Guo and Laura Snip on the greenhouse gas studies; Damien Batstone, Sergi Astals and Paul Jensen on co-digestion during my stay at The University of Queensland; Leiv Rieger, Oliver Schraa and Sergio Beltrán for support and material on the

aeration modelling; and Stefan Diehl, Sebastian Farås, Emma Lundin and Sovanna Tik on the settler modelling.

I thank Ninnie Svensson for the illustration dedicated to the front cover of the thesis.

To my wife Cecilia, daughter Alva and son Carl for always standing by me and allowing me to leave for conference travels and work off hours. I love you! And all other members of my immediate family for your unconditional love and appreciation, making me who I am.

Finally, I acknowledge the financial support by The Swedish Research Council Formas (211-2010-141), The Swedish Water and Wastewater Association (10-106, 12-108), The Swedish Association of Graduate Engineers (Scholarship for Environmental Research), SP Technical Research Institute of Sweden and Lund University. The case studies were funded through contracts by Tekniska Verken in Linköping, Eskilstuna Strängnäs Energi och Miljö, IVL Swedish Environmental Institute and Käppalaförbundet. Furthermore, the Swedish WWT research and education consortium VA-cluster Mälardalen was instrumental for realising this funding.

List of Publications and Author's Contributions

This thesis is based on the following publications, referred to by their Roman numerals:

I **Balancing effluent quality, economic cost and greenhouse gas emissions during the evaluation of (plant-wide) control/operational strategies in WWTPs**

Flores-Alsina X., **Arnell M.**, Amerlinck Y., Corominas L., Gernaey K.V., Guo L, Lindblom E., Nopens I., Porro J., Shaw A., Snip L., Vanrolleghem P.A. and Jeppsson U.
Science of the Total Environment, 2014, 466-467, pp 616-624.

II **Dynamic modelling of nitrous oxide emissions from three Swedish sludge liquor treatment systems**

Lindblom E., **Arnell M.**, Flores-Alsina X., Stenström F., Gustavsson D.J.I., Yang J. and Jeppsson U.
Water Science and Technology, 2016, 73(4), pp 798-806.

III **Aeration system modelling – case studies from three full-scale wastewater treatment plants**

Arnell M. and Jeppsson U.
9th IWA Symposium on Systems Analysis and Integrated Assessment (Watermatex2015), Gold Coast, Queensland, Australia, 14-17 June, 2015.

IV **Parameter estimation for modelling of anaerobic co-digestion**

Arnell M. and Åmand L.
9th IWA World Water Congress and Exhibition (WWC&E2014), Lisbon, Portugal, 21-26 September, 2014.

V **Modelling anaerobic co-digestion in Benchmark Simulation Model no. 2: Parameter estimation, substrate characterisation and plant-wide integration**

Arnell M., Astals S., Åmand L., Batstone D.J., Jensen P.D. and Jeppsson U.
Water Research, 2016, 98, pp 138-146.

VI **Multi-objective performance assessment of wastewater treatment plants combining process models and life cycle assessment**

Arnell M., Rahmberg M., Oliveira F. and Jeppsson U.
Submitted.

All papers are reproduced with permission from their respective publishers.

Author's Contributions

Paper I: Balancing effluent quality, economic cost and greenhouse gas emissions during the evaluation of (plant-wide) control/operational strategies in WWTPs

I had the main responsibility for the writing together with Xavier Flores-Alsina, who did most of the model development. Xavier and myself finalised the model implementation together as well as interpreted the results.

Paper II: Dynamic modelling of nitrous oxide emissions from three Swedish sludge liquor treatment systems

I worked together with Erik Lindblom on developing the MBBR model for the modelling of the nitritation/anammox case. We also worked agile on the calibration and validation of the model. I wrote the paper in close collaboration with Erik Lindblom.

Paper III: Aeration system modelling – case studies from three full-scale wastewater treatment plants

I did the review of aeration models, selected and implemented the model in the Benchmark Simulation Model platform. I performed the modelling case studies based on data from the plant staff. I wrote the main parts of the paper and also gave the presentation at the conference.

Paper IV: Parameter estimation for modelling of anaerobic co-digestion

This work was conducted together with Linda Åmand as part of a PhD-course on modelling of anaerobic digestion. I did the main part of the literature review, was responsible for implementing one of the evaluated models and did the final simulations for the conference paper. I wrote the paper with support from Linda and I also gave the presentation at the conference.

Paper V: Modelling anaerobic co-digestion in Benchmark Simulation Model no. 2: Parameter estimation, substrate characterisation and plant-wide integration

The majority of this work was done by me, with close support of Sergi Astals and Damien Batstone, while I was a visiting researcher at The University of Queensland, Brisbane, Qld,

Australia. I did the model implementation and the simulation studies based on data from Sergi. I did the majority of the writing with much help from the co-authors.

Paper VI: Multi-objective performance assessment of wastewater treatment plants combining process models and life cycle assessment

I did all process model development for this paper and modelling for the case study of Käppala WWTP based on data from the plant staff. Magnus Rahmberg and Felipe Oliveira did the LCA modelling. I wrote the paper with input and comments from the co-authors.

Subsidiary Publications

Peer reviewed papers by the author not included in this thesis:

vii **Plant-wide control of WWTPs – a path to optimal operation**

Rosen C. and **Arnell M.**
10th Nordic Wastewater Conference 2007 (NORDIWA2007), Hamar, Norway, 11-14 November, 2007.

viii **Balancing effluent quality, economical cost and greenhouse gas emissions during the evaluation of plant-wide wastewater treatment control strategies**

Flores-Alsina X., **Arnell M.**, Amerlinck Y., Corominas L., Gernaey K.V., Guo L., Lindblom E., Nopens I., Porro J., Shaw A., Snip L., Vanrolleghem P.A. and Jeppsson U.
IWA Conference on Nutrient Removal and Recovery 2012: Trends in NRR, Harbin, China, 23-25 September, 2012.

ix **A dynamic modelling approach to evaluate GHG emissions from wastewater treatment plants**

Flores-Alsina X., **Arnell M.**, Amerlinck Y., Corominas L., Gernaey K.V., Guo L., Lindblom E., Nopens I., Porro J., Shaw A., Snip L., Vanrolleghem P.A. and Jeppsson U.
3rd IWA World Congress on Water, Climate and Energy (WCE2012), Dublin, Ireland, 13-18 May, 2012.

x **Balancing effluent quality, greenhouse gas emissions and operational cost – developing dynamical models for integrated benchmarking of wastewater treatment plants [in Swedish]**

Arnell M. and Jeppsson U.
VATTEN – Journal of Water Management and Research, 2012, 68(4), pp 295-301.

xi **Practical use of wastewater treatment modelling and simulation as a decision support tool for plant operators – case study on aeration control at Linköping Wastewater Treatment Plant**

Arnell M., Sehlén R. and Jeppsson U.
13th Nordic Wastewater Treatment Conference (NORDIWA2013), Malmö, Sweden, 8-10 October, 2013.

xii **Dynamic modelling and validation of nitrous oxide emissions from a full-scale nitrifying/denitrifying sequencing batch reactor treating anaerobic digester supernatant**

Lindblom E., **Arnell M.**, Stenström F., Tjus K., Flores-Alsina X. and Jeppsson U.
11th IWA Conference on Instrumentation, Control and Automation (ICA2013), Narbonne, France, 18-20 September, 2013.

xiii **Dynamic modelling of nitrous oxide emissions from three Swedish full-scale reject water treatment systems**

Lindblom E., **Arnell M.**, Flores-Alsina X., Stenström F., Gustavsson D.J.I. and Jeppsson U.
9th IWA World Water Congress (WWC&E2014), Lisbon, Portugal, 21-26 September, 2014.

xiv **Modelling chemically enhanced primary settlers for resource recovery purposes**

Lundin E., **Arnell M.**, Tik S., Vanrolleghem P.A. and Carlsson B.
14th Nordic Wastewater Treatment Conference (NORDIWA2015), Bergen, Norway, 4-6 November, 2015.

xv **Simulating the environmental impact of stricter discharge criteria on nitrogen and phosphorous**

Åmand L., Andersson S., **Arnell M.**, Junestedt C., Rahmberg M., Lindblom E., Thunberg A. and Nilsson A.
14th Nordic Wastewater Treatment Conference (NORDIWA2015), Bergen, Norway, 4-6 November, 2015.

xvi **Substrate fractionation for modelling of anaerobic co-digestion with a plant-wide perspective**

Arnell M., Astals S., Åmand L., Batstone D.J., Jensen P.D. and Jeppsson U.
5th IWA/WEF Wastewater Treatment Modelling Seminar (WWTmod2016), Annecy, France, 2-6 April, 2016.

xvii **Evaluating environmental performance of operational strategies at WWTPs**

Arnell M., Rahmberg M., Oliveira F. and Jeppsson U.
10th IWA World Water Congress and Exhibition (WWC&E2016), Brisbane, Australia, 9-13 October, 2016.

Other publications related to the subject by the author:

xviii **Emissions of N_2O and CH_4 from wastewater systems - current state of knowledge**

Arnell M.
SVU report: 2013-11, The Swedish Water and Wastewater Association, Stockholm, Sweden.

xix **Anaerobic co-digestion in plant-wide wastewater treatment models**

Arnell M. and Åmand L.
Technical report, Division of Industrial Electrical Engineering and Automation, Lund University, Lund, Sweden. LUTEDX/(TEIE-7246)/1-26/(2014).

xx **Modelling of N_2O emissions from treatment of anaerobic digester supernatant by SBR and anammox processes**

Lindblom E., **Arnell M.** and Jeppsson U.
SVU report: 2015-17, The Swedish Water and Wastewater Association, Stockholm, Sweden.

xxi **Implementation of the Bürger-Diehl settler model on the benchmark simulation platform**

Arnell M.
Technical report, Division of Industrial Electrical Engineering and Automation, Lund University, Lund, Sweden. LUTEDX/(TEIE-7250)/1-48/(2015).

xxii **Pre-commercial procurement of a mercury free COD analysis method for wastewater and waste products**

Arnell M., Lopez M. and Palmgren T.
SP report 2016:39, SP Technical Research Institute of Sweden, Borås, Sweden.

xxiii **New effluent criteria for Swedish wastewater treatment plants – effects on the plants' total environmental impact**

Åmand L., Andersson S., Oliveira F., Rahmberg M., Junestedt C. and **Arnell M.**
SVU report: 2016-12, The Swedish Water and Wastewater Association, Stockholm, Sweden.

xxiv **Modelling of wastewater treatment plants for multi-criteria evaluation of performance and environmental impact**

Arnell M., Rahmberg M., Oliveira F., Carlsson B. and Jeppsson U.
SVU report: [submitted], The Swedish Water and Wastewater Association, Stockholm, Sweden.

Popular Summary

Water supply is one of society's most important commodities. Water use gives rise to wastewater and for health and environmental protection purposes, treatment of wastewater was one of the great challenges of the past century. The sanitary revolution was voted the greatest medical advance since 1840 by the readers of the distinguished British Medical Journal. Still, wastewater treatment continuously evolve as the awareness of emerging environmental problems grows. The knowledge about the influence of human activities on climate change has widened the scope for treatment plants beyond only effluent water quality and cost. Today greenhouse gas emissions, energy efficiency and resource recovery also need to be considered when evaluating operational strategies.

In the present research, the use of mathematical models has shown the importance of considering the highly dynamic effects of wastewater treatment processes, and at the same time including the up- and down-stream impacts – from resource use and discharge of residues and wastes – that the treatment plant operations give rise to. Simulation of, for example, enhanced primary treatment with chemical precipitants or advanced measures for meeting stricter effluent constraints, show that reduced eutrophication can be achieved along with reduced emissions of greenhouse gases. However, the increased resource consumption, primarily of chemicals, leads to a manyfold increase in depletion of both elemental and fossil resources.

Mathematical modelling and simulation of wastewater treatment processes has a long history and is common practice in the industry in many parts of the world. For this project, a plant-wide modelling platform, The Benchmark Simulation Model no. 2, was adopted and further developed for multi-objective performance assessment. To be able to capture the additional criteria, energy efficiency and greenhouse gases, the model was developed and extended in the following three areas:

Energy for aeration As oxygen supply to the biological unit processes is the most energy intense process of any advanced treatment plant, a detailed dynamic aeration model was implemented in the Benchmark model. The aeration model was tested in three case studies and shown to be adequate for its purpose, robust and easy to adapt to real plants.

Anaerobic co-digestion Energy recovery from the influent organic material via anaerobic digestion is common practise. In anaerobic digestion, organic material in sewage sludge or other materials are degraded, leading to less sludge, and converted to energy-rich biomethane. At many plants redundant digester volumes allow this energy production to be increased by adding external organic substrates (so called co-digestion). The digester model was modified to allow for dynamic simulation of

co-digestion and a procedure to characterise the substrates was proposed. A simulation study showed that modelling is beneficial to assess both digester stability and secondary effects on the water treatment from co-digestion.

Greenhouse gas emissions Repeated measurements on greenhouse gas emissions from wastewater treatment plants have shown a large span of total emissions. The current state of knowledge explains that production and emission of the potent greenhouse gas nitrous oxide (N_2O) in biological treatment processes is highly dynamic and varies greatly with the operational conditions. Therefore, the operational strategy and ambient conditions have a great impact on the total emissions. The model library of the Benchmark model was extended with a biological model that covers the most important production pathways for nitrous oxide. Furthermore, fugitive emissions of carbon dioxide, methane and nitrous oxide from other treatment processes, primarily the sludge treatment, were included. Multiple case studies calibrating the model to experimental data showed the highly dynamic behaviour of the emissions, demonstrating that dynamic models are critical to evaluate greenhouse gas emissions at wastewater treatment plants. However, calibration efforts also indicate that the available models are not yet capturing all the existing processes in the biological reactors and further research is likely required.

All these modifications were included in the Benchmark Simulation Model no. 2 and tested in a full scale case study of a real plant in Sweden. The model outputs were then connected to a life cycle analysis model to capture the off-site up- and down-stream effects of the operations. The use of external goods, such as electrical power and chemicals, leads to resource depletion. Furthermore, discharges of residues (effluent water and sludge) have an impact on the environment downstream. By evaluating the entire wastewater treatment plant considering all these objectives – water quality, energy efficiency, greenhouse gas emission and operational cost – for both on-site effects and off-site environmental impact, the trade-offs between the objectives and different impact categories can be revealed. The presented modelling tool is capable of capturing these trade-offs and the results are essential for decision support when deciding on modifications of operational strategies at wastewater treatment plants.

Populärvetenskaplig sammanfattning

Vattenförsörjning är grundläggande för människan och samhället men vattenanvändning ger också upphov till avloppsvatten. Till skydd av hälsa och miljö samlas avloppsvatten upp i ledningsnät och renas vid avloppsreningsverk. På goda grunder röstades den sanitära revolutionen fram som det största medicinska framsteget sedan 1840 av läsarna av den prominenta vetenskapliga tidskriften British Medical Journal 2007. Trots stora framsteg fortsätter avloppsreningen alltsedan införandet att utvecklas vartefter kunskap, medvetenhet och reningskrav ökar. Kunskapen om den mänskliga påverkan på klimatet genom utsläpp av växthusgaser har vidgat utmaningarna för avloppsreningsverken utöver enbart vattenkvalitet och kostnader. Energieffektivitet och växthusgasutsläpp behöver utvärderas integrerat med vattenkvalitet och driftskostnader för en vidare bedömning av hållbarhet.

Detta forskningsprojekt har med hjälp av matematiska modeller visat på betydelsen av att både inkludera de kraftigt dynamiska effekterna i reningsprocesserna och påverkan från upp- och nedströms processer – såsom produktion av energi och kemikalier och utsläpp av renat vatten – som driften av reningsverk ger upphov till. Simuleringar av bland annat förbättrad primär rening med tillsats av fällningskemikalier eller avancerade reningsprocesser för kraftigt minskade utsläpp har gjorts. Resultaten visar att minskad övergödning kan uppnås samtidigt som utsläppen av växthusgaser minskar. Men den ökade förbrukningen av framförallt kemikalier leder till en flerfalt ökad förbrukning av naturresurser, både fossila- och materialresurser.

Matematisk modellering av avloppsreningsverk har en lång historik och är praxis inom industrin i flera delar av världen. I det här projektet har den reningsverksövergripande modelleringsplattformen *Benchmark Simulation Model nr. 2* använts och vidareutvecklats för multikriterieanalys av avloppsreningsverk. För att kunna simulera energieffektivitet och växthusgasutsläpp tillsammans med utgående vattenkvalitet och driftskostnader har modellplattformen utvecklats inom följande tre områden.

Energi för luftning Då luftning för att syresätta de biologiska reningsprocesserna är den mest energikrävande processen på ett avloppsreningsverk har en detaljerad modell för att utvärdera funktion och energiförbrukning av luftningssystemet implementerats. Luftningsmodellen har testats i tre fallstudier på svenska reningsverk där den visade sig passa bra för syftet samtidigt som den var robust och enkel att anpassa till verkliga förhållanden.

Samrötning Att utvinna energi från organiskt material i avloppsvattnet genom anaerob rötning av avloppsslam är vanligt vid större reningsverk. Vid rötning bryts det organiska materialet ner, vilket inte bara leder till produktion av energirik biogas utan också till mindre slammängder. Många kommunala reningsverk har en överkapacitet i sina rötkammare som innebär att externt organiskt material kan pumpas in (s.k.

samrötning) och på så sätt öka biogasproduktionen. Rötningsmodellen har utvecklats för att kunna göra dynamiska simuleringar av samrötning och en metod för att karakterisera externa substrat har också tagits fram. En simuleringsstudie visar att modellering är ett värdefullt verktyg för att utvärdera gasproduktion, processtabilitet och påverkan på reningsverkets vattenrening.

Växthusgasutsläpp Flera mätkampanjer av växthusgasutsläpp på avloppsreningsverk har tidigare visat på en stor variation av mängderna för olika utsläpp. Den nuvarande förståelsen av detta är att den kraftiga växthusgasen lustgas (N_2O) ofta är den största källan och utsläppen av den dessutom varierar kraftigt beroende på processförhållandena. Driftstrategin och andra yttre förhållanden har därför en stor påverkan på växthusgasutsläppen. Modellbiblioteket i plattformen har därför uppdaterats med en ny bioprocessmodell som inkluderar produktion av lustgas. Dessutom har diffusa utsläpp av koldioxid, metan och lustgas från övriga delar av reningsverket lagts till. Flera fallstudier på olika typer av reningsprocesser har genomförts, vilka visar på den kraftiga variationen i lustgasproduktion och därmed på vikten av att använda dynamiska processmodeller om växthusgasproduktion ska kunna uppskattas. Men kalibreringen av modellerna till mätdata visar också att de modeller som fanns tillgängliga för detta inte fångar alla möjliga produktionsvägar för lustgas och fortsatt forskning behövs inom området.

Alla dessa modifikationer inkluderades i modellplattformen Benchmark Simulation model nr. 2 och testades i en fullskalig fallstudie vid reningsverket Käppala i Lidingö. Processmodellen kopplades till en livscykelanalysmodell för att inkludera processer utanför reningsverket som beror på reningsverkets drift. På så sätt kunde de viktiga och dynamiska processerna på reningsverket beskrivas samt miljöpåverkan från resursanvändning och utsläpp av vatten utvärderas integrerat. Modellverktyget som tagits fram i projektet kan synliggöra motsättningar och avvägningar mellan olika miljöpåverkanskategorier och resultaten användas som beslutsunderlag för möjliga förändringar av avloppsreningsverk.

Nomenclature

Acronyms

AcoD	Anaerobic co-digestion
AD	Anaerobic digester
ADM1	Anaerobic Digestion Model no. 1
ADP	Abiotic depletion potential
ANOX	Anoxic model reactor
AOB	Ammonium oxidising bacteria
AS	Activated sludge
ASM	Activated Sludge Model. Suffixes 1, 1G, 2d and 3 denote model versions no. 1, 1 Greenhouse gas, 2d and 3, respectively
Bio-P	Biological phosphorous removal
BMP	Biomethane potential
BSM	Benchmark Simulation Model platform. Suffixes 1, 2 and 2G denote model versions no. 1, 2 and 2 Greenhouse gas, respectively
CEPT	Chemically enhanced primary treatment
CML	Centrum voor Milieukunde, Leiden University, The Netherlands
CO_2e	Carbon dioxide equivalents
DAF	Dissolved air flotation
DEOX	Non-aerated deoxidation model reactor
DWP	Dynamic wet pressure
EQI	Effluent quality index
FELX	Flexible anoxic/aerated model reactor
FOG	Fat, oil and grease
GHG	Greenhouse gas
GISCOD	General integrated solid waste co-digestion
GWP	Global warming potential
HET	Heterotrophic bacteria
HRT	Hydraulic retention time
IPCC	Intergovernmental Panel on Climate Change
IWA	International Water Association

LCA	Life cycle analysis
LCFA	Long chain fatty acid
LCI	Life cycle inventory
LCIA	Life cycle impact assessment
MBBR	Moving bed bioreactor
NOB	Nitrite oxidising bacteria
OCI	Operational cost index
ODP	Ozone depletion potential
OLR	Organic loading rate
OX	Aerated model reactor
PB	Positive displacement type blower
PCA	Principal component analysis
PI	Proportional-integral controller
RAS	Return activated sludge
SBR	Sequential batch reactor
SSE	Sum of squared errors
STP	Standard temperature and pressure conditions
TB	Turbo type blower
UCT	University of Cape Town
VFA	Volatile fatty acids
WAS	Waste activated sludge
WWT	Wastewater treatment
WWTP	Wastewater treatment plant

Chemical Formulas and Analysis Parameters

ALK	Alkalinity	$g.m^{-3}$
BOD	Biological oxygen demand	$g.m^{-3}$
CH_4	Methane, suffix -C denotes carbon part	$g.m^{-3}$
COD	Chemical oxygen demand	$g.m^{-3}$
CO_2	Carbon dioxide	ppm
DO	Dissolved oxygen	$g.m^{-3}$
HNO_2	Free nitrous acid	$g.m^{-3}$
H_2S	Hydrogen sulphide	$g.m^{-3}$
NH_2OH	Hydroxylamine	$g.m^{-3}$
NH_3	Ammonia, suffix -N denotes nitrogen part	$g.m^{-3}$
NH_4^+	Ammonium, suffix -N denotes nitrogen part	$g.m^{-3}$
NOH	Nitrosyl radical	$g.m^{-3}$
NO^-	Nitrogen oxide, suffix -N denotes nitrogen part	$g.m^{-3}$
NO_2^-	Nitrite, suffix -N denotes nitrogen part	$g.m^{-3}$
NO_3^-	Nitrate, suffix -N denotes nitrogen part	$g.m^{-3}$
N_2	Nitrogen gas	ppm

N_2O	Nitrous oxide, suffix -N denotes nitrogen part	$g.m^{-3}$ / ppm
TN	Total nitrogen	$g.m^{-3}$
TOC	Total organic carbon	$g.m^{-3}$
TP	Total phosphorous	$g.m^{-3}$
TSS	Total suspended solids	$g.m^{-3}$
VS	Volatile solids	$g.m^{-3}$

Model State Variables

S_{aa}	Soluble amino acids COD (ADM)	$g.m^{-3}$
S_{ac}	Soluble acetate COD (ADM)	$g.m^{-3}$
S_{CH4}	Soluble methane COD (ADM)	$g.m^{-3}$
S_{fa}	Soluble long chain fatty acids COD (ADM)	$g.m^{-3}$
S_{IN}	Soluble inorganic nitrogen (ADM)	$g.m^{-3}$
S_I	Soluble inert COD (ASM, ADM)	$g.m^{-3}$
S_{N2O}	Soluble nitrous oxygen nitrogen (ASM)	$g.m^{-3}$
S_{N2}	Soluble methane COD (ASM)	$g.m^{-3}$
S_{ND}	Soluble organic nitrogen (ASM)	$g.m^{-3}$
S_{NH3}	Soluble ammonia nitrogen (ASM)	$g.m^{-3}$
S_{NH}	Soluble ammonium nitrogen (ASM)	$g.m^{-3}$
S_{NO2}	Soluble nitrite nitrogen (ASM)	$g.m^{-3}$
S_{NO3}	Soluble nitrate nitrogen (ASM)	$g.m^{-3}$
S_{NO}	Soluble nitrate oxide nitrogen (ASM1)	$g.m^{-3}$
S_{NO}	Soluble nitric oxide nitrogen (ASM1G)	$g.m^{-3}$
S_O	Dissolved oxygen (ASM)	$g.m^{-3}$
S_{su}	Soluble monosaccharides COD (ADM)	$g.m^{-3}$
S_S	Readily biodegradable COD (ASM)	$g.m^{-3}$
X_{BA1}	Autotrophic biomass for ammonia oxidation (ASM)	$g.m^{-3}$
X_{BA2}	Autotrophic biomass for nitrite oxidation (ASM)	$g.m^{-3}$
X_{BH}	Heterotrophic biomass (ASM)	$g.m^{-3}$
X_{ch}	Particulate carbohydrate COD (ADM)	$g.m^{-3}$
X_c	Particulate composite COD (ADM)	$g.m^{-3}$
X_I	Particulate inert COD (ASM, ADM)	$g.m^{-3}$
X_{li}	Particulate lipid COD (ADM)	$g.m^{-3}$
X_{ND}	Particulate organic nitrogen (ASM)	$g.m^{-3}$
X_{pr}	Particulate protein COD (ADM)	$g.m^{-3}$
X_P	Particulate inert decay COD (ASM)	$g.m^{-3}$
X_S	Slowly biodegradable COD (ASM)	$g.m^{-3}$

Other Symbols

α	Correction factor for oxygen mass transfer in wastewater	-
β	Correction factor for saturation concentration in wastewater	-
δ	Correction factor for liquid column pressure	-

η	Efficiency, indices "motor" and "vfd" denotes motor and variable frequency drive, respectively	-
η_{Haldane}	Parameter in Haldane kinetic term	-
κ	Adiabatic coefficient of air	-
pe	Person equivalents	cap
SOTE	Standard oxygen transfer efficiency	%
Ω	Correction factor for actual barometric pressure	-
ϕ	Relative humidity of air	-
ρ_{g}	Density of air	$g.m^{-3}$
τ	Correction factor for temperature at the gas-liquid interface	-
θ	Arrhenius temperature correction factor	-
B	Biomethane potential, index 0 denotes the maximum	ml CH_4.g VS^{-1}
DO_{Haldane}	Haldane kinetic term	-
F	Fouling factor for the diffusers	-
$f(x)$	Model output in optimisation routine	-
$F_0 \cdot G$	Maximum biomethane potential	ml CH_4.g VS^{-1}
f_{ch}	Fraction of carbohydrates in biodegradable COD	-
f_{d}	Biodegradable fraction of COD	-
f_{li}	Fraction of lipids in biodegradable COD	-
f_{pr}	Fraction of proteins in biodegradable COD	-
h_{sub}	Submersion depth of diffusers	m
I_{fa}	Long chain fatty acid inhibition (ADM)	-
I_{NH}	Ammonium inhibition (ADM)	-
$I_{\text{pH,ac}}$	pH inhibition for uptake of acetate (ADM)	-
k_{hyd}	Hydrolysis rate coefficient	d^{-1}
$K_{\text{I,fa,high}}$	Parameter in long chain fatty acid inhibition, upper limit	kg COD.m^{-3}
$K_{\text{I,fa,low}}$	Parameter in long chain fatty acid inhibition, lower limit	kg COD.m^{-3}
$K_{\text{IO,AOBden}}$	Parameter in Haldane kinetic term	g O_2.m^{-3}
$K_{\text{L}}a$	Volumetric mass transfer coefficient	d^{-1}
$K_{\text{SO,AOBden}}$	Parameter in Haldane kinetic term	g O_2.m^{-3}
M_{g}	Molar mass for air	$g.m^{-3}$
M_{O2}	Molar mass for oxygen	$g.mol^{-1}$
n	Number of data points	-
p	Pressure, indices "g" and "v" denotes air and vapour pressure, respectively	Pa
P_{e}	Total power withdrawal for blowers, indices "shaft", "PB" and "TB" denotes motor shaft, positive displacement or turbo blower type, respectively	kW
Q	Hydraulic flow, indices "was", "ras", "intr" and "carb" denotes waste activated sludge, return activated sludge, internal nitrate recycle and carbon source, respectively	$m^3.d^{-1}$
Q_{CH4}	Biomethane flow	$m^3.d^{-1}$
Q_{gas}	Biogas flow	$m^3.d^{-1}$

Q_g	Flow of air	$m^3.d^{-1}$
R	Molar gas constant	$m^3.Pa.K^{-1}.mol^{-1}$
r_M	Rate of consumption of oxygen in the system	$g.d^{-1}$
$S_{O,sat}$	Saturation concentration for DO in the liquid phase, indices "cw" and "ww" denote clean water and wastewater, respectively	$g.m^{-3}$
T	Operating temperature, index "g" denote air	°C/K
t	Time	d
V_L	Aerated tank volume	m^3
x_{O2}	Oxygen mole fraction for dry gas	-
y	Data values in optimisation routine	-

The main problem in our field is
to keep the main problem the main problem.
– Prof. George Ekama, University of Cape Town

Chapter 1

Introduction

Historically the primary objective for collecting wastewater was sanitation to prevent the spread of water borne diseases, and for a good reason the readers of the distinguished British Medical Journal choose the sanitary revolution as the greatest medical advance since 1840 (Ferriman, 2007). In many countries providing safe drinking water and sanitation are still the great challenges. Since introduction of wastewater treatment plants (WWTPs) the objectives regarding treatment have expanded and the regulations are continuously getting stricter. Today the wastewater treatment plants in developed countries not only remove pathogens but, as importantly, protect the environment from adverse emissions of all kinds. At the same time there is a strong pressure on wastewater utilities to recover resources, increase energy efficiency and reduce greenhouse gas (GHG) emissions, while maintaining the effluent constraints. All of this under a constant pressure to minimise costs.

To optimise the operations of a treatment plant is not an easy task. Firstly, the influent load is constantly varying in flow and concentration, is naturally uncontrolled and arrives every hour of the day, all year round. A wastewater treatment plant cannot allow shutting down for review and maintenance. Secondly, the construction with sequential unit processes in combination with multiple return feeds create numerous feed-back effects that makes the processes interconnected in an intricate manner.

Under such conditions mathematical modelling is a good tool for evaluating performance of WWTPs. The models describe the processes and their interactions in detail considering the ambient conditions. Thereby, the plant-wide effects are captured so that the overall result can be surveyed, analysed and sub-optimisation avoided. Through simulation studies not only the present operations can be evaluated but also future scenarios investigated, for example: load forecasts, plant expansions or alternative operational strategies. Modelling and simulation provide a solid base for decision support when evaluating plant operations.

1.1 Aim and Purpose of Research

The aim of the research presented in this thesis has been to develop a plant-wide modelling tool for simulating how wastewater treatment can be improved in terms of energy efficiency, resource recovery and greenhouse gas emissions, while not compromising effluent quality and still maintaining control of the operational costs. The tool should be used to evaluate wastewater treatment plants and compare operational strategies for the trade-offs between the various objectives. Ultimately, the purpose of the research was to provide detailed information on the impacts of different strategies and for the tool to be used for decision support at utilities.

The model development is based on decades of research on models for wastewater treatment extending existing model platforms with certain elements. The selected developments presented in this thesis are:

- extend the existing modelling tools – presently focussed on effluent water quality – to include a number of significant energy aspects related to treatment plants;
- implement models for greenhouse gas emissions in a plant-wide framework;
- develop procedures and models for simulating important applications of energy recovery as biomethane;
- develop a methodology to perform life cycle analysis (LCA) from results of dynamic benchmark simulations;
- develop new operational / control strategies balancing the multiple objectives included in the tool and demonstrate the implications of various operational strategies; and
- perform cases studies to validate the models and overall results of the simulation tool.

1.2 Delimitations

- The wastewater treatment plants considered in this work are municipal treatment plants with strict effluent standards, i.e. comparable to the regulations in most developed countries.
- The treatment processes included are related to on-site processes but for the life cycle analysis also the off-site processes directly related to the operations are included. Upstream collection systems are not considered.
- Model developments have focused on implementation and use within the Benchmark Simulation Model (BSM) platform.

» Regarding resource recovery only energy recovery as biomethane is considered.

» Micropollutants are not considered.

1.3 Hypothesis

Dynamic process models are essential to assess integrated performance of treatment, energy efficiency, greenhouse gas emissions and operational costs. They are able to capture the highly dynamic nature of wastewater treatment processes where traditional static tools – such as benchmarking using fixed emission factors and performance indicators – fail.

It is possible to construct an integrated model covering on-site processes describing dynamics in detail and couple those results to an LCA model for evaluation of both local and global environmental impacts as well as operational costs. Such a model is suitable for modelling of full-scale treatment plants and provides information not otherwise available.

1.4 Key Contributions

The results from the research have been presented and published in a number of papers and reports listed in the preface. The following six most essential articles are included in Part 2 of the thesis.

Paper I Journal paper published in The Science of the Total Environment (impact factor 2015: 3.98). The paper presents most of the model developments of a plant-wide benchmark simulation model including GHGs. The concept of multi-objective performance assessment is introduced and tested in a simulation study based on four different control strategies. The results visualise the trade-offs between objectives.

Paper II The paper – published in Water Science and Technology (impact factor 2015: 1.06) – describes the application of the developed bioprocess model from Paper I on side-stream treatment of digester supernatant. The model is calibrated to three different process regimes: nitrification/denitrification, nitritation only and anammox. Specific model developments are presented for each case. The results provide novel insights about the predictive capability of the models.

Paper III The paper was presented at the 9th IWA Symposium on Systems Analysis and Integrated Assessment (Watermatex2015). It summarises the developed aeration system model developed for BSM. Results from three full-scale case studies are presented.

Paper IV The paper was presented at the IWA World Water Congress and Exhibition (WWC&E2014). It evaluates methods for estimating substrate dependent parameters when modelling anaerobic co-digestion. The two methods under study are compared for 18 data-sets and a preferred model is concluded.

Paper V Journal paper published in Water Research (impact factor 2015: 5.99). The paper describes a method for including anaerobic co-digestion (AcoD) in plant-wide wastewater treatment models. The presented method includes both substrate characterisation and model integration. Furthermore, a novel term for long-chain fatty acid inhibition is demonstrated. Results from model calibration based on biomethane potential tests and a plant-wide simulation study are presented; this demonstrates how digester stability can be modelled.

Paper VI Paper submitted to a scientific journal. It summarises the overarching methodology of the thesis. Plant-wide models for multi-objective performance assessment integrated with LCA models are presented. The methodology is applied to a case study at Käppala WWTP, Sweden, and an alternative operational strategy is simulated and compared to the current operations. The results show the applicability of the method and that counteractive effects can arise from operational decisions, which cannot be evaluated using traditional tools.

The research can be summarised in four key contributions to the general state of knowledge.

» Detailed models for greenhouse gas emissions, including fugitive emissions, from wastewater treatment processes were included in the Benchmark Simulation Model no. 2 allowing for dynamic modelling of greenhouse gas emissions along with water quality and operational costs.

» An aeration model with adequate complexity versus accuracy was developed for the Benchmark Simulation Model platform. This allows for detailed assessment of aeration control and efficiency, aeration being the largest energy consumer at wastewater treatment plants.

» A systematic procedure for modelling anaerobic co-digestion including both substrate characterisation and model integration in a plant-wide framework was developed and validated. This is instrumental as resource recovery via co-digestion is generally becoming common practice at wastewater treatment plants and digester stability is a critical evaluation parameter.

» A tool for multi-objective performance assessment of wastewater treatment plants integrating process modelling and LCA was developed, including mechanistic models for greenhouse gas emissions and energy production and consumption. This makes

it possible to evaluate all the important dynamic effects of the local treatment plant processes along with the global environmental impact from the operations.

1.5 Outline of Thesis

The work in this thesis covers model developments in several different areas of wastewater treatment, i.e. greenhouse gas emissions, aeration and anaerobic co-digestion. The common theme of these parts is models aimed to assess energy efficiency and greenhouse gas emissions from the operation of wastewater treatment plants. These parts are also combined and tested in plant-wide models for multi-objective performance assessment together with effluent water quality and operational costs.

Chapter 2 gives a background to the topic of the thesis. Wastewater treatment is introduced in a historical context and the development to the current status motivating this work is presented. Special attention is given to the energy requirements for wastewater treatment and the greenhouse gas emissions from the processes. Finally, modelling of wastewater treatment processes is introduced including a brief description of the history of model development and more specifically the Benchmark Simulation Model platform used in this research.

Chapter 3 covers the research on plant-wide modelling of greenhouse gases. After a literature review on the current state of knowledge on greenhouse gas emissions and how they are modelled, the Benchmark Simulation Model no. 2 version greenhouse gas is presented in detail (from Papers I and VI). Thereafter, case studies from Papers I, II and VI are presented together with results and key findings from the respective papers.

In Chapter 4, modelling of aeration systems is presented. The implementations of the selected sub-models of the aeration system are reported separately. Three case studies, partly covered in Paper III, are described in detail to highlight the different parts of, and objectives for, the aeration model. The results in Paper III are presented – with some additional material from other papers and previously unpublished work – to support the key findings.

The research on modelling of anaerobic co-digestion from Papers IV and V is presented in Chapter 5. The developed method for substrate characterisation is outlined following a background description on co-digestion. The chapter covers the work on estimation of substrate dependent parameters from Paper IV as well as the procedure for fractionation of organic material and nitrogen from Paper V. The sensitivity analysis in Paper V supporting this method is presented in detail followed by the implementation of co-digestion in a plant-wide model framework. Finally, the concept is demonstrated by a simulation study on plant-wide co-digestion from Paper V.

In Chapter 6, the plant-wide process model, including relevant parts of the novel implementations, is combined with a life cycle analysis model to assess environmental impacts in several categories from both on-site and off-site processes. The methodology is tested on a case study at a large Swedish wastewater treatment plant, and the development and calibration procedures are outlined (Paper VI). A simulation study is performed where the current operation is compared with an alternative operational strategy with chemically enhanced primary treatment. The simulation results are analysed in detail for both the global environmental impacts and the effects on plant operation, demonstrating their trade-offs.

Finally in Chapter 7, essential conclusions from the preceding chapters are presented and some general conclusions drawn. Identified needs for future research are summarised at the end.

Chapter 2

Background

This chapter provides a background on wastewater treatment and related research topics, such as energy use and greenhouse gas emissions at wastewater treatment plants. Moreover, current practices on performance assessment and modelling of wastewater treatment processes are introduced.

2.1 Scope of Wastewater Treatment

Wherever humans settle and use water we discharge wastewater. It origins from basic water needs, such as water for agriculture, preparing and eating food, hygiene and sanitation. Extended amounts of wastewater arise when we no longer need to collect our water by hand but get tap water in, or in close proximity, to our houses. Wastewater is the collective term for all used water contaminated to the extent that, for most purposes, it cannot be used without treatment. Accumulating amounts of wastewater quickly become a hazard as the contaminants commonly create both health risks – spreading pathogenic deceases – and environmental problems to both natural waters – eutrophication and toxicity – and air by greenhouse gas (GHG) emissions (Metcalf and Eddy, 2014).

The "per capita" (cap) municipal water use in the world ranges from below 50 to over 500 $l.cap^{-1}.d^{-1}$ and there is a clear correlation between economic wealth (i.e. gross domestic product) and water use (FAO, 2016). In developed communities and cities, the water use lies between 150 and 250 $l.cap^{-1}.d^{-1}$, with major cities in The United States at over 400 $l.cap^{-1}.d^{-1}$. Sweden has on an average a specific water consumption of 220 $l.cap^{-1}.d^{-1}$ (IWA, 2014).

In most developed countries the degree of treatment in terms of connected population is very high. However, in countries with low population density a significant part might have single household or community-based treatment not visible in statistics (IWA, 2014). This thesis deals primarily with centralised treatment of wastewater based on modern treatment plants typical for developed countries with strict effluent standards.

In the early days of modern wastewater management the collected wastewater was either discharged untreated downstream the settlements or spread on farm land, which moved the problem out of sight and greatly improved the health and living standards in cities (Cooper, 2001). In the early 20th century, the difference in mortality rate from diseases like typhus and paratyphoid fever in European cities ranged from 1.5 (England) to 43 (Finland) per million people per year, inversely correlating to the number of wastewater treatment plants per capita (Cooper, 2001). With population growth, urbanisation and increased water use in the late 19th century – by industrialisation and improved building standards, introducing for example water closets – larger cities soon experienced environmental problems in the aquatic environment no matter how far away the discharge was moved. Wastewater treatment was consequently introduced. The first modern treatment plants had mechanical separation of sludge and visible contaminants through coarse screens and primary sedimentation, sometimes combined with chemical treatment. However, oxygen depletion and fish death in receiving waters soon made it evident that soluble contaminants needed to be treated as well. The activated sludge system, invented in England in 1914 (Ardern and Lockett, 1914), was very efficient for removing organic matter – measured as biological oxygen demand (BOD) – and was also shown to oxidise ammonium (nitrification). The process quickly became popular and through the introduction of secondary biological treatment, oxygen depletion could in practice be avoided. In the mid 20th century, it was concluded that not only the organics but also the soluble nutrients in the effluent contributed to the recently discovered issue of cultural eutrophication (Parma, 1980). Nutrient removal was developed as a measure. Nitrification was partially already achieved in the activated sludge system and with improved control capabilities in the second half of the 20th century it was mastered to a high degree. The process of denitrification was well known by the time but not until Ludzack and Ettinger (1962) suggested to put preceding anoxic tanks ahead of the aeration basins, with nitrate return to the anoxic tanks, was denitrification applied in a controlled fashion. For phosphorous removal chemical precipitation was gaining renewed application. The concept of biological phosphorous removal (Bio-P) was presented by Barnard (1974) and grew popular, especially in countries with moderate effluent phosphorous limits.

Protecting health and natural waters are still the primary objectives of wastewater treatment. With an influent reflecting the increased use of chemicals in society and discharge into an environment under increasing stress, wastewater treatment plants are in the centre of the environmental business. Therefore, the further development of wastewater treatment is

very much mirroring the perceived environmental problems of society at large. For the last two decades the utilities have experienced an increased pressure not only to meet the continuously increasing effluent standards on organics and nutrients but also to increase energy efficiency and utilise resource recovery, primarily energy and nutrients, while at the same time monitor and mitigate greenhouse gas emissions (Foley et al., 2011). As the general concern about not only heavy metals but also hormones, pesticides, nano-particles and other emerging contaminants are growing, the interest for what happens to these in and after wastewater treatment are likewise growing (Bolong et al., 2009). Even if treatment of micropollutants is not yet regulated and far from common practice, significant amounts of research are carried our in this area and examples exist of full-scale installations (Karlsson-Ottosson, 2015; Kristoffersson, 2014).

2.2 Energy Use and Recovery in Wastewater Treatment

Around 2-3 % of the world energy consumption is used for water (including non-municipal use) (Olsson, 2012b). Wastewater treatment plants are large consumers of energy. The main energy input is in the form of: *i)* electrical power for process equipment, buildings and occasionally for heating, *ii)* heat for anaerobic processes and buildings, *iii)* energy carrying chemicals like carbon source for denitrification, and *iv)* indirect energy use in the manufacturing and transport of intermediate goods. The energy requirements and efficiency of wastewater treatment have been extensively reviewed (Svardal and Kroiss, 2011; Larsen, 2015; Metcalf and Eddy, 2014; Venkatesh and Brattebø, 2011; Nowak, 2003; Balmér, 2000). Olsson (2012b) gives a thorough analysis of the whole area of water and energy, concluding that water is as important for energy production as energy is for water purposes. The specific use of energy for wastewater treatment has been examined in numerous studies. The Swedish Water and Wastewater Association has conducted a 5-year project on energy management including three surveys of the utilities energy use in 2005, 2008 and 2011 (Lingsten and Lundkvist, 2008; Lingsten et al., 2011, 2013; Lingsten, 2014), which not only resulted in a solid knowledge base but also financed measures at plants to increase their energy efficiency and recovery. The results show that the Swedish wastewater utilities consume about 600 GWh of electrical power annually, which is about 0.5 % of the total Swedish consumption (Lingsten, 2014) of 125 $TWh.yr^{-1}$ (The Swedish Energy Agency, 2015, yr 2013). Mizuta and Shimada (2010) did a review of the electrical power consumption of 985 Japanese WWTPs and found that the specific power consumption was in the range of 0.30 to 1.89 $kWh.m^{-3}$ for conventional activated sludge plants, excluding extraordinary side processes. Furthermore, they concluded plant size to be the most influential factor, with larger plants having a smaller specific power consumption. Similar studies have been conducted elsewhere (Balmér, 2000; Frijns et al., 2012) and are supported by theoretical calculations (Nowak, 2003). The main part of the power consumption is used for the actual treatment processes, especially

Table 2.1: Specific power consumption for treatment processes at WWTPs. Part of table from Metcalf & Eddy (Metcalf and Eddy, 2014, Table 17-3).

Process	Power consumption [$kWh.m^{-3}$]
Screens	0.0003-0.0005
Grit removal (aerated)	0.003-0.013
Activated sludge (nitrification / denitrification)	0.23
Return sludge pumping	0.008-0.013
Secondary settling	0.003-0.004
Mesophilic anaerobic digestion of mixed sludge [a]	0.093-0.16
Sludge dewatering (centrifuge)	0.005-0.013

[a] Including electrical and heating power requirements. Heat recovery is not considered.

the blowers for aeration, which typically consume 40-60 % of the electrical power (Olsson, 2012b; Lingsten et al., 2013). Aeration is thereby the sole largest energy consumer at WWTPs and a lot of efforts have been made, both in research and in practise, to optimise aeration. Typical energy consumption numbers for different processes can be found in literature (Metcalf and Eddy, 2014) and a few major ones are re-printed in Table 2.1.

The use of heat in wastewater treatment processes is climate dependent, in cold or temperate climates it is needed for heating anaerobic processes, primarily digesters and buildings during the cold season. In warm climates the case might be the opposite and cooling of buildings and processes is sometimes needed not to jeopardise the biological activity. At Swedish wastewater treatment plants 412 GWh of heat was used in 2011 (Lingsten et al., 2013). This is less than 0.2 % of the total Swedish energy use of 250 $TWh.yr^{-1}$ (excluding electrical power and losses) (The Swedish Energy Agency, 2015, yr 2013). A great variety of heat sources can be used, from external input of primary energy, such as oil or district heating, to self-produced biogas or recovered effluent heat. In Sweden, there is a clear trend that biogas is used for more high value purposes – mainly vehicle fuel or power production – and district heating or recovered low temperature heat are used as heat sources instead.

For input of chemical energy all non-elemental chemicals contain energy following the laws of thermodynamics. However, from a practical perspective the addition of carbon source, such as methanol or ethanol for denitrification, is most relevant as they are energy carriers that could otherwise have been used elsewhere. As the effluent requirements on total nitrogen (TN) are getting stricter the use of external carbon sources is increasing. In Sweden, carbon source equivalent to 60 GWh was added to WWTPs in 2011 (Lingsten et al., 2013). For optimising the energy balance of a treatment plant with anaerobic digestion, there are conflicting interests of using the influent organic matter for denitrification or for biomethane production. Depending on local priorities this can lead to an even larger use of external carbon.

The interest for increasing biogas production is an example of the view that wastewater contaminants rather are "misplaced resources". Based on this view, the wastewater treatment plants can be considered as resource recovery facilities and contribute to the circular economy. In North America the concept is already widely accepted and WWTPs are in the industry commonly referred to as water resource recovery facilities (WRRFs). The influent wastewater contains organics, nutrients and heat that can be reclaimed in different forms (Eitrem Holmgren et al., 2015). The organics can be recovered as energy rich biomethane in digesters or as bioplastics in bioprocesses. The nutrients are needed for fertilisation and can be recycled to arable land either as sludge or after extraction. Various techniques for extraction of both phosphorous and nitrogen have been suggested (Eitrem Holmgren et al., 2015). However, to date the only commercially available process is struvite precipitation, which captures phosphorous and nitrogen in equal amounts on a molar basis. The potential for heat recovery is large, given the great energy content in the influent. However, the temperature is low and heat pumps must be used. The use of heat pumps to recover heat for internal purposes as well as for distribution as district heating is common in countries with temperate or cold climate (Elías-Maxil et al., 2014).

At wastewater treatment plants energy exists primarily in the following five forms (Wett et al., 2016; Metcalf and Eddy, 2014).

Heat energy – Considering the whole urban water cycle, from water extraction at the water works to effluent discharge at the WWTPs, heating of tap water is by far the largest energy input. Up to 90 % of the energy is used for this purpose (Olsson, 2012b) leading to a wastewater with elevated temperature and a significant energy content. Larsen (2015) reports that the energy content of influent wastewater is typically 800 $kWh.pe^{-1}.yr^{-1}$. Heat is also used at plants for heating processes and buildings as stated above.

Calorific energy – Calorific energy in the influent is primarily in the form of COD and macro-nutrients TN and TP but also other compounds contain some energy. Organic matter in wastewater is commonly measured as chemical oxygen demand (COD) with dichromate as oxidising agent (Arnell et al., 2016c). The energy content of the organics depends on the composition of the material and – while the theoretic COD can be calculated – there is no exact correlation between measured COD and energy content due to the incomplete oxidation in the COD analysis using dichromate. The calorific energy can be measured with a bomb calorimeter and studies have shown values from 14.7 to 17.8 $kJ.g^{-1}$ of COD (Shizas and Bagley, 2004; Heidrich et al., 2011). Given some assumptions, Larsen (2015) reports an organic energy content of 150 $kWh.pe^{-1}.yr^{-1}$. The calorific energy content of the in-organics is reported to be about 50 $kWh.pe^{-1}.yr^{-1}$ (Figure 2.1) but this cannot be recovered for direct energy purposes. However, in a system's perspective recycling of nutrients to productive land has a great energy value as it reduces, the normally energy intensive, production of commercial fertilisers. Effluent calorific energy from a WWTP is mainly in sludge and biomethane.

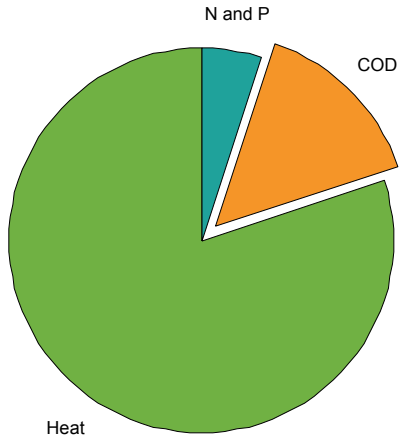

Figure 2.1: Typical energy content in influent municipal wastewater (Larsen, 2015).

Electrical energy – Electrical power is used in the treatment processes. Losses in equipment are converted to heat, which in some cases are transferred to the water (e.g. aeration) but mostly lost to air. The power is commonly bought but can also to some extent be produced at the plant by gas engines and various fuel cell or heat to power concepts (Hofman et al., 2011).

Potential energy – The preferred design of wastewater collection systems is with gravity flow as this minimizes the power needed for pumping. Along with the natural location of most plants close to the recipient this leads to a minimal vertical drop and thus a minimal potential energy. In cases with a significant drop, especially at the outfall, this can be utilised for power generation using a turbine.

Kinetic energy – For completeness the kinetic energy of moving water must be included. This part is normally small and of minor interest in practical applications.

2.3 Greenhouse Gas Emissions from Wastewater Treatment

Following the ubiquitous discussion about climate change and the impact of greenhouse gas (GHG) emissions, many water utilities have become aware of the potential emissions from the operation of WWTPs. Even if it is clear that significant emissions of the strong greenhouse gas nitrous oxide (N_2O) is normally avoided when treating wastewater for nitrogen – as discharged nitrogen otherwise is partly converted and emitted as N_2O in the recipient (IPCC, 2013) – the treatment processes themselves also emit GHGs. Extensive investigations and research have been done over the last two decades to understand the mechanisms

and quantify the emissions. Several studies have concluded that it is primarily carbon dioxide (CO_2), nitrous oxide and methane (CH_4) that can be produced and emitted at treatment plants (IPCC, 2013; Arnell, 2013; Foley et al., 2011). Both CH_4 and N_2O are strong greenhouse gases: on a mass basis CH_4 has a global warming potential (GWP) equivalent to 34 times that of CO_2 and N_2O has a GWP of 298, both calculated in a 100-years perspective and with climate-carbon feedbacks (IPCC, 2013). These GWP factors can be used to convert emissions of various gases into CO_2 equivalents (CO_2e). Greenhouse gas emissions are commonly categorised as direct or indirect emissions, referring to whether they arise at the facility or externally as a consequence of the operations. In global reporting protocols these categories are called Scopes 1, 2 and 3. Scope 1 holds all direct emissions, Scope 2 all indirect emissions from purchased electricity and heat, all other indirect emissions are accounted to Scope 3. For reporting GHG emissions the term "carbon footprint" is frequently used. However, even if different definitions of carbon footprint have been proposed (Wiedmann and Minx, 2007; Wright et al., 2011), there is not one generally accepted definition most authors follow; every author rather includes what fits for a specific case. Consequently, carbon footprint estimates must be evaluated carefully when comparing numbers between studies.

Estimates of total greenhouse gas emissions from wastewater treatment plants have been assessed in a few studies (Gustavsson and Tumlin, 2013; Foley et al., 2011; Bridle et al., 2008; Monteith et al., 2005). Generally, focusing on Scope 1 (direct) emissions CH_4 and N_2O are considered. Carbon dioxide from degraded influent COD is considered biogenic. However, this can be questioned, see Section 2.3.1, but is supported by IPCC (2013). Gustavsson and Tumlin (2013) reported total CO_2e emissions (including Scopes 1, 2 and 3) in the range of 7 to 108 kg per person equivalent (pe) and year (yr) from 16 Scandinavian WWTPs, with an average of 46 $kg.pe^{-1}.yr^{-1}$. This average is in line with other studies (Hofman et al., 2011). The main contribution to GHG emissions was from N_2O, which was also highly variable. Also Foley et al. (2011) reported that N_2O, together with CH_4, were the main contributors to the total GHG emissions from WWTPs, and demonstrating a high variability. In summary, their study found that N_2O made up 2 to 90 % of the total carbon footprint and CH_4 5 to 40 %. Monteith et al. (2005) calculated the GHG emissions for 16 Canadian wastewater treatment plants and found CO_2e emissions in the range of 0.14 to 0.63 $kg.m^{-3}$. These values cannot easily be converted to per person equivalents since no specific wastewater flows are known. However, Gustavsson and Tumlin (2014) report converted numbers for four utilities in the range of 0.2 to 0.45 $kg.m^{-3}$. To put these numbers in perspective, the total per capita CO_2e emissions were (2013) 7 300 $kg.cap^{-1}.yr^{-1}$ for European Union, 16 600 $kg.cap^{-1}.yr^{-1}$ for The United States and 16 900 $kg.cap^{-1}.yr^{-1}$ for Canada (Olivier et al., 2014). Furthermore, the reported emissions from operation of wastewater treatment plants can be compared to the estimated emissions from the discharge of untreated wastewater to natural waters. Using the methodology and emission factors from IPCC (2006) to calculate the emissions of CH_4 and N_2O from a recipient if untreated wastewater would be

discharged, assuming a per capita BOD and TN load of 60 g.pe^{-1}.d^{-1} and 14 g.pe^{-1}.d^{-1}, respectively (Henze et al., 2002), yields CH_4 and N_2O emissions (in CO_2e) of 45 and 12 kg.pe^{-1}.yr^{-1}, respectively.

2.3.1 Carbon Dioxide

Carbon dioxide can be produced and emitted both on- and off-site due to plant operations. The on-site emissions are of two kinds: *i)* CO_2 from combustion of fuels for heat and power generation, these can be both fossil or biogenic depending on the origin of the fuel, and *ii)* CO_2 from the biological respiration of organic material in the treatment processes, such as activated sludge and anaerobic digestion. These emissions are mainly biogenic due to the origin of influent load. However, Law et al. (2013a) have shown that 4 to 14 % of the COD in the influent is of fossil origin. Furthermore, external carbon sources for denitrification and external substrates for digestion can be fossil. If the origin of the organic matter is fossil then the CO_2 produced by respiration should also be considered fossil.

The off-site CO_2 emissions arise due to production of power, chemicals and other goods used for the operation of treatment plants. The CO_2 emissions from wastewater treatment can be controlled by the plant management by making conscious choices of input goods with a small carbon footprint, e.g. renewable power and carbon source.

2.3.2 Methane

Methane is produced and emitted in wastewater systems, both in the collection system and at the treatment plant (Czepiel et al., 1993; Foley et al., 2011; Daelman et al., 2012; IPCC, 2013; Liu et al., 2015). Methane has been reported to make up 75 % of the total GHG emissions from wastewater handling (Foley and Lant, 2007) even if it is usually lower, as stated in the first part of Section 2.3. Measurements in Gold Coast, Qld, Australia showed that methane formation occurred in sewers and that the emissions contributed significantly (25 %) to the total GHG emissions of the wastewater system studied (Foley et al., 2011). Furthermore, the study showed that conditions favourable for hydrogen sulphide (H_2S) formation was so also for methane. Consequently, traditional measures for preventing H_2S formation were also effective for suppressing CH_4. Since the activity of methanogenic organisms is strongly temperature dependent, these results cannot be directly extrapolated to other locations. Gold Cost is situated in a warm climate and the methane formation is lower under colder conditions (Liu et al., 2015).

Also CH_4 emissions from wastewater treatment plants have been examined. The emissions arise from several process steps at the plant. Foley et al. (2011) reported from measurements in The Netherlands and France that substantial amounts of methane are emitted from the

inlet works, i.e. screens, grit removal and primary settlers. Due to the known methane production in the sewers, it is likely that these emissions originate from there and merely are emitted at the plant. These specific studies were not able do differentiate the origin of the CH_4. Other processes showing an elevated risk for methane emissions are primarily those where anaerobic conditions occur, such as anaerobic zones in the activated sludge reactors, thickeners and sludge storage (Daelman et al., 2012). Plants with anaerobic digesters for sludge stabilisation produce methane, which unintentionally can be emitted to the atmosphere, so called fugitive emissions. A survey in Sweden measuring fugitive methane emissions at utilities with anaerobic digestion showed emissions in the range of 0 to 6 % of produced biogas (SWMA, 2012). This and other studies found average methane leakages of 1 to 2 % (SWMA, 2012; Gunnarsson et al., 2005; Fruergaard and Astrup, 2011). The methane produced in digestion is generally collected and utilised for energy recovery, or at least flared to avoid deleterious emissions. But the combustion of biogas in boilers, engines and flares are known not to be complete and a fraction of the gas can pass through to the fumes (Liebetrau et al., 2010). Methane emissions from one year storage of digested and dewatered sludge were measured by Jönsson et al. (2015). They reported CH_4-C emissions from 0.8 to 7.5 $kg.ton^{-1}$ volatile solids (VS) (converted to CH_4 1.1-10 $kg.ton^{-1}$ VS), where the lower value represents thermophilic sludge stored under cover. For the total CH_4 emissions from WWTPs Foley et al. (2011) reported levels from less than 0.0004 to as high as 0.048 kg COD_{CH4} per kg $COD_{influent}$. Converted to kg of CH_4 these emissions correspond to 0.1 -12 $g.kg^{-1}$ COD (the COD content of CH_4 is 4 kg COD per kg of CH_4).

2.3.3 Nitrous Oxide

It has been known for a long time that the biological processes in wastewater treatment can emit nitrous oxide (Robertson, 1991; Björlenius, 1994; von Schulthess et al., 1994). Initially, it was assumed that the production of N_2O was only due to incomplete reduction of nitrate to nitrogen gas by heterotrophic bacteria (HET), as it was known that N_2O is a mandatory intermediate in the denitrification reduction chain. However, recent advances in research on production mechanisms of nitrous oxide show that other production pathways exist and can be significant (Kampschreur et al., 2009b). Both heterotrophic and autotrophic bacteria can produce N_2O. The production pathways are indicated in Figure 2.2. Ammonia oxidising bacteria (AOB) can produce N_2O both through hydroxylamine oxidation in the first step of nitrification and through nitrifier denitrification as a side process to the second step. It is generally accepted that nitrite oxidising bacteria (NOB) do not contribute to N_2O production (Law et al., 2012b). The same applies for anammox bacteria (Kampschreur et al., 2009a) and the small N_2O emissions reported from nitritation/anammox processes are generally considered to be associated with heterotrophic activity in the reactors (Yang et al., 2013).

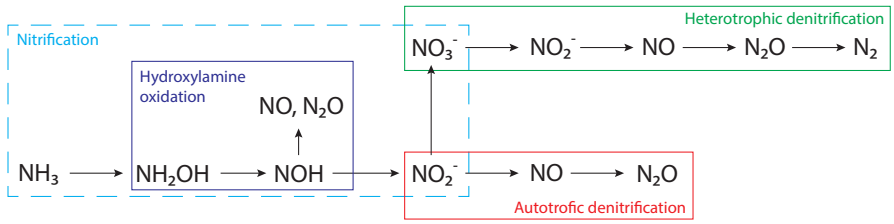

Figure 2.2: Conventional nitrogen conversion cycle over nitrate with N_2O production pathways indicated.

The hydroxylamine production pathway occurs in the first step of nitrification. AOB converts ammonia (NH_4) to nitrite (NO_2^-) over hydroxylamine (NH_2OH) mediated by the enzyme *ammonia mono-oxygenase*. The oxidation from NH_2OH to NO_2^- is catalysed by another enzyme, *hydroxylamine oxidoreductase*, and is in fact a two-step process with a nitrosyl radical (NOH) as an intermediate. This allows for electrons to be accepted and transferred simultaneously. In both these steps – from ammonia to nitrite – AOB require molecular oxygen for energy and as an electron acceptor. Being a radical, NOH is extremely unstable and it can chemically degrade to NO and N_2O if accumulated (Law et al., 2012b). In a balanced process both hydroxylamine and nitrosyl are rapidly consumed and do not occur at significant levels and no N_2O is produced. However, recent studies indicate that various process disturbances can lead to significant N_2O production via this pathway (Law et al., 2012b; Ni and Yuan, 2015; Peng et al., 2014). Any process conditions leading to increased ammonia oxidation rates can cause unbalanced AOB activity and hence incomplete hydroxylamine oxidation with N_2O as the final product rather than NO_2^-. The two main conditions suggested are elevated ammonia levels and rapidly increasing levels of dissolved oxygen (DO), for example under transient conditions (Law et al., 2012b; Peng et al., 2014).

Ammonia oxidising bacteria can also produce nitrous oxide via the so called nitrifier denitrification pathway (Foley et al., 2011). In several studies, this pathway has been shown to be dominating (Åmand et al., 2016; Lindblom et al., 2016; Peng et al., 2014; Stenström et al., 2014; Gustavsson and la Cour Jansen, 2011; Foley et al., 2011). This is possible since AOB have the capability of reducing NO_2^- to NO and further to N_2O (Figure 2.2). The genome of AOB has been shown to possess the capability of expressing the NO_2^- and NO reductases but not N_2O reductase, implying that N_2O rather than N_2 is the end product of nitrifier denitrification. One condition shown to stimulate nitrifier denitrification is accumulation of NO_2^- (Tallec et al., 2006; Kampschreur et al., 2009b; Wunderlin et al., 2012). In turn, nitrite accumulation is promoted under anoxic and sub-oxic conditions (Peng et al., 2014) and has been shown to be the dominating contributor to N_2O production in some studies (Foley et al., 2011). Peng et al. (2014) used isotopic measurements to evaluate the contribution of nitrifier denitrification and hydroxylamine oxidation under varying DO conditions (range 0 to 3 $g.m^{-3}$) and found that nitrifier denitrification was dominating and that the

combination of DO and NO_2^- concentrations were regulating the balance. Their study shows that the AOB denitrification is decreasing with increasing DO, while the opposite is seen for hydroxylamine oxidation.

Heterotrophic denitrification is a four-step process reducing nitrate (NO_3^-) to N_2 over NO_2^-, NO and N_2O (Figure 2.2). The four consecutive reactions use organic carbon as electron donor and are catalysed by different enzymes in each step. Under normal conditions the reduction of NO and N_2O is three to four times faster that the reduction of NO_3^- and NO_2^- leading to complete reduction to N_2 as the final product (von Schulthess et al., 1994). However, various operating conditions, such as DO, pH and sulphide, have been shown (Pan et al., 2013b) to disturb the reduction reactions leading to accumulation of the intermediate compounds. Pan et al. (2013b) for example report that pH causes a stronger inhibitory effect on N_2O reduction than on the other steps of denitrification. It is likely that the N_2O reduction is the most sensitive one, leading to accumulation of N_2O (Pan et al., 2013b). Furthermore, Pan et al. (2013a) have shown that a low COD to nitrogen ratio will lead to electron competition, which also stimulates accumulation of N_2O.

Nitrous oxide has a relatively high solubility in water and accumulation of N_2O in the aqueous phase must not lead to instant emissions to the atmosphere. If subsequent processes have the capability of reducing N_2O, the conversion to N_2 could be completed there. However, if the reactor or downstream reactors are aerated the N_2O will normally be stripped to the atmosphere (Kampschreur et al., 2009b).

2.4 Performance Assessment of Wastewater Treatment Plants

Municipal water services, including wastewater management, is a legal monopoly in many countries, for example the countries of the European Union. This makes it very important for utilities to be able to show that the business is managed in an efficient and cost effective way (Matos et al., 2003). One of the traditional tools in strategic planning and management is evaluation using performance indicators. Performance indicators is a monitoring tool where the business is evaluated based on historical data aggregated to key indicators that are followed over time (Matos et al., 2003). Typically the data is averaged to annual or monthly values and the method is suitable for strategic planning and monitoring on utility level. Performance indicators are useful for evaluating both treatment efficiency, energy efficiency, costs, etc. Key performance indicators are commonly used for benchmarking between businesses. Even if it is possible to go deep into the operations and perform process benchmarking this is a tool for steady-state monitoring of historical results with limited details regarding the treatment process itself.

Life cycle analysis (LCA) is a widely applied tool for assessing the environmental impact of a product or service. In LCA the global environmental impacts of the process and all related activities are evaluated for the entire life cycle. As related activities production of input goods and waste handling count. LCA has been applied to wastewater treatment systems historically (Baresel et al., 2016; Corominas et al., 2013a,b). Typically the data used in LCA are annual averages and default values from generic databases. This gives an indication of the global environmental impact and are useful for comparisons and benchmarking. It is also possible to use LCA in scenario planning. However, LCA gives few insights regarding process details and specific conditions and does not cover other areas of interest, such as costs.

For penetrating deeper in evaluation of treatment processes, mass and energy balances offer more detailed insights (Barker and Dold, 1995). With such calculations the performance of separate unit processes can be evaluated. This is an attractive method since for example flows, concentrations and tank volumes are calculated from explicit equations. This kind of spread-sheet calculations also offers the possibility to do similar steady-state evaluations of for example costs. Calculations using such simple steady-state models are useful in many applications and are used both for historical evaluation and design of future reconstruction and change in operations (Ekama, 2009).

To date, the most detailed and powerful tool known to evaluate wastewater treatment processes is simulation using mechanistic process models (Daigger, 2011). The detailed mathematical descriptions of the unit processes in the models provide unmatched insights on the mechanisms of the plant. Process models allow for both steady-state and dynamic simulations, the latter capturing dynamic effects, such as variations in load and temperature as well as seasonal effects. Furthermore, not only treatment efficiency can be evaluated. Successful studies have been performed including criteria such as energy efficiency (Fiter et al., 2005), greenhouse gas emissions (Guo, 2014; Sweetapple, 2014) and costs (Jeppsson et al., 2007). Another area where dynamic process models have proven superior is for development and evaluation of control and operational strategies (Gernaey et al., 2014; Åmand, 2014; Åmand et al., 2013; Olsson, 2012a).

2.5 History of Process Modelling

The development of process models for wastewater treatment systems started in the 1950s. Prior to that simpler empirical equations had been used. The development of mechanistic models of the biological processes became possible after Monod (1949) had presented a mathematical description for microbial growth. Some of the most fundamental developments on bioprocess models for activated sludge systems was done at University of Cape Town, Republic of South Africa (Jeppsson, 1996). The early steady-state model by Marais

and Ekama (1976) evolved into a dynamic model including both biomass growth and the death-regeneration principle (Dold et al., 1980). This is the basis for process models to this day (Makinia, 2010). In the 1980s, the current state of knowledge was synthesised into a state of the art model for activated sludge systems, the Activated Sludge Model no. 1 (ASM1) (Henze et al., 1987), which over time has become accepted both by the research community and practitioners. One of the key elements for this success was that the ASM1 had a reliable set of default parameters. The research community continued the model development and new processes like biological phosphorous removal was added, which became ASM2d. Furthermore, the mechanisms of ASM1 was improved to better mimic reality in ASM3 (Henze et al., 2000). During the 1990s the research on detailed modelling of anaerobic digestion started (Siegrist et al., 1993), which was later compiled into a standard model, Anaerobic Digestion Model no. 1 (ADM1) (Batstone et al., 2002).

Another fundamental unit process at WWTPs that gained a lot of attention in modelling was settlers, mainly secondary settling. Settler models are instrumental to facilitate the simulation of a complete activated sludge unit. The primary objective for a settler is to separate water and sludge, return the sludge to the activated sludge reactor and extract a specified wastage flow. For this purpose initially ideal point settler models were used. A point settler is simply an ideal separation unit without internal volume and can still be used when effluent TSS concentration or hydraulics are of minor importance. For developing more capable models many different principles have been proposed (Makinia, 2010). The principle of the very common layered, one-dimensional settler models describing the convective flux and concentration dependent settling velocity of particles stem from the early work by for example Stenstrom (1975) and Vitasovic (1985) using the theory of Kynch (1952) (Jeppsson, 1996). Later, Takács et al. (1991) added a modified settling velocity flux function allowing for a more realistic effluent TSS. However, the Takács et al. (1991) model was derived directly from mass balances without considering some important numerical aspects, which means that it can produce incorrect numerical solutions if the concentration profile in the settler is not monotonically increasing. This problem has been solved by Bürger et al. (2013), who derived a consistent modelling methodology from the integral form of the settling equation. The model by Bürger and Diehl also allows for including the influence of compression and dispersion on the settling flux. Furthermore, it is possible to increase the number of layers for improved numerical accuracy and to calculate the sludge blanket height (Arnell, 2015).

When the fundamental bioprocess models for both the water and sludge train were accepted it became possible to construct plant-wide models for WWTPs. Models for support systems like primary clarifiers, thickeners and aeration systems were incorporated and interfaces between the different sets of state variables were developed (Nopens et al., 2010; Volcke et al., 2006). Models have been used frequently in parallel with actual process development for fundamental understanding of the biological processes. As the process development

has continued, with for example new pathways (i.e. anammox) and side-stream treatment, models for these processes have been established as well and incorporated into plant-wide platforms.

As the models proved to be reliable they also came into use in the industry (Daigger, 2011). Today several commercial software packages exist for specifically modelling wastewater treatment systems. These basically use ASM and ADM style models but usually have code specific adjustments to improve realism, simulation speed and enhance their ease of use.

2.6 Benchmark Simulation Model Platform

The Benchmark Simulation Model (BSM) platform was developed with the purpose of making model-based comparisons of strategies for operation and, more specifically, automatic control at wastewater treatment plants (Gernaey et al., 2014). For example, different process configurations and various control strategies, such as dissolved oxygen control, can be evaluated. The performance of control strategies are in practice difficult to compare – due to varying conditions, such as loads, disturbances and plant design – and simulation models are therefore practical in order to make fair comparisons. The BSM platform consists of six elements: *i)* standardised treatment plant layout with fixed tank volumes, *ii)* set of process models for all the included treatment steps, *iii)* predefined influent flow and loads, characterised by the model state variables allowing for both steady-state and dynamic simulations, *iv)* large number of sensor models for monitoring the process realistically and actuator models to implement control strategies, *v)* predefined simulation protocol, and *vi)* given evaluation scheme including an aggregated effluent quality index (EQI), operational cost index (OCI) and risk index. The Benchmark platform has been developed for both stand-alone activated sludge units – Benchmark Simulation Model no. 1 (BSM1) – and for a plant-wide WWTP (BSM2). For the scope of this thesis emphasis will be put on BSM2 in the following description.

The BSM2 plant is designed to be a standard treatment plant with effluent standards similar to modern plants in developed countries (Figure 2.3). The water line consists of a primary clarifier of 900 m^3, an activated sludge unit with five reactors in series where reactors 1 and 2 have volumes of 1500 m^3 each and reactors 3 to 5 are equally sized volumes of 9000 m^3 in total. In the default set-up reactors 1 and 2 are anoxic and reactors 3 to 5 aerated; reactor 5 and reactor 1 are connected by internal recycling. Feed and recycle flows are flexible and air and carbon source can be added to all reactors allowing for different process configurations. The activated sludge reactors are followed by a secondary settler with a volume of 6000 m^3 and an area of 1500 m^2. In the sludge train the waste activated sludge is thickened and digested together with the primary sludge in an anaerobic digester of 3400 m^3 liquid volume. Finally, the sludge is dewatered and the supernatant is recycled to the water line

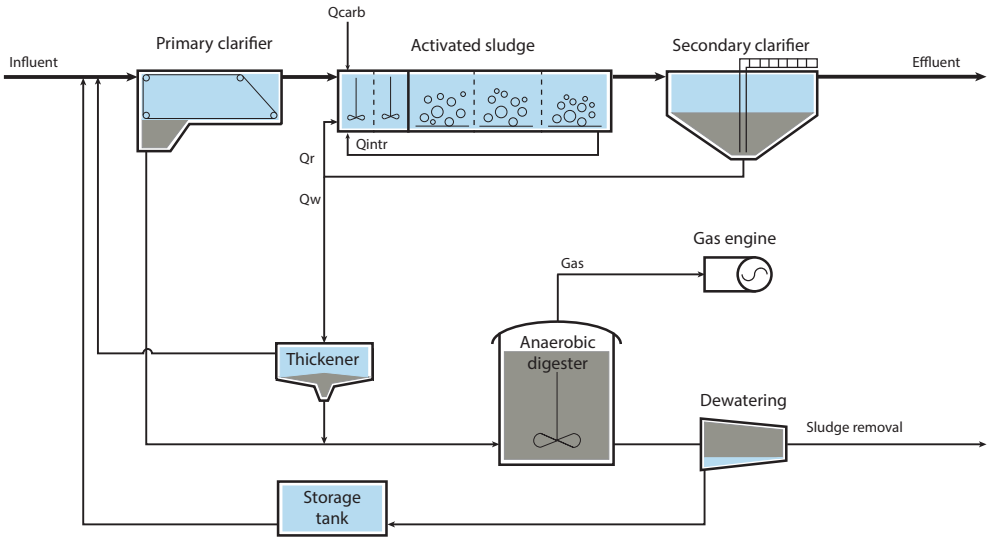

Figure 2.3: Principal plant layout of the treatment plant in Benchmark Simulation Model no. 2.

via a storage tank. In the sludge line there is also a co-generation unit for heat and electrical power generation from the produced biogas. The heat is only used for heating the digester.

For the model set-up the primary settler is modelled using an empirical mass balance model by Otterpohl and Freund (1992). The ASM1 was chosen for the activated sludge process followed by the one-dimensional 10-layer model by Takács et al. (1991) for the secondary settler. In the sludge line the digestion process is modelled using the ADM1 and the thickener and dewatering units are described by simple ideal separation models.

Following the defined simulation protocol for BSM2, the plant is simulated for 609 days with a defined dynamic influent containing everything from short-term diurnal variations and weekend effects to long-term variations for temperature and holiday periods. The first 245 days are used for stabilising the plant with the simulated control settings and the final 364 days are used for performance evaluation. In the evaluation scheme the EQI measures the effluent water quality as a weighted average of effluent COD, BOD, ammonia, nitrate and total solids loads whereas the OCI provides a relative comparison for the operational costs including, power for mixing, aeration and pumping, carbon source addition, heating of the digester, utilisation of biogas and disposal of sludge.

The BSM platform is continuously expanded and refined in order to allow for evaluation of operation and control in emerging areas. Many specialised versions exist today, including for example, greenhouse gas (BSM2G), micropollutants (BSM2X) and a plant-wide version

including phosphorous and a complete physico-chemical model (BSM2P) (Jeppsson et al., 2013).

For the modelling activities in the presented research the software package Matlab/Simulink has been used (MATLAB 7.1-8.4, The Mathworks Inc., Natwick, MA, USA, 2010-2014).

Chapter 3

Modelling Greenhouse Gas Emissions

This chapter aims to describe the extensions made to the Benchmark Simulation Model no. 2 with respect to greenhouse gas emissions. To introduce the topic, a brief literature review is presented with regard to modelling of greenhouse gas production. The details of the developed model and its implementation are described. Finally, the related Papers I, II *and* VI *are introduced and key results presented.*

3.1 Modelling N_2O Production

The research area of modelling greenhouse gas emissions (GHG) emissions in wastewater treatment processes has developed along with the process understanding of GHG production in wastewater treatment. Several research groups have been active in the field and have suggested various models. The development has recently been reviewed by Mannina et al. (2016) and Ni and Yuan (2015).

The principles for modelling GHG emissions at wastewater treatment plants (WWTPs) can roughly be divided into three categories (Mannina et al., 2016): *i)* simple emission factor based models at system level, *ii)* comprehensive WWT models including static emission factors for GHG emissions at unit process level, and *iii)* detailed mechanistic models at unit process level. The models used in this work belong to the third category.

Mechanistic models for biological production of GHG include emissions of CO_2, through respiration of COD and emissions of CH_4 and CO_2 from the anaerobic digester modelled using ADM1. However, the development of mechanistic models for N_2O production has been more important and intricate. The models suggested in literature all try to explain the observed emissions through modelling of one or several of the production pathways

described in Section 2.3.3. One of the mostly used models is the one by Hiatt and Grady (2008) describing HET production of N_2O by including all four sequential steps in denitrification (Figure 2.2). Being one of the three intermediate compounds, N_2O is included as a state variable, which allows for modelling of accumulation and subsequent emission. One of the features making this model popular is that it, apart from the four-step denitrification, also splits nitrification into two steps with separate state variables for AOB and NOB biomass. Although the Hiatt and Grady-model does not include neither AOB denitrification nor hydroxylamine oxidation, the two-step nitrification description has proven the model suitable for expansion to include N_2O production by AOB (Porro et al., 2011; Flores-Alsina et al., 2011; Corominas et al., 2012). Disregarding this, other models have been proposed for modelling of the heterotrophic N_2O production. Kaelin et al. (2009) suggested a simpler two-step extension of the ASM3 model (Henze et al., 2000) including N_2O. On the other hand, Pan et al. (2013b) argued that a more complicated modelling approach with four-step denitrification including electron competition was necessary to explain the N_2O production under COD limited conditions.

Models including N_2O production by AOB are commonly categorised as one- or two-pathway models to indicate if they include only one or both of the hypothesised pathways (Peng et al., 2015b). Several one-pathway models including AOB denitrification have been suggested (Mampaey et al., 2013; Ni et al., 2011). The models by Mampaey et al. (2013) and Ni et al. (2011) differ in terms of substrate, ammonia vs. ammonium, and because the model by Ni et al. (2011) describes ammonia oxidation as a two-step process with NH_2OH as an intermediate. Furthermore, the Ni et al. (2011) model has some additional inhibition and reduction steps. Law et al. (2012a) proposed a model including the NH_2OH pathway by AOB. Both models by Ni et al. (2011) and Law et al. (2012a) build on the concept of modelling the electron transport, which significantly adds to the model complexity. To compare the predictive capabilities, Peng et al. (2015b) have validated four different one-pathway models against several data sets. None of the models were capable of fully describing the dynamics of all the data. It was concluded that the two pathways are active under different conditions and to fully describe data with large variations both pathways are needed (Peng et al., 2015b). Following from that, Ni et al. (2014) recently suggested a two-pathway model based on three oxidation processes and three reduction processes, including modelling of electron transport. This model has been further developed to include dependency of N_2O formation on inorganic carbon (Peng et al., 2015a).

The first plant-wide model including GHG emissions was presented by Monteith et al. (2005). The model is based on static factors on unit process level with the possibility of applying case specific conditions and data. This methodology was further developed by Bridle et al. (2008) and the fundamentals were brought into the models used in this research by Flores-Alsina et al. (2011). However, in the early attempts to calculate plant-wide estimates of GHG emissions only CO_2 and CH_4 were considered and N_2O neglected

(Rosso and Stenstrom, 2008; Gori et al., 2013). As the importance of N_2O was discovered it was also included in process modelling. The first plant-wide models including N_2O together with other emissions were based on existing dynamic modelling tools expanded with either mechanistic (Flores-Alsina et al., 2011, 2012a,b) or static (Corominas et al., 2012; Rodriguez-Garcia et al., 2012) model components for N_2O emissions. Through this development the paramount importance of considering dynamics in N_2O production has been clarified (Guo, 2014; Flores-Alsina et al., 2014; Arnell and Jeppsson, 2012; Lindblom et al., 2013). Therefore, the recent research has focused on mechanistic modelling of N_2O and incremental contributions have been presented, leading up to the point where we are today (Porro et al., 2011; Corominas et al., 2012; Sweetapple, 2014; Guo, 2014; Flores-Alsina et al., 2014; Snip et al., 2014).

3.2 Description of BSM2G

The Benchmark Simulation Model no. 2 Greenhouse gas (BSM2G) is an extension of the standard BSM2 described in Section 2.6. Out of the six parts of the BSM platform – plant layout, model setup, influent load, sensors and actuators, simulation procedure and evaluation scheme – modifications were required for the model set-up, influent load and evaluation scheme. The final version of BSM2G developed and used for this work and presented in Papers I, II and VI are described in this section. Fundamental contributions to this development were also presented by Flores-Alsina et al. (2011) and Guo and Vanrolleghem (2014).

The BSM2G plant layout with the included GHG emissions are shown in Figure 3.1. In BSM2G both direct emissions from the plant and indirect – off-site – emissions are included.

Direct Emissions

- CO_2 from biological respiration of COD in the activated sludge unit, anaerobic digester and biological side-stream treatment. CO_2 assimilated by autotrophic growth is credited. Calculated in the bioprocess models.
- N_2O from nitrogen conversion processes in activated sludge and side-stream reactors. Calculated in the bioprocess models.
- Fugitive emissions of CO_2 and CH_4 from the anaerobic digester and co-generation unit. Dissolved CH_4 in the digester effluent is stripped and a CO_2 credit is included for power production from biomethane. Calculated dynamically using emission factors.
- CO_2, N_2O and CH_4 from sludge storage. Calculated dynamically using emission factors.

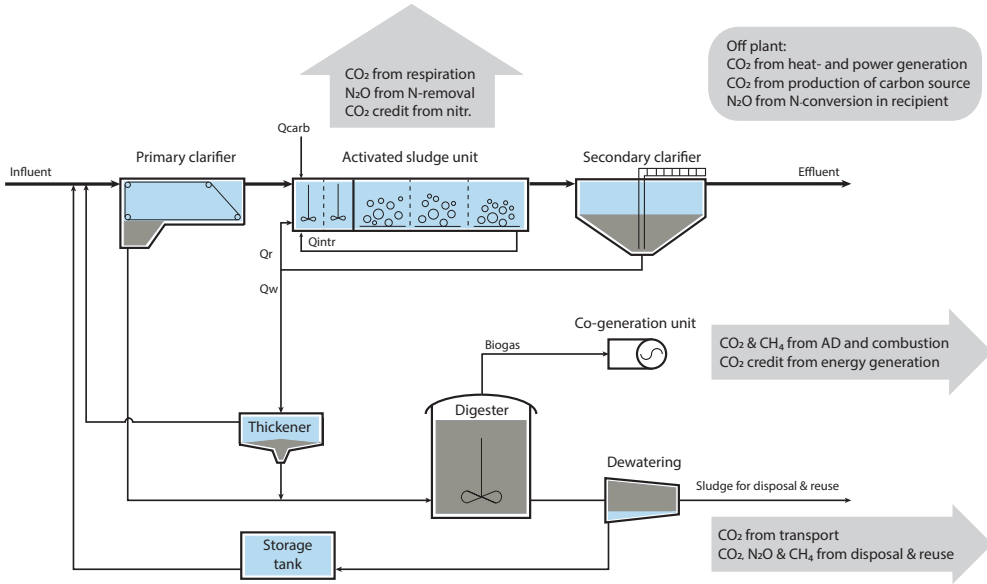

Figure 3.1: Principal wastewater treatment plant layout of the treatment plant in Benchmark Simulation Model no. 2 Greenhouse gas (BSM2G) with included greenhouse gas emissions indicated in grey boxes.

Indirect Emissions

- CO_2 from off-site heat and power generation. Calculated using static emission factors.
- CO_2 from production of external carbon source. Calculated using static emission factors.
- N_2O from conversion of effluent nitrogen in recipient. Calculated using static emission factors.
- CO_2 for transport of sludge for disposal. Calculated using static emission factors.
- CO_2, N_2O and CH_4 from disposal of sludge. Calculated using static emission factors.

3.2.1 BSM2G Model Library

Activated Sludge Unit

The bioprocess model ASM1 used in BSM2 was updated with reaction kinetics for biological N_2O production. Two major model amendments were made. The principles described by Hiatt and Grady (2008) with two-step nitrification and four-step denitrification were included, featuring heterotrophic N_2O production. Reaction specific model parameters

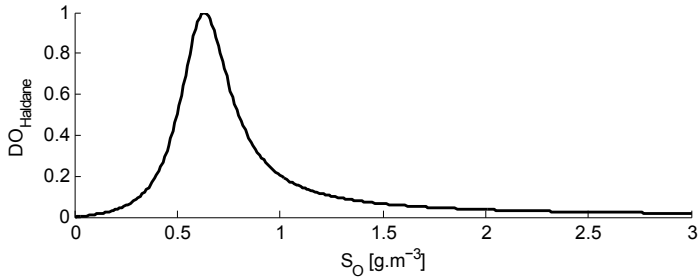

Figure 3.2: Haldane kinetic term as a function of modelled dissolved oxygen concentration (S_O) for limiting denitrification by ammonia oxidising bacteria to sub-oxic conditions.

are used for each of the four denitrification steps. As a complement, AOB denitrification was included following Mampaey et al. (2013) where AOB have the capability of reducing NO_2^- to NO and N_2O. To limit the AOB denitrification to sub-oxic conditions the Haldane kinetic term suggested by Guo and Vanrolleghem (2014) was included,

$$DO_{\text{Haldane}} = \frac{S_O}{K_{SO,AOBden} + \eta_{\text{Haldane}} \cdot S_O + S_O^2 / K_{IO,AOBden}} \tag{3.1}$$

where, $K_{SO,AOBden}$ [g O_2.m^{-3}], η_{Haldane} [-] och $K_{IO,AOBden}$ [g O_2.m^{-3}] are kinetic parameters.

This limits the AOB denitrification reaction rate to a maximum at a specified (low) DO and a declining rate at concentrations above that peak, see Figure 3.2.

All state variables used in the amended model (ASM1G) (Guo and Vanrolleghem, 2014) are listed in Table 3.1. There are 15 reactions in the ASM1G model.

1. Heterotrophic growth under aerobic conditions with S_S as substrate and S_O as electron acceptor.
2. Heterotrophic growth under anoxic conditions with S_S as substrate and S_{NO3} as electron acceptor.
3. Heterotrophic growth under anoxic conditions with S_S as substrate and S_{NO2} as electron acceptor.
4. Heterotrophic growth under anoxic conditions with S_S as substrate and S_{NO} as electron acceptor.
5. Heterotrophic growth under anoxic conditions with S_S as substrate and S_{N2O} as electron acceptor.

Table 3.1: State variables of the model ASM1G. For nitrogen variables only the nitrogen part of the compound is considered. See Nomenclature section for units.

Symbol	Description	Symbol	Description
S_I	Soluble inert COD	X_I	Particulate inert COD
S_S	Readily biodegradable COD	X_S	Slowly biodegradable COD
S_O	Dissolved oxygen	X_{BH}	Heterotrophic biomass
S_{NO3}	Soluble nitrate	X_{BA1}	Ammonia oxidising biomass
S_{NO2}	Soluble nitrite	X_{BA2}	Nitrite oxidising biomass
S_{NO}	Soluble nitric oxide	X_P	Particulate inert decay
S_{N2O}	Soluble nitrous oxide	X_{ND}	Particulate organic nitrogen
S_{N2}	Soluble dinitrogen	TSS	Total suspended solids
S_{NH}	Ammonia nitrogen	ALK	Alkalinity
S_{ND}	Soluble organic nitrogen	Q	Flow

6. Autotrophic growth of X_{BA1} under aerobic conditions with free ammonia as substrate and S_O as partial electron acceptor (ammonia oxidation).
7. Autotrophic growth of X_{BA1} under sub-oxic conditions with free nitrous acid (HNO_2) as substrate, NH_3 as electron donor and S_O as partial electron acceptor (AOB denitrification).
8. Autotrophic growth of X_{BA1} under sub-oxic conditions with S_{NO} as substrate, NH_3 as electron donor and S_O as partial electron acceptor (AOB denitrification).
9. Autotrophic growth of X_{BA2} under aerobic conditions with S_{NO2} as substrate and S_O as electron acceptor (nitrite oxidation).
10. Decay of X_{BH}.
11. Decay of X_{BA1}.
12. Decay of X_{BA2}.
13. Conversion of S_{ND} to S_{NH}.
14. Hydrolysis of X_S to S_S.
15. Hydrolysis of X_{ND} to S_{ND}.

The emissions of CO_2 from respiration of organic material are calculated based on the amount of COD degraded and the nitrogen credit is calculated based on the biomass growth using a value of 0.31 $kg.kg^{-1}$ $N_{nitrified}$.

Sludge Train

In the sludge train fugitive emissions from the anaerobic digester and co-generation unit are included. For the digester the literature review (Section 2.3.2) showed that a slip of

raw gas in the range 1 to 2 % is likely and hence, 1 % was implemented in BSM2G. The slip volume is accounted to the GHG emissions and subtracted from the produced gas volume. The remaining gas is fed to the co-generation unit. In the gas engine 1.7 % of the raw gas is assumed to pass uncombusted to the fumes (Liebetrau et al., 2010). The dissolved CH_4 in effluent sludge (S_{CH4}) from the digester is assumed to be fully stripped in the dewatering unit and emitted to the atmosphere. The quantity is calculated dynamically in the simulations and the S_{CH4} after stripping is set to zero.

In the downstream biosolids handling it is assumed that the sludge is stored uncovered for 12 months before transported to disposal and reuse. Based on measurements of emissions from sludge storage by Jönsson et al. (2015) it was assumed that degradation processes in the dewatered sludge give rise to CH_4 emissions of 8.68 $kg.ton^{-1}$ VS and that 1.1 % of TN in sludge diffuse as N_2O-N. The COD and TN contents of the sludge are adjusted accordingly.

Indirect and Off-Site Emissions

Different values have been used for the CO_2 emissions from net power production. In Paper I, the default value from Flores-Alsina et al. (2011) was used, 0.94 $kg.kWh^{-1}$ corresponding to Australian coal fired power plants. For the general BSM2G this value was updated to the more adequate European production mix of 0.359 $kg.kWh^{-1}$ (IEA, 2011). For the case study in Paper VI, a case specific value of 0.041 $kg.kWh^{-1}$ corresponding to Swedish electricity production (2012) was used.

Emissions of CO_2 for production of methanol were included by Flores-Alsina et al. (2011) using an emission factor of 1.54 $kg.kg^{-1}$ of methanol.

The remaining TN content in the effluent water is known to partly convert to N_2O in the recipient. N_2O-N emissions corresponding to lakes and rivers were included in the BSM2G based on an emission factor of 5 $g.kg^{-1}$ TN discharged to the recipient (IPCC, 2006).

In the standard BSM2G three different sludge disposal alternatives are included. Flores-Alsina et al. (2011) laid out the principles for including CO_2 emissions from mineralisation of sludge COD. To this, additional emission factors for CH_4 and N_2O were added.

Agriculture 38 % of the sludge; transport distance 150 km; emission factor N_2O-N = 0.01 $kg.kg^{-1}$ TN.

Forestry 17 % of the sludge; transport distance 144 km; emission factor N_2O-N = 0.01 $kg.kg^{-1}$ TN, CH_4 = 0.0075 $kg.kg^{-1}$ TOC (TOC represents total organic carbon).

Composting 45 % of the sludge; transport distance 20 km; emission factor N_2O-N = 0.01 $kg.kg^{-1}$ TN.

3.2.2 BSM2G Influent Load and Evaluation Scheme

The influent load profiles and evaluation scheme of BSM2 were updated by Flores-Alsina et al. (2011). The updated influent profiles follow the principles of Gernaey et al. (2006) with the additional biomass and nitrogen states added to the influent accordingly.

In the evaluation procedure, the two weighted indices EQI and OCI are calculated together with the time in violation of effluent constraints, i.e. the fraction of a year that the effluent quality exceeds the stipulated effluent constraints. Only the EQI needed to be modified after including GHG production models. All four oxidation states of nitrogen were included using the weighting factor for nitrate and the additional biomass states were added to the TSS, COD and BOD estimates. The calculated GHG emissions are converted to CO_2 equivalents (CO_2e) using GWP factors for a 100-year time horizon from IPCC (2013): 34 for CH_4 and 298 for N_2O, including climate-carbon feedbacks. The various emissions in the model are reported separately and a selection of which emissions to report can be made case-by-case (for example in total or excluding biogenic emissions).

3.3 Integrated Evaluation of Greenhouse Gas Emissions, Effluent Water Quality and Costs

The developed model platform, BSM2G, was used for its original purpose – benchmarking of control strategies – in Paper 1. The default control strategy of BSM2 was compared with four alternative strategies. The results were evaluated including the aspect of GHG emissions together with the traditional EQI and OCI.

The default control strategy in the BSM2G used as base case in Paper 1 consists of two control loops. In the first one, the DO concentration in the second aerated reactor is controlled towards a set-point of 2 $g.m^{-3}$ using a proportional-integral (PI) controller manipulating the airflow rate, i.e. the volumetric oxygen transfer rate coefficient (K_La). The K_La inputs to the first and third aerated reactors are set to equal and half of the K_La for the controlled reactor, respectively. The second PI controller regulates the nitrate return flow (Q_{intr}) from reactor five to reactor one based on a set-point for nitrate in the second anoxic reactor. Furthermore, the wastage flow of activated sludge (Q_{was}) was varied seasonally with $Q_{was,summer}$ = 450 $m^3.d^{-1}$ and $Q_{was,winter}$ = 300 $m^3.d^{-1}$. The flow rates for return activated sludge (Q_{ras}) and carbon source addition (Q_{carb}) were kept constant for the whole simulation period.

Four alternative control strategies were tested for comparisons in Paper 1.

i. Impact of DO control by varying the set-point value between 1 and 3 $g.m^{-3}$. Default value 2 $g.m^{-3}$.

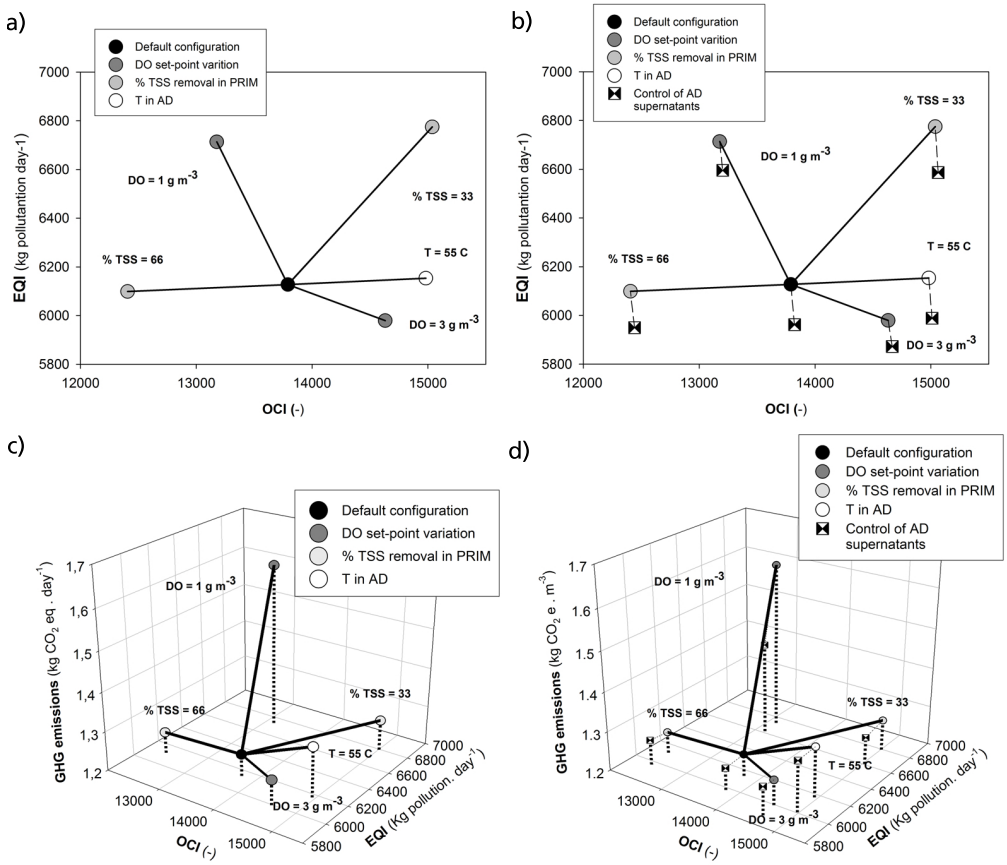

Figure 3.3: Results from Paper I presenting effluent quality index (EQI), operational cost index (OCI) and greenhouse gas emissions for the simulated control strategies. Figure from Paper I.

ii. Impact of primary clarifier efficiency by varying the TSS removal efficiency in the primary clarifier from 33 % to 66 %, default value 50 %.

iii. Impact of the anaerobic digester operating mode by changing the temperature in the anaerobic digester from mesophilic (35 °C) to thermophilic (55 °C), default value 35 °C.

iv. Impact of anaerobic digestion (AD) supernatants by controlling the return flow rate. The timer-based control strategy stores the dewatering liquor during daytime (when the plant is high loaded) and returns it at night (when the plant is low loaded). Note that the default BSM2 strategy does not use this control approach and liquors are simply returned as they are generated.

The resulting EQI, OCI and GHG emissions for the simulated control strategies are summarised in Figure 3.3. It is evident from the results that Strategy *i*, varying the DO set-

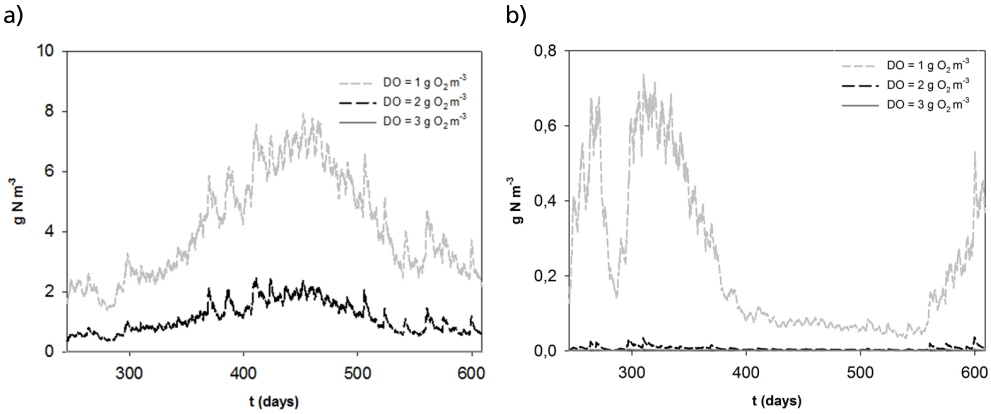

Figure 3.4: Dynamic profiles of ammonium nitrogen (left) and nitrite nitrogen (right) in the case with varying dissolved oxygen (DO) set-point. For both graphs the concentrations at DO = 3 $g.m^{-3}$ is zero or close to zero. Figure from Paper I.

point, has the largest effect on GHG emissions out of the tested strategies. Reducing the DO set-point in the AS leads to increased S_{NO2} concentration, which in turn stimulates AOB denitrification – and hence N_2O production – in the model, see Figure 3.4. The S_{NO2} profile shows a pronounced seasonal variation proving the paramount importance of taking the dynamic variations into account when considering N_2O formation. Even if the reduced aeration at the same time leads to lower indirect CO_2 emissions from power generation, the overall CO_2e increases. The degree of TSS removal in the primary clarifier has little impact on GHG emissions in this study but increased removal improves the effluent quality and reduces the operational costs substantially. The small increase in GHG emissions at higher removal efficiency is due to higher N_2O production that exceeds the credit from increased biogas production. Furthermore, the results show that with a stable and sufficiently sized digester in the base case very little is gained through switching to a thermophilic regime in the AD. The operational costs increase as well and so do the GHG emissions due to the increased heat requirements. Lastly, the effect of Strategy *iv* – controlling the return pumping of sludge liquors – are shown for all cases. This strategy leads to a small improvement in the effluent quality for all cases by reducing the S_{NH4} peaks, but has no effect on GHG emissions for almost all cases. A reduction in GHG emissions is gained in combination with low DO, which follows from the fact that low DO and high ammonia is a risk combination for high N_2O production. All details on the results and a comprehensive discussion about the realism of the models are given in Paper I.

3.4 Modelling N_2O Production in Side-Stream Treatment

Sidestream treatment of high strength AD supernatant has grown in popularity since the launch of industrial processes applying novel nitrogen removal pathways, such as nitritation/denitritation and anaerobic ammonia oxidation (known as anammox). The kinetics for N_2O production in ASM1G was thoroughly tested on sludge liquor side-treatment systems in Paper II. Three data sets: *i)* measurements on a nitrifying/denitrifying sequencing batch reactor (SBR) at Slottshagen WWTP, Norrköping, Sweden, by Stenström et al. (2014), *ii)* measurements by Gustavsson and la Cour Jansen (2011) on a nitritation only SBR at Sjölunda WWTP, Malmö, Sweden, and *iii)* data from a pilot-scale one-stage nitritation/anammox moving bed biofilm reactor (MBBR) by Yang et al. (2013). For details on the measurements the interested reader is referred to the original papers. In this section, results supporting the key conclusions on modelling of N_2O will be recaptured. For details on the models, calibration and comprehensive discussion about the results, see Paper II and Lindblom et al. (2015).

3.4.1 Nitrification/Denitrification Sequencing Batch Reactor

In the dataset used for calibration of the nitrification/denitrification SBR, the N_2O production rate in the initial non-aerated phase almost equal the nitrification rate, indicating that the last step of the heterotrophic denitrification is almost totally inhibited, Figures 3.5b and 3.5g. The N_2O production immediately stops at t = 1.5 h when ethanol is dosed and the accumulated N_2O is reduced to N_2. This rapid switch indicates a strong dependency of the heterotrophic N_2O production on COD availability. The standard formulation of denitrification in Hiatt and Grady (2008) does not capture this and an additional state for ethanol ($S_{S,EtOH,5}$) was implemented. With a high value of the half-saturation constant for the uptake of S_{N2O} utilising S_S and in contrary a low value when utilising $S_{S,EtOH}$, the large and rapid change could be described. However, the simulation results do not fully support the fact that N_2O production relates to the kind of carbon substrate. A more complex model like the recent four-step denitrification model by Pan et al. (2013b) might better capture this phenomenon (Pan et al., 2015).

Excluding anomalies stemming from the denitrification phase, the measured emissions of N_2O, occurring during the aerated phase, are fairly well described by the model (Figure 3.5f). Parameter adjustments were made to capture the seemingly high correlation with ammonia and there is support in literature for AOB denitrification being the dominating N_2O production pathway under such conditions (Ni et al., 2014).

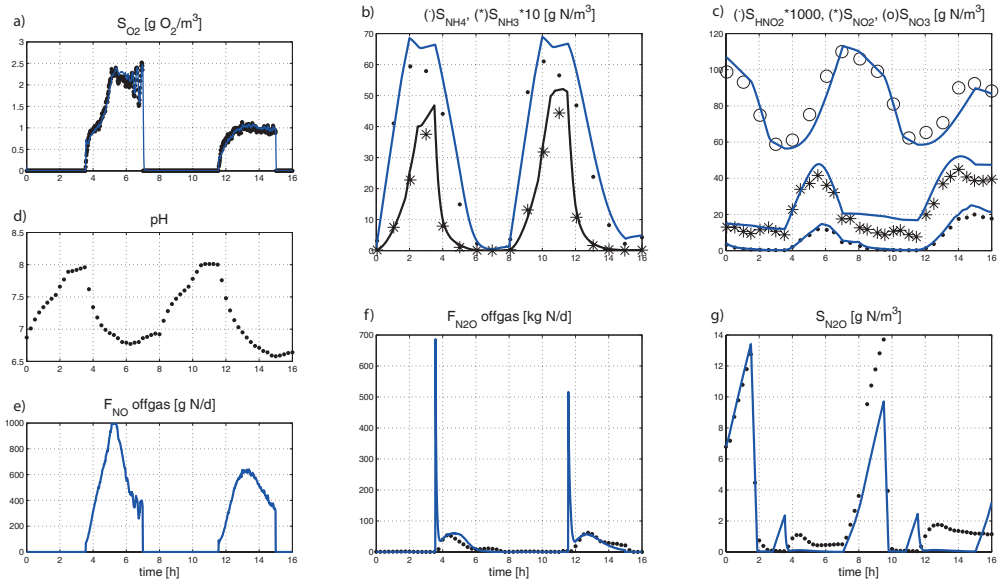

Figure 3.5: Results from the nitrification/denitrification SBR case study. a) dissolved oxygen, b) ammonia and ammonium, c) free nitrous acid, nitrite and nitrate, d) pH, e) nitrogen oxide flux to off-gas, f) nitrous oxide flux to off-gas, and g) dissolved nitrous oxide. Black markers represent data, blue line represents simulation results. Figure from Paper II.

3.4.2 Nitritation Sequencing Batch Reactor

The simulation results from the nitritation only SBR at Sjölunda WWTP are shown in Figure 3.6. The N_2O-N emissions exhibit a quick rise to 30-75 $kg.m^{-3}$ when aeration is switched on. After the peak it declines throughout the aeration phase (Figure 3.6e). The measurements at Sjölunda WWTP include off-gas NO concentrations, which are relatively stable. Considering the equations for nitrifier denitrification in the applied model dissolved nitrogen oxide (S_{NO}) was not believed to explain the dynamic N_2O emissions.

The sharp simulated peaks at the beginning of each phase (Figure 3.6e) are due to stripping of accumulated N_2O during anoxic conditions. These peaks are not seen in measurement data, see Figure 3.6e. As stripping according to the model occurs fast, the decrease in N_2O production throughout the aeration phase must be explained by AOB activity. However, by analysing data along with simulation results it was concluded that neither NO_2^- nor DO concentrations were the major cause for N_2O production. The applied model for AOB denitrification could only be reasonably calibrated assuming a unique half-saturation constant – not present in the original model – for ammonia using a very high value, $K_{NH3,AOB,DN}$ = 1.0 $g.m^{-3}$. It was concluded that the ASM1G was not suitable for describing this data set.

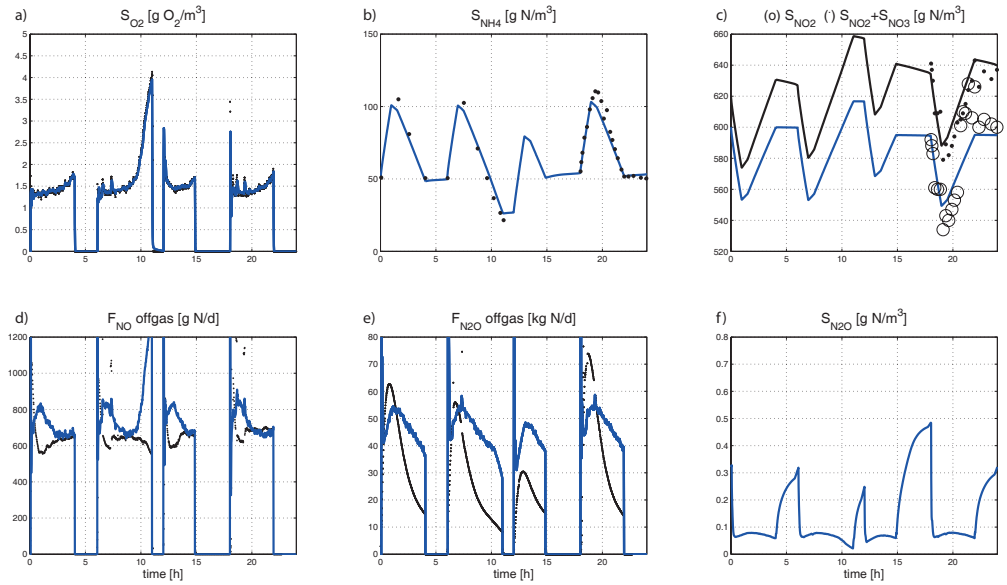

Figure 3.6: Results from the nitritation only SBR case study. a) dissolved oxygen b) ammonium c) nitrite and nitrite+nitrate d) nitrogen oxide flux to off-gas e) nitrous oxide flux to off-gas and f) dissolved nitrous oxide. Black markers represent data, blue line represents simulation results. Figure from Paper II.

It has been shown in laboratory experiments (Law et al., 2013b) and by modelling (Ni et al., 2014) that the high nitrite nitrogen concentrations (500-600 $g.m^{-3}$, Figure 3.6a), in combination with moderate DO concentrations (1.2-2.0 $g.m^{-3}$, Figure 3.6c), would imply that the contribution of the NH_2OH pathway to the total N_2O emissions is substantial. A NH_2OH pathway model, for example the one presented by Law et al. (2012a), could potentially describe the data better.

3.4.3 Nitritation/Anammox Moving Bed Biofilm Reactor

The pilot-scale anammox reactor was operated with intermittent aeration to achieve both nitritation and anaerobic ammonium oxidation. The dataset contains both soluble in-tank and off-gas N_2O concentration measurements. To model the MBBR, a biofilm model was constructed (see Paper II for details) and combined with ASM1G for biological reactions, both in the biofilm and the bulk liquid.

The model was calibrated to a part of the data with moderate nitrogen load and an intermittent aeration strategy where the reactor was aerated for 45 minutes out of 60. Simulation results show that, compared to the other case studies in Paper II, the relatively low N_2O emissions of 0.5 % during the studied period can be explained by heterotrophic denitrific-

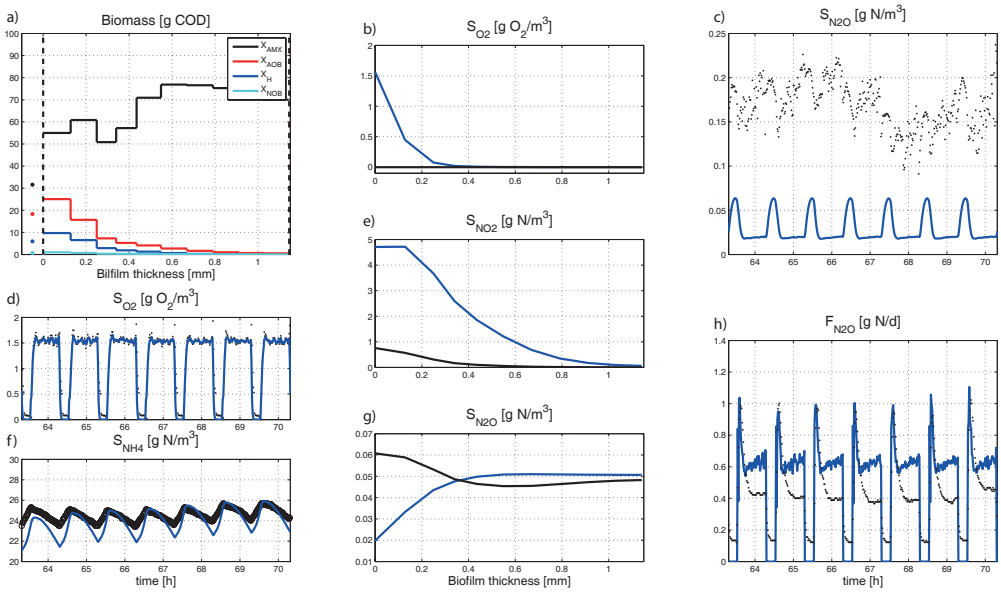

Figure 3.7: Results from the nitritation/anammox MBBR case study. a) biomass in biofilm (lines) and bulk liquid (markers), b) dissolved oxygen in biofilm, c) dissolved nitrous oxide in bulk liquid, d) dissolved oxygen in bulk liquid, e) dissolved nitrite in biofilm, f) dissolved ammonium in bulk liquid, g) dissolved nitrous oxide in biofilm, and h) nitrous oxide flux to off-gas. In Figures c), d), f) and h) black markers represent data, blue line represents simulation results. In Figures b), e) and g) blue and black lines represent simulation results under aerated and anoxic conditions, respectively. Figure from Paper II.

ation, Figure 3.7. Approximately 3 % of the influent ammonium is converted via nitrification and heterotrophic denitrification and 20 % out of this amount is accumulated as S_{N2O}, probably because of low S_S concentrations from hydrolysis of particulates in the biofilm. The resulting emissions of N_2O are similar to the measurements, Figure 3.7h. Although much lower, emissions were also measured during non-aerated phases, a phenomenon that was not explained by the model. The simulated and measured dissolved N_2O concentrations are shown as time-series in (Figure 3.7c). S_{N2O} accumulates during anoxic conditions, which is also seen as peaks in the N_2O emission as aeration is turned on. The measurement data do not show a clear pattern but occasionally it can be seen that S_{N2O} increases during anoxic conditions. The simulated S_{N2O} concentrations are generally lower than the measured ones. Based on the implemented model it is difficult to calibrate this effect because the N_2O flux – which is quite well predicted – is proportional to S_{N2O} and N_2O-K_La. Thus, if the measurements are correct, either the stripping model – including the diffusion coefficients – or the estimated K_La need to be modified.

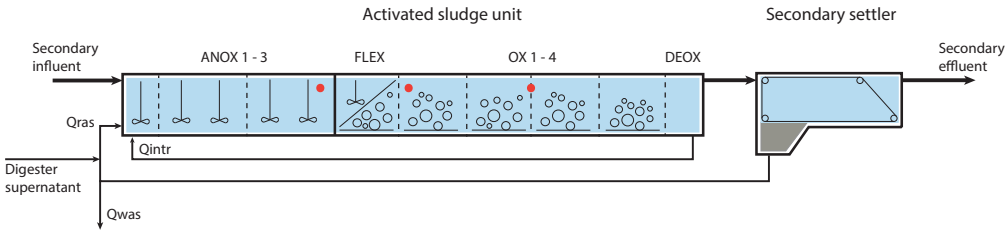

Figure 3.8: Schematic process configuration of the activated sludge reactors at Käppala wastewater treatment plant, Lidingö, Sweden. Red markers indicate positions for in-tank measurements of N_2O. Figure from Arnell et al. (2016b).

3.5 Calibration of N_2O Production in a Full-Scale Activated Sludge Unit

As part of the major case study at Käppala WWTP in Lidingö, Sweden, measurements of N_2O were conducted in one out of five parallel AS blocks at the plant. The case study is fully described in Paper VI and generally summarised in Chapter 6 but the specific details on calibration of the N_2O production are given in this section. Measurements were performed over a period of about 100 days in both liquid and gaseous phases. The in-tank concentrations were measured with an in-situ probe. To capture the processes along the reactor length the sensor was moved two times during the measurement period and data from all three locations were registered. Measurement positions are indicated in Figure 3.8, see Paper VI for details. Since the plant is covered, the gas phase measurements were made in the ventilation channel collecting off-gas from the selected AS block. Together with ventilation flow measurements the mass flux of N_2O was calculated.

From the measured N_2O concentration in the reactor it was evident that no N_2O production occurred in the anoxic zones, see Figure 3.9. The soluble N_2O concentration was very low at the end of the last anoxic zone even if no forced stripping had occurred. However, in the aerated zones the N_2O concentration was higher and increasing along the reactor. Taking the stripping, due to aeration, into consideration it was concluded that the major part of the production and emission of N_2O occurred from the aerated zones. The reason for this is assumed to be the relatively high NO_2-N concentrations measured, around 0.3 $g.m^{-3}$. As seen in Figure 3.10, the average level of the modelled emissions is in line with measured values. However, the full dynamics of the measured emissions were not well predicted by the model. The model predicts a constant base line for the N_2O-N emissions of about 30 $kg.d^{-1}$ even when the measured emissions decrease around day 425, Figure 3.10. The model behaviour follows from the model equations for AOB denitrification. However, recent publications emphasise the importance of using a two-pathway model – including both hydroxylamine oxidation and AOB denitrification – under dynamic conditions (Peng et al., 2015b). Such models predict that the N_2O production relates to the rate of nitritation

– i.e. AOB activity – rather than DO. These new two-pathway models were not available at the time when conducting the case study at the Käppala WWTP but the present results support that additional reaction pathways need to be considered in future work. One trade-off made in favour of getting proper emissions to air, was that the N_2O concentration in the aqueous phase had to be calibrated to lower than measured values for the aerated zones.

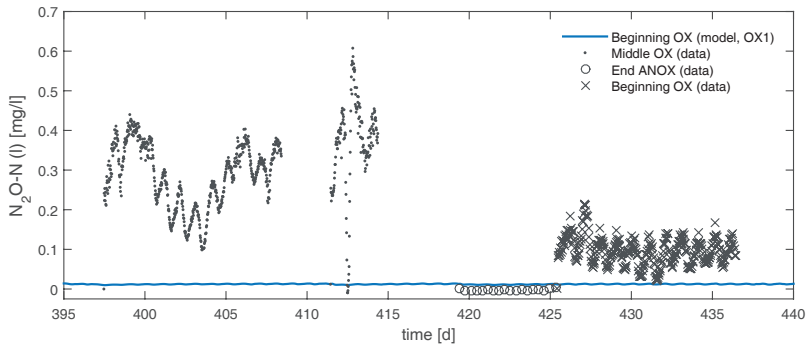

Figure 3.9: N_2O-N in aqueous phase at Käppala wastewater treatment plant. Measurements in the three different locations (grey markers) indicated in Figure 3.8 and modelled S_{N2O} in the first aerated zone (blue line). The time scale represents simulation days, where 395 corresponds to 29th of May. Figure from Paper VI.

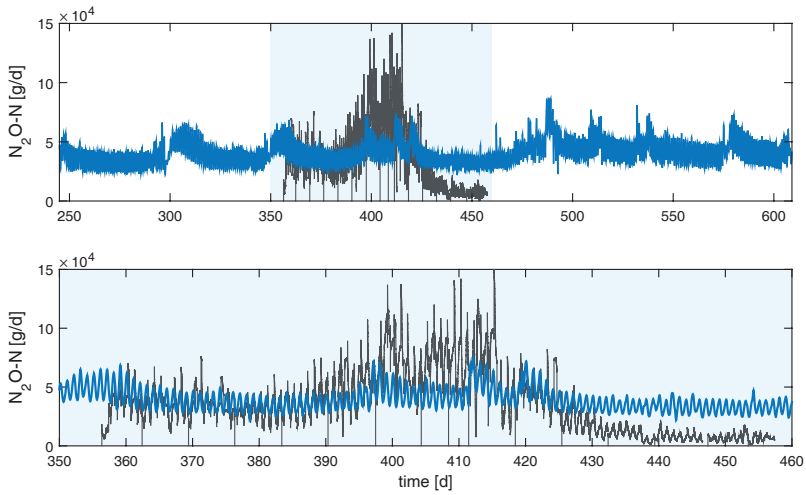

Figure 3.10: N_2O in off-gas at Käppala wastewater treatment plant. Measured data (grey line) and model result (blue line). Full year simulation (top) and day 350 to 460 covering the N_2O measurement campaign (bottom). The time represents simulation days, where 245 corresponds to 1st January and day 350 corresponds to 14th of April. Figure from Paper VI.

3.6 Summary of Key Findings

» The inclusion of greenhouse gas emissions provides an additional criterion when evaluating control/operational strategies in a wastewater treatment plant (WWTP), offering more knowledge about the overall "sustainability" of plant control/operational strategies.

» Results from simulations of different control strategies show the trade-offs that can arise. For example, the energy-related (aeration energy for activated sludge/energy recovery from anaerobic digestion) optimization procedures and the opposite effect that N_2O may have on the overall greenhouse gas emissions of the wastewater treatment plant.

» The importance of considering the water and sludge lines together and their combined impact on the total quantity of greenhouse gas emissions are shown when the temperature regime is modified, the anaerobic digestion supernatant return flows are controlled and the removal efficiency in the primary clarifier is varied.

» The implemented biological process model, together with physical models for the sequencing batch reactor (SBR) and moving bed bioreactor (MBBR) processes, can partly describe the N_2O emission data from the three side-stream treatment case studies. For the two SBR processes, necessary model and parameter adjustments indicate that N_2O production by NH_2OH oxidation was contributing as well. The four-step denitrification model could be used to model accumulation of dissolved N_2O during anoxic conditions in the nitrifying/denitrifying SBR. The N_2O emissions from the studied MBBR anammox process data were satisfactory simulated by assuming heterotrophic denitrification only.

» The stripping equation in the implemented model may be overly simplified. It results in sharp N_2O gas emission peaks that are not observed experimentally. Furthermore, the dissolved concentrations and off-gas flux of N_2O could not be matched at the same time due to the formulation of the stripping equation. For simulation of full-scale N_2O emission data in general, the retention time of the gas including the measurement devices would probably improve the conclusions that can be drawn regarding N_2O formation pathways.

» The model was calibrated to a measured N_2O emissions from a real plant, the Käppala WWTP in Lidingö, Sweden. The calibration shows that the model is suitable for this conventional municipal treatment process under current operational conditions. However, it is not possible to capture the full dynamics in N_2O production and emissions seen in the data. From this fact it is concluded that a model describing autotrophic and heterotrophic denitrification N_2O production only is not sufficient. Additional production pathways need to be considered.

» Although the observations are WWTP specific, the practical use of the developed tools is demonstrated and the model framework can also be applied to other systems.

Chapter 4

Aeration System Modelling

This chapter summarises the development of an aeration system model for evaluating airflow and energy performance of aeration in the Benchmark Simulation Model platform. Three case studies are presented from Paper III*, supplemented with results from Arnell et al. (2013) and some previously unpublished results for two of the cases.*

4.1 Introduction to Aeration System Modelling

At wastewater treatment plants several unit processes require forced aeration of tanks for various purposes. Air is used in grit chambers for increasing the removal efficiency of heavy particles, in pre-aeration tanks for oxidation of odorous compounds and in dissolved air flotation systems to improve buoyancy (Metcalf and Eddy, 2014). But most of all, aeration is used in aerobic biological treatment units to supply oxygen for oxidation of organic matter and nitrogen. Aeration of secondary biological treatment, such as activated sludge, is facilitated by a low pressure compressed air system. The basic components of the system include (Figure 4.1a):

- blower units of various kinds, including internal control systems;
- an air distribution system including pipings with bends, fittings, contractions and other obstructions;
- valves, sensors, instruments and other related equipment for control; and
- aerators / diffusers.

It has been shown in many studies that aeration is one of the most energy consuming processes at wastewater treatment plants (WWTPs), commonly accounting for 40 - 60 % of the

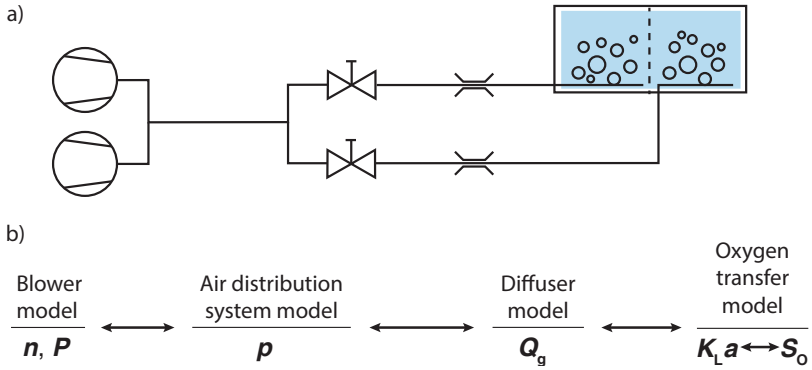

Figure 4.1: Schematic figure of a general aeration system (top) and aeration model structure (bottom). Principal model elements indicated showing the relation between: blower electrical power requirements (P) and rotation speed (n), distribution system pressure (p), airflow (Q_g), the volumetric oxygen transfer coefficient ($K_L a$) and dissolved oxygen concentration (S_O).

total electrical power demand (Olsson, 2012b; Reardon, 1995; Lingsten et al., 2013). Therefore, aeration comprises one of the major operational costs for any WWTP with secondary biological treatment facilitating nitrification. Due to the major cost, the aeration system has been the main focus for automatic control over the last 40 years or so (Olsson, 2012a; Åmand et al., 2013). Naturally, also the modelling community has engaged in the optimisation of aeration efficiency. For that purpose, various aeration system models have been presented. Modelling of aeration systems implies including a sub-model for the mechanical components providing air to the activated sludge system and further, to model the oxygen transfer from air to liquid. The principal layout of a submerged pressurised aeration system is sketched in Figure 4.1a.

Which parts of the aeration system that need to be modelled depends on the intended use of the model. Generally, there are three levels: *i)* predicting airflow and improve understanding – only airflow needs to be modelled (Paper III), *ii)* evaluating control strategies and calculating power requirements – the main components of the entire system needs to be modelled (Arnell et al., 2013; Rieger et al., 2006; Alex et al., 2002; Sniders and Laizans, 2006), and *iii)* designing aeration systems including sizing blowers, air distribution, controller tuning, etc. – the whole actual system needs to be included in detail (Beltrán et al., 2013; Crosby et al., 2010). A schematic model structure for an aeration system can be seen in Figure 4.1b. In addition to the model of the physical aeration system it may in some cases be important to add a cost model (i.e. for electrical power). This should reflect the tariffs' construction with time dependency, peak tariffs, etc. (Aymerich et al., 2015). Depending on purpose the approach can vary. For Levels *i* and *ii* it is feasible to use the backwards calculations sketched in Figure 4.1b. For the more complex tasks at Level *iii* a forward modelling approach – better describing the real plant situation, where air is pushed into the reactors – may be required.

4.2 Including an Aeration Model in BSM

The Benchmark Simulation Model (BSM) platform is a generic modelling platform originally developed to compare control strategies on an objective basis. As energy consumption has grown increasingly important, a more detailed aeration model than just the default volumetric mass transfer coefficient (K_La) of oxygen supply, is required (Gernaey et al., 2014). Since the BSM plant layout is a fictive construction intended to be comparable but not identical to any conventional WWTP, designing a full aeration system in detail was not considered meaningful. Consequently, for the purpose of BSM the backwards modelling principle sketched in Figure 4.1 was selected. In this section, the model implemented in BSM and used in parts for Papers III and VI and Arnell et al. (2013) is described.

4.2.1 Oxygen Transfer Model

The consumption of oxygen in the biological reactors is well described by the biokinetic models as a reaction term in the differential equations for aerobic biomass growth. Applying the two-film theory (Whitman, 1962) for mass transfer of oxygen from gas phase to bulk liquid, the oxygen transfer can be calculated by the equation from Lewis and Whitman (1924),

$$\frac{dS_O}{dt} = K_La(S_{O,sat} - S_O) - r_M \tag{4.1}$$

where,

S_O is the dissolved oxygen (DO) concentration in the reactor [g.m^{-3}];
K_La is the volumetric mass transfer coefficient in the liquid phase [d^{-1}];
$S_{O,sat}$ is the saturation concentration for DO in the liquid phase [g.m^{-3}];
r_M is the rate of consumption of oxygen in the system [g.m^{-3}.d^{-1}].

Equation (4.1) can be used to calculate the required K_La to maintain a desired DO concentration. To calculate the airflow required to reach this mass transfer the aeration devices, such as diffusers, sliced tubes or other equipment releasing air in the tanks, need to be considered. Depending on the design – leading to different bubble characteristics – the oxygen transfer rate will be different. The difference depends on the interfacial velocity gradient between the air inside the bubble and the bulk liquid, which increases with bubble size (Rosso et al., 2008). The oxygen transfer efficiency of aeration devices is measured by standardised tests (ASCE, 2007) reporting the efficiency in clean water under standard conditions (STP: 20 °C, DO = 0 g.m^{-3}, atmospheric pressure). This is called standard oxygen transfer efficiency (SOTE, %). SOTE for fine pore diffusers is typically varying with design configuration – i.e. submersion depth and floor coverage – and airflow, see example in

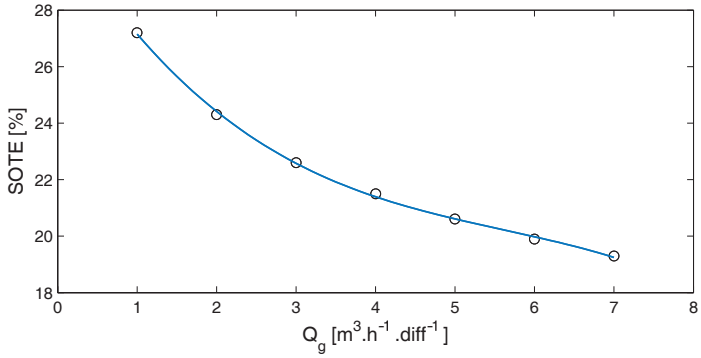

Figure 4.2: Profile over the standard oxygen transfer efficiency (SOTE) for a membrane diffuser disc (black markers) with polynomial fit (blue line) against the airflow through the diffuser (Q_g). Figure from Arnell et al. (2013).

Figure 4.2. Furthermore, the contaminants in wastewater are affecting the oxygen transfer (Rosso and Stenstrom, 2006; Amerlinck et al., 2016). The rate limiting effects of oxygen transfer in wastewater are lumped into the α-factor, which is calculated as:

$$\alpha = \frac{K_{\mathrm{L}}a_{\mathrm{ww}}}{K_{\mathrm{L}}a_{\mathrm{cw}}} \tag{4.2}$$

where $K_{\mathrm{L}}a_{\mathrm{ww}}$ and $K_{\mathrm{L}}a_{\mathrm{cw}}$ are the volumetric oxygen transfer coefficients for wastewater and clean water, respectively (Metcalf and Eddy, 2014). The suppression of oxygen transfer is caused by surfactants, which attach to the bubble as it rises and affect both the bubble size and the oxygen transfer rate. This phenomenon is more pronounced for fine bubble aeration systems since coarse bubbles cause higher turbulence (Rosso and Stenstrom, 2006). The oxygen transfer efficiency for diffused aeration systems is known to deteriorate even further over time. This is due to scaling and fouling of diffusers by biofilms and inorganic salts (in the following referred to as fouling, F). Fouling changes the diffuser's characteristics in terms of bubble size but also increases the pressure drop over the diffuser. The formation of fouling is site-specific but is commonly seen within two years of operation of an aeration system (Kaliman et al., 2008). The salinity of the wastewater also affects the solubility of oxygen, i.e. $S_{\mathrm{O,sat}}$, in relation to clean water as:

$$\beta = \frac{S_{\mathrm{O,sat,ww}}}{S_{\mathrm{O,sat,cw}}} \tag{4.3}$$

where, $S_{\mathrm{O,sat,ww}}$ and $S_{\mathrm{O,sat,cw}}$ are the oxygen saturation concentrations for wastewater and clean water, respectively.

Given specific equipment with corresponding SOTE-profile and process water conditions, the $K_{\mathrm{L}}a$ to airflow, can be calculated. Various expressions have been suggested, from simple empirical input-output relations (Makinia, 2010; Olsson and Newell, 1999; Lindberg, 1997)

over empirical models including selected information about the system (Dold and Fairlamb, 2001; Johnson and McKinney, 1994) to mechanistic models with only physical and measurable system-specific parameters (Beltrán et al., 2013; Metcalf and Eddy, 2014). In Beltrán et al. (2013) the proposed equation is:

$$K_{\mathrm{L}}a = \alpha \cdot F \cdot (\theta^{T-20}) \frac{SOTE_{\mathrm{STP}} \cdot x_{\mathrm{O2}} \cdot M_{\mathrm{O2}} \cdot \rho_{\mathrm{g,STP}}}{V_{\mathrm{L}} \cdot M_{\mathrm{g}} \cdot \delta \cdot S_{\mathrm{O,sat,STP}}} \cdot Q_{\mathrm{g}} \tag{4.4}$$

$$S_{\mathrm{O,sat}} = \tau \cdot \Omega \cdot \beta \cdot \delta \cdot S_{\mathrm{O,sat,STP}} \tag{4.5}$$

where,

α is the oxygen transfer correction factor for wastewater [-];
F is the fouling factor for the diffusers [-];
θ is the temperature correction factor, a value of 1.024 is used [-];
T is the operating temperature [°C];
$SOTE$ is the standard oxygen transfer efficiency as function of submersion depth (h_{sub}) and airflow. Calculated by fitting a polynomial to manufacturer data, Figure 4.2 [-];
x_{O2} is the oxygen mole fraction for dry gas [-];
M_{O2} is the molar mass for oxygen [g.mol^{-1}];
$\rho_{\mathrm{g,STP}}$ is the density of air at standard conditions [g.m^{-3}];
V_{L} is the aerated tank volume [m^3];
M_{g} is the molar mass for air [g.mol^{-1}];
δ is a correction factor for liquid column pressure [-];
$S_{\mathrm{O,sat,STP}}$ is the saturation concentration for DO in the liquid phase at standard conditions [g.m^{-3}];
Q_{g} is the flow rate of air [m^3.d^{-1}];
τ is the correction factor for temperature at the gas-liquid interface [-];
Ω is the correction factor for actual barometric pressure [-];
β is the correction factor for saturation concentration in wastewater [-].

4.2.2 Modelling Air Distribution

If a specific aeration system is of interest (or assumed) it can be piecewise modelled from all its components (Crosby et al., 2010; Beltrán et al., 2011). Referring to Figure 4.1 and assuming that the airflow has been modelled, the whole distribution system to the blower head can be described by Bernoulli's equation, with the pressure losses approximated by the modified Darcy-Weisbach equation (Metcalf and Eddy, 2014). Thereby the pressure losses for every component in the system (pipes, bends, valves and fittings) are summed up and added to the static pressure.

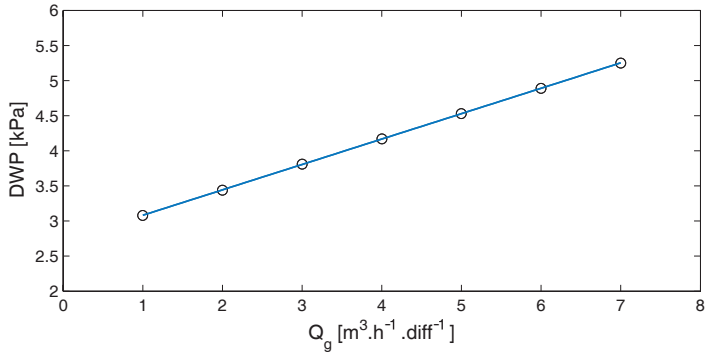

Figure 4.3: Dynamic wet pressure (DWP) profile for a membrane diffuser disc (black markers) and polynomial fit (blue line) against the airflow through the diffuser (Q_g). Figure from Arnell et al. (2013).

For the purpose of the aeration system model in BSM, simplifications of this approach were made. Since a major part of the total pressure drop arises from the aeration device, in order to ensure an even air distribution in the basin – 90 % of the total pressure drop according to USEPA (1989) – the air diffusers are the most important part for an accurate model. That means that the remaining part of the distribution system can be simplified and generalised without losing too much accuracy. Alex et al. (2002) have proposed an approach where the piping, including fittings, etc., are lumped into elements of equivalent resistance. The modelled variables are temperature, pressure and airflow. The most important parts, i.e. blowers, control valves and air diffusers, are still described separately in the model by fitting polynomials to manufacturers' data of pressure drop to airflow. An example for a specific diffuser is shown in Figure 4.3. Only diffusers and blowers have been included in the case studies performed in this work.

4.2.3 Blower Models

There are many types of blowers. The two main types are positive displacement type blowers (PBs) and turbo type blowers (TBs). The main difference between the two types, from a control perspective, is that PBs delivers a constant airflow depending primarily on blower speed and less on head pressure, whereas TBs airflow is highly dependent on head pressure. Apart from that there are also significant differences in characteristics like efficiency (TBs are generally more effective), control range, control options, response time to control actions, etc. Moreover, blowers are often custom designed by manufacturers for clients. Various modelling approaches have been proposed (Amerlinck et al., 2016; Beltrán et al., 2013; Crosby et al., 2010; Alex et al., 2002). The expression from Beltrán et al. (2013) was selected

for implementation in BSM for TBs with low compression ratios,

$$P_{\mathrm{e,TB}} = \frac{\rho_{\mathrm{g,i}} \cdot R \cdot T_{\mathrm{g_i}} \cdot \kappa}{\eta \cdot M_{\mathrm{g,i}} \cdot (\kappa - 1)} \cdot \left[\left(\frac{p_{\mathrm{g,o}}}{p_{\mathrm{g,i}}} \right)^{1-\frac{1}{\kappa}} - 1 \right] \cdot \frac{p_{\mathrm{g,i,STP}} - \phi_{\mathrm{i,STP}} \cdot p_{\mathrm{v,i,STP}}}{p_{\mathrm{g,i}} - \phi_{\mathrm{i}} \cdot p_{\mathrm{v,i}}} \cdot \frac{T_{\mathrm{g,i}}}{T_{\mathrm{g,i,STP}}} \cdot Q_{\mathrm{g,STP}} \quad (4.6)$$

where,

$P_{\mathrm{e,TB}}$ is the total power withdrawal for a TB [W];
p_{g} is the air absolute pressure [Pa];
R is the molar gas constant [Pa.m^3.mol^{-1}.K^{-1}];
T_{g} is the air temperature [K];
κ is the adiabatic coefficient of air [-]; and
η is the overall blower efficiency [-] calculated for each operating point;
subscripts *i* and *o* refer to blower inlet and outlet, respectively; and
remaining variables are defined for Equation (4.4).

The total airflow supplied to the AS reactors is corrected for the blower inlet conditions in the second part of Equation (4.4) where,

$p_{\mathrm{g,i}}$ barometric pressure [Pa];
ϕ is relative humidity [-];
$p_{\mathrm{v,i}}$ vapour pressure [Pa]; and
T temperature [K].

PBs have to be modelled quite differently. Most commercial software packages include some simple model for the power consumption of PBs. All the equations found by the author were empirical to some extent, including the fitting of some relation to manufacturers' data. For the work in Arnell et al. (2013), a PB model based on manufacturers' data (Figure 4.4) with additional efficiency corrections was used,

$$P_{\mathrm{e,PB}} = \frac{P_{\mathrm{e,shaft}}}{\eta_{\mathrm{motor}}\, \eta_{\mathrm{vfd}}} \quad (4.7)$$

where,

$P_{\mathrm{e,PB}}$ is the total power consumption for a PB [kW];
$P_{\mathrm{e,shaft}}$ is the shaft power requirements, from polynomial fit of manufacturers' data in relation to airflow [kWh.d^{-1}];
η_{motor} is the motor efficiency [-];
η_{vfd} is the efficiency of the variable frequency drive [-].

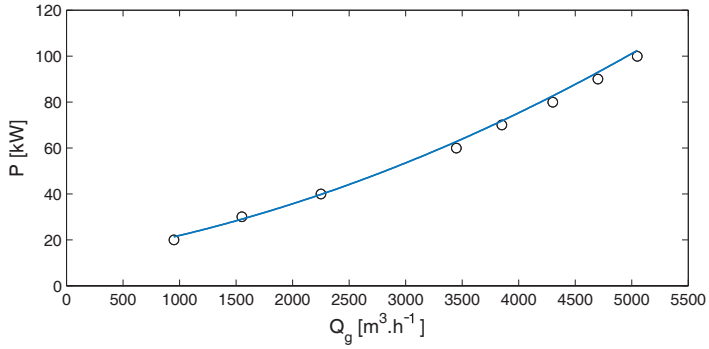

Figure 4.4: Shaft power (P) profile for a lobe rotor positive displacement blower (black markers) with polynomial fit (blue line) against the output airflow from the blower (Q_g). Figure from Arnell et al. (2013).

4.3 Case Studies on Aeration Modelling

The aeration system model described (Section 4.2) was applied in three case studies presented in Paper III. The three WWTPs were Käppala WWTP, Lidingö, Sweden (WWTP 1), Ekeby WWTP, Eskilstuna, Sweden (WWTP 2) and Linköping WWTP, Linköping, Sweden (WWTP 3). Key data on plant loads, dimensions and aeration system designs are given in Paper III, Table 1. The overall results on calibrated airflows are given in Paper III, Figure 3 and Table 2. In the following three subsections, some details from the three case studies are presented together with selected results and discussion of key aspects related to the aeration model. It should be made clear that the aeration system modelling was integrated in a larger water-train or plant-wide model in all three cases. The main objective of the models was generally not to specifically evaluate the aeration system but rather general treatment efficiency related questions.

4.3.1 Käppala WWTP

The main purpose of the Käppala WWTP case study was to implement and evaluate the full modelling tool developed in this project and presented in Paper VI (see Chapter 6 and Paper VI for plant layout and details on the plant-wide model). In the following section, the details of the aeration systems modelling from Paper III will be discussed.

The AS unit at Käppala was designed in five parallel lines with identical design and common pumping of return activated sludge (RAS). The DO control in the five lines differed as line one to three had a controller design providing a tapered and decreasing airflow along the aerated zones based on two DO measurements (Åmand, 2014). Lines four and five were upgraded with an ammonium feed-back control. The strategy was based on individual DO

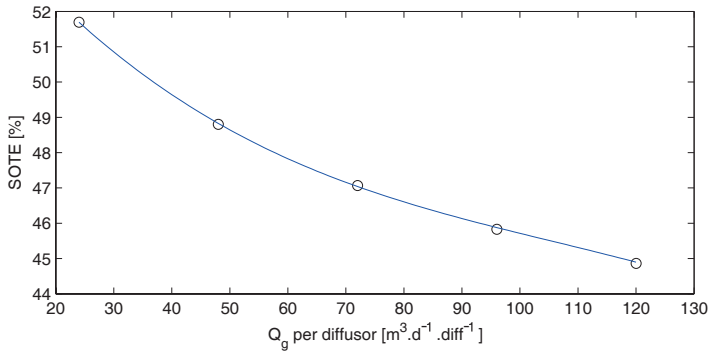

Figure 4.5: Profile over the standard oxygen transfer efficiency (SOTE) for the aerators used at Käppala WWTP (black markers) with polynomial fit (blue line) against the airflow through the diffuser (Q_g). Part of figure from Paper III.

measurements in the four aerated reactors in each activated sludge line and measurements of effluent NH_4-N after the secondary settlers. An upgrade of all lines to the ammonium feed-back control was planned and the load was assumed equal to all lines. Consequently, the five AS reactors were for the purpose of this project modelled as one and the ammonium feed-back control was applied for the entire activated sludge system. Fine pore diffusers (Sanitaire Silver Series II) for aeration of swing- and aerated zones are mounted at the bottom of the quite deep, 10 m, AS reactors. Basic data on the plant and aeration system is given in Paper III, Table 1.

For the purpose of the modelling study, only the oxygen transfer was modelled for Käppala WWTP using Equations (4.1), (4.4) and (4.5). A 3rd degree polynomial was fitted to the SOTE profile for the diffusers, Figure 4.5. No off-gas measurements were available for estimating actual α or fouling factors. The combined αF was – after consultation with the diffuser manufacturer – assumed to be 0.8. The distribution system was not modelled in this case and the specific aeration power consumption was calculated using a static case-specific factor of 0.025 kWh.Nm^{-3} (Arnell et al., 2016b). The resulting airflow profile is shown in Figure 4.6. On an average the fit of the total airflow to data was acceptable for the purpose of the model. The deviation was 4.4 %, which was the best out of the three case studies in Paper III. Looking at a 7-day profile (Figure 4.6, right), the behaviour matches well the real plant (see Paper II for goodness of fit estimates). It is evident from the full-year simulation results (Figure 4.6, left) that the simulated airflow is smoother than the data. This may be explained by the fact that the real plant only has the advanced ammonium feed-back DO control with four DO sensors in two out of five parallel lines. In the model, ammonium feed-back control was used for the whole volume.

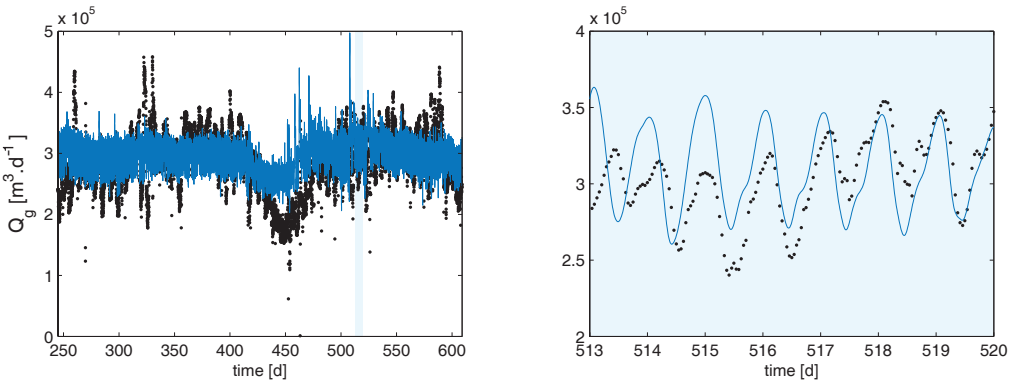

Figure 4.6: Total airflow (Q_g) at Käppala WWTP. Full-year simulation (left) and 7-day selection (right). Data (black markers) and model fit (blue line). The time represents simulation days, where 245 corresponds to 1st January and 513 corresponds to 24th October. Part of Figure 3, Paper III.

4.3.2 Eskilstuna WWTP

The water utility *Eskilstuna Strängnäs Energi och Miljö* ordered a modelling study to evaluate alternatives for improved nitrogen removal at the Ekeby WWTP in Eskilstuna, Sweden. Independent from this, according to the maintenance plan, a renewal of the diffusers in the AS reactors were at the time for the project already contracted. The existing diffusers Nopon PIK 300 were to be changed to Atek iDISC 260. Therefore, as an additional part of the modelling project, the aeration model implemented in BSM was used to simulate the performance of the two diffuser installations. These results have not been publicly published before.

The modelled plant layout of the water train of Ekeby WWTP is shown in Figure 4.7 (top). The three parallel activated sludge reactors are very long and narrow and show a pronounced plug-flow behaviour, Figure 4.7 (bottom). Investigating the hydraulics applying the principles of Fujie et al. (1983) indicated that no less than 34 tanks in series were required to describe the hydraulic behaviour. Even if less reactors would probably have been sufficient for the purpose of the model, this number quite well suited the physical sectioning of the tanks and was therefore used. The aeration system is a fine pore bottom aeration system with circular discs and rubber membranes. The diffusers are evenly distributed in four sections with a tapered and decreasing diffuser density along the reactor length. Furthermore, the final anoxic zones have diffusers and are used as swing zones during the cold season, with a constant airflow. The diffusers are supplied with air from two turbo-type blowers in parallel. The DO in the four aerated zones are controlled by two PI-controllers. The first controller manipulates the airflow to the first two zones based on measurements of DO about ¼ into the aerated zones and the second manipulates the airflow to the two final

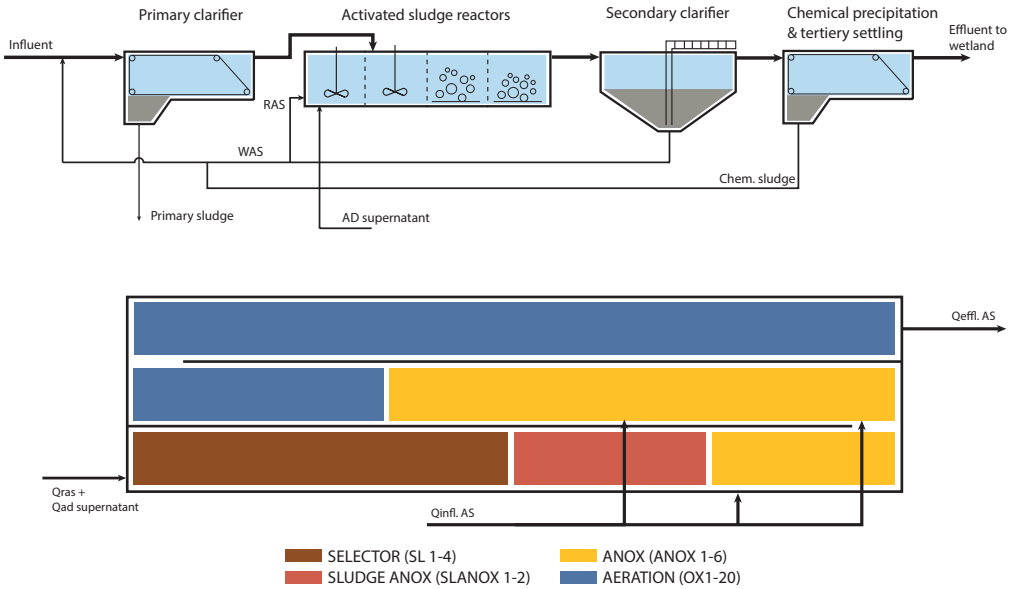

Figure 4.7: Plant layout for Ekeby wastewater treatment plant. Water train treatment process (top) and activated sludge reactor configuration (bottom). One of three parallel three-pass reactors.

zones based on DO measurements just prior to the effluent of the activated sludge reactor. The set-point for the first DO controller is 2.25 $g.m^{-3}$ and for the second 2.5 $g.m^{-3}$. For the purpose of comparing performance of the two different diffuser installations only the oxygen transfer model, Equation (4.4), was used. The SOTE curves for the two diffusers were retrieved from the manufacturers and 3rd degree polynomials were fitted to the data. Figure 2 in Paper III (middle) exemplifies the SOTE curve for the Nopon membranes. The SOTE for the Atek iDISC 260 is about 2 % higher at the same depth and diffuser density.

At the time when the nutrient removal process, using a selector for treating the AD supernatant, was designed and built at Ekeby WWTP the α values were measured. The results turned out higher than for conventional Ludzack-Ettinger configurations, which is coherent with later work by Rosso et al. (2008). No recent measurements were available and considering the quite aged aeration system a lumped αF factor was assumed. According to theory in the cited work the α should increase along the reactor and a tapered setting of αF along the model reactors were used, i.e. [0.5, 0.4, 0.6, 0.85, 0.95] from swing zones and though the aerated zones. For the new diffusers the lower values were assumed to be 20 % higher in absence of fouling effects, i.e. [0.6, 0.48, 0.72, 0.85, 0.95].

Simulation results for the two diffuser installations are shown in Figures 4.8 to 4.10. The required airflows to reach the DO set-points are about 25 % lower for the new Atek diffusers compared to the old Nopon membranes, Figure 4.8. Since the DO concentration is

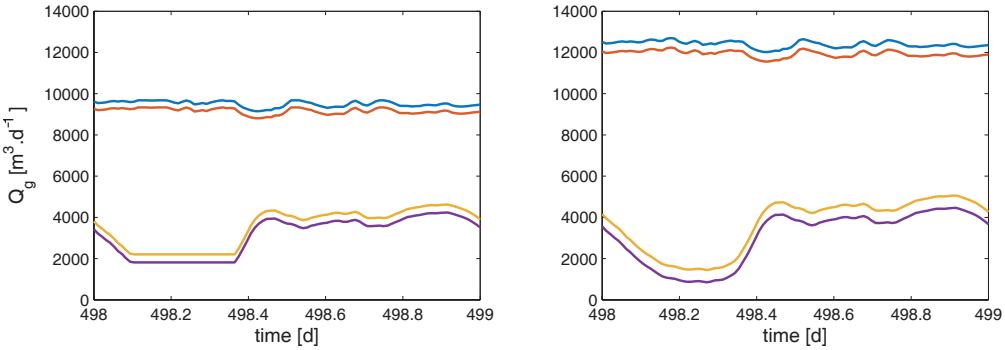

Figure 4.8: Simulated airflows (Q_g) in the aerated reactors for the two diffuser types: Atek iDISC IDA-260 (left) and Nopon PIK 300 (right). Lines represent dissolved oxygen concentration in model reactor OX 1-5 (blue), OX 6-10 (red), OX 11-15 (yellow), OX 16-20 (purple). The time represents simulation days, where 498 corresponds to 10th October.

controlled this makes little difference on the simulated S_O concentration (Figure 4.9) but saves energy. This saving is related to the slightly higher SOTE for the Atek membrane but even more to the assumed fouling of the Nopon diffusers. However, fouling will in due time also show on any new diffusers (Kaliman et al., 2008). A result affecting the treatment efficiency is that the higher simulated aeration efficiency for the Atek diffusers gives significantly higher DO concentration in the swing zones when aerated during winter, Figure 4.10.

The calibration of the airflow to available daily averages reported in Paper III, Figure 3 and Table 2, was successful for the intended purpose of the model. However, the plant is affected by events of severe nitrification failure during winter that the model was not capable of capturing. This is not a shortfall of the aeration model but rather the AS model set-up and ASM1 implementation.

4.3.3 Linköping WWTP

The Linköping WWTP operated by *Tekniska Verken in Linköping* were facing new stricter effluent requirements and a forecasted load increase. A modelling project was conducted to investigate possible changes of the control and configuration of the processes for improved nitrogen removal and possible expansion with another AS block to cope with the higher load.

A plant-wide model was built, Figure 4.11. There were three parallel AS blocks at the plant, all with individual secondary clarifiers and sludge systems. Since the blocks had different loads, reactor sizes and dimensions, they were modelled separately. However, the parallel lines within each block (eight in total) were modelled as one. All three blocks had sub-

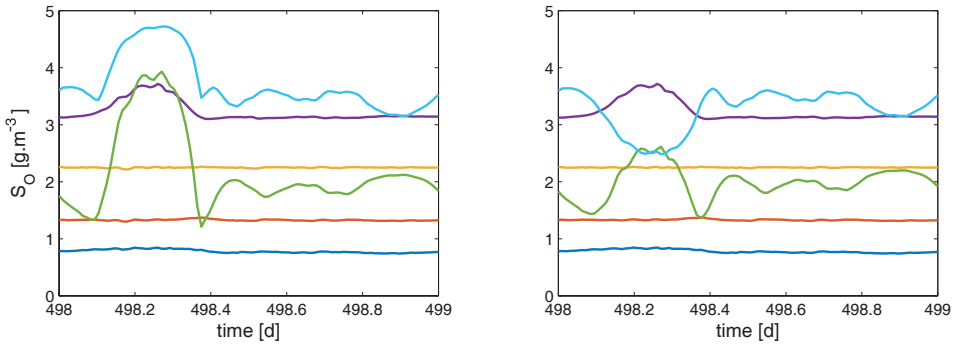

Figure 4.9: Simulated dissolved oxygen concentrations (S_O) in the AS reactors for the two diffuser types: Atek iDISC IDA-260 (left) and Nopon PIK 300 (right). Lines represent DO in model reactor OX 1 (blue), OX 3 (red), OX 6 (yellow), OX 10 (purple), OX 15 (green), OX 20 (light blue). The time represents simulation days, where 282 corresponds to 10th October.

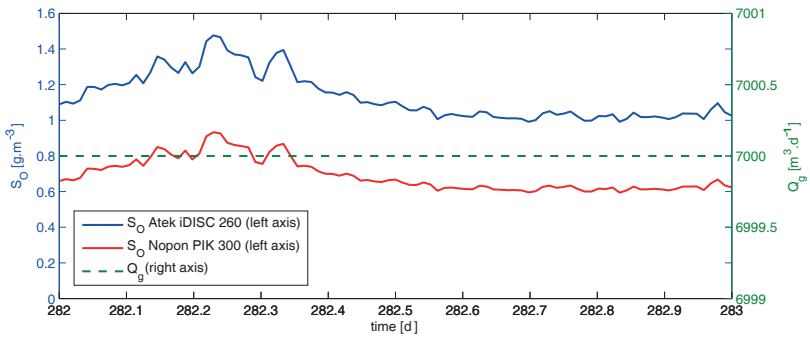

Figure 4.10: Modelled dissolved oxygen concentrations (S_O) near the end of the anoxic swing zones during an aerated period during winter. A constant airflow (Q_g, green, right y-axis) is resulting in different S_O for the two diffusers Atek (blue, left y-axis) and Nopon (red, left y-axis). The time represents simulation days, where 498 corresponds to 6th February.

merged fine pore aeration with circular membrane discs, Sanitaire Silver Series II diffusers. The three AS blocks were supplied with air from five lobe-rotor (PB type) blowers. Due to varying depth between the AS blocks the air supply system was split into two pressure zones. For DO control each AS line was split in two legs (natural partitioning since the tanks were U-shaped). A cascade controller design featured firstly PI controllers manipulating air-supply valve position based on DO measurements in each reactor (individual DO measurements about ¾ into the reactor) and, secondly, controllers manipulating blower speed based on in-line pressure. On top of that an over-arching control manipulated the DO set-point based on measurements of NH_4-N and NO_3-N at the end of two master-lines. This facilitated both intermittent aeration allowing for denitrification and nitrification in-

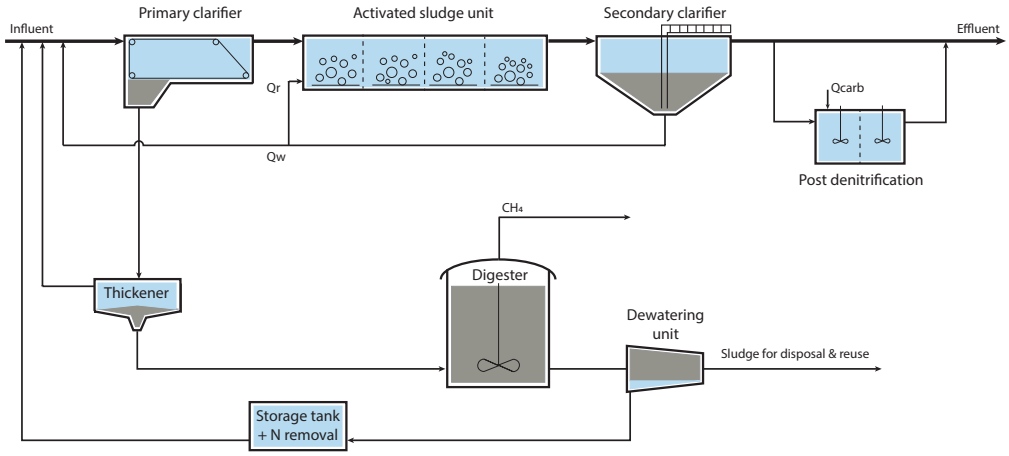

Figure 4.11: Plant layout for the Linköping wastewater treatment plant model.

termittently based on actual load and a variable DO set-point during aerated periods based on NH_4-N concentration (Rosen and Arnell, 2007).

The plant-wide model was developed in steps as the aim of the modelling evolved. In the first step, the standard BSM2 influent profile was used as basis for the influent characterisation. This since no data was available for short-term (hour, day, week) calibration; the model was rather calibrated on annual and seasonal averages. All three components of the aeration system were modelled, following the principles outlined in Section 4.2. The oxygen transfer rate was modelled by Equations (4.1), (4.4) and (4.5) by fitting 3rd degree polynomials to SOTE data from the manufacturer of the diffusers. This was done independently for the activated sludge blocks with different depths, see example in Paper III, Figure 2. The pressure in the air distribution system was also modelled. A linear model was fitted to data for the dynamic wet pressure of the diffusers, Figure 4.3. Together with the static head pressure – according to the submersion depth – the aeration system pressure was in agreement with data (not shown). This means that the aeration system design is consistent with the recommendations in USEPA (1989), i.e. the diffusers make up the major part of the pressure total drop in the system. Pressure drops in pipings and valves were not modelled. Given the fact that PBs were used, the modelled pressure in the air distribution system was not used. The blower station was instead modelled using Equation (4.7) and the polynomial fit is shown in Figure 4.4. The five blowers were modelled individually and a look-up table principle was used to mimic the plant strategy for stepwise changing the number of operating blowers in the two pressure zones.

Figure 4.12 shows the simulated concentration profiles for DO, NH_4-N and NO_3-N in one of the AS reactors for one day. One of the key findings at this stage of the plant modelling

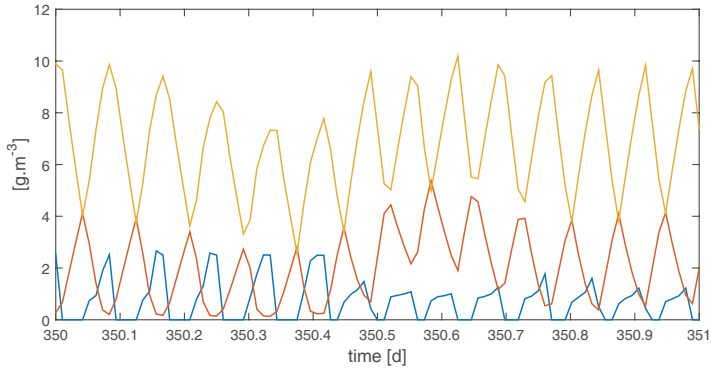

Figure 4.12: Concentrations of dissolved oxygen (blue), NH_4-N (red) and NO_3-N (yellow) at the end of activated sludge block no. 1. The time represents simulation days, where 350 corresponds to 13th October.

was that the periodic DO dips, seen in the second half of Figure 4.12, could be explained by limitations in the air supply. This was something the plant operators had not been able to explain without the simulation results. This insight initiated an up-grade of the aeration system at the plant.

Simulations were performed to compare three aeration control strategies:

i. the default control regime based on intermittent aeration and ammonium/nitrate feedback;

ii. constant aeration with DO control; and

iii. constant aeration using ammonium feedback control according to Åmand et al. (2013).

The results in Figure 4.13 and Table 4.1 – also presented in Arnell et al. (2013) – show that Strategy *iii* is the most favourable one with respect to energy consumption and overall effluent quality, measured as EQI. The energy use for Strategy *iii* is only 71 % of that for Strategy *i*. Moreover, the effluent NH_4-N is 1.3 g.m^{-3} compared to 3.2 g.m^{-3} for the default strategy. Evaluating effluent NH_4-N Strategy *ii* is actually best since the NH_4-N set-point for Strategy *iii* was set to 2.5 g.m^{-3}. However, taking into consideration that the permit allows for 3.5 g.m^{-3} effluent NH_4-N but only 10 g.m^{-3} TN means that Strategy *i* solely manages the TN limit by utilising the redundant volumes from the elevated NH_4-N concentration in the best way for denitrification. However, the effluent TN is close to 10 g.m^{-3} also for Strategy *iii* and it cannot be excluded that this strategy could be further optimised to manage the effluent standards.

In a further investigation, the model was upgraded with an influent characterisation using the real plant influent profile, following the principles outlined in Åmand et al. (2016). This

Table 4.1: Simulation results for three control strategies for the aeration of the activated sludge reactors at Linköping WWTP. Strategy *i* is intermittent aeration with ammonium and nitrate feedback, Strategy *ii* is fixed set-point DO control and Strategy *iii* is ammonium feedback control (Arnell et al., 2013).

Evaluation Criteria\Control Strategy	*i*	*ii*	*iii*
NH_4-N [g.m^{-3}]	3.2	0.71	1.3
TN [g.m^{-3}]	8.9	17.3	10.4
EQI [kg pollutant.d^{-1}]	12 300	13 900	11 200
Aeration energy [kWh.d^{-1}]	5 300	5 200	3 800

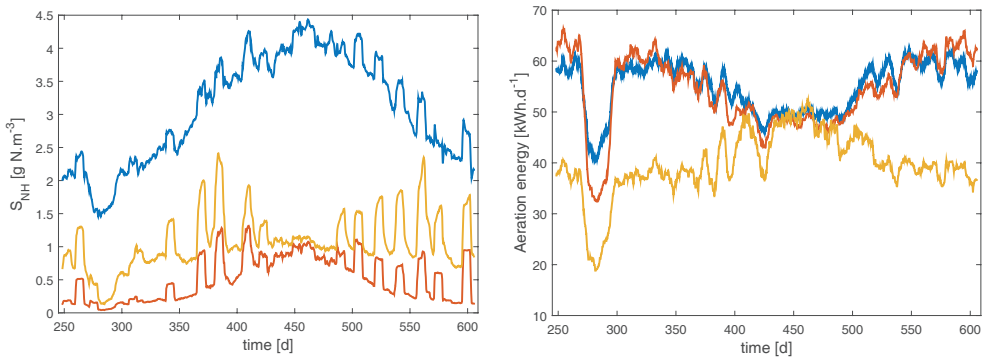

Figure 4.13: Simulation results for the three evaluated control strategies: Intermittent aeration (blue line); fixed set-point dissolved oxygen control (red); and ammonium feedback control (yellow). Effluent ammonium (left) and aeration energy consumption (right). The time represents simulation days, where 245 corresponds to 1st July.

allows for comparison with plant data on a short-term basis. Results are presented in Paper III, Figure 3 and Table 2.

4.4 Summary of Key Findings

» A model structure with backwards calculation of the quantities in the aeration system was found to be appropriate. Relationships for the various parts, from oxygen transfer to blowers, were selected and implemented in the Benchmark Simulation Model platform.

» The model was tested in three real plant case studies. It proved to be simple and robust. Acceptable accuracy were reached for all three cases by simple adjustments of mainly polynomials for the standard oxygen transfer efficiency and airflow limitations. Limiting the air supply to actual values was shown to be critical in dynamic simulations.

» The results emphasise the importance of modelling the aeration system beyond just input of the volumetric mass transfer coefficient (K_La) for oxygen. Airflow is a crit-

ical variable for evaluating air consumption, aeration energy consumption and for communicating simulation results to utility staff. Including a blower model allows for assessing dynamics in power consumption.

Chapter 5

Modelling Anaerobic Co-Digestion in Plant-Wide Models

This chapter addresses the energy recovery at wastewater treatment plants through anaerobic digestion. Co-digestion of sewage sludge together with other organic substrates is an emerging practice, which needs to be included in versatile modelling tools. The implementation of co-digestion in Benchmark Simulation Model no. 2 is described along with methods for estimation of substrate dependent parameters and characterisation of substrate in model state variables. Results from the simulation studies in Papers IV *and* V *are briefly presented.*

5.1 Energy Recovery Through Anaerobic Digestion

Apart from optimising the major energy consuming processes at wastewater treatment plants (WWTPs), the key to an improved energy balance at treatment plants is to recover energy from the influent wastewater. As described in Section 2.2, the influent wastewater contains energy primarily in three forms: thermal, calorific in organic compounds and calorific in inorganic compounds. Recovering energy from organics through anaerobic digestion (AD) of internal sludges – such as primary and secondary (waste activated) sludges – is the most applied option in practice. Several studies have reported that production of biogas (the raw gas from digesters) containing energy-rich biomethane provides an opportunity for WWTPs to become energy neutral (Gao et al., 2014; Frijns et al., 2012; Hofman et al., 2011; Jenicek et al., 2012). This fact have increased the interest in optimising the digestion process for increased biogas production (Strömberg, 2015; Lingsten, 2014; Jenicek et al., 2012). If capacity is available there is an opportunity to further increase the gas production by adding external or internal organic substrates (called co-substrate) directly to

the digester. The organic matter in the co-substrate is partially degraded in the AD process and converted to biogas. However, in the degradation also nutrients are mobilised and recirculated to the water train via AD supernatant. Typically this internal load – if not treated separately – makes up 10 to 20 % of the influent total nitrogen (TN) to a WWTP. At WWTPs without chemical precipitation, i.e. Bio-P plants, also total phosphorus (TP) is mineralised and recirculated. Therefore, one of the key factors for succeeding with anaerobic co-digestion (AcoD) is to select suitable co-substrates and a good feed strategy (Nordell and Wiberg, 2013). Co-substrate characteristics and applicability have been extensively reviewed by Mata-Alvarez et al. (2014). Ideally, co-substrates have a high methane potential, minimum impact on residual solids production and a nutrient composition suitably balanced for the host WWTP (Nordell and Wiberg, 2013). Generally, this means that co-substrate characteristics will differ from those of WWTP sludges in terms of composition and degradation kinetics. While there are a large number of potential co-substrates suitable for digestion at WWTPs, local substrate availability and transport costs will constrain the options for individual plants.

Many digestion facilities at WWTPs are under-utilised. Commonly, the organic loading rate (OLR) is well below what is known to be feasible and the dilute sludge feed occupies unnecessary large volumes (Lundkvist, 2005). However, the current operations can with proven measures, such as thickening of feed sludge, improved mixing and stable heating, be optimised (Thunberg et al., 2013; Jenicek et al., 2012). Such measures not only improve the digester stability but usually increase the hydraulic retention time (HRT) in the reactor. If, which is usually the case for mesophilic ADs, the HRT is above approximately 25 days the digester can be considered to have redundant volumes. With low OLR and redundant volume, a utility can utilise this resource by applying anaerobic co-digestion (AcoD) (Batstone and Virdis, 2014; Mata-Alvarez et al., 2014). Co-digestion is defined as digestion of co-substrates together with the primary substrate, which at WWTPs are the internal sludges. Co-substrates can be internal, such as fat from grease traps, or external, such as food industry wastes or other non-polluted organic wastes (Mata-Alvarez et al., 2014, 2011). In many parts of the world AcoD is an emerging practice (Lingsten, 2014; Mata-Alvarez et al., 2014).

5.1.1 Digestion Modelling in BSM2

The digester in Benchmark Simulation model no. 2 (BSM2) is a traditional continuously stirred tank reactor with a volume of 3 500 m^3 (3 400 m^3 liquid volume). The default operational strategy gives a hydraulic retention time of about 19 days. Temperature compensation of model parameters are fully implemented according to Batstone et al. (2002), which means that the digester model could be operated in the entire mesophilic range without

recalculating parameter values. As default the AD operates at mesophilic temperature of 35 °C. With parameter adjustments modelling of thermophilic digestion is also possible.

In the original Anaerobic Digestion Model no. 1 (ADM1), particulate substrate is fed to the digester model as particulate composite material (X_c). This acts as a pool for all particulate organic material including dead biomass. The first process of ADM1 is the disintegration step, describing the breakdown of X_c into carbohydrates (X_{ch}), proteins (X_{pr}), lipids (X_{li}) and inerts (X_I). This step was included to model the extracellular and non-biological processes, like lysis and decomposition of complex materials. The disintegration is modelled by first-order kinetics dividing X_c into X_{ch} (30 %), X_{pr} (30 %), X_{li} (30 %) and X_I (10 %). The second process of ADM1 is hydrolysis of X_{ch}, X_{pr} and X_{li} into small soluble compounds, i.e. monosaccharides (S_{su}), amino acids (S_{aa}) and long chain fatty acids (LCFA, S_{fa}). This is also modelled by first-order kinetics with individual rate parameters. This model formulation has a few implications, One is that all material pooled into X_c will have the same stoichiometric composition with regards to X_{ch}, X_{pr}, X_{li} and X_I, dead biomass included. Another one is that placing two reactions with first-order kinetics after one another means that the slower reaction will become rate limiting.

The implementation of ADM1 in BSM2 is consistent with the original description by Batstone et al. (2002) to a great extent (Arnell et al., 2016a; Arnell and Åmand, 2014). One significant exception is, however, the degradation of particulate substrates in the digester. An interface is needed to convert the ASM1 state variables into the corresponding ADM1 ditto (Nopens et al., 2009). In the interface, all COD in the feed are converted directly into X_{ch}, X_{pr}, X_{li} and X_I rather than X_c. This allows for an adapted composition depending on substrate and separates feed from dead biomass. The disintegration step is kept only for dead biomass. However, since the disintegration step is rate limiting with the default ADM1 parameters, the hydrolysis rate coefficients need to be adjusted accordingly to get a realistic degradation rate. This adjustment is not done in the standard BSM2 parameterisation, leading to a too effective digestion process, which overestimates capacity and gas production in the digester. In the present work, estimation of hydrolysis rate coefficients from many batch experiments on various sludges and substrates have been made, presented in Paper IV and Arnell and Åmand (2014). A suggestion for an updated default hydrolysis rate coefficient of mixed sludge is presented.

Not many studies on integration of AcoD in plant-wide wastewater treatment plant models have been presented (Razaviarani and Buchanan, 2015). Key aspects of such a model is flexibility to model common substrates and feed strategies, ability to evaluate both energy recovery and plant-wide effects on the treatment plant and compatibility with practical characterisation procedures.

5.1.2 Modelling Anaerobic Co-Digestion

There are several studies on modelling of anaerobic co-digestion at stand-alone digestion systems using ADM1, based on various approaches. The task includes both substrate characterisation and integration of multiple substrates in the model feed. The simplest approach is to characterise the actual feed mix, composed of an arbitrary number of substrates, to get the stoichiometric composition of X_c, i.e. fractions of X_c for X_{ch}, X_{pr}, X_{li} and X_I (Derbal et al., 2009). This is successful in terms of model prediction but leads to a static model since the substrate mix cannot be varied without repeating the characterisation process, i.e. only simulations with static model inputs are possible. To increase flexibility, Esposito et al. (2008) and Galí et al. (2009) suggest some modifications of ADM1. They implement multiple pools of X_c with individual stoichiometry and degradation kinetics to which specific substrates are associated. This allows for dynamic model inputs but code adjustments are required each time the number of substrates is to be altered.

The most general and flexible method for including AcoD in ADM1, is the general integrated solid waste co-digestion (GISCOD) model (Zaher et al., 2009). Unlike the above examples, this approach uses the ADM1 formulation of BSM2, i.e. feeding particulate substrates as X_{ch}, X_{pr}, X_{li} and X_I, and using X_c only for biomass decay. To keep the hydrolysis for different substrates apart, the GISCOD model virtually separates the hydrolysis step from the remaining processes of ADM1, further explained in Section 5.4. This makes the model flexible for dynamic feeds and easy to adapt when varying the number of substrates.

5.2 Substrate Characterisation

One of the most important aspects for a successful modelling project is characterisation of the substrate feed. In the characterisation both the substrate-dependent biokinetic parameters of the model must be identified, and organic and nitrogen content of the substrates be fractioned into the 26 state variables of ADM1. Since the ADM1 model was published in 2002 several methods for fractionation of substrate COD and TN have been suggested in literature (Kleerebezem and van Loosdrecht, 2006; Zaher et al., 2009; Nopens et al., 2009; Girault et al., 2012; Astals et al., 2013; Jimenez et al., 2015). While some of these methods are comprehensive and provide a detailed feed characterisation, they are also complicated and include analytical methods not commonly used in AD testing. The problem of input characterisation remains a major challenge, as identified in a recent key review of AD modelling, particularly for mixed digesters (Batstone et al., 2015). The feasibility of a characterisation method for engineering purposes is determined by simplicity, transparency, affordability and fit for purpose accuracy.

In Paper V, a detailed method for substrate characterisation is proposed. An input model in two steps was developed to apply AcoD in BSM2 and plant-wide models in general. The input modelling methodology is divided in two steps:

i. a method to estimate the biodegradable part of COD (f_{d}, fully correlating to the maximum biomethane potential, B_0) and the substrate dependent model parameters, i.e. the hydrolysis parameters ($k_{\mathrm{hyd,i}}$) for particulate matter;

ii. a scheme for fractionation of COD and TN into the classification of ADM1 state variables, based on the estimated f_{d} and basic physico-chemical data of the substrate.

5.2.1 Estimation of Substrate Dependent Parameters

Provided the modification of ADM1 in BSM2 – substrate fed as macro molecules rather than composite material – the most important substrate-dependent parameters are the hydrolysis rate coefficients ($k_{\mathrm{hyd,i}}$) for X_{ch}, X_{pr} and X_{li}. The model allows for differentiated hydrolysis rate coefficients for the different molecules but a lumped value is commonly used (Batstone et al., 2009). In the present work, three different methods / models have been evaluated and compared.

The hydrolysis rate for a substrate can be estimated from batch digestion tests, so called biomethane potential (BMP) tests. In a BMP test, the substrate is degraded with excess of inoculum and the produced biogas- and biomethane volumes are measured. The cumulative production curve retrieved is used to calculate the parameters B_0, f_{d} and k_{hyd} (Angelidaki et al., 2009). These parameters are estimated simultaneously by fitting a model to data, using an optimisation routine. In the present work, three different models have been evaluated for estimating B_0 [ml CH_4.g VS $^{-1}$] and k_{hyd} [d^{-1}]. In Paper IV, the following first-order function (Angelidaki et al., 2009; Jensen et al., 2011),

$$B(t) = B_0 \cdot (1 - e^{-k_{\mathrm{hyd}} \cdot t}) \tag{5.1}$$

where B [ml CH_4.g VS $^{-1}$] is the biomethane production at time t [d], is compared to a Monod-type function proposed by Koch and Drewes (2014),

$$B(t) = \frac{F_0 \cdot G \cdot k_{\mathrm{hyd}} \cdot t}{1 + k_{\mathrm{hyd}} \cdot t} \tag{5.2}$$

where, $F_0 \cdot G$ [ml CH_4.g VS $^{-1}$] is the amount of degradable particulate matter at the beginning of the test converted to volume of CH_4. This can be interpreted as the ultimate methane yield of the substrate added but values differ from B_0 in Equation (5.1).

As can be seen in Figure 5.1, the two models differ in their principal behaviour. The first-order function reaches a maximum gas production and the rate coefficient, k_{hyd}, is corresponding to the time constant of the model, meaning the time it takes for the gas production

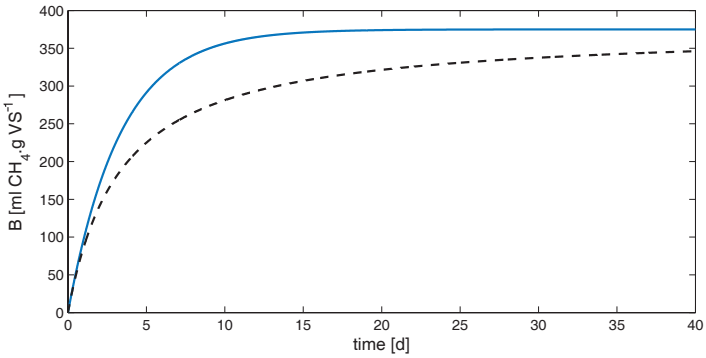

Figure 5.1: Examples of model outputs for the first-order function (Equation 5.1), blue line) and the Monod-type function (Equation 5.2), black dashed line). Figure from Paper IV.

to reach 63 % of B_0. Equation (5.2), on the other hand, continues to increase and does not reach a maximum within the stop time of the BMP test and rather $1/k_{\mathrm{hyd}}$ is interpreted as the half-saturation value, that is the time it takes to reach 50 % of $F_0 \cdot G$.

The optimal parameter values were found using an optimisation routine adjusting k_{hyd} and B_0 or $F_0 \cdot G$ according to a selected cost function. The original publications for the models, Angelidaki et al. (2009) and Koch and Drewes (2014), both linearise the respective models and use linear optimisation. The optimisation procedure is thereby simplified. However, the linearisation is also known to increase the errors in the low range of the dataset. The straightforward method for non-linear models is instead to use non-linear optimisation. In Paper IV, the optimisation was performed in MATLAB using the function `fminsearch`, which runs a simplex search algorithm (Nelder and Mead, 1965). For the optimisation a cost function is needed. The cost function measures the error between the model output ($f(x)$) and data (n data points y), which is to be minimised. The most common cost function is the sum of squared errors (SSE),

$$\mathrm{SSE} = \sum_{i=1}^{n} \Big(y(i) - f(x(i)) \Big)^2 \tag{5.3}$$

Other alternatives have been proposed. In the work by Koch and Drewes (2014), the sum of absolute errors was used with the motivation that it is less sensitive to outliers, which otherwise have a large impact when squared as in SSE. Outliers in the low range of measured data is potentially a problem with the linearised version of Equation (5.2) used by Koch and Drewes (2014) since the reciprocal values, $1/t$ and $1/B_0$, are part of the linearised equation amplifying small values. However, optimisation with the sum of absolute errors is more likely to result in several minima and for the solution to be unstable than with SSE. In Paper IV, the two cost functions were evaluated for both models and results compared. Uncertainty analysis was performed based on the Frequentist's approach using

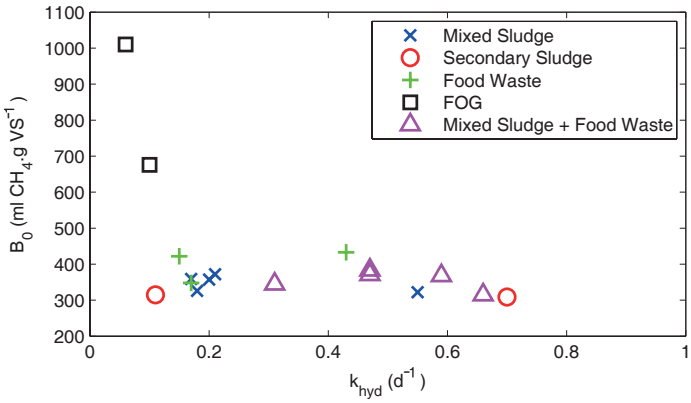

Figure 5.2: The outputs B_0 and k_{hyd} for the 18 data sets using the first-order function model, Equation (5.1). Figure from Paper IV.

the Maximum Likelihood Estimate (Nocedal and Wright, 2006) to calculate the covariance of the two parameters and confidence bounds for the estimates. More information on the uncertainty analysis is provided in Paper IV and Arnell and Åmand (2014).

For the model evaluation 18 data sets were collected of BMP tests from Swedish and German universities and Swedish WWTPs. The substrates were secondary sludge, mixed sludge, food waste, vegetable waste and "fat, oil and grease" (FOG). More information about the data sets is presented in Paper IV, Table 2.

The resulting parameter estimates are visualised in Figure 5.2. The hydrolysis coefficient estimated with Equation (5.1) ranged from 0.08 to 0.70 d^{-1}. The range for B_0 was 315 to 1010 ml CH_4.g VS^{-1}. This is in the same range as reported elsewhere (Batstone et al., 2009). From the detailed results in Paper IV – comparing both models using the two cost functions with a thorough uncertainty analysis – it was concluded that the first-order function (Equation 5.1) with SSE outperformed the Monod-type function and sum of absolute errors in all combinations for almost all data sets.

In Paper V, estimations of B_0 and k_{hyd} were also performed from BMP test data. In this work, the full ADM1 model was used to model the dynamic response of the BMP tests. Using the full model provides more realistic estimates if the same model is to be used for implementing the parameters in subsequent simulations. Moreover, using the ADM1 model allows for including the effect of inhibition that some substrates exhibit in mono-substrate BMP tests. In Paper V, a novel inhibition function (I_{fa}) was implemented for inhibition by LCFA (S_{fa}) on acetate (S_{ac}) uptake, as:

$$I_{\mathrm{fa}} := \begin{cases} e^{-2.77259((S_{\mathrm{fa}}-K_{\mathrm{I,fa,low}})/(K_{\mathrm{I,fa,high}}-K_{\mathrm{I,fa,low}}))^2} & \text{for } S_{\mathrm{fa}} > K_{\mathrm{I,fa,low}} \\ 1 & \text{for } S_{\mathrm{fa}} \leqslant K_{\mathrm{I,fa,low}} \end{cases} \tag{5.4}$$

Table 5.1: Resulting parameter estimates for three slaughterhouse wastes in Paper v.

Parameter \ Substrate	Paunch	Blood	DAF
B_0 [ml CH_4.g VS $^{-1}$]	299	520	1044
k_{hyd} [d^{-1}]	0.125	0.310	0.103
$K_{I,fa,low}$ [kg COD.m^{-3}]	–	–	0.406
$K_{I,fa,high}$ [kg COD.m^{-3}]	–	–	0.714

The function has two additional parameters ($K_{I,fa,low}$ and $K_{I,fa,high}$) to be estimated for substrates rich on lipids. The parameter estimation was performed in MATLAB using the function `lsqcurvefit` parametrised to use a Levenberg-Marquardt optimisation algorithm (Nocedal and Wright, 2006). The method was applied to three fractions of slaughterhouse waste: paunch, blood and dissolved air flotation (DAF) sludge, each rich on carbohydrates, protein and fat, respectively. The resulting parameters are shown in Table 5.1. The simulated and measured BMP profiles are displayed in Paper v, Figure 3. The fit to data is good for paunch and blood, while it is less accurate for DAF sludge. Thanks to the novel inhibition function for LCFA, the model captures the main process impacts due to LCFA inhibition. This motivates the use of the more complex ADM1 model for parameter estimation in this case.

5.2.2 Substrate Fractionation

Following the first step of the characterisation procedure – parameter estimation – the substrate COD and TN need to be fractionated into the state variables of ADM1. For the most influential state variables – considering relevant output variables, such as gas production, volatile solids (VS) destruction and digestate composition – a sensitivity analysis was performed, see Section 5.3 below.

The fractionation procedure is illustrated in Figure 5.3. The particulate and soluble fractions of COD are calculated using values for filtered COD and the estimated f_d. For the remaining biodegradable part of particulate COD, proteins and lipids are fractionated into X_{pr} and X_{li} by converting analysed values into COD, and thereafter the remaining part is assigned to X_{ch}. This principle, previously also suggested by Galí et al. (2009), is chosen since proteins and lipids are generally easier to analyse than carbohydrates for solid substrates, and still leaves enough degrees of freedom to close the mass balance. For the soluble state variables the volatile fatty acids (VFAs) can be calculated directly from measurements. Assuming the soluble COD is small (< 10 % of total COD), the state variables for mono-saccharides (S_{su}), amino acids (S_{aa}) and LCFA (S_{fa}) can be fractionated in the same way as their corresponding particulates.

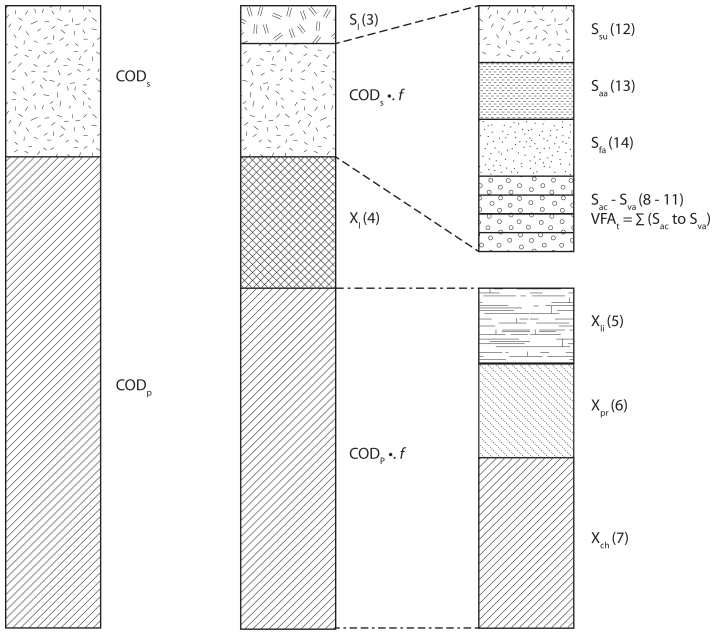

Figure 5.3: The proposed COD fractionation scheme. Numbers in brackets refer to equation numbers in Paper v. Figure from Paper v.

This fractionation procedure is described in detail with explicit equations for all steps and limitations in Paper v. The data requirements to follow the suggested fractionation scheme are: total solids (TS), VS, total COD, filtered COD, VFA (i.e. acetate, propionate, butyrate and valerate), proteins, lipids, total ammonia nitrogen and a BMP test.

The three types of slaughterhouse wastes – paunch, blood and DAF sludge – were fractionated using the proposed methodology. The resulting model feed compositions are presented in Paper v, Table 1. Given the simulation results of the BMP tests the fractionation results were satisfactory.

5.3 Sensitivity Analysis

As previously shown by Solon et al. (2015) and Galí et al. (2009), not all of the 26 state variables of ADM1 have equally large impact on the model output variables. To prioritise which state variables that were most important for the purpose of this study, a sensitivity analysis was performed. The sensitivity analysis was made by Monte Carlo simulations of the isolated AD block of BSM2 with varying feed compositions. Evaluation was made on relevant output variables for assessment of plant-wide performance of AcoD, i.e. gas flow

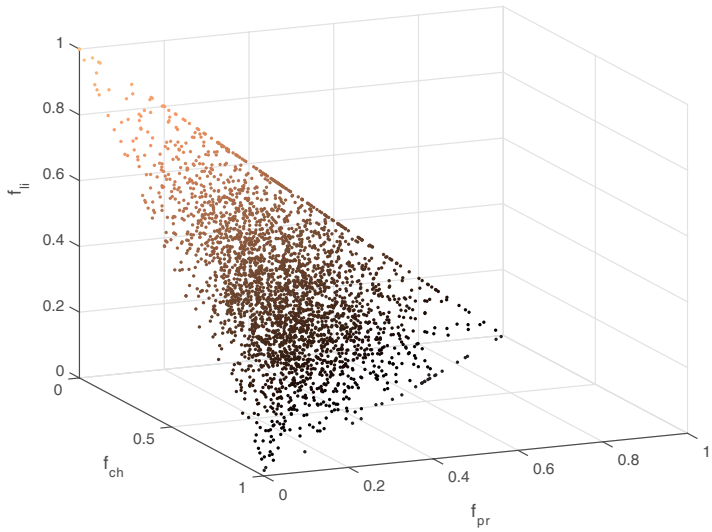

Figure 5.4: Combinations of f_{ch}, f_{pr} and f_{li} for the 3 000 samples used for Monte Carlo simulations in the sensitivity analysis. Figure from supplementary information to Paper v.

(Q_{gas}), methane flow (Q_{CH4}), inorganic nitrogen (S_{IN}), pH and VFAs. The Monte Carlo simulations were designed following Batstone (2013) using 3 000 influent profiles with varying feed compositions. To the average sludge COD load of 2.4 kg.m^{-3}.d^{-1} from BSM2 an additional 8.4 kg.m^{-3}.d^{-1} of co-substrate COD was added. The co-substrate normally distributed samples with varying fractions of X_{ch}, X_{pr} and X_{li} out of biodegradable particulate COD (f_{ch}, f_{pr} and f_{li}) were generated using normalised inverted random numbers. The resulting samples of f_{ch}, f_{pr} and f_{li} are depicted in Figure 5.4.

The simulations were run for 130 days with constant influent conditions (i.e. steady-state without feed-back effects from the WWTP).

The results were evaluated using principal component analysis (PCA), see Figure 5.5. The variations in the results are explained to 71.5 % by Component 1 and 25.2 % by Component 2. The variation in Component 1 is positively related to biogas and methane flow and negatively to VFA. Component 2 is mostly influenced by the S_{IN} concentration in the effluent digestate. From Figure 5.5 three distinctive regions are identified.

I. The substrate compositions positive in Component 1 and negative in Component 2 represent a well-functioning digester with low VFAs and good methane production.

II. As the protein content increases the output gradually moves from Region I into II, i.e. negative in Component 1 but positive in Component 2, towards the upper-left corner. These substrate compositions are at, or close to, digester failure as the ammonia

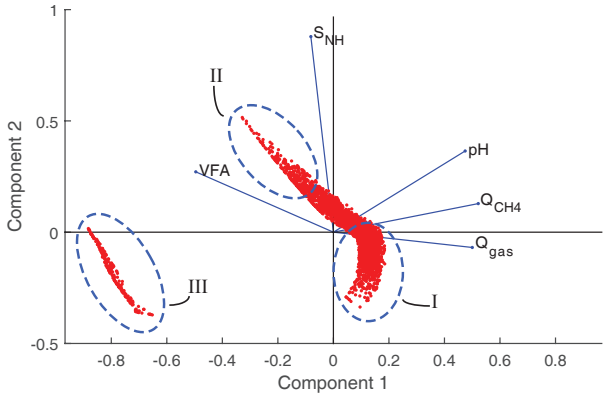

Figure 5.5: Principal component analysis for the Monte Carlo simulations with varying anaerobic digester feed composition. Figure from Paper v.

inhibition is gradually increasing (Figure 5.7, second-top middle) along with VFAs leading to decreasing methane production.

III. The clustered samples negative in both Components 1 and 2 are all high in X_{li} and represent a disruptive digester failure due to LCFA inhibition, where methane production totally stops and VFA increases dramatically leading to total pH inhibition. There is a relatively rapid switch from Region I to Region III due to the threshold nature of inhibition, specifically, when 58 % of the co-substrate COD load of 8.4 $kg.m^{-3}.d^{-1}$ consists of X_{li}, see Figure 5.7 (second-bottom right).

This leads to the conclusion that apart from f_d, the two most important input model parameters for digester stability with co-digestion are the fractions determining X_{pr} and X_{li}. The results in Figure 5.6 (top left) also show that X_{ch} is relevant for the total gas production, because a higher X_{ch} fraction leads to increased CO_2 production, which is coherent with Solon et al. (2015). Moreover, Figures 5.6 and 5.7 reveal that high loads of carbohydrates will lead to pH inhibition subsequent to high VFA production. It is also clear from Figure 5.7 (second-bottom right) that the estimated inhibition parameters for LCFA (Table 5.1) results in a on-off behaviour of the I_{fa} function. As seen, it is in the simulated cases either 1 or 0. This also explains why Region III, Figure 5.5, is separated from Regions I and II.

5.4 Implementing Anaerobic Co-Digestion in BSM2

Anaerobic co-digestion not only leads to higher biomethane production but also has effects on gas composition, digester stability, biosolids production and AD supernatant strength.

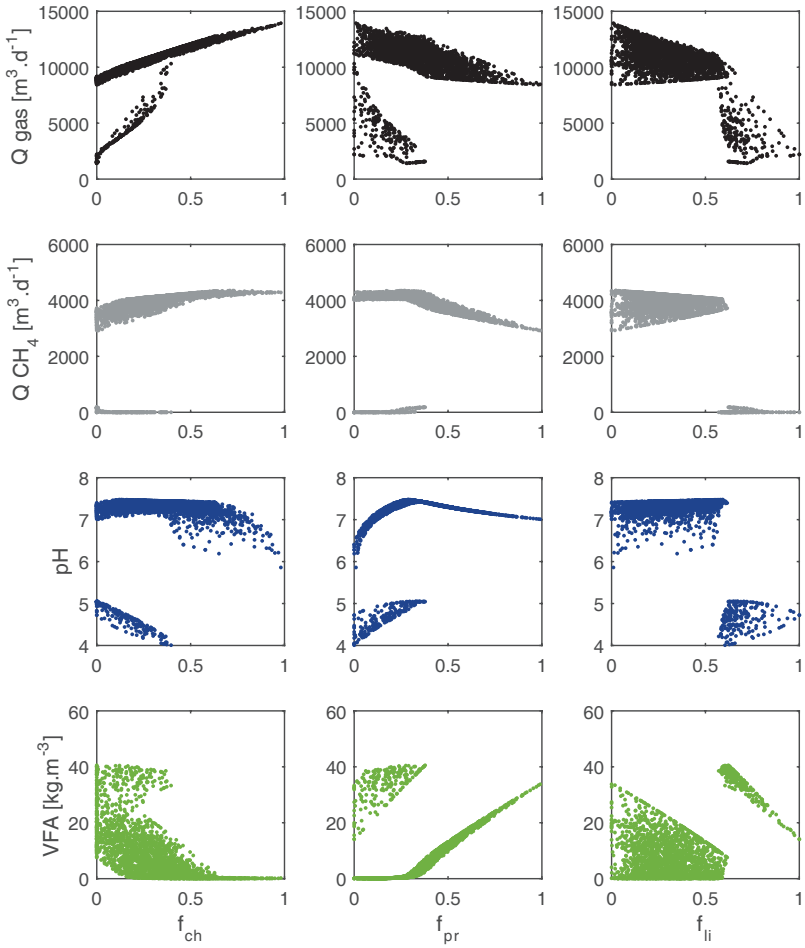

Figure 5.6: Output state variables from the Monte Carlo simulations. From top to bottom the rows depict, Q_{gas}, Q_{CH4}, pH and VFA. Each output variable is plotted against the fractions of biodegradable COD f_{ch}, f_{pr} and f_{li}, respectively, from left to right. Each point represents one simulation where the sum of f_{ch}, f_{pr} and f_{li} adds up to 1. Consequently, points with a high proportion of one component are necessarily low in the others. Figure from supplementary information to Paper v.

These effects can be positive, negative or a combination of both for the overall plant operation. Therefore, simulation studies using plant-wide models are a powerful tool to evaluate co-substrates and digester feed strategies as well as the overall plant impacts.

AcoD was implemented in BSM2 using the GISCOD model introduced in Section 5.1.2. This means that the co-substrates were characterised independently following the procedure presented in Paper v, identifying substrate-dependent parameters and fractionating the COD and TN of the substrates. The ASM to ADM interface for mixed sludge was kept intact. For the model implementation, the hydrolysis reactions were virtually separated

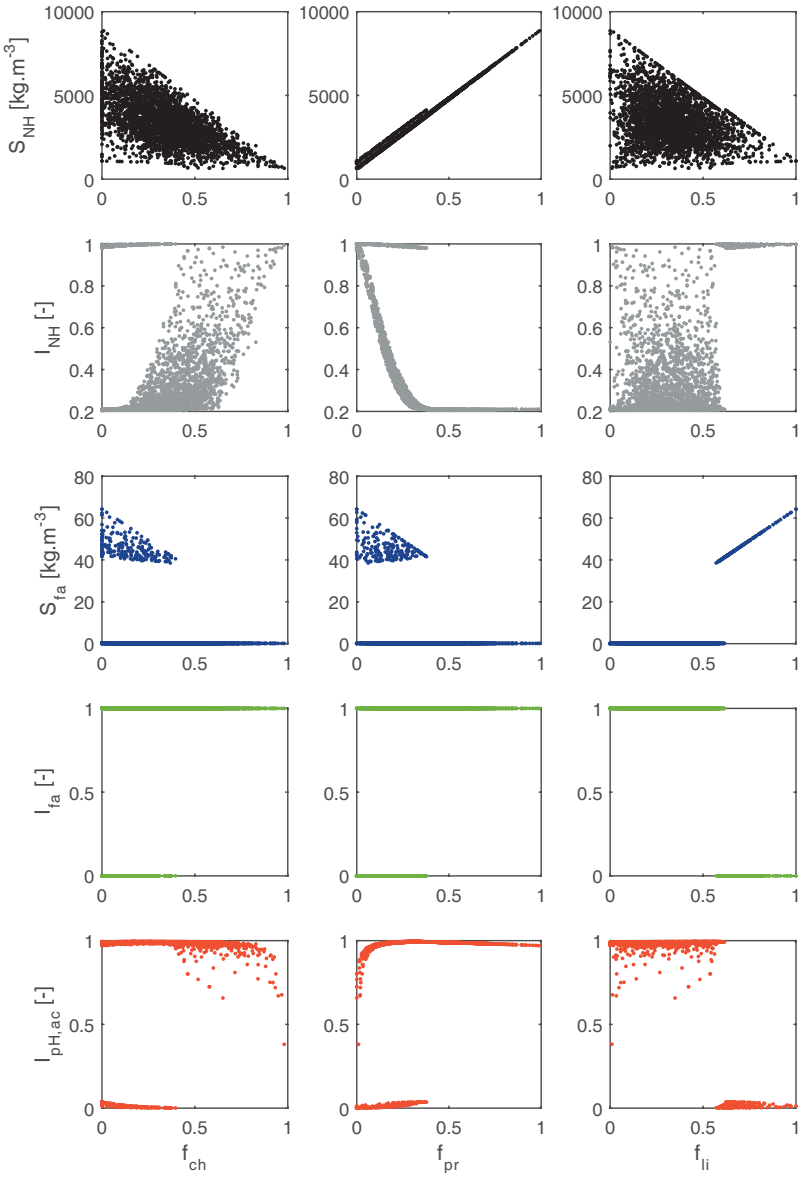

Figure 5.7: AD inhibitions and corresponding inhibitory compound from the Monte Carlo simulations. From top to bottom the rows depict, S_{NH}, ammonium inhibition (I_{NH}), S_{fa}, I_{fa} and pH inhibition for uptake of acetate ($I_{\mathrm{pH,ac}}$). Each state variable is plotted against the fractions of biodegradable COD f_{ch}, f_{pr} and f_{li}, respectively, from left to right. Each point represents one simulation where the sum of f_{ch}, f_{pr} and f_{li} adds up to 1. Consequently, points with a high proportion of one component are necessarily low in the others. Figure from supplementary information to Paper v.

from the remaining processes of ADM1. The substrates were fed to individual model reactors in which only the hydrolysis step of ADM1 was active. Following the hydrolysis-reactor

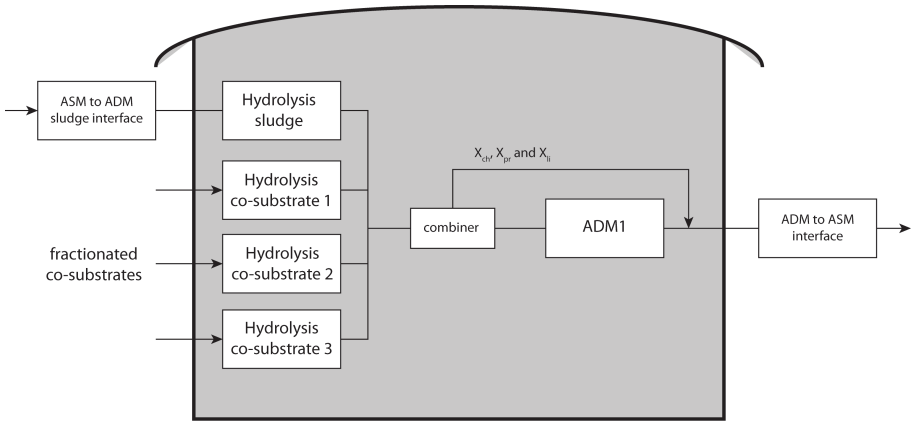

Figure 5.8: Model layout for the anaerobic digester block in Benchmark Simulation Model no. 2 with integrated GISCOD model for anaerobic co-digestion. Figure from Paper v.

blocks the hydrolysed streams are combined and input to a common model reactor with the remaining steps of the model active, see Figure 5.8. The small remaining parts of substrate particulates (X_{ch}, X_{pr} and X_{li}) after hydrolysis are bypassed the ADM1 block. For clarity it should be emphasised that there is one physical digester and it is only virtually separated in the model.

5.4.1 Simulation Study for Plant-Wide Assessment of Anaerobic Co-Digestion

A simulation study was designed to test the developed model for AcoD at WWTPs and exemplify how plant-wide effects of AcoD can be assessed using BSM2. The co-digestion feed consisted of paunch, blood and DAF sludge based on the substrate characterisation presented in Section 5.2. The sludge COD feed was of on an average 2.38 $\mathrm{kg.m^{-3}.d^{-1}}$ to the digester. In addition to that, an external feed-mix was designed with a base-line of about 50 % additional COD. For stressing the system further, two periods with peak loads – with blood days 350-410 and DAF sludge days 500-521 – were included. The total profile for the organic loading rate, OLR, is depicted in Figure 5.9 (bottom). For details on the co-substrate feed-mix, see Paper v. For the sludge hydrolysis a value for $k_{\mathrm{hyd,sludge}}$ = 0.32 $\mathrm{d^{-1}}$ was used, based on Arnell and Åmand (2014).

The main simulation results are compared with the BSM2 default values in Table 5.2. Dynamic profiles for the methane production, OLR, internal nitrogen load and effluent NO_3-N are shown in Figures 5.9 and 5.10. The co-substrates had a positive effect on the methane production leading to a reduction in the overall operational cost index (OCI) from 11 630 to 10 490. However, at the same time the effluent water quality deteriorated from the increased nitrogen load in the water train, due to AD supernatant recirculation, increasing

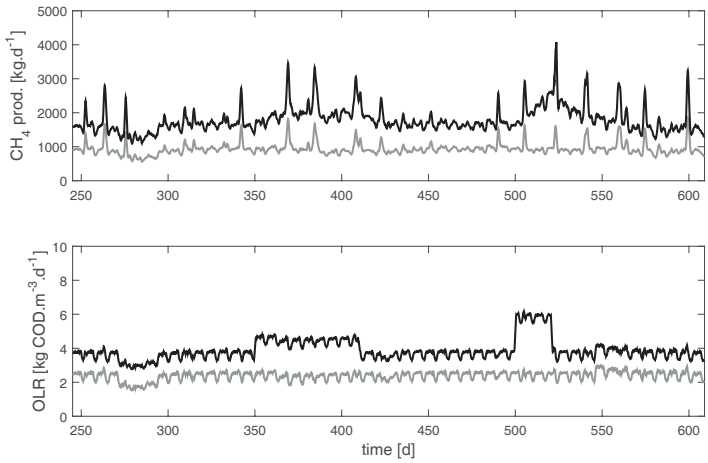

Figure 5.9: Simulated effect of anaerobic co-digestion on the anaerobic digester in Benchmark Simulation Model no. 2 (BSM2). Methane production (top), organic loading rate (OLR) (bottom). Grey lines are standard BSM2 results without co-digestion and black lines are the simulated scenario with co-digestion (filtered values). The time represents simulation days, where 245 corresponds to 1st July. Figure from Paper v.

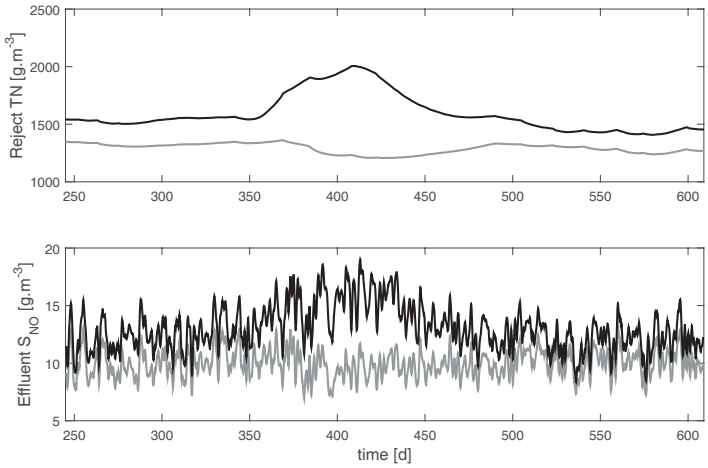

Figure 5.10: Simulated effect of anaerobic co-digestion on the Benchmark Simulation Model no. 2 processes. Anaerobic digester supernatant total nitrogen (TN) concentration (top) and effluent nitrate (S_{NO}, bottom). Grey lines are standard BSM2 results without co-digestion and black lines are the simulated scenario with co-digestion (filtered values). The time represents simulation days, where 245 corresponds to 1st July. Figure from Paper v.

the effluent quality index (EQI) from 5330 to 5970. The reduction in OCI corresponds to a total reduction of the operational costs for the WWTP by 10 % (not considering gate fees for the co-substrates). This significant reduction was achieved because the revenue from selling co-generated power from the produced methane increased by 92 %, although both the aeration energy and the sludge production at the same time increased by 6 and 39 %,

Table 5.2: Simulation results for BSM2 with co-digestion compared to the default values. Table from Paper v.

	BSM2 default	**BSM2 with AcoD**
Operational cost index [–]	11 600	10 050
Effluent quality index [kg pollutant.d^{-1}]	5 330	5 970
Average aeration energy [kWh.d^{-1}]	4 130	4 380
Methane production [kg.d^{-1}]	935	1 800
Sludge production [kg TSS.d^{-1}]	3 480	4 730
Effluent S_{NH} [g.m^{-3}]	0.49	0.44
Effluent S_{NO} [g.m^{-3}]	9.81	12.9
Effluent TN [g.m^{-3}]	12.3	15.4
Time in violation TN [%]	0.17	15.0

respectively. The increase in EQI was mainly due to a higher effluent total nitrogen (TN) concentration, 15.4 g.m^{-3}, caused by the nitrogen load from the protein rich co-substrate, which elevated the S_{NH} concentration in the returning AD supernatant from an average of 1290 g.m^{-3} to 1610 g.m^{-3} (Figure 5.10). This led to a time in violation of the effluent constrains for TN of 15 %, compared to 0.17 % without AcoD. The violation of the effluent constrains would in reality be an unacceptable effect of AcoD and shows the importance of selection and dose strategy of the co-substrate. The primary cause of high effluent TN was elevated effluent S_{NO} caused by insufficient carbon availability for denitrification rather than poor nitrification (Table 5.2, Figure 5.10). The reason for this is that the default control strategy of the closed loop BSM2 has a DO control in the activated sludge unit responding to the increased ammonia load but only a fixed dosage of methanol. If the same total load of blood would have been dosed over the whole period the methanol scarcity might had been less pronounced, or if it had been dosed for an even shorter period the nitrification capacity would have been exceeded as well. Effluent limit violations could have been avoided if simulating an increased or controlled methanol dosage. The drawback of the increased nitrogen load would then have manifested itself as increased methanol consumption instead of effluent violation. While being outside the scope of this work, the strategies to cope with increased nitrogen load can easily be tested and evaluated with additional simulations (results not shown). This demonstrates how simulating AcoD in plant-wide WWTP models allows to design an optimal co-substrate composition and feed strategy and simultaneously control the effects on the water train. Nordell and Wiberg (2013) have shown in lab- and full-scale experiments of AcoD at Linköping WWTP in Sweden how a wise, i.e. nitrogen poor, co-substrate selection can have positive plant-wide effects and contribute to the nitrogen removal of the plant by assimilation of nitrogen in biosolids.

The effects of the simulated co-digestion case on digester stability and inhibition are further discussed in Paper v.

5.5 Summary of Key Findings

Non-linear parameter estimation was used to estimate the first-order hydrolysis coefficient (k_{hyd}) and the ultimate methane yield from 18 datasets of biomethane potential (BMP) batch data.

- The parameter uncertainty was lower when fitting data to a first-order model compared to a Monod-type function since this model could better describe the shape of the cumulative gas production in the BMP tests.
- The Monod-type function resulted in higher estimates of the hydrolysis coefficient and the ultimate methane yield compared to the first-order model.
- The smoother the BMP curve and the more samples in the test, the smaller the confidence interval of the estimated gas production.
- The hydrolysis coefficients for the studied substrates were in the range 0.08 to 0.70 d^{-1}.

Anaerobic co-digestion was for the first time implemented in Benchmark Simulation Model no. 2. The GISCOD model was used to describe anaerobic co-digestion (AcoD), complemented by a Gaussian long chain fatty acid inhibition function.

- A new input model for fractionation of COD was developed based on feasible and affordable tests. The method was proven reliable based on modelling of BMP tests of three substrates: paunch, blood and dissolved air flotation sludge.
- A performance assessment study of anaerobic co-digestion was performed using a dynamic feed mix. It revealed that the overall operational cost was reduced by 10 %. However, the high nitrogen content in blood increased ammonia inhibition in the digester, leading to lower digester performance and overloaded the denitrification capacity of the water train and deteriorated the effluent water quality.
- A sensitivity analysis on co-substrate feed characteristics showed that apart from the biodegradable fraction of COD, protein and lipid fractions of particulate biodegradable COD were the two most important state variables for digester stability and methane production, and that different substrates caused different modes of failure.

Chapter 6

Multi-Objective Performance Assessment Using Coupled Process Models and Life Cycle Assessment

This chapter describes the over-arching methodology of coupling the plant-wide process model to a life cycle analysis model to assess not only the on-site effects but also the off-site environmental impact of the operations, both up-stream from production of input goods and downstream from discharge of treated water and disposal of sludge. The specific model developments on greenhouse gas emissions, aeration and anaerobic co-digestion described in Chapters 3 to 5 are included in the tool. The case study in Paper VI*, using the tool to model Käppala wastewater treatment plant, is described together with a simulation study on chemically enhanced primary clarification. This work has also been presented in Arnell et al. (2016b) and Arnell et al. (2016d). Finally, another simulation study demonstrating the effect of stricter effluent regulations from Åmand et al. (2016), based on the Käppala model, is presented.*

6.1 Combining Process Modelling and Life Cycle Assessment

As has been demonstrated in the preceding chapters, dynamic process models are essential when evaluating operational strategies at wastewater treatment plants. For example, N_2O emissions can manyfold due to short-term concentration fluctuations in the activated sludge unit having a major impact on greenhouse gas emissions, demand peaks in aeration have a non-linear impact on cost and unreliable co-substrate availability makes steady-state simulations obsolete when evaluating plant-wide impacts of anaerobic co-digestion (AcoD). However, along with these on-site effects the plant operations at the same time have global

environmental impacts due to production of input goods, discharge of residues and discarding of wastes. These impacts are only covered to a limited extent in process models. Greenhouse gas (GHG) emissions from production of power and some chemicals, residual effluent nitrogen and disposal of sludge are for example included in the Benchmark Simulation Model no. 2, version greenhouse gas (BSM2G). Other impacts are not considered but could very well be crucial for the overall environmental impact of the operations. If, for example, operational strategies for dealing with stricter effluent constraints are compared, several alternatives may be able to meet the treatment requirements and the total environmental impact could be decisive.

Global environmental impacts of products and processes are commonly assessed by life cycle analysis (LCA) (Baumann and Tillman, 2004). In LCA, the object under study is evaluated for the environmental impacts that the inputs and outputs give rise to over the course of the entire life cycle. All processes and transports are included, from extraction of resources to handling of residuals and wastes. Following the international standard for LCA, a study is performed in four mandatory steps (ISO 14040, 2006): *i)* definition of goal and scope for the analysis, *ii)* life cycle inventory (LCI), where the environmental loads from the entire system are calculated, *iii)* life cycle impact assessment (LCIA), where the loads are characterised in equivalent units by the selected impact categories to get aggregated measures of the potential environmental impacts, and *iv)* evaluation of the LCA. Urban water services and wastewater treatment plants have been subjected to LCA in several studies (Baresel et al., 2016; Heimersson et al., 2016; Corominas et al., 2013a; Lundie et al., 2004). To assess the operational performance and effects on-site along with the potential global environmental impacts, process models have been combined with LCA (Meneses et al., 2016; Arnell et al., 2016b; de Faria et al., 2015; Corominas et al., 2013b). In Paper VI, a methodology in two steps was proposed for combining process models and LCA.

i. The plant-wide process model platform BSM2G was used to evaluate: effluent water quality, energy efficiency, on-site GHG emissions and operational costs. Full-year dynamic simulations were evaluated and averaged results of inputs and outputs for all sub-processes were exported.

ii. An LCA model was constructed following ISO 14040 (2006) for the plant covering the same unit operations as the process model but extended with up-stream processes for production of input goods and downstream impact of residuals and wastes. The exported results from the process model were imported to the LCA model.

The applied process model BSM2G is described in Section 3.2. When combining the BSM2G with the LCA model two exceptions from the default procedure were made. The off-site processes, production of power and chemicals, together with the downstream ones in recipient and from sludge disposal, are excluded from the evaluation procedure of BSM2G. Instead the impacts from these processes are included in the LCA.

6.2 Life Cycle Analysis Model

The coupled LCA model was developed for the case study of Käppala WWTP presented in Section 6.3. The model development followed ISO 14040 (2006) and the four steps listed in Section 6.1.

i. The goal and scope of the LCA were to perform a comparative assay of the operational strategies simulated using the process model. The system boundaries for the study (Figure 6.1) were therefore chosen to be the treatment plant itself with direct emissions to water, soil and air and the production and transport of power and chemicals from resource extraction to the plant. The benefit of utilising the produced biomethane was accounted for by expanding the system to include the benefiting process, i.e. as vehicle fuel. For the purpose of comparing operational strategies, one year of operation was considered and construction and demolition phases were excluded as these have been shown to have only limited impact for most conventional advanced WWTPs (Corominas et al., 2013a).

ii. To manage the LCI, the Gabi software tool was used (Gabi software 6.3, Thinkstep, Leinfelden-Echterdingen, Germany, 2013). The process model simulation outputs were used together with generic data from the Ecoinvent database (Wernet et al., 2016). Functional unit for the inventory was chosen to be 1 m^3 of treated wastewater.

iii. For the LCIA characterisation the procedures of Centrum voor Milieukunde at Leiden University, The Netherlands (CML) were applied (Guinée et al., 2002). The six most important impact categories were selected based on previous studies (Corominas et al., 2013a) for which impacts were calculated: abiotic depletion potential of elemental (ADP elements) and fossil (ADP fossil) resources, eutrophication potential, acidification potential, global warming potential (GWP) and ozone depletion potential (ODP).

iv. Except for the performance evaluation of the on-site process with BSM2G, the six LCA impact categories were evaluated individually in reference to the corresponding total European impacts to indicate relative significance.

6.3 Case Study on Käppala Wastewater Treatment Plant

The Käppala WWTP in Lidingö outside Stockholm, Sweden, receives wastewater from 11 municipalities in the northern part of the greater Stockholm area with a total load of 440 000 person equivalents (pe). The plant is mainly an underground facility built into the mountain on the island Lidingö in the archipelago. The effluent requirements are 10 $g.m^{-1}$ TN (annual average) and 0.3 $g.m^{-1}$ TP (quarterly average). This is achieved by a treatment

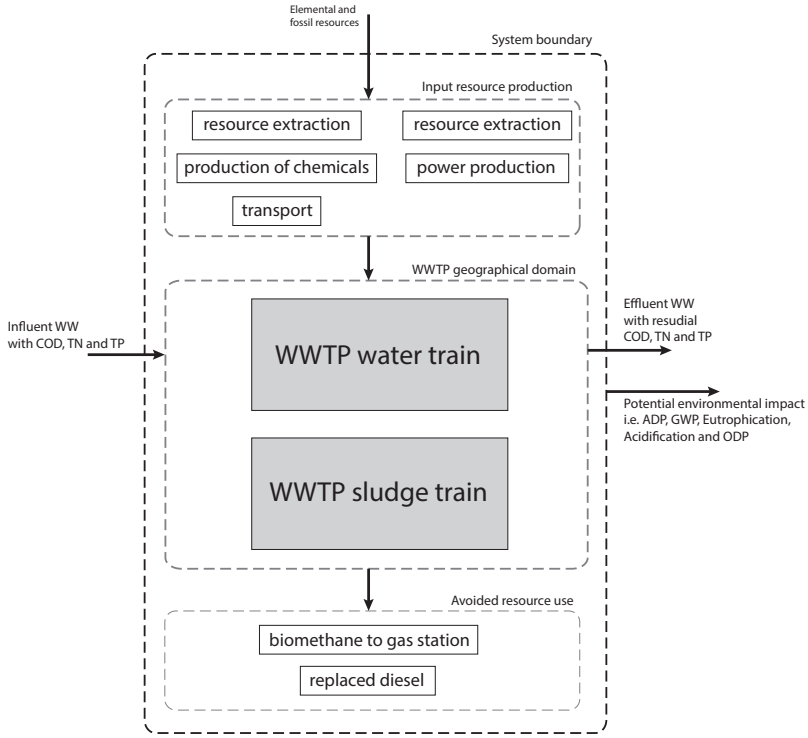

Figure 6.1: System boundaries and modelled activities for the life cycle analysis. Modified figure from Paper VI.

process based on primary mechanical treatment, secondary biological treatment and tertiary filtration (Figure 6.2). The original part of the plant, built in the 1960s, treats about 40 % of the influent flow (2012) in a treatment train applying a UCT Bio-P process in the activated sludge unit. The plant was expanded during the 1990s with a parallel treatment train handling the remaining 60 % in a modified Ludzack-Ettinger configuration (Figure 6.2). For this project only the new part of the plant was modelled and the influent load was adjusted accordingly.

The platform BSM2G (Section 3.2) was modified with regard to plant layout, model library and influent load to mimic the treatment process at Käppala. The plant layout was adjusted according to Figure 6.2, with the five parallel lines in the AS unit modelled as one and split into 9 consecutive reactors – three anoxic (ANOX), one swing zone (FLEX), four aerated (OX) and one final non-aerated deox zone (DEOX) – following the principles for hydraulic modelling of activated sludge tanks proposed by Fujie et al. (1983) (Figure 3.8). The submodel library of BSM2G was complemented by an ideal model for the sand filter unit, see model description in Paper VI. For the modified influent load see Section 6.3.1.

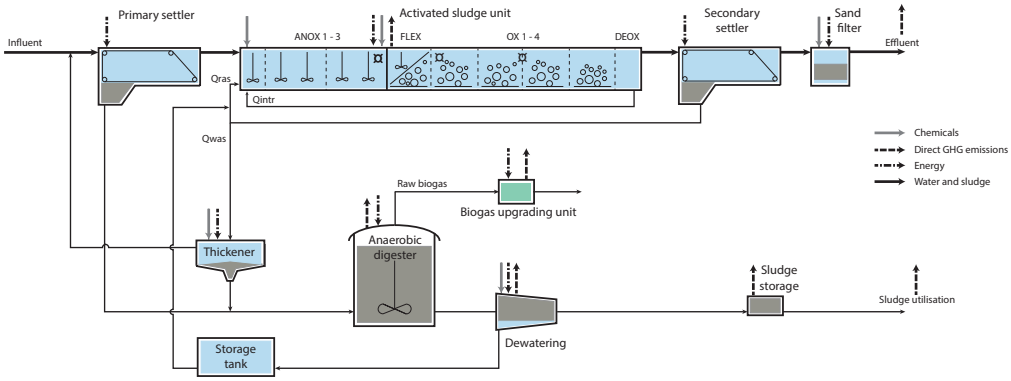

Figure 6.2: Process flow diagram of the modelled unit processes at the Käppala wastewater treatment plant. Arrows indicate flows of water and sludge (solid black), chemical input (solid grey), direct greenhouse gas emissions (dashed black) and energy input (dot-dashed black). The measurement points for aqueous N_2O are indicated in the activated sludge unit (¤). Figure from Paper VI.

Consumption of resources, such as energy and chemicals, were either modelled dynamically (i.e. carbon source addition) or calculated based on specific consumption numbers. Specific data were mainly retrieved from the utility but some generic BSM2G data were used when specific data were missing. Values are tabulated in the supplementary information of Paper VI, Table S.1. The specific consumption factors have, when possible, been coupled to dynamically modelled flows and volumes but for a few energy related processes static consumptions per day provided the most reliable information.

The general description of the LCA model in Section 6.2 was modified for the case study. For gas utilisation, external use of the upgraded biomethane as vehicle fuel was assumed by substitution of diesel in heavy vehicles (i.e. public transport). The off-site reuse of biosolids was not included due to lack of data. Case specific inventory data were used. Assumptions and data can be found in Paper VI and its supplementary information.

6.3.1 Calibration and Validation of the Process Model

For influent fractionation and calibration the procedures in Rieger et al. (2012) were followed. Data from the year 2012 was selected for calibration and from 2014 for validation. The results from 2012 were chosen for presentation as this was a year with several severe rain events challenging the treatment process. A dynamic influent profile was created from plant data for the years 2012 and 2014. The actual measurements were used for influent flow along with a synthetic diurnal load pattern created from the averaged and normalised diurnal flow rate during dry weather. The procedure in five steps was inspired from Lindblom (2011).

i. The high resolution influent flow profile for a full year was split into 365 individual diurnal curves, and all days with a representative dry weather flow were selected.

ii. For every 15 minutes of the day (i.e. the resolution of the model) an average flow was calculated from the selected daily curves from Step *i* creating an average flow profile.

iii. The averaged flow profile from Step *ii* was normalised to one and the diurnal variation was assumed to apply equally to all influent load variations to the plant.

iv. The normalised load profile from Step *iii* was multiplied by the average daily loads of COD, NH_4-N, NO_3-N and TSS to retrieve the individual load profiles in $g.d^{-1}$. The average daily loads during dry weather were used in order to get a fair representation of the influent loads without dilution from stormwater. Compensation for groundwater intrusion was not made.

v. Finally, the created load profiles were divided with the full actual flow profile for the whole 609 d period. Data from the beginning of May 2011 to the end of December 2012 were used for 2012 and similarly for 2014.

In summary, this procedure provides dynamic, 609 day long, concentration profiles for all state variables considering diurnal variations and dilution according to the actual flow pattern.

The calibration results are tabulated in the supplementary information of Paper VI, Table S.4. More information on the calibration and results are also presented in Arnell et al. (2016b). The calibration was satisfactory according to the stop-criteria established for effluent water quality (Figure 6.3), biogas production and air supply to the AS unit. To achieve this, the calibration was primarily focused on establishing a correct sludge age for the AS unit in order to gain realistic nitrification. Although inert suspended solids were introduced in the influent as well as in the AS – corresponding to the sludge production from simultaneous precipitation – the TSS level in and WAS production from the simulated AS unit had to be lowered.

6.3.2 Simulation of Chemically Enhanced Primary Clarification

During recent years there has been a strong focus on resource recovery at WWTPs and more specifically at energy recovery through anaerobic digestion (Eitrem Holmgren et al., 2015). This follows from the understanding of climate change that has been growing over the last decade promoting renewable energy. In Sweden, this has created a strong trend for WWTPs to upgrade their biogas to vehicle fuel quality, which provides a greater economical and environmental value. Consequently, the interest has also grown for increasing biogas production (Lingsten, 2014). As shown in Chapter 5, anaerobic co-digestion provides an opportunity to substantially increase the gas production. However, also the influent

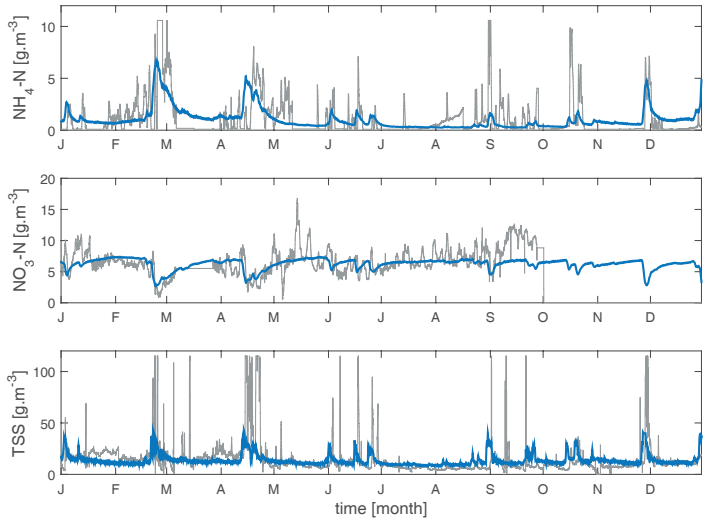

Figure 6.3: Calibration results. Dynamic profile of secondary effluent concentrations of NH_4-N (top), NO_3-N (middle) and TSS (bottom). Data (grey line) vs. calibrated and filtered simulation results (blue line). Figure from Arnell et al. (2016b).

COD is a valuable resource. Being less degraded, the primary sludge has higher biomethane potential than secondary sludge (see Paper IV). Therefore, if the COD reduction over the primary clarifier could be increased more potent sludge could be fed to the digester. At the same time, the organic load on the AS would be reduced leading to lower energy requirements for aeration. Altogether this points to the importance of the primary mechanical treatment steps at WWTPs (Bachis et al., 2015; Lundin et al., 2015). A common way to improve primary clarification is to implement chemically enhanced primary treatment (CEPT), where pre-precipitation with metal salts and/or polymers is used to improve the removal efficiency (Ødegaard, 1998). However, extensive removal in the primary treatment might lead to COD deficiency for denitrification in the AS, i.e. there is a conflicting competition for the influent organic matter, whether it is best used for denitrification or for biogas production.

A simulation study was designed to assess the total environmental impact of the CEPT strategy using the proposed methodology. For realism and comparison, the calibrated model of the Käppala WWTP was used. The base case represents the current operation (simulation results for 2012) of the treatment plant. The alternative strategy with CEPT was modelled with the following modifications: the COD removal efficiency over the primary clarifier was increased to 60 % by increasing the parameter `f_corr` to 0.8 and move the modelling of precipitation – addition of inert suspended solids – prior to the primary clarifier. A reduction of that magnitude is possible if the plant has efficient primary clarifiers, which is the case at Käppala. The goal of the simulation of CEPT was to analyse the change

Table 6.1: Process model outputs from the case study on chemically enhanced primary treatment (CEPT). From Paper VI.

	Base case	CEPT
EQI [kg pollutant.d^{-1}]	17 470	17 040
Biomethane prod. [kg CH_4.d^{-1} / kWh.d^{-1}]	4 930 / 68 400	5 610 / 77 900
Power for aeration [kWh.d^{-1}]	6 590	6 480
Precipitation chemicals [kg Fe.d^{-1}]	178	1 260
Methanol [kg COD.d^{-1}]	0	2 060
N_2O emissions from AS [kg CO_2e.d^{-1}]	19 040	14 400

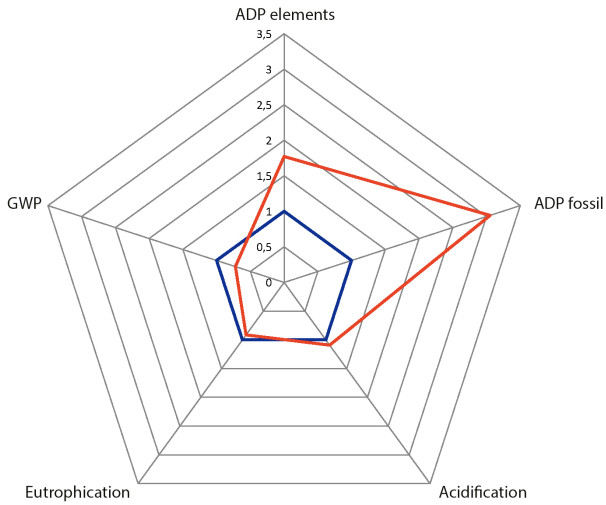

Figure 6.4: Diagram showing five out of six evaluated environmental impact categories in the life cycle analysis for Käppala wastewater treatment plant. Simulation results for the base case (blue line) compared with simulation results from implementing chemically enhanced primary treatment (red line). The categories are: Abiotic Depletion Potential (ADP) elemental, ADP fossil, Acidification, Eutrophication and Global Warming Potential (GWP). Results for Ozone Depletion Potential (ODP) not shown in figure. All results are normalised to the base case. Figure from Paper VI.

in environmental impact from that strategy assuming the same effluent quality. Therefore, the operation was tuned to match the same effluent standards as for the base case. To achieve this it was necessary to add methanol to the anoxic zones to match the denitrification in the CEPT case. This was done by a 50/50 addition to ANOX 1 and 2 with a PI-regulator controlling the methanol flow towards a set-point of 6.7 g.m^{-3} NO_3-N in the effluent from the DEOX.

Selected results are presented in Table 6.1, while full results are presented in Paper VI (with supplementary information) and also in Arnell et al. (2016b). The LCA results (5 categories) for the base case and the CEPT strategy are compared in Figure 6.4. Looking at the Eutrophication category it can be seen that the aim not to affect the effluent quality has been reached. The resulting EQI from the process simulation (Table 6.1) confirms this and

it can therefore be concluded that other off-site processes are not affecting Eutrophication substantially. One of the main goals of the simulated strategy was to reduce the emission of GHGs. As can be seen, the overall GWP is reduced by 28 % (Figure 6.4). This is achieved by an increase in biomethane production (14 %) and reduced N_2O emissions from the AS (14 %, Table 6.1), despite the increased emissions from production and transport of methanol and precipitation chemicals. It is hypothesised that the decreased N_2O emissions are due to the reduced load on the AS with CEPT. The TN in the primary effluent was reduced and methanol was dosed, which improves the carbon to nitrogen ratio. Setting up the strategy it was also expected that the aeration energy should be reduced. The results in Table 6.1 show that this was not realised, likely due to the methanol addition to the AS keeping the organic load high.

The improvement in GWP comes with a cost in terms of resource use. The ADP elements and ADP fossil are increased by 77 and 305 %, respectively (Figure 6.4). This rise is completely explained by the increased use of chemicals for precipitation and denitrification, Figure 6.5. The origin of the methanol was here assumed to be fossil based, which has a major impact on ADP fossil. The impact category with the largest relative change was Ozone Depletion Potential (ODP), with CEPT it increased by 450 % (Paper VI, Table 2). As is further explained in Paper VI, the absolute values are very small and also when normalised to the total European emissions the ODP was 2 to 4 orders of magnitude lower than that of the other categories. Even if the increase was relatively large, it was from a low initial level. The impact of CEPT on Acidification potential is negative but very small. The change is solely caused by production and transport of chemicals, especially methanol, which penalises CEPT in this case.

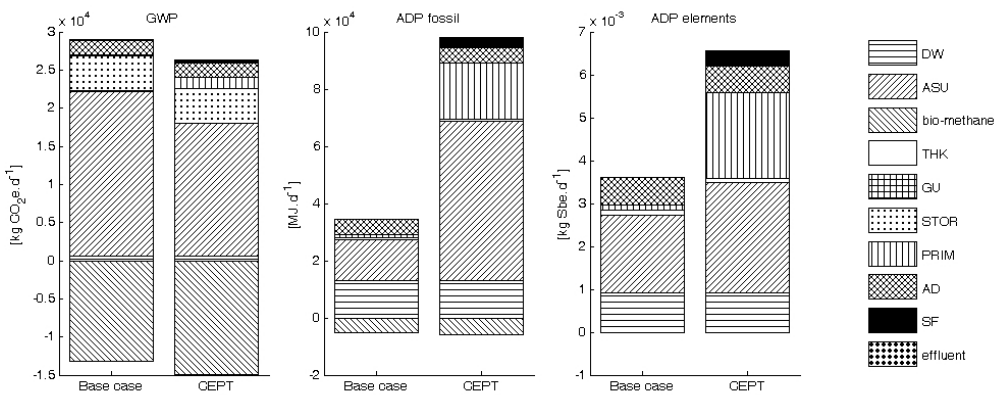

Figure 6.5: Life cycle analysis results for the base case compared to chemically enhanced primary treatment (CEPT) in three categories: Global Warming Potential (GWP), Abiotic Depletion Potential (ADP) fossil, and ADP elements. Results presented for individual unit processes: sludge dewatering unit (DW), activated sludge unit (ASU), utilisation of biomethane as vehicle fuel (biomethane), thickener (THK), biogas upgrading unit (GU), storage tank (STOR), primary clarifier (PRIM), anaerobic digester (AD), sand filter (SF) and effluent water (effluent). Figure from Paper VI.

Table 6.2: Simulated scenarios. From Åmand et al. (2016).

Scenario	Load	Treatment process	Effluent limits
1	Present	Present	Present
2	Present	Future	Future
3	Future	Future	Future

The increase in consumption of chemicals can be found in Table 6.1. The cost for operations increases with the cost of chemicals but the net operational cost could not be reported since the revenue from selling the biomethane was not publicly available.

6.3.3 Simulation of Stricter Effluent Limits

In a parallel project, the process-LCA model for the Käppala WWTP (2012) was used in another assessment study simulating the effect of enforcing stricter effluent constraints on the plant (Åmand et al., 2015). A simulation study was designed to compare the impact of the current operations with a situation where firstly, the plant is modified to cope with the stricter limits and secondly, adding a forecasted load increase from 440 000 to 900 000 pe. The three scenarios are shown in Table 6.2. The stricter constraints were TN = 6 $g.m^{-3}$, TP = 0.2 $g.m^{-3}$ and BOD = 6 $g.m^{-3}$, all as monthly averages. In the project this analysis was done for three different WWTPs, see Åmand et al. (2016) for detailed descriptions.

The process modifications and how they are modelled are described in detail in Åmand et al. (2016). In brief the modifications for Käppala WWTP were:

- switching P-removal from simultaneous precipitation to CEPT using ferric chloride;
- introducing complementary one-sludge post-denitrification in the DEOX zone;
- side-stream treatment of AD supernatant in an anammox process; and
- peak-flow treatment with chemical precipitation on a partial by-pass flow.

Three assumptions in the LCA were identified as especially important and uncertain: choice of functional unit, origin of carbon source for denitrification and whether or not a credit is counted for vehicle fuel from biogas replacing diesel. A sensitivity analysis was made on those variables.

The simulation results showed that the plant cannot manage the stricter limits without process modifications (Åmand et al., 2016). However, implementing the proposed measures the effluent quality is satisfactory for all scenarios, Table 6.3. It is likely that not all four modifications would have been necessary in Scenario 2, i.e. with current load, however, in Scenario 3 they were.

Table 6.3: Effluent quality for the three scenarios. From Åmand et al. (2016).

	Scenario 1	Scenario 2	Scenario 3
TN [$g.m^{-3}$]	8.5	4.2	4.4
NH_4-N [$g.m^{-3}$]	1.3	0.74	0.92
NO_3-N [$g.m^{-3}$]	5.9	2.8	2.7
TP [$g.m^{-3}$]	0.2	0.12	0.12

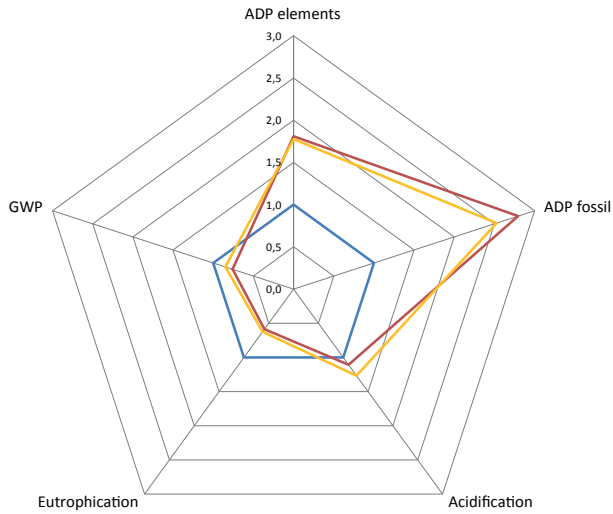

Figure 6.6: Life cycle analysis results – in five impact categories: Global Warming Potential (GWP), Abiotic Depletion Potential (ADP) elements, ADP fossil, Acidification, and Eutrophication – from simulating alternatives for handling stricter effluent limits at Käppala wastewater treatment plant. Scenario 1 (blue line), Scenario 2 (red line) and Scenario 3 (yellow line). All results are normalised to Scenario 1. Figure from Åmand et al. (2016).

The LCA results displayed in Figure 6.6 show a similar structure as for the CEPT case presented in Section 6.3.2. In Scenarios 2 and 3, the Eutrophication is significantly reduced as the effluent quality is intentionally improved. Also the GWP declines at the expense of higher ADP of elements and fossil resources due to use of precipitation chemicals and external carbon source.

The sensitivity analysis revealed some interesting results, see Figures 6.7 and 6.8. The functional unit used in the LCA has an impact when comparing results for the different scenarios. Comparing three different functional units – 1 m^3 of treated wastewater, 1 kg of removed TN and 1 pe load – it can be seen (Figure 6.7) that using removed nitrogen made the improvements in GWP and Eutrophication even larger and the increase in ADP a bit less pronounced. Switching to person equivalents have little or no effect on Scenario 2 but for Scenario 3, with an increased load to the plant, four out of five impacts are substantially reduced with acidification even changing from a predicted increase to a decrease

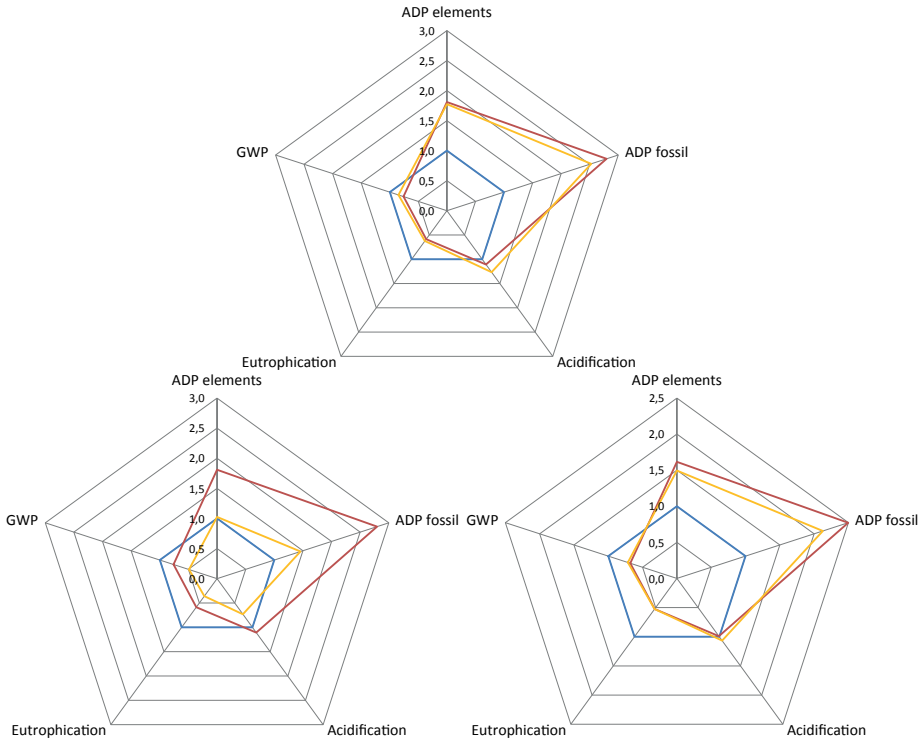

Figure 6.7: Results from the sensitivity analysis on alternative functional units. Life cycle analysis results – in five impact categories: Global Warming Potential (GWP), Abiotic Depletion Potential (ADP) elements, ADP fossil, Acidification, and Eutrophication – from comparing: per m^3 (top), per pe (bottom left), and per removed nitrogen (bottom right). Each diagram shows Scenario 1 (blue line), Scenario 2 (red line) and Scenario 3 (yellow line). All results are normalised to Scenario 1. Figure from Åmand et al. (2016).

compared to Scenario 1. The difference in results between the per m^3 and per pe is due to a proportionally lower increase in influent flow than in influent loads in Scenario 3.

Altering the type of carbon source was also evaluated, Figure 6.8. In the standard simulations methanol of fossil origin was assumed. For the sensitivity analysis three alternatives were tested: ethanol (USA), ethanol (Brasil) and waste glycerol from airports. The results show that altering carbon source has an impact on ADP while the other categories are mostly unaffected. Ethanol has a lower impact on ADP fossil but a higher impact on ADP elements. Brazilian ethanol from sugar cane has a lower environmental impact than the one produced from corn in USA. With waste glycerol the climate impact is reduced for all categories compared to the other types of carbon sources examined. Consequently, the choice of carbon source has a major impact on the results.

Also the sensitivity analysis on crediting of vehicle fuel replacing diesel had an impact on the results. Including the credit reduced the GWP with 45 %, 67 % and 67 % for Scenarios

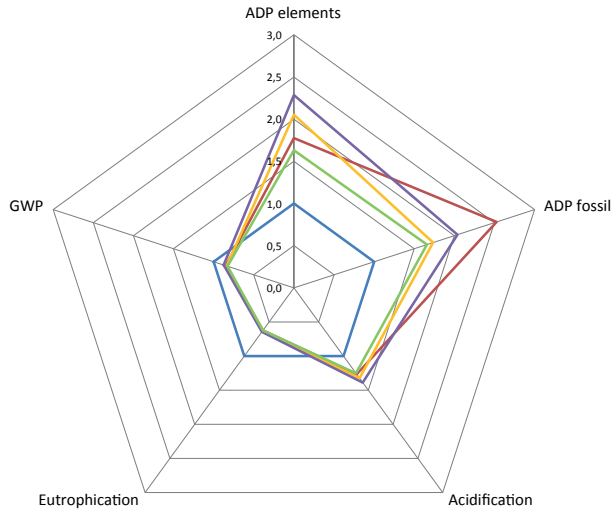

Figure 6.8: Results from the sensitivity analysis on origin of carbon source. Life cycle analysis results – in five impact categories: Global Warming Potential (GWP), Abiotic Depletion Potential (ADP) elements, ADP fossil, Acidification and Eutrophication – from comparing Scenario 1 with fossil based methanol (blue line) with Scenario 3 with four alternative types of carbon source: fossil based methanol (red line), ethanol Brasil (yellow line), ethanol USA (purple line) and waste glycol (green line). All results are nomalised to Scenario 1. Figure from Åmand et al. (2016).

1 to 3, respectively. The higher reductions for Scenarios 2 and 3 is due to a higher biogas production. Also the Acidification potential was reduced with 30 % for all three scenarios.

6.4 Using Results for Decision Support

The results from the simulated case studies show the multidimensional, and often conflicting, impacts that various operational strategies can lead to. When the operations are evaluated, for multiple objectives, the assessment grows more complex. From the results it is evident that in the presented cases detailed process models are necessary to assess, for example, N_2O production in the activated sludge reactors. This has been shown previously for other cases, i.e. Flores-Alsina et al. (2014), Guo (2014) and Corominas et al. (2013b). The effects can rarely be calculated by traditional spread-sheet methods (Rieger et al., 2012). At the same time, the increase in resource use and energy recovery, for these two simulation studies, leads to an altered environmental impact off-site, which is not captured by the process model but only by LCA. To combine process modelling and LCA is useful for comparing alternative operational strategies at WWTPs and provides a more thorough and comprehensive base for decision making.

The different impact categories in LCA measure different things expressed in different units and are not comparable per se. The standard for LCA studies, ISO 14040, states that

weighted comparison of the impact categories is an optional part of the LCA, conducted separately after the LCIA. This is good praxis since the subjective process of grading and weighting the results should not be mixed with the objective impact assessment. The weighting step was not performed in this study since it was focused on developing a methodology for impact assessment. However, if the results are to be used for decision making then this weighting and comparison of the different impact categories' mutual importance have to be done at a later stage. For example, to decide if a sought improvement in eutrophication or climate impact is worthwhile if other categories are worsened. This exercise can be performed by skilled decision makers involved in conducting the LCA. It is important that a representative group of stakeholders is engaged in this process. Principles, guidance and examples on weighting and multi-criteria analysis can be found in literature (ISO 14040, 2006; Baumann and Tillman, 2004; Malmqvist et al., 2006).

6.5 Summary of Key Findings

» The model platform Benchmark Simulation Model no. 2 Greenhouse Gas was extended to – in addition to effluent quality and operational cost – also evaluate fugitive GHG emissions, more detailed energy efficiency models and global environmental impact.

» To assess the global environmental impact the dynamic process models have been coupled with a life cycle analysis (LCA) model. This novel approach to combine a detailed plant-wide model including dynamic energy and GHG calculations and LCA captures both direct effects and off-site impacts, for example from production of electricity and chemicals.

» The model concept was calibrated to a real plant, the Käppala WWTP in Lidingö, Sweden. The model calibration under current operational conditions shows that the model is suitable to describe a conventional municipal wastewater treatment process.

» A simulation study on altering the operational strategy at the Käppala WWTP in Lidingö, Sweden, was performed. The current strategy with simultaneous precipitation and predenitrification utilising internal COD was compared to a strategy with extensive preprecipitation and adding methanol in the anoxic zones. The comparative simulations show that several of the initial goals with the strategy are fulfilled, i.e. higher biogas production, lower aeration energy requirements and an overall decrease in global warming potential (28 %). However, at the same time the LCA reveals that the abiotic depletion of both elemental and fossil resources increases by 77 % and 305 %, respectively. Also the ozone layer depletion increases manyfold but from a very low initial level.

» The study shows that the method is applicable for use at WWTPs. The coupled process and LCA modelling methodology captures plant-wide and global effects that would not only have been hard to determine with standard spread-sheet calculations but would also remain hidden using any of the models separately. The results from this type of combined study create a good basis for selecting operational strategies at WWTPs.

Chapter 7

Conclusions and Future Research Needs

The key findings of the separate studies are summarised in general conclusions of the research. Furthermore, identified areas for further research are outlined.

7.1 General Conclusions

A tool for performance assessment of wastewater treatment plants (WWTPs) evaluating multiple objectives was developed. The tool combines plant-wide process models for long-term dynamic simulations to evaluate treatment plant performance – including effluent water quality, operational cost and greenhouse gas emissions – with life cycle analysis (LCA) to assess global environmental impacts of the plant operation. For this purpose, the plant-wide model Benchmark Simulation Model no. 2 (BSM2) was expanded to include additional processes, increase the level of detail in important areas and allow for simulation of common and realistic operational strategies. Specifically, the developments were the following.

BSM2 was upgraded with models for production and emission of greenhouse gases. Process models for direct and indirect emissions of carbon dioxide (CO_2), methane (CH_4) and nitrous oxide (N_2O) were added, including fugitive emissions. The biokinetic model in BSM2, Activated Sludge Model no. 1 (ASM1), was expanded with two-step nitrification including nitrifier denitrification and four-step denitrification to describe two important production pathways for nitrous oxide. The expanded model, ASM1G, was used in several case studies: a simulation study evaluating control strategies, three treatment processes for

digester supernatant and a plant-wide study of a full-scale WWTP. The key findings of the studies can be summarised in the following conclusions.

» The inclusion of greenhouse gas emissions provides an additional criterion when evaluating control / operational strategies in a WWTP, offering more knowledge about the overall "sustainability" of the plant.

» The implemented biological process model, together with physical models for the sequencing batch (SBR) and moving bed biofilm (MBBR) reactors, can partly describe the N_2O emission data from the three side-stream treatment case studies. For the two SBR processes necessary model and parameter adjustments indicate that, while not included in the model, N_2O production by NH_2OH oxidation, is contributing as well. The N_2O emissions from the studied MBBR anammox process are satisfactory simulated by assuming heterotrophic denitrification only.

» The plant-wide model concept was calibrated to a real plant, the Käppala WWTP in Lidingö, Sweden. The model calibration under current operational conditions shows that the model is suitable for this type of conventional municipal treatment process. However, the model could not capture the full dynamics in the measurements of production and emission of N_2O. From this fact it is concluded that a model containing N_2O production from autotrophic and heterotrophic denitrification only is not sufficient.

To improve the energy assessment in BSM2 a more detailed aeration model was developed including oxygen transfer through diffusers, air distribution system and blowers. The conclusions from the three full-plant case studies can be summarised in three points.

» An aeration-model structure with backwards calculation of the quantities in the aeration system was found to be appropriate. Relationships for the various parts, from oxygen transfer to blowers, were selected and implemented in the BSM system.

» The tested aeration model proved to be simple and robust. With straightforward adjustments – mainly of the SOTE polynomial and airflow limitations – acceptable accuracy was achieved for all three cases. Limiting the air supply to actual values was shown to be critical in dynamic simulations.

» The results emphasise the importance of modelling the aeration system beyond just K_La input. Airflow rate is a critical variable for evaluating air consumption, aeration energy performance and for communicating simulation results to utility staff. Including a blower model allows for assessing dynamics in power consumption.

Models and procedures for including anaerobic co-digestion in BSM2 were developed. The plant-wide integration of a flexible co-digestion model structure was presented. Moreover,

a procedure for substrate characterisation, including both estimation of substrate dependent parameters and fractionation of organics and nitrogen, was suggested. The following conclusions can be drawn from the work on co-digestion.

- Non-linear parameter estimation was used to estimate the first-order hydrolysis coefficients and the ultimate methane yields from 18 datasets using BMP batch data. The parameter uncertainty was lower when fitting data to a first-order model compared to a Monod-type function since a first-order model could better describe the shape of the cumulative gas production in the BMP tests.
- The hydrolysis rate coefficients for the studied substrates were in the range 0.08 to 0.70 d^{-1}, i.e. comparable to results found in other studies.
- A new input model for fractionation of COD was developed, based on feasible and affordable tests. The method was proven reliable by modelling of BMP tests of the three substrates paunch, blood and flotation sludge.
- A sensitivity analysis of co-substrate feed characteristics showed that, apart from the biodegradable fraction of COD, protein and lipid fractions of particulate biodegradable COD were the two most important state variables for determining digester stability and methane production, and that different substrates caused different modes of failure.

To assess the global environmental impact, the dynamic process models were coupled to a life cycle analysis (LCA) model. For the first time, this model concept was calibrated to a real plant, the Käppala WWTP in Lidingö, Sweden. Two simulation studies were performed leading to the following conclusions.

- The current operational strategy, with simultaneous precipitation and predenitrification utilising internal COD, was compared to a strategy with extensive preprecipitation and adding methanol in the anoxic zones. The comparative simulations show that several of the initial goals for the strategy are fulfilled, i.e. higher gas production and an overall decrease in Global Warming Potential (28 %). However, at the same time the LCA reveals that the Abiotic Depletion of both elemental and fossil resources increase by 77 % and 305 %, respectively. Also the Ozone Layer Depletion increases manyfold but from a very low initial level.
- The simulation study imposing stricter effluent constraints showed that process modifications were necessary to manage the treatment and that the change at the same time increased the off-site environmental impacts in some categories. The choice of input goods, such as carbon source and electrical power, had a significant impact on the results.

From the general results of the research it can be concluded that – although the results from the different studies are specific for the case studies – the models could successfully be applied and calibrated to several different treatment plants. This demonstrates that the methodology is applicable for use at other similar conventional wastewater treatment plants with minor modifications. The coupled dynamic process and LCA modelling methodology captures plant-wide and global effects that would not only have been impossible to detect with standard spread-sheet calculations but would also remain hidden using any of the models separately. The importance of considering the water and sludge line together when evaluating changes in the anaerobic digestion or sludge systems are evident, as it was shown to have effects on both greenhouse gas emissions and treatment efficiency. Generally, the examined operational strategies in the different studies revealed several trade-offs between, for example effluent quality, greenhouse gas emissions and resource use. The results from this type of combined study create a much better basis for selecting operational strategies at WWTPs.

7.2 Future Research

Items of interest for future research were identified in each of the four modelling areas in this work: greenhouse gas emissions, aeration, co-digestion and multi-objective assessment including on- and off-site processes.

Production and emission of greenhouse gases at wastewater treatment plants are hot topics. On-going research continuously increase our knowledge of these processes and it is reasonable to expect that the current state of knowledge is not complete. Also in modelling of greenhouse gases, specifically for N_2O, new developments have been presented regularly during the research work presented here. Of necessity, one process model configuration had to be selected for implementation in the plant-wide model. The best model available at the time was used. However, new models. incorporating the latest process understanding, have recently been presented. The conclusions from the case studies on side-stream treatment and full-scale treatment at Käppala wastewater treatment plant indicate that models including additional production pathways need to be considered in future work. The emissions of N_2O also indicate that the stripping model may be overly simplified. Alternative descriptions allowing for in-tank concentrations and emissions to air to better align with measurement data should be investigated. Regarding the emissions of CO_2, the distinction of biogenic and non-biogenic emissions should be visualised by acknowledging the origin of the organic material degraded. Furthermore, for completeness it would be informative if the CH_4 emissions in the headworks, originating from the sewer network, were included.

The aeration model presented has been tested in several case studies. However, the air distribution and blower part of the model were only partly included in these studies. More

case studies should be conducted to validate these sub-models. Furthermore, including the characteristics of control valves for the airflow have not been tested. In conjunction to the important energy consumption for aeration there are other major energy consuming units at wastewater treatment plants. Pumping is one process where dynamic models have been presented, which could be considered for inclusion in future work.

The proposed method for characterising co-substrates is limited to solid substrates and modifications for soluble substrates should be investigated. Moreover, the method still includes an analysis of total COD, which is known to be unreliable for complex substrates. Future research should search for characterisation procedures where this analysis could be replaced by better alternatives. Although digester stability was addressed in this work, an extended anaerobic digestion model – capturing more of the processes destabilising digesters at high organic loading rates – should be developed to even better benefit from modelling of co-digestion.

In the presented work on including off-site environmental impact through coupling dynamic process models to LCA, the operational costs were not fully incorporated. An analysis of operational costs, in line with the standard Benchmark Simulation Model platform, should be included in future versions of the tool. To achieve this, specific costs for some transports and input goods must be included along with gate fees for external co-substrates. Furthermore, in the case study at the Käppala treatment plant the impact of sludge disposal was not included. For other cases, data might be available to include transport and disposal of dewatered sludge in the LCA model. Sludge disposal is important to include in future studies using the tool, especially if the evaluated operational strategies have a significant impact on sludge production.

References

Alex, J., Binh To, T., Hartwig, P., 2002. Improved design and optimization of aeration control for WWTPs by dynamic simulation. Water Science and Technology 45(4-5), 365–372.

Amerlinck, Y., Bellandi, G., Amaral, A., Weijers, S., Nopens, I., 2016. Detailed off-gas measurements for improved modelling of the aeration performance at the WWTP of Eindhoven. Water Science and Technology 74(1), 203–211.

Angelidaki, I., Alves, M., Bolzonella, D., Borzacconi, L., Campos, J.L., Guwy, A.J., Kalyuzhnyi, S., Jenicek, P., van Lier, J.B., 2009. Defining the biomethane potential (BMP) of solid organic wastes and energy crops: a proposed protocol for batch assays. Water Science and Technology 59(5), 927–934.

Ardern, E., Lockett, W.T., 1914. Experiments on the oxidation of sewage without the aid of filters. Journal of the Society of Chemical Industry 33(10), 523–539.

Arnell, M., 2013. Utsläpp av lustgas och metan från avloppssystem – en granskning av kunskapsläget. Technical report SVU 2013-11. The Swedish Water and Wastewater Association, Stockholm, Sweden.

Arnell, M., 2015. Implementation of the Bürger-Diehl settler model on the benchmark simulation platform. Technical report LUTEDX/(TEIE-7250)/1-48/(2015). Division of Industrial Electrical Engineering and Automation, Lund University, Lund, Sweden.

Arnell, M., Astals, S., Åmand, L., Batstone, D.J., Jensen, P.D., Jeppsson, U., 2016a. Substrate fractionation for modelling of anaerobic co-digestion with a plant-wide perspective. 5th IWA/WEF Wastewater Treatment Modelling Seminar (WWTmod2016), Annecy, France, 2-6 April, 2016.

Arnell, M., Jeppsson, U., 2012. Balancing effluent quality, greenhouse gas emissions and operational cost – developing dynamical models for intergrated benchmarking of wastewater treatment plants. Vatten – Journal of Water Management and Research 68(4), 295–301.

Arnell, M., Jeppsson, U., Rahmberg, M., Oliveira, F., Carlsson, B., 2016b. Modellering av avloppsreningsverk för multikriteriebedömning av prestanda och miljöpåverkan. Technical report SVU 2016 [submitted]. The Swedish Water and Wastewater Association, Stockholm, Sweden.

Arnell, M., Lopez, M., Palmgren, T., 2016c. Förkommersiell innovationsupphandling av kvicksilverfri COD-analys. Technical report SP 2016-39. SP Technical Research Institute of Sweden, Borås, Sweden.

Arnell, M., Rahmberg, M., Oliveira, F., Jeppsson, U., 2016d. Evaluating environmental performance of operational strategies at WWTPs. 10th IWA World Water Congress and Exhibition (WWC&E2016), Brisbane, Australia, 9-13 October, 2016.

Arnell, M., Sehlén, R., Jeppsson, U., 2013. Practical use of wastewater treatment modelling and simulation as a decision support tool for plant operators – case study on aeration control at Linköping wastewater treatment plant. 13th Nordic Wastewater Treatment Conference (NORDIWA2013), Malmö, Sweden, 8-10 October, 2013.

Arnell, M., Åmand, L., 2014. Anaerobic co-digestion in plant-wide wastewater treatment models. Technical report CODEN:LUTEDX/(TEIE-7246)/1-26/(2014). Division of Industrial Electrical Engineering and Automation, Lund University, Lund, Sweden.

ASCE, 2007. Measurement of oxygen transfer in clean water. Technical report ASCE/EWRI 2-06. American Society of Civil Engineers, New York, NY, USA.

Astals, S., Esteban-Gutierrez, M., Fernandez-Arevalo, T., Aymerich, E., Garcia-Heras, J.L., Mata-Ahiarez, J., 2013. Anaerobic digestion of seven different sewage sludges: A biodegradability and modelling study. Water Research 47(16), 6033–6043.

Aymerich, I., Rieger, L., Sobhani, R., Rosso, D., Corominas, L., 2015. The difference between energy consumption and energy cost: Modelling energy tariff structures for water resource recovery facilities. Water Research 81, 113–123.

Bachis, G., Maruejouls, T., Tik, S., Amerlinck, Y., Melcer, H., Nopens, I., Lessard, P., Vanrolleghem, P.A., 2015. Modelling and characterization of primary settlers in view of whole plant and resource recovery modelling. Water Science and Technology 72(12), 2251–2261.

Balmér, P., 2000. Operation costs and consumption of resources at Nordic nutrient removal plants. Water Science and Technology 41(9), 273–279.

Baresel, C., Dalgren, L., Almemark, M., Lazic, A., 2016. Environmental performance of wastewater reuse systems: impact of system boundaries and external conditions. Water Science and Technology 73(6), 1387–1394.

Barker, P.S., Dold, P.L., 1995. COD and nitrogen mass balances in activated-sludge systems. Water Research 29(2), 633–643.

Barnard, J.L., 1974. Cut P and N without chemicals. Water and Wastes Engineering 11(7), 33–36.

Batstone, D.J., 2013. Teaching uncertainty propagation as a core component in process engineering statistics. Education for Chemical Engineers 8(4), 132–139.

Batstone, D.J., Keller, J., Angelidaki, R.I., Kalyuzhnyi, S.V., Pavlostathis, S.G., Rozzi, A., Sanders, W.T.M., Siegrist, H., Vavilin, V.A., 2002. Anaerobic Digestion Model No. 1. Technical report IWA Scientific and Technical Report No. 13. IWA Publishing, London, UK.

Batstone, D.J., Puyol, D., Flores-Alsina, X., Rodriguez, J., 2015. Mathematical modelling of anaerobic digestion processes: applications and future needs. Reviews in Environmental Science and Bio/Technology 14(4), 595–613.

Batstone, D.J., Tait, S., Starrenburg, D., 2009. Estimation of hydrolysis parameters in full-scale anerobic digesters. Biotechnology and Bioengineering 102(5), 1513–1520.

Batstone, D.J., Virdis, B., 2014. The role of anaerobic digestion in the emerging energy economy. Current Opinion in Biotechnology 27, 142–149.

Baumann, H., Tillman, A.M., 2004. The hitch hiker's guide to LCA (Life Cycle Assessment): an orientation in Life Cycle Assessment methodology and application. Studentlitteratur, Lund, Sweden.

Beltrán, S., Logroño, C., Maiza, M., Ayesa, A., 2013. Model-based optimization of aeration systems in WWTPs. 11th IWA Conference on Instrumentation, Control and Automation (ICA2013), Narbonne, France, 18-20 September, 2013.

Beltrán, S., Maiza, M., de la Sota, A., Villanueva, J.M., Odriozola, V., Ayesa, A., 2011. Model-based optimization of aeration systems in WWTPs. 8th IWA Symposium on Systems Analysis and Integrated Assessment (Watermatex2011), San Sebastián, Spain, 20-22 June, 2011.

Björlenius, B., 1994. Lustgasutsläpp från kommunala reningsverk. Technical report No. 4390. Swedish Environmental Protection Agency, Solna, Sweden.

Bolong, N., Ismail, A.F., Salim, M.R., Matsuura, T., 2009. A review of the effects of emerging contaminants in wastewater and options for their removal. Desalination 239(1-3), 229–246.

Bridle, T., Shaw, A., Cooper, S., Yap, K., Third, K., Domurad, M., 2008. Estimation of greenhouse gas emissions from wastewater treatment plants. 5th IWA World Water Congress (WWC2008), Vienna, Austria, 7-12 September, 2008.

Bürger, R., Diehl, S., Farås, S., Nopens, I., Torfs, E., 2013. A consistent modelling methodology for secondary settling tanks: a reliable numerical method. Water Science and Technology 68(1), 192–208.

Cooper, P.F., 2001. Historical aspects of wastewater treatment, in: Lens, P., Zeeman, G., Lettinga, G. (Eds.), Decentralised sanitation and reuse: Concepts, systems and implementation. IWA Publishing, London, UK.

Corominas, L., Flores-Alsina, X., Snip, L., Vanrolleghem, P.A., 2012. Comparison of different modeling approaches to better evaluate greenhouse gas emissions from whole wastewater treatment plants. Biotechnology and Bioengineering 109(11), 2854–2863.

Corominas, L., Foley, J., Guest, J.S., Hospido, A., Larsen, H.F., Morera, S., Shaw, A., 2013a. Life cycle assessment applied to wastewater treatment: State of the art. Water Research 47(15), 5480–5492.

Corominas, L., Larsen, H.F., Flores-Alsina, X., Vanrolleghem, P.A., 2013b. Including life cycle assessment for decision-making in controlling wastewater nutrient removal systems. Journal of Environmental Management 128, 759–767.

Crosby, C., Brown, K., Sheehan, M., Fullerton, R., Roge, W., 2010. A step forward in the simulation of diffused aeration systems. 51st Water New Zealand Annual Conference and Expo, Rotorua, New Zealand, 3 August, 2010.

Czepiel, P.M., Crill, P.M., Harriss, R.C., 1993. Methane emissions from municipal wastewater treatment processes. Environmental Science and Technology 27(12), 2472–2477.

Daelman, M.R.J., van Voorthuizen, E.M., van Dongen, U., Volcke, E.I.P., van Loosdrecht, M.C.M., 2012. Methane emission during municipal wastewater treatment. Water Research 46(11), 3657–3670.

Daigger, G.T., 2011. A practitioner's perspective on the uses and future developments for wastewater treatment modelling. Water Science and Technology 63(3), 516–526.

Derbal, K., Bencheikh-Iehocine, M., Cecchi, F., Meniai, A.H., Pavan, P., 2009. Application of the IWA ADM1 model to simulate anaerobic co-digestion of organic waste with waste activated sludge in mesophilic condition. Bioresource Technology 100(4), 1539–1543.

Dold, P., Fairlamb, M., 2001. Estimating oxygen transfer K_La, SOTE and air flow requirements in fine bubble diffused air systems. 74th Water Environment Federation's Annual Technical Exhibition and Conference (WEFTEC2001), Atlanta, Georgia, 13-17 October, 2001.

Dold, P.L., Ekama, G.A., Marais, G.v.R., 1980. The activated sludge process 1. A general model for the activated sludge process. Progress in Water Technology 12(6), 47–77.

Eitrem Holmgren, K., Li, H., Verstraete, W., Cornel, P., 2015. State of the art compendium report on resource recovery from water. Technical report IWA Resource Recovery Cluster. International Water Association, London, UK.

Ekama, G.A., 2009. Using bioprocess stoichiometry to build a plant-wide mass balance based steady-state WWTP model. Water Research 43(8), 2101–2120.

Elías-Maxil, J.A., van der Hoek, J.P., Hofman, J., Rietveld, L., 2014. Energy in the urban water cycle: Actions to reduce the total expenditure of fossil fuels with emphasis on heat reclamation from urban water. Renewable and Sustainable Energy Reviews 30, 808–820.

Esposito, G., Frunzo, L., Panico, A., d'Antonio, G., 2008. Mathematical modelling of disintegration-limited co-digestion of OFMSW and sewage sludge. Water Science and Technology 58(7), 1513–1519.

FAO, 2016. AQUASTAT Main Database. Food and Agriculture Organization of the United Nations (FAO). Website accessed [01/08/2016 8:32].

de Faria, A.B.B., Sperandio, M., Ahmadi, A., Tiruta-Bama, L., 2015. Evaluation of new alternatives in wastewater treatment plants based on dynamic modelling and life cycle assessment (DM-LCA). Water Research 84, 99–111.

Ferriman, A., 2007. BMJ readers choose the "sanitary revolution" as greatest medical advance since 1840. BMJ: British Medical Journal 334, 111.

Fiter, M., Guell, D., Comas, J., Colprim, J., Poch, M., Rodriguez-Roda, I., 2005. Energy saving in a wastewater treatment process: An application of fuzzy logic control. Environmental Technology 26(11), 1263–1270.

Flores-Alsina, X., Arnell, M., Amerlinck, Y., Corominas, L., Gernaey, K., Guo, L., Lindblom, E., Nopens, I., Porro, J., Shaw, A., 2012a. A dynamic modelling approach to evaluate GHG emissions from wastewater treatment plants. IWA World Congress on Water, Climate and Energy (WCE2012), Dublin, Ireland, 13-18 May, 2012.

Flores-Alsina, X., Arnell, M., Amerlinck, Y., Corominas, L., Gernaey, K.V., Guo, L., Lindblom, E., Nopens, I., Porro, J., Shaw, A., Snip, L., Vanrolleghem, P.A., Jeppsson, U., 2012b. Balancing effluent quality, economical cost and greenhouse gas emissions during the evaluation of plant-wide wastewater treatment control strategies. IWA Conference on Nutrient Removal and Recovery 2012: Trends in NRR, Harbin, China, 23-25 September, 2012.

Flores-Alsina, X., Arnell, M., Armerlinck, Y., Corominas, L., Gernaey, K.V., Guo, L., Lindblom, E., Nopens, I., Porro, J., Shaw, A., Snip, L., Vanrolleghem, P.A., Jeppsson, U., 2014. Balancing effluent quality, economic cost and greenhouse gas emissions during the evaluation of (plant-wide) control/operational strategies in WWTPs. Science of the Total Environment 466(1), 616–624.

Flores-Alsina, X., Corominas, L., Snip, L., Vanrolleghem, P.A., 2011. Including greenhouse gas emissions during benchmarking of wastewater treatment plant control strategies. Water Research 45(16), 4700–4710.

Foley, J., Lant, P., 2007. Fugitive greenhouse gas emissions from wastewater systems. Technical report 192076030X. Water Services Association of Australia, Melbourne, Vic., Australia.

Foley, J., Yuan, Z., Keller, J., Senante, E., Chandran, K., Willis, J., van Loosdrecht, M.C.M., van Voorthuizen, E., 2011. N_2O and CH_4 emission from wastewater collection and treatment systems. Technical report GWRC 2011-30. Global Water Research Coalition, London, UK.

Frijns, J., Middleton, R., Uijterlinde, C., Wheale, G., 2012. Energy efficiency in the European water industry: learning from best practices. Journal of Water and Climate Change 3(1), 11–17.

Fruergaard, T., Astrup, T., 2011. Optimal utilization of waste-to-energy in an LCA perspective. Waste Management 31(3), 572–582.

Fujie, K., Sekizawa, T., Kubota, H., 1983. Liquid mixing in activated sludge aeration tank. Journal of Fermentation Technology 61(3), 295–304.

Galí, A., Benabdallah, T., Astals, S., Mata-Alvarez, J., 2009. Modified version of ADM1 model for agro-waste application. Bioresource Technology 100(11), 2783–2790.

Gao, H., Scherson, Y.D., Wells, G.F., 2014. Towards energy neutral wastewater treatment: methodology and state of the art. Environmental Science: Processes and Impacts 16(6), 1223–1246.

Gernaey, K., Jeppsson, U., Vanrolleghem, P., Copp, J., 2014. Benchmarking of control strategies for wastewater treatment plants. Technical report IWA Scientific and Technical Report No. 21. IWA Publishing, London, UK.

Gernaey, K., Rosen, C., Jeppsson, U., 2006. WWTP dynamic disturbance modelling – an essential module for long-term benchmarking development. Water Science and Technology 53(4-5), 225–234.

Girault, R., Bridoux, G., Nauleau, F., Poullain, C., Buffet, J., Steyer, J.P., Sadowski, A.G., Beline, F., 2012. A waste characterisation procedure for ADM1 implementation based on degradation kinetics. Water Research 46(13), 4099–4110.

Gori, R., Giaccherini, F., Jiang, L.M., Sobhani, R., Rosso, D., 2013. Role of primary sedimentation on plant-wide energy recovery and carbon footprint. Water Science and Technology 68(4), 870–878.

Guinée, J., Gorrée, M., Heijungs, R., Huppes, G., Kleijn, R., de Koning, A., van Oers, L., Wegener Sleeswijk, A., Suh, S., Udo de Haes, H., de Bruijn, H., van Duin, R., Huijbregts, M., 2002. Handbook on life cycle assessment. Operational guide to the ISO standards. I: LCA in perspective. IIa: Guide. IIb: Operational annex. III: Scientific background. Kluwer Academic Publishers, Dordrecht, The Netherlands.

Gunnarsson, I., von Hoffman, V., Holmgren, M., Kristensson, I., Liljemark, S., Pettersson, A., 2005. Metoder att mäta och reducera emissioner från system med rötning och uppgradering av biogas. Technical report RVF Utveckling 2005:07. The Swedish Waste and Management Association, Stockholm, Sweden.

Guo, L., 2014. Greenhouse gas emissions from and storm impacts on wastewater treatment plants: Process modelling and control. Ph.D. thesis. Université Laval, Québec, Canada.

Guo, L.S., Vanrolleghem, P.A., 2014. Calibration and validation of an activated sludge model for greenhouse gases no. 1 (ASMG1): prediction of temperature-dependent N_2O emission dynamics. Bioprocess and Biosystems Engineering 37(2), 151–163.

Gustavsson, D.J.I., la Cour Jansen, J., 2011. Dynamics of nitrogen oxides emission from a full-scale sludge liquor treatment plant with nitritation. Water Science and Technology 63(12), 2838–2845.

Gustavsson, D.J.I., Tumlin, S., 2013. Carbon footprints of Scandinavian wastewater treatment plants. Water Science and Technology 68(4), 887–893.

Gustavsson, D.J.I., Tumlin, S., 2014. Carbon footprint for wastewater treatment plants. Technical report SVU 2014-02. The Swedish Water and Wastewater Association, Stockholm, Sweden.

Heidrich, E.S., Curtis, T.P., Dolfing, J., 2011. Determination of the internal chemical energy of wastewater. Environmental Science and Technology 45(2), 827–832.

Heimersson, S., Svanström, M., Laera, G., Peters, G., 2016. Life cycle inventory practices for major nitrogen, phosphorus and carbon flows in wastewater and sludge management systems. International Journal of Life Cycle Assessment 21(8), 1197–1212.

Henze, M., Grady Jr, C.P.L., Gujer, W., Marais, G.v.R., Matsuo, T., 1987. Activated Sludge Model No. 1. Technical report Scientific and Technical Report No. 1. IWA Publishing, London, UK.

Henze, M., Gujer, W., Mino, T., van Loosdrecht, M.C.M., 2000. Activated Sludge Models ASM1, ASM2, ASM2d and ASM3. Technical report IWA Scientific and Technical Report No. 9. IWA Publishing, London, UK.

Henze, M., Harremoës, P., la Cour Jansen, J., Arvin, E., 2002. Wastewater treatment: biological and chemical processes. 3rd ed., Springer Science and Business Media, Berlin, Germany.

Hiatt, W.C., Grady, C.P.L., 2008. An updated process model for carbon oxidation, nitrification, and denitrification. Water Environment Research 80(11), 2145–2156.

Hofman, J., Hofman-Caris, R., Nederlof, M., Frijns, J., van Loosdrecht, M.C.M., 2011. Water and energy as inseparable twins for sustainable solutions. Water Science and Technology 63(1), 88–92.

IEA, 2011. Emissions from fuel combuistion. Highlights. Technical report. International Energy Agency, Paris, France.

IPCC, 2006. Wastewater treatment and discharge, in: Eggleston, H.S., Buendia, L., Miwa, K., Ngara, T., Tanabe, K. (Eds.), 2006 IPCC guidelines for national greenhouse gas inventories, vol. 5, Waste. Institute for Global Environmental Strategies, Hayama, Japan.

IPCC, 2013. Climate change 2013: the physical science basis. Contribution of working group I to the fifth assessment report of the intergovernmental panel on climate change. Cambridge University Press, Cambridge, United Kingdom and New York, NY, USA.

ISO 14040, 2006. Environmental management - Life cycle assessment - Principles and framework. International Organization for Standardization, Geneva, Switzerland.

IWA, 2014. International statistics for water services 2014. Technical report. International Water Association, London, UK.

Jenicek, P., Bartacek, J., Kutil, J., Zabranska, J., Dohanyos, M., 2012. Potentials and limits of anaerobic digestion of sewage sludge: Energy self-sufficient municipal wastewater treatment plant? Water Science and Technology 66(6), 1277–1281.

Jensen, P.D., Ge, H., Batstone, D.J., 2011. Assessing the role of biochemical methane potential tests in determining anaerobic degradability rate and extent. Water Science and Technology 64(4), 880–886.

Jeppsson, U., 1996. Modelling aspects of wastewater treatment processes. Ph.D. thesis. Lund University, Lund, Sweden, ISBN: 91-88934-00-4.

Jeppsson, U., Alex, J., Batstone, D.J., Benedetti, L., Comas, J., Copp, J.B., Corominas, L., Flores-Alsina, X., Gernaey, K.V., Nopens, I., Pons, M.N., Rodriguez-Roda, I., Rosen, C., Steyer, J.P., Vanrolleghem, P.A., Volcke, E.I.P., Vrecko, D., 2013. Benchmark simulation models, quo vadis? Water Science and Technology 68(1), 1–15.

Jeppsson, U., Pons, M.N., Nopens, I., Alex, J., Copp, J.B., Gernaey, K.V., Rosen, C., Steyer, J.P., Vanrolleghem, P.A., 2007. Benchmark Simulation Model no. 2: general protocol and exploratory case studies. Water Science and Technology 56(8), 67–78.

Jimenez, J., Aemig, Q., Doussiet, N., Steyer, J.P., Houot, S., Patureau, D., 2015. A new organic matter fractionation methodology for organic wastes: Bioaccessibility and complexity characterization for treatment optimization. Bioresource Technology 194, 344–353.

Johnson, T.L., McKinney, R.E., 1994. Modeling full-scale diffused aeration systems: critical issues in water and wastewater treatment. ASCE National Conference on Environmental Engineering, ASCE, Boulder, Colorado, USA, 11-13 July, 1994.

Jönsson, H., Junestedt, C., Willén, A., Yang, J., Tjus, K., Baresel, C., Rodhe, L., Trela, J., Pell, M., Andersson, S., 2015. Minska utsläpp av växthusgaser från rening av avlopp och hantering av avloppsslam. Technical report SVU 2015-02. The Swedish Water and Wastewater Association, Stockholm, Sweden.

Kaelin, D., Manser, R., Rieger, L., Eugster, J., Rottermann, K., Siegrist, H., 2009. Extension of ASM3 for two-step nitrification and denitrification and its calibration and validation with batch tests and pilot scale data. Water Research 43(6), 1680–1692.

Kaliman, A., Rosso, D., Leu, S.Y., Stenstrom, M.K., 2008. Fine-pore aeration diffusers: Accelerated membrane ageing studies. Water Research 42(1-2), 467–475.

Kampschreur, M.J., Poldermans, R., Kleerebezem, R., van der Star, W.R.L., Haarhuis, R., Abma, W.R., Jetten, M.S.M., van Loosdrecht, M.C.M., 2009a. Emission of nitrous oxide and nitric oxide from a full-scale single-stage nitritation-anammox reactor. Water Science and Technology 60(12), 3211–3217.

Kampschreur, M.J., Temmink, H., Kleerebezem, R., Jetten, M.S.M., van Loosdrecht, M.C.M., 2009b. Nitrous oxide emission during wastewater treatment. Water Research 43(17), 4093–4103.

Karlsson-Ottosson, U., 2015. Första svenska reningssteget för läkemedel installerat. Volume 2015-10-19 of *Ny Teknik*. Talentum Media, Stockholm, Sweden.

Kleerebezem, R., van Loosdrecht, M.C.M., 2006. Waste characterization for implementabon in ADM1. Water Science and Technology 54(4), 167–174.

Koch, K., Drewes, J.E., 2014. Alternative approach to estimate the hydrolysis rate constant of particulate material from batch data. Applied Energy 120, 11–15.

Kristoffersson, T., 2014. Vatten renas med ozon. Volume 2014-07-07 of *Östgöta Correspondenten*. NTM – Norrköpings Tidningars Media AB, Linköping, Sweden.

Kynch, G.J., 1952. A theory of sedimentation. Transactions of the Faraday Society 48, 166–176.

Larsen, T.A., 2015. CO_2-neutral wastewater treatment plants or robust, climate-friendly wastewater management? A systems perspective. Water Research 87, 513–521.

Law, Y., Jacobsen, G.E., Smith, A.M., Yuan, Z.G., Lant, P., 2013a. Fossil organic carbon in wastewater and its fate in treatment plants. Water Research 47(14), 5270–5281.

Law, Y., Lant, P., Yuan, Z.G., 2013b. The confounding effect of nitrite on N_2O production by an enriched ammonia-oxidizing culture. Environmental Science and Technology 47(13), 7186–7194.

Law, Y., Ni, B.J., Lant, P., Yuan, Z.G., 2012a. N_2O production rate of an enriched ammonia-oxidising bacteria culture exponentially correlates to its ammonia oxidation rate. Water Research 46(10), 3409–3419.

Law, Y.Y., Ye, L., Pan, Y.T., Yuan, Z.G., 2012b. Nitrous oxide emissions from wastewater treatment processes. Philosophical Transactions of the Royal Society of London. Series B, Biological Sciences 367(1593), 1265–1277.

Lewis, W.K., Whitman, W.G., 1924. Principles of gas absorption. Industrial and Engineering Chemistry 16(12), 1215–1220.

Liebetrau, J., Clemens, J., Cuhls, C., Hafermann, C., Friehe, J., Weiland, P., Daniel-Gromke, J., 2010. Methane emissions from biogas-producing facilities within the agricultural sector. Engineering in Life Sciences 10(6), 595–599.

Lindberg, C.F., 1997. Control and estimation strategies applied to the activated sludge process. Ph.D. thesis. Uppsala University, Uppsala, Sweden, ISBN: 91-506-1202-6.

Lindblom, E., 2011. Uppställande och kalibrering av simuleringsmodell för test av driftstrategier på Bromma reningsverk. Technical report. Sweco Environment AB, Stockholm, Sweden.

Lindblom, E., Arnell, M., Flores-Alsina, X., Stenström, F., Gustavsson, D.J.I., Yang, J., Jeppsson, U., 2016. Dynamic modelling of nitrous oxide emissions from three Swedish sludge liquor treatment systems. Water Science and Technology 73(4), 798–806.

Lindblom, E., Arnell, M., Jeppsson, U., 2015. Modellering av lustgasemissioner från SBR- och anammoxprocesser för rejektvattenbehandling . Technical report SVU 2015-17. The Swedish Water and Wastewater Association, Stockholm, Sweden.

Lindblom, E., Arnell, M., Stenström, F., Tjus, K., Flores-Alsina, X., Jeppsson, U., 2013. Dynamic modelling and validation of nitrous oxide emissions from a full-scale nitrifying/denitrifying sequencing batch reactor treating anaerobic digester supernatant. 11th IWA Conference on Instrumentation, Control and Automation (ICA2013), Narbonne, France, 18-20 September, 2013.

Lingsten, A., 2014. Summering report for "Water and wastewater utilities contribution to Sweden's energy efficiency". Technical report SVU 2014-05. The Swedish Water and Wastewater Association, Stockholm, Sweden.

Lingsten, A., Lundkvist, M., 2008. Nulägesbeskrivning av VA-verkens energianvändning. Technical report SVU 2008-01. The Swedish Water and Wastewater Association, Stockholm, Sweden.

Lingsten, A., Lundkvist, M., Hellström, D., 2013. Swedish water and wastewater utilities use of energy in 2011. Technical report SVU 2013-17. The Swedish Water and Wastewater Association, Stockholm, Sweden.

Lingsten, A., Lundkvist, M., Hellström, D., Balmér, P., 2011. VA-verkens energianvändning 2008. Technical report SVU 2011-04. The Swedish Water and Wastewater Association, Stockholm, Sweden.

Liu, Y.W., Ni, B.J., Sharma, K.R., Yuan, Z.G., 2015. Methane emission from sewers. Science of the Total Environment 524, 40–51.

Ludzack, F.J., Ettinger, M.B., 1962. Controlling operation to minimize activated sludge effluent nitrogen. Journal Water Pollution Control Federation 34(9), 920–931.

Lundie, S., Peters, G.M., Beavis, P.C., 2004. Life Cycle Assessment for sustainable metropolitan water systems planning. Environmental Science and Technology 38(13), 3465–3473.

Lundin, E., Arnell, M., Tik, S., Vanrolleghem, P.A., Carlsson, B., 2015. Modelling chemically enhanced primary settlers for resource recovery purposes. 14th Nordic Wastewater Treatment Conference (NORDIWA2015), Bergen, Norway, 4-6 November, 2015.

Lundkvist, M., 2005. Energieffektivisering – rapport till möte med energimyndigheten. Technical report Sweco Report 2005-01-14T. Sweco Viak AB, Halmstad, Sweden.

Makinia, J., 2010. Mathematical modelling and computer simulation of activated sludge systems. IWA Publishing, London. UK.

Malmqvist, P., Heinicke, G., Kärrman, E., Stenström, T., Svensson, G., 2006. Strategic planning of sustainable urban water management. IWA Publishing, London, UK.

Mampaey, K.E., Beuckels, B., Kampschreur, M.J., Kleerebezem, R., van Loosdrecht, M.C.M., Volcke, E.I.P., 2013. Modelling nitrous and nitric oxide emissions by autotrophic ammonia-oxidizing bacteria. Environmental Technology 34(12), 1555–1566.

Mannina, G., Ekama, G., Caniani, D., Cosenza, A., Esposito, G., Gori, R., Garrido-Baserba, M., Rosso, D., Olsson, G., 2016. Greenhouse gases from wastewater treatment – A review of modelling tools. Science of the Total Environment 551, 254–270.

Marais, G.v.R., Ekama, G.A., 1976. The activated sludge process: Part 1 - steady state behaviour. Water SA 2, 163–200.

Mata-Alvarez, J., Dosta, J., Macé, S., Astals, S., 2011. Codigestion of solid wastes: A review of its uses and perspectives including modeling. Critical Reviews in Biotechnology 31(2), 99–111.

Mata-Alvarez, J., Dosta, J., Romero-Güiza, M.S., Fonoll, X., Peces, M., Astals, S., 2014. A critical review on anaerobic co-digestion achievements between 2010 and 2013. Renewable and Sustainable Energy Reviews 36, 412–427.

Matos, R., Cardoso, A., Duarte, P., Ashley, R., Molinari, A., Schulz, A., 2003. Performance indicators for wastewater services. IWA Publishing, London, UK.

Meneses, M., Concepcion, H., Vilanova, R., 2016. Joint environmental and economical analysis of wastewater treatment plants control strategies: a benchmark scenario analysis. Sustainability 8(4), 1–20.

Metcalf and Eddy, 2014. Wastewater engineering: treatment and resource recovery. 5th ed., McGraw-Hill Education, New York, NY, USA.

Mizuta, K., Shimada, M., 2010. Benchmarking energy consumption in municipal wastewater treatment plants in Japan. Water Science and Technology 62(10), 2256–2262.

Monod, J., 1949. The growth of bacterial cultures. Annual Reviews in Microbiology 3(1), 371–394.

Monteith, H.D., Sahely, H.R., MacLean, H.L., Bagley, D.M., 2005. A rational procedure for estimation of greenhouse-gas emissions from municipal wastewater treatment plants. Water Environment Research 77(4), 390–403.

Nelder, J.A., Mead, R., 1965. A simplex method for function minimization. The Computer Journal 7(4), 308–313.

Ni, B.J., Peng, L., Law, Y.Y., Guo, J.H., Yuan, Z.G., 2014. Modeling of nitrous oxide production by autotrophic ammonia-oxidizing bacteria with multiple production pathways. Environmental Science and Technology 48(7), 3916–3924.

Ni, B.J., Ruscalleda, M., Pellicer-Nacher, C., Smets, B.F., 2011. Modeling nitrous oxide production during biological nitrogen removal via nitrification and denitrification: extensions to the general ASM models. Environmental Science and Technology 45(18), 7768–7776.

Ni, B.J., Yuan, Z.G., 2015. Recent advances in mathematical modeling of nitrous oxides emissions from wastewater treatment processes. Water Research 87, 336–346.

Nocedal, J., Wright, S., 2006. Numerical optimization. 2nd ed., Springer Science and Business Media, New York, NY, USA.

Nopens, I., Batstone, D.J., Copp, J.B., Jeppsson, U., Volcke, E.I.P., Alex, J., Vanrolleghem, P.A., 2009. An ASM/ADM model interface for dynamic plant-wide simulation. Water Research 43(7), 1913–1923.

Nopens, I., Benedetti, L., Jeppsson, U., Pons, M.N., Alex, J., Copp, J.B., Gernaey, K.V., Rosen, C., Steyer, J.P., Vanrolleghem, P.A., 2010. Benchmark Simulation Model no. 2: finalisation of plant layout and default control strategy. Water Science and Technology 62(9), 1967–1974.

Nordell, E., Wiberg, L., 2013. Concomitant increase in biogas production and improved nitrogen removal by co-digestion of low nitrogen content substrates and primary sludge. 1st IWA conference on Holistic Sludge Management (HSM2013), Västerås, Sweden, 6-8 May, 2013.

Nowak, O., 2003. Benchmarks for the energy demand of nutrient removal plants. Water Science and Technology 47(12), 125–132.

Olivier, J.G.J., Janssens-Maenhout, G., Muntean, M., Peters, J.A.H.W., 2014. Trends in global CO_2 emissions: 2014 report. Technical report PBL1490 / JRC93171. PBL Netherlands Environmental Assessment Agency, The Hague, The Netherlands.

Olsson, G., 2012a. ICA and me – A subjective review. Water Research 46(6), 1585–1624.

Olsson, G., 2012b. Water and energy – Threats and opportunities. IWA Publishing, London, UK.

Olsson, G., Newell, B., 1999. Wastewater treatment systems: modelling, diagnosis and control. IWA Publishing, London, UK.

Otterpohl, R., Freund, M., 1992. Dynamic models for clarifiers of activated sludge plants with dry and wet weather flows. Water Science and Technology 26(5-6), 1391–1400.

Pan, Y.T., Ni, B.J., Bond, P.L., Ye, L., Yuan, Z.G., 2013a. Electron competition among nitrogen oxides reduction during methanol-utilizing denitrification in wastewater treatment. Water Research 47(10), 3273–3281.

Pan, Y.T., Ni, B.J., Lu, H.J., Chandran, K., Richardson, D., Yuan, Z.G., 2015. Evaluating two concepts for the modelling of intermediates accumulation during biological denitrification in wastewater treatment. Water Research 71, 21–31.

Pan, Y.T., Ni, B.J., Yuan, Z.G., 2013b. Modeling electron competition among nitrogen oxides reduction and N_2O accumulation in denitrification. Environmental Science and Technology 47(19), 11083–11091.

Parma, S., 1980. The history of the eutrophication concept and the eutrophication in the Netherlands. Hydrobiological Bulletin 14(1-2), 5–11.

Peng, L., Ni, B.J., Erler, D., Ye, L., Yuan, Z.G., 2014. The effect of dissolved oxygen on N_2O production by ammonia-oxidizing bacteria in an enriched nitrifying sludge. Water Research 66, 12–21.

Peng, L., Ni, B.J., Ye, L., Yuan, Z.G., 2015a. N_2O production by ammonia oxidizing bacteria in an enriched nitrifying sludge linearly depends on inorganic carbon concentration. Water Research 74, 58–66.

Peng, L., Ni, B.J., Ye, L., Yuan, Z.G., 2015b. Selection of mathematical models for N_2O production by ammonia oxidizing bacteria under varying dissolved oxygen and nitrite concentrations. Chemical Engineering Journal 281, 661–668.

Porro, J., Guo, L., Sharma, K., Benedetti, L., Van Hulle, S., Vanrolleghem, P., Amerlinck, Y., Yuan, Z., Shaw, A., Nopens, I., 2011. Towards a benchmarking tool for minimizing wastewater utility greenhouse gas footprints. 8^{th} IWA Symposium on Systems Analysis and Integrated Assessment (Watermatex2011), San Sebastián, Spain, 20-22 June, 2011.

Razaviarani, V., Buchanan, I.D., 2015. Calibration of the Anaerobic Digestion Model No. 1 (ADM1) for steady-state anaerobic co-digestion of municipal wastewater sludge with restaurant grease trap waste. Chemical Engineering Journal 266, 91–99.

Reardon, D.J., 1995. Turning down the power. Civil Engineering 65(8), 54–56.

Rieger, L., Alex, J., Gujer, W., Siegrist, H., 2006. Modelling of aeration systems at wastewater treatment plants. Water Science and Technology 53(4-5), 439–447.

Rieger, L., Gillot, S., Langergraber, G., Ohtsuki, T., Shaw, A., Tak, I., Winkler, S., 2012. Guidelines for using activated sludge models. Technical report IWA Scientific and Technical Report No. 22. IWA Publishing, London, UK.

Robertson, K., 1991. Emissions of N_2O in Sweden – Natural and anthropogenic sources. Ambio 20(3-4), 151–155.

Rodriguez-Garcia, G., Hospido, A., Bagley, D.M., Moreira, M.T., Feijoo, G., 2012. A methodology to estimate greenhouse gases emissions in life cycle inventories of wastewater treatment plants. Environmental Impact Assessment Review 37, 37–46.

Rosen, C., Arnell, M., 2007. Plant-wide control of WWTPs – a path to optimal operation. 10th Nordic Wastewater Conference (NORDIWA2007), Hamar, Norway, 11-14 November , 2007.

Rosso, D., Larson, L.E., Stenstrom, M.K., 2008. Aeration of large-scale municipal wastewater treatment plants: state of the art. Water Science and Technology 57(7), 973–978.

Rosso, D., Stenstrom, M.K., 2006. Surfactant effects on alpha-factors in aeration systems. Water Research 40(7), 1397–1404.

Rosso, D., Stenstrom, M.K., 2008. The carbon-sequestration potential of municipal wastewater treatment. Chemosphere 70(8), 1468–1475.

von Schulthess, R., Wild, D., Gujer, W., 1994. Nitric and nitrous oxides from denitrifying activated sludge at low-oxygen concentration. Water Science and Technology 30(6), 123–132.

Shizas, I., Bagley, D.M., 2004. Experimental determination of energy content of unknown organics in municipal wastewater streams. Journal of Energy Engineering – ASCE 130(2), 45–53.

Siegrist, H., Renggli, D., Gujer, W., 1993. Mathematical modelling of anaerobic mesophilic sewage sludge treatment. Water Science and Technology 27(2), 25–36.

Sniders, A.A., Laizans, D., 2006. Invariant control of wastewater aeration, in: Elleithy, K., Sobh, T., Mahmood, A., Iskander, M., Karim, M. (Eds.), Advances in computer, information, and systems sciences, and engineering. Springer, Dordrecht, The Netherlands.

Snip, L.J.P., Boiocchi, R., Flores-Alsina, X., Jeppsson, U., Gernaey, K.V., 2014. Challenges encountered when expanding activated sludge models: a case study based on N_2O production. Water Science and Technology 70(7), 1251–1260.

Solon, K., Flores-Alsina, X., Gernaey, K.V., Jeppsson, U., 2015. Effects of influent fractionation, kinetics, stoichiometry and mass transfer on CH_4, H_2 and CO_2 production for (plant-wide) modelling of anaerobic digesters. Water Science and Technology 71(6), 870–877.

Stenstrom, M.K., 1975. A dynamic model and computer compatible control strategies for wastewater treatment plants. Ph.D. thesis. Clemson University, Clemson, SC, USA.

Stenström, F., Tjus, K., la Cour Jansen, J., 2014. Oxygen-induced dynamics of nitrous oxide in water and off-gas during the treatment of digester supernatant. Water Science and Technology 69(1), 84–91.

Strömberg, S., 2015. Developments in feedstock analysis and process control for biogas production. Ph.D. thesis. Lund University, Lund, Sweden, ISBN: 978-91-7000-290-8.

Svardal, K., Kroiss, H., 2011. Energy requirements for waste water treatment. Water Science and Technology 64(6), 1355–1361.

Sweetapple, C.G., 2014. Developing strategies for the reduction of greenhouse gas emissions from wastewater treatment. Ph.D. thesis. University of Exeter, Exeter, UK.

SWMA, 2012. Sammanställning av mätningar inom Frivilligt åtagande 2007 - 2012. Technical report U2012:15. The Swedish Waste Management Association, Malmö, Sweden.

Takács, I., Patry, G.G., Nolasco, D., 1991. A dynamic-model of the clarification thickening process. Water Research 25(10), 1263–1271.

Tallec, G., Garnier, J., Billen, G., Gousailles, M., 2006. Nitrous oxide emissions from secondary activated sludge in nitrifying conditions of urban wastewater treatment plants: Effect of oxygenation level. Water Research 40(15), 2972–2980.

The Swedish Energy Agency, 2015. Energiläget 2015. Technical report ET2015:08. The Swedish Energy Agency, Stockholm, Sweden.

Thunberg, A., Sundin, A.M., Palmgren, T., 2013. Ten years of optimising the biogas production at Käppala WWTP. 1st IWA conference on Holistic Sludge Management (HSM2013), Västerås, Sweden, 6-8 May, 2013.

USEPA, 1989. Design manual: Fine pore aeration systems. Technical report EPA/625/1-89/023. U.S. Environmental Protection Agency, Office of Research and Development, Cincinnati, OH, USA.

Venkatesh, G., Brattebø, H., 2011. Energy consumption, costs and environmental impacts for urban water cycle services: Case study of Oslo (Norway). Energy 36(2), 792–800.

Vitasovic, Z.Z., 1985. An integrated control system for the activated sludge process. Ph.D. thesis. Rice University, Houston, TX, USA.

Volcke, E.I.P., van Loosdrecht, M.C.M., Vanrolleghem, P.A., 2006. Continuity-based model interfacing for plant-wide simulation: A general approach. Water Research 40(15), 2817–2828.

Wernet, G., Bauer, C., Steubing, B., Reinhard, J., Moreno-Ruiz, E., Weidema, B., 2016. The ecoinvent database version 3 (part I): overview and methodology. International Journal of Life Cycle Assessment 21(9), 1218–1230.

Wett, B., Aichinger, P., Al-Omari, A., Jimenez, J., Wadhawan, T., Takács, I., Murthy, S., 2016. Combining energy- with mass-flow based process models within the fence of a wastewater treatment plant: energy fractionation for process characterization. 5th IWA/WEF Wastewater Treatment seminar (WWTmod2016), Annecy, France, 2-6 April, 2016.

Whitman, W.G., 1962. The two film theory of gas absorption. International Journal of Heat and Mass Transfer 5(5), 429–433.

Wiedmann, T., Minx, J., 2007. A definition of 'carbon footprint'. Technical report ISA UK Research Report 07-01. ISA UK Research and Consulting, Durham, UK.

Wright, L.A., Kemp, S., Williams, I., 2011. 'Carbon footprinting': towards a universally accepted definition. Carbon Management 2(1), 61–72.

Wunderlin, P., Mohn, J., Joss, A., Emmenegger, L., Siegrist, H., 2012. Mechanisms of N_2O production in biological wastewater treatment under nitrifying and denitrifying conditions. Water Research 46(4), 1027–1037.

Yang, J.J., Trela, J., Plaza, E., Tjus, K., 2013. N_2O emissions from a one stage partial nitrification/anammox process in moving bed biofilm reactors. Water Science and Technology 68(1), 144–152.

Zaher, U., Li, R., Jeppsson, U., Steyer, J.P., Chen, S., 2009. GISCOD: General Integrated Solid Waste Co-Digestion model. Water Research 43(10), 2717–2727.

Åmand, L., 2014. Ammonium feedback control in wastewater treatment plants. Ph.D. thesis. Uppsala University, Uppsala, Sweden, ISBN: 978-91-554-8900-7.

Åmand, L., Andersson, S., Arnell, M., Junestedt, C., Rahmberg, M., Lindblom, E., Thunberg, A., Nilsson, A., 2015. Simulating the environmental impact of stricter discharge criteria on nitrogen and phosphorous. 14th Nordic Wastewater Treatment Conference (NORDIWA2015), Bergen, Norway, 4-6 November, 2015.

Åmand, L., Andersson, S., Oliveira, F., Rahmberg, M., Junestedt, C., Arnell, M., 2016. New effluent criteria for Swedish wastewater treatment plants – effects on the plants' total environmental impact. Technical report SVU report 2016-12. The Swedish Water and Wastewater Association, Stockholm, Sweden.

Åmand, L., Olsson, G., Carlsson, B., 2013. Aeration control – a review. Water Science and Technology 67(11), 2374–2398.

Ødegaard, H., 1998. Optimised particle separation in the primary step of wastewater treatment. Water Science and Technology 37(10), 43–53.

Scientific publications

Paper 1

Science of the Total Environment 466–467 (2014) 616–624

Contents lists available at ScienceDirect

Science of the Total Environment

journal homepage: www.elsevier.com/locate/scitotenv

Balancing effluent quality, economic cost and greenhouse gas emissions during the evaluation of (plant-wide) control/operational strategies in WWTPs

Xavier Flores-Alsina [a,b], Magnus Arnell [a,c], Youri Amerlinck [d], Lluís Corominas [e], Krist V. Gernaey [b], Lisha Guo [f], Erik Lindblom [a,g], Ingmar Nopens [d], Jose Porro [d,h], Andy Shaw [i,j], Laura Snip [b], Peter A. Vanrolleghem [f], Ulf Jeppsson [a,*]

[a] Division of Industrial Electrical Engineering and Automation (IEA), Department of Measurement Technology and Industrial Electrical Engineering (MIE), Lund University, Box 118, SE-221 00 Lund, Sweden
[b] Center for Process Engineering and Technology (PROCESS), Department of Chemical and Biochemical Engineering, Technical University of Denmark, Building 229, DK-2800 Kgs. Lyngby, Denmark
[c] CIT Urban Water Management, Gjuterigatan 1D, SE-582 73 Linköping, Sweden
[d] BIOMATH, Department of Mathematical Modelling, Statistics and Bioinformatics, Ghent University, Coupure Links 653, B-9000 Ghent, Belgium
[e] ICRA, Catalan Institute for Water Research, Scientific and Technological Park of the University of Girona, H_2O Building, Emili Grahit 101, 17003 Girona, Spain
[f] ModelEAU, Département de génie civil et de génie des eaux, Université Laval, 1065 Avenue de la Médecine, Québec G1V 0A6, QC, Canada
[g] Sweco Environment, Gjörwellsgatan 22, SE-100 26 Stockholm, Sweden
[h] Laboratory of Chemical and Environmental Engineering (LEQUiA), University of Girona, Faculty of Sciences, Campus Montilivi s/n, 17071, Girona, Spain
[i] Black & Veatch, 8400, Ward Parkaway, Kansas City, MO 64114, USA
[j] Illinois Institute of Technology, 3300 South Federal Street, Chicago, IL 60616, USA

HIGHLIGHTS

- A 3-D graphical representation shows the interactions among effluent quality, operational cost and GHG emissions during the evaluation of operational/control strategies in WWTP.
- The study points out the importance of taking into account the existing interactions among the water and sludge line.
- The potentially undesirable effects of local energy optimization (aeration/biogas) are highlighted when calculating the total plant's overall global warming potential.

GRAPHICAL ABSTRACT

The 3-D representation of effluent quality (EQI), operational cost (OCI) and greenhouse gas emissions (GHG) during the evaluation of several (plant-wide) control/operational strategies: (1) modification of the DO set point, (2) modification of the primary clarifier TSS removal efficiency and (3) modification of the anaerobic digester temperature regime.

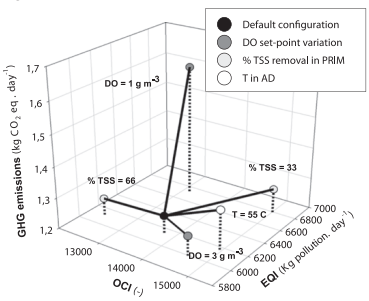

* Corresponding author at: Division of Industrial Electrical Engineering and Automation (IEA), Department of Measurement Technology and Industrial Electrical Engineering (MIE), Lund University, Box 118, SE-221 00 Lund, Sweden. Tel.: +46 46 222 92 87.
E-mail address: ulf.jeppsson@iea.lth.se (U. Jeppsson).

0048-9697/$ – see front matter © 2013 Elsevier B.V. All rights reserved.
http://dx.doi.org/10.1016/j.scitotenv.2013.07.046

ARTICLE INFO

Article history:
Received 2 April 2013
Received in revised form 2 July 2013
Accepted 13 July 2013
Available online 19 August 2013

Editor: Simon Pollard

Keywords:
Benchmarking
Global warming
Model-based evaluation
Multi-criteria decision making
Process control
Sustainability

ABSTRACT

The objective of this paper was to show the potential additional insight that result from adding greenhouse gas (GHG) emissions to plant performance evaluation criteria, such as effluent quality (EQI) and operational cost (OCI) indices, when evaluating (plant-wide) control/operational strategies in wastewater treatment plants (WWTPs). The proposed GHG evaluation is based on a set of comprehensive dynamic models that estimate the most significant potential on-site and off-site sources of CO_2, CH_4 and N_2O. The study calculates and discusses the changes in EQI, OCI and the emission of GHGs as a consequence of varying the following four process variables: (i) the set point of aeration control in the activated sludge section; (ii) the removal efficiency of total suspended solids (TSS) in the primary clarifier; (iii) the temperature in the anaerobic digester; and (iv) the control of the flow of anaerobic digester supernatants coming from sludge treatment. Based upon the assumptions built into the model structures, simulation results highlight the potential undesirable effects of increased GHG production when carrying out local energy optimization of the aeration system in the activated sludge section and energy recovery from the AD. Although off-site CO_2 emissions may decrease, the effect is counterbalanced by increased N_2O emissions, especially since N_2O has a 300-fold stronger greenhouse effect than CO_2. The reported results emphasize the importance and usefulness of using multiple evaluation criteria to compare and evaluate (plant-wide) control strategies in a WWTP for more informed operational decision making.

© 2013 Elsevier B.V. All rights reserved.

1. Introduction

The main focus in assessing the operation of wastewater treatment plants has historically been the effluent water quality under constraints of technical feasibility and cost. This certainly still holds, but the discussions on sustainability in general and the issue of climate change due to greenhouse gas (GHG) emissions in particular (Foley et al., 2011; Law et al., 2012; Rodriguez-Garcia et al., 2012) have widened the scope for the utilities. An increasing interest in GHG emissions calls for novel approaches to evaluate the performance of control and operational strategies in order to include additional performance indicators related to GHG emissions.

Aside from evaluating control and operational strategies (Nopens et al., 2010) before full-scale implementation (Ayesa et al., 2006), dynamic activated sludge models (ASM) (Henze et al., 2000) have been widely used for multiple purposes in wastewater engineering such as benchmarking (Gernaey et al., 2013), diagnosis (Olsson, 2012; Rodriguez-Roda et al., 2002), design (Rieger et al., 2012; Flores et al., 2007), teaching (Hug et al., 2009) and optimization (Rivas et al., 2008). Based on new knowledge on the chemical and biochemical mechanisms of GHG production, recent efforts have been made to capture the production and emissions of CO_2, CH_4 and N_2O and integrate these processes in the traditional ASM models (Batstone et al., 2002; Hiatt and Grady, 2008; Ni et al., 2013; Mampaey et al., 2013; Guo and Vanrolleghem, 2013).

Nevertheless, there are few studies discussing the additional benefit of adding a new dimension related to GHG production and emission to the traditional effluent quality and operational cost indices within the performance evaluation procedures (Flores-Alsina et al., 2011; Corominas et al., 2012; Guo et al., 2012). In this paper, an extended version of the International Water Association (IWA) Benchmark Simulation Model No. 2 (BSM2), i.e., BSM2G, is used for all simulations to demonstrate the benefit of adding this additional GHG emissions dimension.

A novelty of this paper includes the evaluation of plant-wide control/operational strategies through an integrated GHG modeling approach, representing the major pathways known to contribute significantly the plant-wide carbon footprint. These strategies involve changes related to the following process variables: (i) the dissolved oxygen (DO) set point of the aeration system in the activated sludge section; (ii) the removal efficiency of the total suspended solids (TSS) in the primary clarifier; (iii) the temperature in the anaerobic digester (AD); and (iv) the control of the flow of anaerobic digester supernatants from sludge treatment. Further, the authors in this paper consider the main interactions between the water and the sludge line. Finally, changes in effluent quality index (EQI), operational cost index (OCI) and CO_2, CH_4 and N_2O emissions are analyzed by means of a 3-D representation and thoroughly discussed. As a side effect, synergies and trade-offs between local energy optimization and the overall GHG production is studied in detail.

2. Methods

2.1. Wastewater treatment plants under study

The WWTP under study (BSM2G) has the same layout as the IWA BSM2 platform proposed by Nopens et al. (2010). The plant is treating an influent flow rate of 20,648 $m^3 \cdot day^{-1}$ and a total COD and N load of 12,240 and 1140 $kg \cdot day^{-1}$, respectively. Influent characteristics are generated following the principles stated in Gernaey et al. (2011). The activated sludge (AS) unit is a modified Ludzack-Ettinger configuration consisting of 5 tanks in series. Tanks 1 (ANOX1) and 2 (ANOX2) are anoxic (total volume = 3000 m^3), while tanks 3 (AER1), 4 (AER2) and 5 (AER3) are aerobic (total volume = 9000 m^3). AER3 and ANOX1 are linked by means of an internal recycle with the purpose of nitrate recycle for pre-denitrification. The BSM2G plant further contains a primary (PRIM) (900 m^3) and a secondary (SEC) clarifier (6000 m^3), a sludge thickener (THK), an anaerobic digester (AD) (3400 m^3), a storage tank (ST) (160 m^3) and a dewatering unit (DW). Additional information about the plant design and operational conditions can be found in Flores-Alsina et al. (2011).

The biological process model used in the study is described in detail in Guo and Vanrolleghem (2013). From the original set of models of BSM2, the Activated Sludge Model No. 1 (ASM1) (Henze et al., 2000) has been expanded with the principles proposed by Hiatt and Grady (2008) and Mampaey et al. (2013). The Hiatt and Grady model incorporates two nitrifying populations: ammonia oxidizing bacteria (AOB) and nitrite oxidizing bacteria (NOB) using free ammonia (NH_3) and free nitrous acid (FNA) as nitrogen substrate, respectively. The model also considers sequential reduction of nitrate (NO_3^-) to nitrogen gas (N_2) via nitrite (NO_2^-), nitric oxide (NO) and nitrous oxide (N_2O) using individual reaction-specific parameters. Additionally, the ideas summarized in Mampaey et al. (2013) are used to consider NO and N_2O formation from the nitrification pathway assuming ammonia (NH_3) as the electron donor. To account for seasonal variability, liquid–gas saturation constants, kinetic parameters, transfer coefficients and equilibrium reactions are temperature dependent. Stripping equations for the gases were implemented as in Foley et al. (2011). The interfaces presented in Nopens et al. (2009) have been modified to link the modified activated sludge model and the anaerobic digestion model (Batstone et al., 2002), by considering COD, N and charge balances for all oxidized nitrogen compounds. Further information about the GHG models and parameter values can be found in Corominas et al. (2012) and Guo et al. (2012).

Nomenclature

AD	anaerobic digester
ADM	anaerobic digestion model
AE	aeration energy (kWh·day^{-1})
AER	aerobic section
AOB	ammonium oxidizing bacteria
ANOX	anoxic section
ASM	activated sludge model
BOD	biochemical oxygen demand (g·m^{-3})
BSM2	Benchmark Simulation Model No 2
CH_4	methane (kg CH_4·day^{-1})
CO_2	carbon dioxide (kg CO_2·day^{-1})
CO_2e	equivalent carbon dioxide (kg CO_{2e}·day^{-1})
COD	chemical oxygen demand (g·m^{-3})
DO	dissolved oxygen concentration (g·m^{-3})
DW	dewatering unit
EC	consumption of external carbon source (kg COD·day^{-1})
EQI	effluent quality index (kg pollution·day^{-1})
GHG	greenhouse gas
GWP	global warming potential
HE	heating energy (kWh·day^{-1})
k_La	volumetric oxygen transfer coefficient (day^{-1})
ME	mixing energy (kWh·day^{-1})
MP	methane production (kg CH_4·day^{-1})
N	nitrogen
NH_4^+	ammonium nitrogen (g N·m^{-3})
NO	nitric oxide nitrogen (g N·m^{-3})
N_2O	nitrous oxide nitrogen (kg N·day^{-1})
NOB	nitrite oxidizing bacteria
NO_2^-	nitrite nitrogen (g N·m^{-3})
NO_3^-	nitrate nitrogen (g N·m^{-3})
NO_x	oxidized forms of nitrogen (g N·m^{-3})
OCI	operational cost index (cost unit·year^{-1})
PE	pumping energy (kWh·day^{-1})
PRIM	primary clarifier
PI	proportional integral controller
Q_{carb}	external carbon source flow rate (m^3·day^{-1})
Q_e	effluent flow rate (m^3·day^{-1})
Q_{intr}	internal recycle flow rate (m^3·day^{-1})
Q_r	external recirculation flow rate (m^3·day^{-1})
Q_w	waste sludge flow rate (m^3·day^{-1})
SEC	secondary clarifier
SP	sludge production (kg TSS·day^{-1})
SRT	sludge retention time (day)
ST	storage tank
THK	thickener
TKN	total Kjeldahl nitrogen (g·m^{-3})
TN	total nitrogen (g·m^{-3})
TSS	total suspended solids (g·m^{-3})
WWTP	wastewater treatment plant

2.2. Control strategy and simulated scenarios

The plant is simulated in a closed loop regime, which includes two PI control loops. The first loop controls the dissolved oxygen concentration in AER2 by manipulating the air supply rate, here implemented as the oxygen transfer coefficient K_La4 (set point = 2 g O_2 g·m^{-3}). K_La3 is set equal to K_La4 and K_La5 is set to half its value. The second loop controls the nitrate concentration in ANOX2 by manipulating the internal recycle flow rate (Q_{intr}). Two different waste sludge flow rates (Q_{w_winter} = 300 m^3·day^{-1} // Q_{w_summer} = 450 m^3·day^{-1}) are imposed in SEC depending on the time of the year in order to sustain the nitrifying biomass in the system during the winter period. Noise and delays are applied to sensor and actuator models to give the simulations more realism. The external recirculation flow rate (Q_r) and carbon source addition (Q_{carb}) remain constant throughout the simulations. Additional details about the default operational strategy can be found in Flores-Alsina et al. (2011). The selection of the different scenarios is intended to demonstrate the relative effects of logical control strategies that may be implemented by operators to increase energy efficiency and/or improve overall plant performance. The following four selected scenarios are simulated in the presented case study:

- Impact of DO control (commonly used to reduce aeration costs) by varying the set point value between 1 and 3 g·m^{-3} (default value 2 g · m^{-3}).
- Impact of primary clarifier efficiency by varying the TSS removal efficiency in PRIM from 33% to 66% (default value 50%). Although in reality this does not happen without chemical addition, the effect of improving TSS removal, such as through chemical addition, is the change of interest.
- Impact of the anaerobic digester operating mode by changing the temperature in the anaerobic digester from mesophilic (35 °C) to thermophilic (55 °C) (default value 35 °C).
- Impact of anaerobic digester supernatants by controlling the return flow rate originating from the DW unit. This timer-based control strategy stores the dewatering liquor during daytime (when the plant is high loaded) and returns it at night (when the plant is low loaded). Note that the default BSM2 strategy does not use this control approach and liquors are simply returned as they are generated.

2.3. Evaluation criteria

2.3.1. Effluent quality (EQI) and operational cost (OCI) indices

The overall pollution removal efficiency is obtained using the effluent quality index (EQI) from the standard BSM2 (Nopens et al., 2010). EQI is an aggregated weighted index of all pollution loads: TSS, COD, BOD_5, total Kjeldahl nitrogen (TKN) and the oxidized forms of nitrogen (NO_X), leaving the plant. The economic objectives are evaluated using the operational cost index (OCI) (Nopens et al., 2010). It consists of the sum of all major operating costs in the plant: aeration energy (AE), pumping energy (PE), mixing energy (ME), sludge production (SP), external carbon addition (EC), methane production (MP) and the net heating energy (HE^{net}). EQI and OCI are based on simulation results with the 609 days of dynamic influent data generated following the principles outlined in Gernaey et al. (2011), although only the last 364 days are used for the evaluation itself.

2.3.2. Greenhouse gas (GHG) emissions

The comprehensive method proposed by Flores-Alsina et al. (2011) is used to calculate GHG emissions in the WWTP. The emissions considered are:

- Direct secondary treatment emissions: The emissions from the activated sludge section include the CO_2 generated from biomass respiration and BOD oxidation, the N_2O generated from nitrogen removal and the CO_2 credit from nitrification. Although in theory possible from anaerobic digester supernatants return and from the influent, CH_4 stripping/emissions in the secondary treatment were not considered, as they are not yet predicted by the plant-wide models.
- Sludge processing: The GHG emissions during sludge treatment are mainly generated in the anaerobic digester. In this case, it is assumed that the biogas is fed directly into a gas-fired combustion turbine converting the CH_4 into CO_2 and generating electricity and heat (in turn used to heat the anaerobic digester influent). The CO_2 generated during anaerobic digestion and the CO_2 produced in the combustion process are assumed to be released to the atmosphere.
- Net power GHG: The difference between energy usage and production. Energy consumption involves aeration, pumping, mixing and

heating. Energy production comes from the electricity generated by the turbine. A value of 0.94 kg $CO_2 \cdot (kWh)^{-1}$ is assumed for any external energy production required (based on the efficiency of a coal-burning power plant (Bridle et al., 2008)).

- Chemicals: The GHG emissions from production of carbon source for denitrification are accounted for (from industrial production of methanol data (Dong and Steinberg, 1997)).
- Sludge disposal and reuse: The disposal of sludge is accounted for by CO_2 emissions from transport and mineralization of organic matter at the disposal site considering three different fates. Compost (45 %) and agriculture (38%) are the main fates, while a small fraction is sent to forestry (17 %). When it comes to transport, forestry and agriculture imply further distance (≈150 km) than compost (≈20 km).

GHG emissions are also evaluated over a one-year period following the same principles. Finally, in order to deal with the different nature of the generated GHG emissions (CO_2, CH_4 and N_2O) they are converted into units of CO_2 equivalents (CO_2e). The assumed global warming potentials (GWP) for N_2O and CH_4 are 298 kg CO_2e per kg N_2O and 25 kg CO_2e per kg CH_4, respectively (IPCC, 2007).

It is important to highlight that this methodology accounts for the main sources of GHG emissions. However, the selected types of emissions and how they are included in the evaluation procedures can be user-defined based on various objectives and boundaries of interest. For example, it is possible to break down the plant's global warming potential into biogenic/non-biogenic emissions or within (on-site) and outside (off-site) the fence emissions.

3. Results

EQI, OCI and GHG values for the different simulated scenarios are shown in Fig. 1. As mentioned previously, the selection of the different scenarios is intended to demonstrate the relative effects of logical control strategies that may be implemented by operators to optimize plant performance. However, the main underlying reason for the scenario selection is the desire of showing the benefit of including the additional dimension dealing with GHG emissions when implementing changes across the whole plant. This is highlighted by moving from the 2-D to the 3-D representation and showing the results for a variety of situations. Hence, it is possible to see how the overall picture changes when (1) EQI and OCI are considered only or (2) when adding the total quantity of CO_2, N_2O and CH_4 emissions (quantified in kg CO_2e. m^{-3} of treated wastewater). From the generated results one can see that (1) the dissolved oxygen set point in the activated sludge section has a paramount importance on the plant's total GHG emissions (*z*-axis) next to the well-known impacts on effluent quality and operating costs; (2) better TSS removal efficiency in PRIM mainly improves effluent quality and operational cost (*x*- and *y*-axes), but the total GHG emissions remain almost equal; (3) thermophilic conditions in the anaerobic digester reveal that a higher operating temperature appears to be a more expensive way to operate the plant (with higher operational cost, *y*-axis) without having substantial benefits in terms of increased gas production (Fig. 4); and (4) control of the anaerobic digester supernatants return flow rate slightly improves effluent quality, increases cost but does not have an effect on the GHG emissions unless

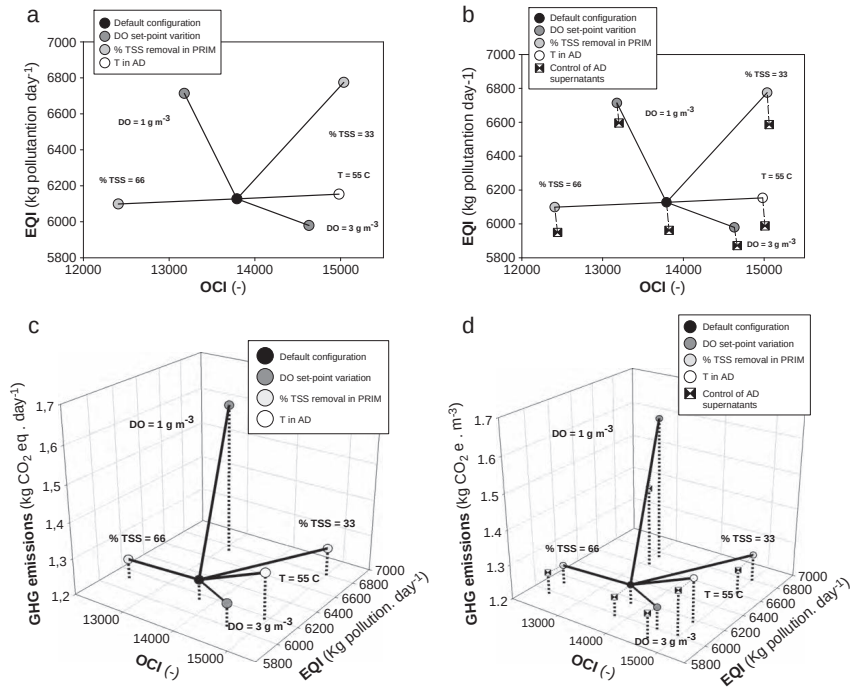

Fig. 1. Effluent quality (a, b, c, d), operational cost (a, b, c, d) and greenhouse gas emissions (c, d) for the different control strategies with (b, d) and without (a, c) controlling the anaerobic digester supernatant.

DO is very low (see dotted lines in Fig. 1, right). Figs. 2–4, show the dynamic variation of selected process variables and their seasonal variation (simulation start date: 1st of July, day = 245, total time: 364 days). Further details and discussion of these results are provided in the following sub-sections.

3.1. Effect of dissolved oxygen concentration

Low DO set points lead to a reduction of the off-site CO_2 production due to lower energy consumption and subsequently lower operational cost (detailed results not shown), but the overall GHG emissions are increased compared to the default case. The reason for this GHG increase is the increased formation of N_2O and its approximately 300-fold stronger greenhouse effect compared to CO_2. In this case, the N_2O increase is mainly caused by accumulation of NO_2^- (see Fig. 2, right) due to incomplete nitrification (see the increase of the EQI values in Fig. 1 and the dynamics of NH_4^+ in Fig. 2, left). High DO set points increase aeration energy and operational costs but improve effluent quality (see *x*- and *y*-axes in Fig. 1 and dynamic profiles in Fig. 2). Despite higher off-site emissions of CO_2, the overall GHG emissions are still lower due to a reduced N_2O contribution. In all cases (Figs. 2–4), the sudden drop around day 290 is caused by the holidays simulated in summer (for further details, see Gernaey et al., 2011).

3.2. Effect of primary clarifier efficiency

High PRIM efficiency (TSS removal = 66%) decreases the quantity of TSS entering the activated sludge section and improves the overall nitrification efficiency leading to better effluent quality (even though denitrification is significantly worsened because of a lack of readily biodegradable organic material). There is a reduction in the operational cost mainly due to (i) the lower aeration energy in the activated sludge section and (ii) the increased biogas production, which leads to higher energy recovery in the sludge line (see Fig. 3, right). However, the lower organic load entering the biological reactor increases the overall N_2O emissions due to the low C/N ratio of the primary clarifier effluent (see Fig. 3, left), especially in warm temperatures (days 245 to 350 and 550 to 609). Conversely, a low PRIM efficiency (TSS removal = 33%) decreases the effluent quality due to reactor overloading. Operational costs are higher due to (i) increased energy demand in the aerobic section and (ii) low energy recovery from the sludge line. In terms of GHG emissions, lower TSS removal in PRIM causes (i) an increase of the CO_2 emissions from BOD oxidation and biomass decay in the bioreactor and (ii) higher off-site CO_2 emissions due to increased energy demand in the aerobic section and low-energy recovery in the AD. All in all, the overall variations of the total GHG emissions seem to be very small when changing PRIM efficiency (*z*-axis in Fig. 1). However, the specific GHG compounds emitted and their origin change substantially in the different simulated scenarios (see the discussion section).

3.3. Effect of digester performance

Fig. 4 shows the results of changing the digester's operating temperature from 35 °C (mesophilic conditions) to 55 °C (thermophilic conditions). In this system, no substantial benefits can be observed in either biogas production or off-site CO_2 emissions. However, thermophilic conditions substantially increase the operational cost (Fig. 1) due to higher energy requirements for heating (Fig. 4, left) without significantly improving the digester performance (Fig. 4, right). Subsequently, this also leads to higher CO_2 emissions from off-site power generation. The effect on effluent quality variables is negligible (see discussion section).

3.4. Effect of controlling the return flows of anaerobic digester supernatants

In Fig. 1, the effect of controlling the anaerobic digester supernatants return flows is shown. In all cases, there is a slight improvement in the effluent quality (all evaluated scenarios have lower values of the EQI, *x*-axis) when control of the anaerobic digester supernatants returns is activated. This reduction is attributed to the storage tank's capability to reduce the effect of ammonium peaks originating from the sludge treatment line when the plant is already high loaded. Fig. 5 shows the smoothing effect on the effluent ammonium nitrogen of controlling the anaerobic digester supernatants return flows. On the other hand, the slight increase in the OCI (*y*-axis) of Fig. 1 is due to the extra pumping. Finally, with regard to GHG generation, there is no substantial benefit unless the DO concentration is very low. As mentioned before, low DO levels combined with high ammonium loads substantially increase the total N_2O emissions. The simulation results show that N_2O decrease can be achieved by dampening the ammonium peaks.

4. Discussion

The results reported in this case study pave the way to several discussions. Indeed, the additional dimension provided by the quantification of the N_2O, CH_4 and CO_2 generation from the WWTP changes the overall picture of the evaluation procedure giving a better idea about the "sustainability" of the different alternatives.

4.1. Importance of plant-wide control

The study presents an important result to the wastewater community showing the potential impacts of energy optimization, particularly in the aeration/anaerobic digester system and the importance of plant-wide evaluation. For example, Fig. 1 shows the clear advantages of increasing the % TSS removal in the PRIM. Firstly, the load to the activated

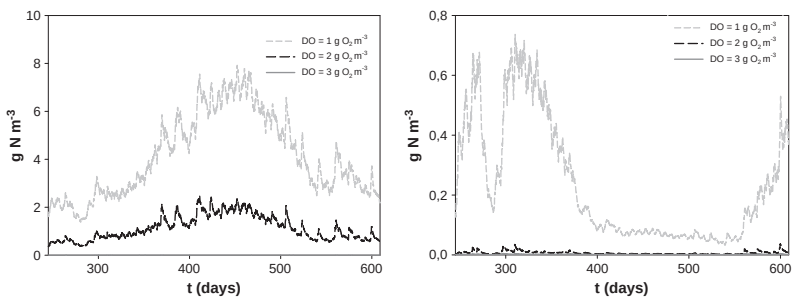

Fig. 2. Effect of dissolved oxygen on nitrification: NH_4^+ (left) and NO_2^- (right) in the effluent.

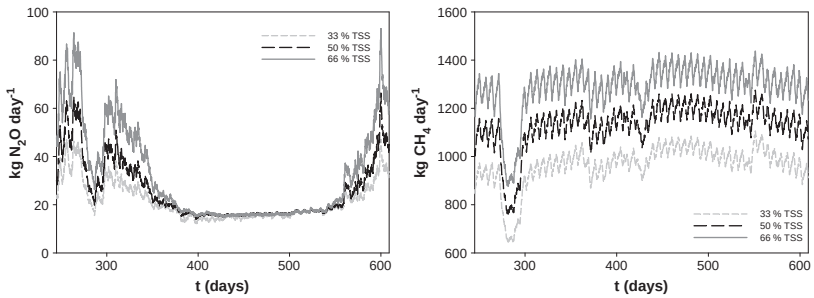

Fig. 3. Effect of TSS removal efficiency in PRIM: N_2O emissions from the activated sludge (left) and CH_4 from the anaerobic digester (right).

sludge section is substantially reduced (and thus the off-site CO_2 emissions due to aeration). Secondly, there is an increase of energy recovery from the anaerobic digestion (higher CO_2 credit). However, the total quantity of GHG emissions does not change since there is a substantial increase of N_2O emissions due to the inadequate C/N ratios that result (poor denitrification). Finally, this analysis provides insights with regard to decision making and evaluating operational options. Indeed, based on the results, operating a plant at low DO concentrations cannot be recommended due to the decrease in effluent quality despite the substantial savings in OCI (see Fig. 1a, b). The situation becomes even worse when GHG emissions are included in the analysis (Fig. 1c, d) and the substantial contribution of N_2O in the total plant's global warming potential would rank that alternative even lower. This demonstrates the usefulness of a third GHG dimension for deciding on the optimum DO control strategy to meet a specific plant's objectives.

4.2. The case study

As the integrated GHG modeling framework used in this paper incorporates AOB denitrification and heterotrophic denitrification N_2O pathways, it is promising to see the results reported in this paper lead to similar observations as the experiments reported in von Schulthess and Gujer (1996) and Kampschreur et al. (2009), related to DO, C/N ratios and N_2O emissions, which helps to validate the models' assumptions and structures and gain confidence in the relative effects observed. There is also good agreement with the studies of the effects of soluble/particulate compounds in activated sludge processes and their relation with the overall GWP of the plant (Gori et al., 2011). However, there are also aspects that warrant further attention. For example, there is suggested evidence that N_2O production increases during winter time (Kampschreur et al., 2009), although lower winter emissions have been reported as well (Daelman et al., 2013). With the ASM1G model used, lower temperatures lead to lower N_2O emissions, as explained in detail by Guo and Vanrolleghem (2013). Further investigations are still being conducted in order to better understand and describe the potential seasonal variability of GHG emissions.

The authors are aware of the fact that a TSS removal of 66% in PRIM is hard to achieve in many treatment plants without the addition of chemicals (Tchobanoglous et al., 2003). Further research is necessary to consider the role of such chemicals on the OCI, and the overall GWP in a similar way as is done for carbon source usage, i.e., kg CO_2e for each kg of chemical used. As mentioned previously, only the TSS removal effect of the chemical is studied in this paper.

Finally, it should be mentioned that traditionally thermophilic conditions should substantially increase biogas production (Tchobanoglous et al., 2003). The limited improvement in digester performance shown in this study can be explained by the following points: (i) the used ASM/ADM interfaces (Nopens et al., 2009) where the disintegration process (limiting factor in many digestion processes) is instantaneous; (ii) the low biodegradable fraction coming with the influent (Gernaey et al., 2011), consequently bringing limited amounts of organic material to the anaerobic digester (although kinetics are faster at thermophilic conditions, there is no more material to be converted); and (iii) the large digester volume, i.e., the digester was originally designed with a sufficiently long hydraulic retention time to convert all potentially digestible organics into methane under mesophilic conditions. If additional external organic waste would be available to make use of the extra digestion capacity in thermophilic conditions, results and conclusions would likely be different.

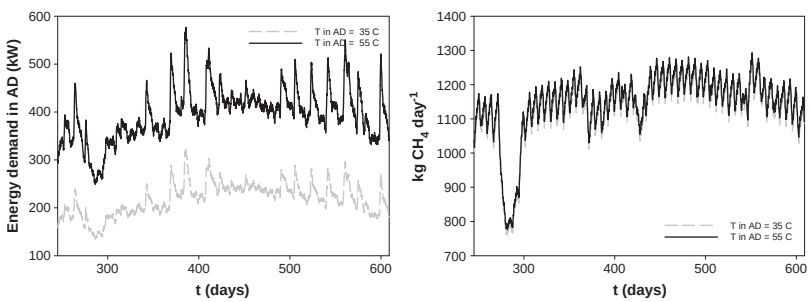

Fig. 4. Effect of modified T regime on the anaerobic digester's performance: energy demand (left) and CH_4 (right) in anaerobic digester.

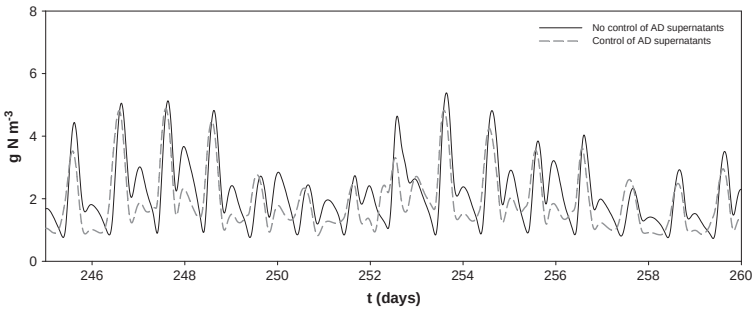

Fig. 5. Effect on the effluent ammonium of controlling the anaerobic digester supernatants (15 day snapshot of 364 days simulation).

4.3. Accounting (framing) for the plant's global warming potential

The case study shows that wastewater treatment system models are useful to quantify the different GHG emissions when evaluating different control strategies or operational procedures by taking into account the different sources of CO_2, CH_4 and N_2O. However, from a climate change point of view, not all these sources have the same importance. For example, biogenic sources of CO_2, such as the CO_2 emissions from the aerobic/anaerobic treatment of organics contained in the wastewater, are part of the natural carbon cycle, as long as they do not originate from fossil fuel based household products, such as detergents. On the other hand, there are non-biogenic sources, such as the off-site CO_2 emissions due to electricity consumption or production of chemicals that should be avoided. The methodology presented herein allows making this distinction when computing the plant's overall carbon footprint. A clear example can be found in scenario 2 (% TSS removal efficiency), where the total emission of GHG is almost the same, but their type and origin are quite different. For instance, the percentage of biogenic/non-biogenic CO_2 varies when the TSS removal efficiency is either decreased or increased: 30/70 and 20/80, respectively.

A similar type of differentiation can be made regarding on-site and off-site emissions. Thus, for the default case study the ratio between off-site and on-site emissions is 0.28. It is important to highlight that this ratio may change for example when the DO set point is decreased or increased. When the DO is decreased and the plant's total energy consumption is decreased (and consequently off-site emissions), the ratio is reduced to 0.18. On the other hand, when the DO set point is increased and there is a high energy demand to maintain 3 g O_2 m^{-3} in the biological reactor, the ratio increases to 0.33 due to higher off-site emission.

4.4. Energy-mix-related consideration issues

It must be noted that the value of 0.94 kg $CO_2e \cdot (kWh)^{-1}$ used for external energy production is an accurate value for a coal-burning power plant, but the electricity mix of any given country can be quite different than sole coal burning (being one of the dirtiest technologies when it comes to CO_2 emissions). In order to evaluate how this value may affect the results of benchmarking studies, the variation in the GWP was also evaluated assuming the average European (0.462 kg $CO_2e \cdot (kWh)^{-1}$) and US (0.731 kg $CO_2e \cdot (kWh)^{-1}$) energy mix value. The effect of DO set point variation is used as an example. Calculations reveal (for this particular case study) that cleaner energy mixes may change the net power GHG ($CO_2e \cdot m^{-3}$) by up to 50%. Nevertheless, the overall effect on the carbon footprint as accounted for in this study will still be very small (<5% in all cases). Note that this percentage may change depending on the framing (biogenic/non biogenic and on-site/off-site emissions).

4.5. General application of the method

The shown numeric results are case study specific, but the presented tools are generic. The influent characteristics (Gernaey et al., 2011) can be scaled to different situations (Flores-Alsina et al., in press). The same applies for the WWTP design (Nopens et al., 2010), which can be modified to describe full-scale process dynamics (Arnell et al., in press). In a recent study, the same ASM model structure has been tested calibrated/validated with a SBR plant treating anaerobic digester supernatants (Lindblom et al., in press). Naturally, some of the parameters had to be re-adjusted to better represent the new system, but the match between experiments and simulations was fairly close. It should be stressed that the modification of the model could give an under/overestimation of the total emissions, but the general conclusions would remain almost the same. The reader should be reminded that although the strong weight of N_2O in the GWP of the simulated plant, it is just one of an extensive list of emissions.

The same applies for CH_4 behaviour (Blumensaat and Keller, 2005). In case of doing so, the environmental impact of the different pollutants used to quantify the EQI has to be changed. Moreover, future users will have to update the relative importance of energy, chemicals and sludge treatment and collection costs used to quantify the OCI in accordance to their own (local) requirements.

Regarding the parameters used to quantify the different GHG emissions, some changes may be necessary. For example, (i) the external energy source will have a strong influence when converting $kWh \cdot day^{-1}$ to kg $CO_2e \cdot day^{-1}$, (ii) the utilization (or not) of biogas for sludge heating and plant electricity (cogeneration), (iii) the transport distances, and (iv) the sludge fate (incineration, landfill etc.) might change from one case to another.

Taking these factors into account, the presented set of models can be used as a decision support tool for control and process engineers, water authorities and regulators when evaluating the "sustainability" of different engineering applications for (i) design, (ii) process optimization and (iii) evaluation of alternatives for plant upgrading/expansion.

4.6. Limitations

It is important to highlight that the N_2O models used in the study are still under development and are in the process of being validated with full-scale data. Results thus far have been promising (Lindblom et al., in press). In this paper, the N_2O production by AOB is based on denitrification with NH_4^+ as electron donor. Other possible mechanisms, such as the formation of N_2O as a by-product of incomplete oxidation of hydroxylamine (NH_2OH) to NO_2^-, are not considered. Recent investigations demonstrate that both the autotrophic denitrification and the NH_2OH oxidation are involved in N_2O production, although the latter to a minor degree (Wunderlin et al., 2013). Nevertheless, a unified model

that describes both mechanisms independently does not yet exist (Ni et al., 2013). Therefore, the results reflect the assumptions built into the N_2O model structure of Mampaey et al., 2013.

Finally, the reader should be aware that the list of emissions on which this study is based is not complete. There are other sources of GHG that potentially contribute to the overall emissions of the plant. N_2O can be observed in the plant effluent (either because not all N_2O is stripped out in bioreactor or because the effluent NH_4^+ can be converted into N_2O after discharging into the river). Experimental observations have revealed that substantial stripping of methane might take place at the inlet of the WWTP (Guisasola et al., 2009). Also, no fugitive emissions of methane are considered from the anaerobic digester or the gas turbine (Daelman et al., 2012). In the ADM–ASM interface (Nopens et al., 2009), the quantity of methane that remains in the liquid phase is stripped, but not quantified in the model. Finally, while CO_2 is included, the potential N_2O and CH_4 emissions from sludge disposal and reuse are not considered either although they might be up to 40% of the total emissions (EPA, 2010; Brown et al., 2010).

5. Conclusions

The key observations of the presented study can be summarized in the following points:

- The inclusion of GHG emissions provides an additional criterion when evaluating control/operational strategies in a WWTP, offering a better idea about the overall "sustainability" of plant control/operational strategies.
- Simulation results show the risk of energy-related (aeration energy in AS/energy recovery from AD) optimization procedures, and the opposite effect that N_2O and its 300-fold stronger GHG effect (compared to CO_2) might have on the overall GWP of the WWTP.
- The importance of considering the water and sludge lines together and their impact on the total quantity of GHG emissions are shown when the temperature regime is modified and the anaerobic digester supernatants return flows controlled.
- While these observations are WWTP specific, the use of the developed tools is demonstrated and can be applied to other systems.

Acknowledgements

The authors acknowledge the financial support obtained through the Swedish Research Council Formas (211-2010-141), the Swedish Water & Wastewater Association (10-106, 11-106), the J. Gust. Richert Memorial Fund (PIAH/11:58), the TECC project of the Québec Ministry of Economic Development, Innovation and Exports (MDEIE) and FWO-Flanders (G.A051.10). Xavier Flores-Alsina gratefully acknowledges the financial support provided by the People Program (Marie Curie Actions) of the European Union's Seventh Framework Programme FP7/2007-2013 under REA agreement 329349 (PROTEUS). Lluís Corominas received the "Juan de la Cierva" scholarship from the Science Ministry of Spain (jci-2009-05604), and the career integration grant (PCIG9-GA-2011-293535) from EU. Laura Snip has received funding from the People Program (Marie Curie Actions) of the European Union's Seventh Framework Programme FP7/2007-2013, under REA agreement 289193 (SANITAS). Peter Vanrolleghem holds the Canada Research Chair in Water Quality Modelling.

References

Arnell M, Sehlen R, Jeppsson U. Practical use of wastewater treatment modelling and simulation as a decision support tool for plant operators—case study on aeration control at Linköping wastewater treatment plant. 13th Nordic Wastewater Conference, Malmö, Sweden, 8-10 October; 2013. [in press].

Ayesa E, De la Sota A, Grau P, Sagarna JM, Salterain A, Suescun J. Supervisory control strategies for the new WWTP of Galindo-Bilbao: the long run from the conceptual design to the full-scale experimental validation. Water Sci Technol 2006;53(4–5):193–201.

Batstone DJ, Keller J, Angelidaki I, Kayuznyi SV, Pavlostathis SG, Rozzi A, et al. Anaerobic Digestion Model No 1. IWA Scientific and Technical Report No 13. London, UK: IWA Publishing; 2002.

Blumensaat F, Keller J. Modelling of two-stage anaerobic digestion using the IWA Anaerobic Digestion Model No. 1 (ADM1). Water Res 2005;39(1):171–83.

Bridle T, Shaw A, Cooper S, Yap KC, Third K, Domurad M. Estimation of greenhouse gas emissions from wastewater treatment plants. Proceedings IWA World Water Congress 2008. Vienna (Austria), 7-12 September; 2008.

Brown S, Beecher N, Carpenter A. Calculator tool for determining greenhouse gas emissions for biosolids processing and end use. Environ Sci Technol 2010;44(24):9509–15.

Corominas L, Flores-Alsina X, Snip L, Vanrolleghem PA. Comparison of different modelling approaches to better understand greenhouse gas emissions from wastewater treatment plants. Biotechnol Bioeng 2012;109(11):2855–63.

Daelman MRJ, van Voorthuizen EM, van Dongen UGJM, Volcke EIP, van Loosdrecht MCM. Methane emission during municipal wastewater treatment. Water Res 2012;46(11):3657–70.

Daelman MRJ, De Baets B, van Loosdrecht MCM, Volcke EIP. Influence of sampling strategies on the estimated nitrous oxide emission from wastewater treatment plants. Water Res 2013;47(9):3120–30.

Dong Y, Steinberg M. Hynol: an economical process for methanol production from biomass and natural gas with reduced CO_2 emission. Int J Hydrogen Energy 1997;22(10–11):971–7.

EPA. Methane and Nitrous Oxide Emissions from Natural Sources. Technical Report; 2010. [published April 2010].

Flores X, Poch M, Rodríguez-Roda I, Bañares-Alcántara R, Jiménez L. Systematic procedure to handle critical decisions during the conceptual design of activated sludge systems. Ind Eng Chem Res 2007;46(17):5600–13.

Flores-Alsina X, Corominas L, Snip L, Vanrolleghem PA. Including greenhouse gas emissions during benchmarking of wastewater treatment plant control strategies. Water Res 2011;45(16):4700–10.

Flores-Alsina X, Saagi R, Lindblom E, Thirsing C, Thornberg D, Gernaey KV, et al. Calibration and validation of a phenomenological dynamic influent pollutant disturbance scenario generator using full-scale data. 11th IWA Conference on Instrumentation, Control and Automation (ICA 2013), Narbonne, France, 18-20 September; 2013. [in press].

Foley J, Yuan Z, Keller J, Senante E, Chandran K, Willis J, et al. N_2O and CH_4 emission from wastewater collection and treatment systems. Technical report. London, UK: Global Water Research Coalition; 2011.

Gernaey KV, Flores-Alsina X, Rosen C, Benedetti L, Jeppsson U. Dynamic influent pollutant disturbance scenario generation using a phenomenological modelling approach. Environ Model Softw 2011;26(11):1255–67.

Gernaey KV, Jeppsson U, Vanrolleghem PA, Copp JB, editors. Benchmarking of Control Strategies for Wastewater Treatment Plants. IWA Scientific and Technical Report. London, UK: IWA Publishing; 2013. [to appear].

Gori R, Jiang LM, Sobhani R, Rosso D. Effects of soluble and particulate substrate on the carbon and energy footprint of wastewater treatment processes. Water Res 2011;18(15):5858–72.

Guisasola A, Sharma KR, Keller J, Yuan Z. Development of a model for assessing methane formation in rising main sewers. Water Res 2009;43(11):2874–84.

Guo L, Vanrolleghem PA. Calibration and validation of an Activated Sludge Model for Greenhouse Gases no. 1 (ASMG1): Prediction of temperature-dependent N2O emission dynamics. Bioprocess Biosyst Eng 2013. http://dx.doi.org/10.1007/s00449-013-0978-3.

Guo L, Porro J, Sharma K, Benedetti L, Van Hulle S, Vanrolleghem PA, et al. Towards a benchmarking tool for minimizing wastewater utility greenhouse gas footprints. Water Sci Technol 2012;66(11):2483–95.

Henze M, Gujer W, Mino T, van Loosdrecht MCM. Activated Sludge Models ASM1, ASM2, ASM2d and ASM3. IWA Scientific and Technical Report No 9. London, UK: IWA Publishing; 2000.

Hiatt WC, Grady Jr CPL. An updated process model for carbon oxidation, nitrification, and denitrification. Water Environ Res 2008;80(11):2145–56.

Hug T, Benedetti L, Hall ER, Johnson BR, Morgenroth E, Nopens I, et al. Wastewater treatment models in teaching and training: the mismatch between education and requirements for jobs. Water Sci Technol 2009;59(4):745–53.

Intergovernmental Panel on Climate Change (IPCC). In: Solomon S, Qin D, Manning M, Chen Z, Marquis M, Averyt KB, Tignor M, Miller HL, editors. Contribution of working group I to the fourth assessment report of the Intergovernmental Panel on Climate Change. Cambridge, United Kingdom and New York, NY, USA: Cambridge University Press; 2007.

Kampschreur MJ, Temmink H, Kleerebezem R, Jetten MSM, van Loosdrecht MCM. Nitrous oxide emission during wastewater treatment. Water Res 2009;43(17):4093–103.

Law Y, Ye L, Pan Y, Yuan Z. Nitrous oxide emissions from wastewater treatment processes. Phil Trans R Soc B 2012;367:1265–77.

Lindblom E, Arnell M, Stenström F, Tjus K, Flores-Alsina X, Jeppsson U. Dynamic modelling and validation of nitrous oxide emissions from a full-scale nitrifying/denitrifying sequencing batch reactor treating anaerobic digester supernatant. 11th IWA Conference on Instrumentation, Control and Automation (ICA 2013), Narbonne, France, 18-20 September; 2013. [in press].

Mampaey KE, Beuckels B, Kampschreur MJ, Kleerebezem R, van Loosdrecht MCM, Volcke EIP. Modelling nitrous and nitric oxide emissions by autotrophic ammonia-oxidizing bacteria. Environ Technol 2013. http://dx.doi.org/10.1080/09593330.2012.758666.

Ni BJ, Yuan Z, Chandran K, Vanrolleghem PA, Murthy S. Evaluating mathematical models for N_2O production by ammonia-oxidizing bacteria: Towards a unified model. Biotechnol Bioeng 2013;110(1):152–63.

Nopens I, Batstone DJ, Copp JB, Jeppsson U, Volcke E, Alex J, et al. An ASM/ADM model interface for dynamic plant-wide simulation. Water Res 2009;43(7):1913–23.

Nopens I, Benedetti L, Jeppsson U, Pons M-N, Alex J, Copp JB, et al. Benchmark simulation model no 2: finalisation of plant layout and default control strategy. Water Sci Technol 2010;62(9):1967–74.
Olsson G. ICA and me: a subjective review. Water Res 2012;46(6):1586–624.
Rieger L, Gillot S, Langergraber G, Ohtsuki T, Shaw A, Takács I, et al. Guidelines for using activated sludge models. Scientific and Technical Report No.22. London, UK: IWA Publishing; 2012.
Rivas A, Irizar I, Ayesa E. Model-based optimisation of wastewater treatment plants design. Environ Model Softw 2008;23(4):435–50.
Rodriguez-Garcia G, Hospido A, Bagley DM, Moreira MT, Feijoo G. A methodology to estimate greenhouse gases emissions in Life Cycle Inventories of wastewater treatment plants. Environ Impact Assess Rev 2012;37:37–46.
Rodriguez-Roda I, Sànchez-Marrè M, Comas J, Baeza J, Colprim J, Lafuente J, et al. A hybrid supervisory system to support WWTP operation: implementation and validation. Water Sci Technol 2002;45(4–5):289–97.
Tchobanoglous G, Burton FL, Stensel HD. Wastewater Engineering: Treatment, Disposal and Reuse. New York, USA: McGraw-Hill; 2003.
von Schulthess R, Gujer W. Release of nitrous oxide (N_2O) from denitrifying activated sludge: verification and application of a mathematical model. Water Res 1996;30(3):521–30.
Wunderlin P, Lehmann MF, Siegrist H, Tuzson B, Joss A, Emmenegger L, et al. Isotope signatures of N_2O in a mixed microbial population system: constraints on N_2O producing pathways in wastewater treatment. Environ Sci Technol 2013;47(3):1339–48.

Paper II

Dynamic modelling of nitrous oxide emissions from three Swedish sludge liquor treatment systems

E. Lindblom, M. Arnell, X. Flores-Alsina, F. Stenström, D. J. I. Gustavsson, J. Yang and U. Jeppsson

ABSTRACT

The objective of this paper is to model the dynamics and validate the results of nitrous oxide (N_2O) emissions from three Swedish nitrifying/denitrifying, nitritation and anammox systems treating real anaerobic digester sludge liquor. The Activated Sludge Model No. 1 is extended to describe N_2O production by both heterotrophic and autotrophic denitrification. In addition, mass transfer equations are implemented to characterize the dynamics of N_2O in the water and the gas phases. The biochemical model is simulated and validated for two hydraulic patterns: (1) a sequencing batch reactor; and (2) a moving-bed biofilm reactor. Results show that the calibrated model is partly capable of reproducing the behaviour of N_2O as well as the nitritation/nitrification/denitrification dynamics. However, the results emphasize that additional work is required before N_2O emissions from sludge liquor treatment plants can be generally predicted with high certainty by simulations. Continued efforts should focus on determining the switching conditions for different N_2O formation pathways and, if full-scale data are used, more detailed modelling of the measurement devices might improve the conclusions that can be drawn.

Key words | ASMN, autotrophic denitrification, greenhouse gases, heterotrophic denitrification, modelling, sludge liquor treatment

E. Lindblom
M. Arnell
U. Jeppsson
Division of Industrial Electrical Engineering and Automation (IEA), Department of Biomedical Engineering, Lund University,
PO Box 118, SE-221 00 Lund,
Sweden

E. Lindblom (corresponding author)
Stockholm Vatten, SE-106 36 Stockholm,
Sweden
E-mail: *erik.lindblom@stockholmvatten.se*

M. Arnell
SP Technical Research Institute of Sweden,
Gjuterigatan 1D, SE-582 73 Linköping,
Sweden

X. Flores-Alsina
Department of Chemical and Biochemical Engineering, Technical University of Denmark,
DK-2800 Lyngby,
Denmark

F. Stenström
Water and Environmental Engineering, Department of Chemical Engineering, Lund University,
PO Box 118, SE-221 00 Lund,
Sweden
and
VA-Ingenjörerna AB, Trädgårdsgatan 12,
SE-702 12 Örebro,
Sweden

D. J. I. Gustavsson
VA SYD, PO Box 191, SE-201 21 Malmö,
Sweden
and
Sweden Water Research, Ideon Science Park,
Scheelevägen 15, SE-223 70 Lund,
Sweden

J. Yang
Department of Sustainable Development, Environmental Science and Engineering,
Royal Institute of Technology (KTH),
Teknikringen 76, SE-100 44, Stockholm,
Sweden
and
Swedish Environmental Research Institute (IVL),
Valhallavägen 81, SE-100 31, Stockholm,
Sweden

INTRODUCTION

Efficient municipal wastewater treatment plant (WWTP) engineering and operation call for plant-wide process understanding, which can be summarized as mathematical models (Gernaey *et al.* 2014). Results from recent

investigations have shown that some 'optimal' WWTP operational strategies, e.g. operation with intermittent aeration (Yu *et al.* 2010) and/or low dissolved oxygen (DO) setpoints (Kampschreur *et al.* 2009) might be 'sub-optimal' in certain respects because of the risk of elevated emissions of the undesired greenhouse gas nitrous oxide (N_2O). This is possibly due to lack of generally applicable knowledge and models that capture all aspects related to N_2O formation and thus an inability of WWTP simulators to predict the emissions with certainty.

Based on new knowledge of the biological mechanisms of N_2O production, recent efforts have been made to capture the production and emission of N_2O and integrate these processes with the traditional activated sludge models (ASM) (Henze *et al.* 2000; Hiatt & Grady 2008; Mampaey *et al.* 2013; Ni *et al.* 2013; Pan *et al.* 2014). The aim is to increase the understanding of the N_2O production mechanisms and eventually to allow for mitigation of the emission, e.g. by developing appropriate control strategies. The paper by Flores-Alsina *et al.* (2014) clearly demonstrates how seemingly good control strategies for WWTPs in terms of improved effluent quality and lower operational costs may actually lead to a dramatic increase in greenhouse gas emissions, thereby partly counteracting the original purpose of the control.

In this study, process models for sequencing batch reactor (SBR) and biofilm systems – including available N_2O production models – for treating sludge liquors from anaerobic digestion of municipal primary, secondary and chemical sludge have been developed, implemented in the software (*Matlab-Simulink*®) and evaluated to test if a combination of the above-mentioned biological reaction models can be calibrated and validated using full-scale data.

MATERIAL AND METHODS

Full-scale data sets

The models are calibrated to reproduce the data sets from three Swedish full-scale systems denoted *SBR_N/DN*, *SBR_NO2* and *MBBR_AMX*:

- ***SBR_N/DN*:** N_2O measurements performed by Stenström *et al.* (2014), who investigated a nitrification(N)-denitrification(DN) SBR process at Slottshagen WWTP (Norrköping, Sweden);
- ***SBR_NO2*:** N_2O measurements performed by Gustavsson & la Cour Jansen (2011), who investigated a *nitritation only* SBR process at Sjölunda WWTP (Malmö, Sweden);
- ***MBBR_AMX*:** N_2O measurements performed by Yang *et al.* (2013), who investigated a one-stage nitritation-anammox moving-bed biofilm reactor (MBBR) process at Hammarby-Sjöstad pilot plant (Stockholm, Sweden).

The three case studies involve treatment of real anaerobic digestion sludge liquor and all include measurements of traditional wastewater variables (online and grab samples) and online measurements of N_2O (water and/or gas phase). The reader is referred to the original papers for further details about the experiments.

Mathematical models

Considering the experimental data of the three case studies, a biological process model including heterotrophic ($X_{B,H}$) and ammonia oxidizing bacteria (X_{AOB}) denitrification was hypothesized to be able to describe the measurements. The model was initially based on the ideas summarized in Hiatt & Grady (2008). This model (ASMN) extends the well-recognized ASM1 (Henze *et al.* 2000) with two nitrifying populations: X_{AOB} and nitrite oxidizing bacteria (X_{NOB}). The use of ASMN is partly motivated by the fact that free ammonia (S_{NH3}) and nitrous acid (S_{HNO2}) are considered as substrates for X_{AOB} and X_{NOB}, respectively. These components are temperature- and pH-dependent, which is important to consider while modelling sludge liquor treatment processes. Moreover, the sequential four-step heterotrophic denitrification of nitrate (S_{NO3}) to nitrogen gas (N_2) in the model is via nitrite (S_{NO2}), nitric oxide (S_{NO}) and nitrous oxide (S_{N2O}); both S_{NO2} and S_{NO} are important components to consider for N_2O production by X_{AOB} (Chandran *et al.* 2011). ASMN does not include AOB N_2O production, which, as pointed out by Gustavsson & la Cour Jansen (2011) and Stenström *et al.* (2014) amongst others, potentially is a governing process for N_2O formation in biological sludge liquor treatment systems. To date, N_2O is believed to be produced by AOB through two different pathways (Chandran *et al.* 2011; Ni *et al.* 2014): (1) AOB denitrification; and (2) incomplete oxidation of hydroxylamine, hereby denoted the NH_2OH pathway. In Ni *et al.* (2013), four different models, each including one of the pathways, were compared with data sets from different systems. None of the models could describe all data sets accurately and recently, Ni *et al.* (2014) therefore presented an integrated model in which both pathways are included. Thereby it is suggested that shifts of the dominating pathway, due to different process conditions during nitrification (mainly DO and NO_2^- concentrations), can be

predicted. Unfortunately, the two-pathway model adds significantly to model complexity as electron competition, with several additional model parameters, is included. Since this work considers N_2O production also by heterotrophic denitrification it was, to confine the model complexity, decided to implement a one-pathway model for AOB N_2O production, i.e. the AOB denitrification pathway. Moreover, the model by Ni *et al.* (2014) was not available by the time this project had to decide upon which model to apply. Among the two AOB denitrification models evaluated by Ni *et al.* (2013), the one proposed by Mampaey *et al.* (2013) was selected for implementation because it does not contain additional model components and therefore is relatively easy to integrate with ASMN. In the resulting integrated model, X_{AOB} are also capable of reducing S_{HNO2} to S_{NO} and further into S_{N2O}. The assumed reaction rates for X_{AOB} denitrification ($r_{NO/N2O,AOB,den}$ [g N m^{-3} d^{-1}]) are shown in Equations (1) and (2):

$$r_{NO,AOB,den} = f_{DNT,A} \cdot \frac{\mu_{AOB}}{Y_{AOB}} \cdot \left(\frac{S_O}{K_{O,AOB} + S_O}\right) \cdot \left(\frac{S_{NH3}}{K_{NH3,AOB} + S_{NH3}}\right) \cdot \left(\frac{S_{HNO2}}{K_{HNO2,AOB} + S_{HNO2}}\right) \cdot X_{AOB} \quad (1)$$

$$r_{N2O,AOB,den} = \frac{\mu_{AOB}}{Y_{AOB}} \cdot \left(\frac{S_O}{K_{O,AOB} + S_O}\right) \cdot \left(\frac{S_{NH3}}{K_{NH3,AOB} + S_{NH3}}\right) \cdot \left(\frac{S_{NO}}{K_{NO,AOB} + S_{NO}}\right) \cdot X_{AOB} \quad (2)$$

In the original model, the same half-saturation coefficients $K_{O,AOB}$ and $K_{NH3,AOB}$ are assumed for X_{AOB} aerobic ammonia oxidation and X_{AOB} denitrification. The parameters $K_{HNO2,AOB}$ and $K_{NO,AOB}$ are unique for X_{AOB} denitrification. It should be highlighted that, although not included in the presented model, incomplete oxidation of NH_2OH may also play an important role in the N_2O production of the three case studies. Finally, growth and decay processes of anammox active biomass (X_{AMX}) according to Hao *et al.* (2002) were included in the biological process model. X_{AMX} convert S_{NH4} and S_{NO2} to mainly nitrogen gas and also S_{NO3} in the absence of oxygen.

Stripping (mass transfer) equations for the gases were implemented as in Foley *et al.* (2011). In the three case studies, the monitored DO concentration is used as the input to a controller that adjusts the k_La_{O2} of the modelled systems. The applied diffusivities of N_2O and O_2 are 1.77 10^{-9} m^2/s and 2.12·10^{-9} m^2/s, respectively, yielding $k_La_{N2O} = 0.91$ k_La_{O2}. The simulated flux of N_2O in the off-gas (F_{N2O} [kg N d^{-1}]), which is used to validate the model behaviour with the measured emissions, is then given by $F_{N2O} = k_La_{N2O} \cdot S_{N2O} \cdot V_{AER}$, with V_{AER} [m^3] denoting the aerated water volume. The simulated k_La_{O2} values are within the range of 300 to 600 d^{-1}. Thus, the half-life of possibly accumulated S_{N2O} during stripping is only a few minutes. Any long-term dynamic variation of N_2O emissions is therefore, according to the model, due to variations of the biological reaction rates. However, the stripping/flux equation might represent an overly simplified version of reality. For example, the retention time of the bubbles in the reactor, the measurement devices and stripping during non-aerated conditions have not been taken into account.

The reactive settler model developed within the benchmark simulation model (BSM) framework (Flores-Alsina *et al.* 2012) was expanded with variable layer heights (e.g. during filling) and layer mixing (e.g. during aeration) to describe the SBR behaviour of the *SBR_N/DN* and *SBR_NO2* systems.

The biofilm model, used to model the MBBR anammox system (*MBBR_AMX*), was inspired by the implementation in the commercial software platform WEST 3.7.3 (DHI 2011). According to this model, the bulk water volume is separated from the biofilm, which, in turn, is divided into 10 layers. Soluble components are transported by diffusion between the biofilm layers and bulk, proportionally to the concentration gradients. Particulate material attaches to the outermost layer of the biofilm and detachment occurs from all layers as the biofilm thickness exceeds a user defined maximum value.

RESULTS AND DISCUSSION

In this section, the results of the three case studies are shown and discussed. A summary of applied parameter values is given in Table 1.

Nitrification/denitrification SBR, case SBR_N/DN

Recorded DO and pH values (Figures 1(a) and 1(d)) as well as flow rate data were directly used as model inputs. The process temperature was constant (30.3 °C).

During the measurement period of 16 hours used for model calibration the NH_4^+-N load to the SBR plant was 180 kg N d^{-1}. The *SBR_N/DN* cycle of 8 hours starts with 3.5 hours of anoxic denitrification including 2 hours of

Table 1 | Calibrated model parameter values for the three case studies

	K_{SS} [g COD·m^{-3}]	$K_{S,EtOH,5}$ [g COD·m^{-3}]	$K_{IS,HNO2}$ [g N·m^{-3}]	b_{AOB} [d^{-1}]	μ_{AOB} [d^{-1}]	$f_{ANT,A}$ [-]
Reference	*40*[a]		*0.0007–0.001*[b]	*0.13*[c]	*2.13*[d], *2.05*[c]	*0.028*[d]
SBR_N/DN	100	1	0.001	0.23	2.00	0.120
SBR_NO2	40	–	–	0.23	0.85	0.075
MBBR_AMX	40	–	–	0.08	1.41	–
	Y_{AOB} [g COD·(g N)$^{-1}$]	$K_{O,AOB}$ [g O_2·m^{-3}]	$K_{NH3,AOB}$ [g N m^{-3}]	$K_{NH3,AOB,DN}$ [g N m^{-3}]	$K_{HNO2,AOB}$ [g N m^{-3}]	$K_{NO,AOB}$ [g N m^{-3}]
Reference	*0.18*[a], *0.15*[b,c]	*0.6*[a], *0.5*[d]	*0.0075*[a], *1.0*[d]	*1.0*[d]	*0.002*[d]	*1.0*[d]
SBR_N/DN	0.18	1.0	0.053	0.368	0.003	0.06
SBR_NO2	0.18	1.0	0.140	1.000	0.001	0.06
MBBR_AMX	0.18	1.0	0.053	–	–	–

Values from original publications given in italics:
[a]Hiatt & Grady (2008).
[b]Zhou *et al.* (2008).
[c]Hao *et al.* (2002) at T = 30 °C.
[d]Wampaey *et al.* (2013) at T = 35 °C.

filling. Initially, the accumulation rate of S_{N2O} is almost equal to the denitrification rate of S_{NO3} indicating that the final step of heterotrophic denitrification is inhibited (Figures 1(c) and 1(g)). At $t = 1.5$ h ethanol is dosed to the process and S_{N2O} in the water phase is immediately reduced. To model these observations with ASMN the heterotrophic N_2O denitrification process without ethanol must be almost completely inhibited. The original ASMN inhibition term for S_{NO} was replaced by S_{NO2} inhibition (Zhou *et al.* 2008) since no information of S_{NO} concentrations was available. Despite several attempts this drastic shift, between complete and no inhibition because of a low availability of readily biodegradable substrate (S_S), could not be captured by the original ASMN model and motivated the extension with an additional model component representing ethanol, $S_{S,EtOH,5}$ [g COD·m^{-3}]. This state variable was assumed to affect the process in the same way as S_S, with the exception that the half-saturation coefficient ($K_{S,EtOH,5}$) for the last step of denitrification, heterotrophic growth with $S_{S,EtOH,5}$ as substrate and N_2O as electron acceptor, is set to a low value (1 g COD·m^{-3}). For the same process, but with S_S from the influent sludge liquor as substrate, the half-saturation coefficient (K_{S5}) was given a high value (100 g COD·m^{-3}). Although there might be a physical explanation for the varying values of the half-saturation coefficients, they should in this case be considered as lumped values to model the inhibition without external carbon. However, according to the simulation results, S_{N2O} starts to accumulate again as ethanol is consumed, a phenomenon that was not measured and indicates that separated growth on internal and added substrates is not necessarily the actual process governing the S_{N2O} formation. Pan *et al.* (2014) recently published a new model for the denitrification process that, in comparison with ASMN, better describes electron competition and the dynamics of denitrification intermediates in a number of experiments. Adopting the concepts of this model might be a way to fully describe the observed heterotrophic denitrification process of the *SBR_N/DN* case.

Ammonia oxidation starts instantly when aeration is initiated at $t = 3.5$ h (Figures 1(a) and 1(b)). The associated N_2O emissions are shown in Figure 1(f). A sharp peak in the simulated emission is seen at the start of the aeration due to stripping of the partially faulty prediction of anoxic N_2O accumulation (Figure 1(g) between $t = 3.0$–3.5 h). The maximum measured N_2O emission is reached after 1 hour of aeration with absence of measured accumulated S_{N2O} from the preceding anoxic phase. Thus, the emission is mainly due to N_2O production during aerobic conditions and according to the implemented model to AOB

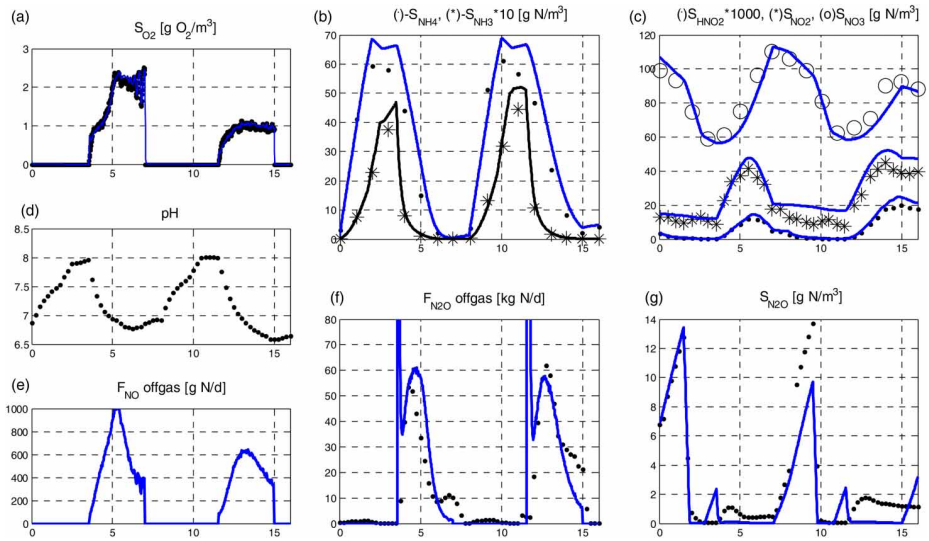

Figure 1 | Measured (markers) and simulated (solid lines) concentrations and mass flows for the nitrification/ denitrification SBR process (*SBR_N/DN*). Measurements of NO (e) were not available. The *x*-axes show time in hours.

denitrification. The X_{AOB} affinity coefficient for S_{HNO2} appears relatively low since S_{HNO2} peaks after 2.5 hours of aeration (Figure 1(c)). As will be shown in the next case study as well, the studied emission seems to be correlated with S_{NH3} and in the model this has been accounted for by choosing a separate half-saturation coefficient for S_{NH3} during AOB denitrification, $K_{NH3,AOB,DN}$ [g N·m^{-3}]. The used value is seven times higher compared with the value of $K_{NH3,AOB}$ (0.053 g N·m^{-3}) for aerobic ammonia oxidation, see Table 1. It must be stated that incomplete NH_2OH oxidation might also contribute to the emission but according to results in Ni *et al.* (2014), the moderate concentrations of NO_2^- (15–40 mg N L^{-1}) and DO (1–2 mg O_2 L^{-1}) supports the assumption that AOB denitrification is the dominating pathway in this case.

Nitritation only SBR, case *SBR_NO2*

During the measurement period of 24 hours used for model calibration the NH_4^+-N load to the SBR plant was 710 kg N d^{-1}. The temperature in the SBR process was similar to *SBR_N/DN*, 31.7 °C. An important difference is, however, that in *SBR_NO2* the pH was controlled at 6.8. The *SBR_NO2* cycle of 6 hours starts with aeration and filling. S_{NH4} increases until filling stops after 1.5 hours (Figure 2(b)). During the subsequent aerobic batch mode phases, the nitritation process proceeds until aeration is switched off. A fixed constant airflow is applied during each cycle but the total length of the aerated phases is varied. This also means that the time periods for the anoxic settling phases that make up the end of each cycle vary.

The SBR process had been operated for nitritation only during several months prior to this measurement campaign and the sludge was therefore enriched with X_{AOB}. The DO data (Figure 2(a)) indicate that the oxygen demand of the sludge decreases when S_{NH4} decreases below 50 g N m^{-3}, which was modelled by a half-saturation coefficient ($K_{NH3,AOB}$) value of 0.14 g N m^{-3}, corresponding to 24 g NH_4-N L^{-1}.

The sharp simulated peaks at the beginning of each phase (not reflected in the measurement data) are due to stripping of accumulated S_{N2O} during anoxic conditions. Consequently, as stripping according to the model occurs fast, the decrease in N_2O production throughout the aeration phase must be explained by aerobic biological N_2O production.

The N_2O emissions reach 30–75 kg N d^{-1} and decrease to 10–15 kg N d^{-1} at the end of the aerobic phases (Figure 2(e)). In the most extreme cycle (#4, t = 18–24 h), the emission at the end of the aerated phase is only 20% of the maximum

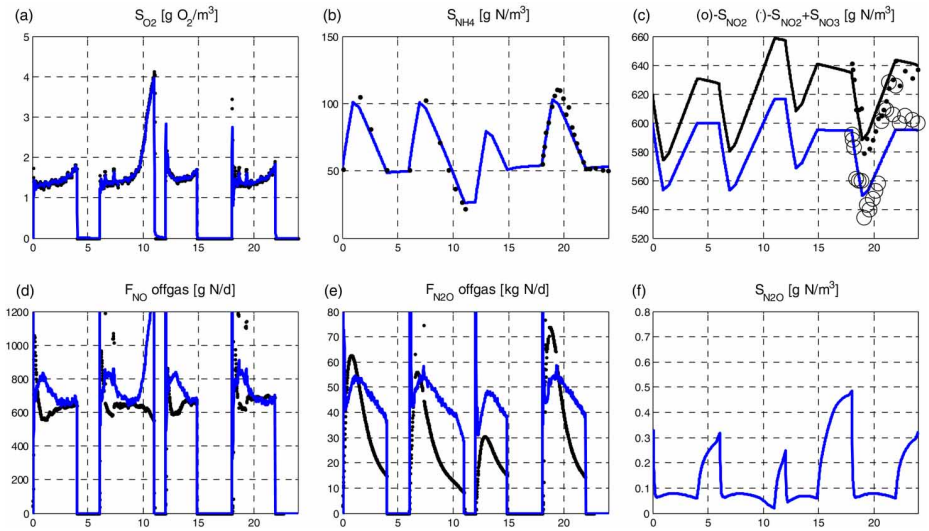

Figure 2 | Measured (markers) and simulated (solid lines) concentrations and mass flows for the nitritation only SBR process (*SBR_NO2*). Measurements of dissolved N_2O (f) were not available. The *x*-axes show time in hours.

emission during that same phase. Considering Equation (1), S_{NO2} in the process varies around 500–600 g N m^{-3} during the nitritation phase (Figure 2(c)). This variation corresponds to 0.15–0.18 g HNO_2-N·m^{-3} with the pH being controlled at = 6.8 and a temperature of 31.7 °C. Since the concentrations are always high they are believed not to represent any major cause for the varying N_2O emissions. S_O actually increases throughout the aeration phase, a phenomenon that according to the model could increase the N_2O production (in contrast to the observations).

Opposite to the *SBR_N/DN* case this study includes measurements of NO offgas concentrations, which were relatively stable. This is reflected by the almost constant calculated NO emissions shown in Figure 2(d). Considering Equation (2), S_{NO} does therefore not explain the dynamic N_2O emissions.

The attempt to fit the AOB denitrification model (Equations (1) and (2)) to the measurement data is not successful and requires the inclusion of – as was also done for *SBR_N/DN* – a unique S_{NH3} half-saturation coefficient for AOB denitrification ($K_{NH3,AOB,DN}$). By choosing a high value (1.0 g N m^{-3}) the S_{NH3} dependency changes towards a linear relation and part of the dynamics can be modelled.

In the original paper describing the experimental data (Gustavsson & la Cour Jansen 2011), a linear relation between the length of the anoxic phase and emitted mass of N_2O was proposed. The implemented model can be adjusted to explain this phenomenon as seen in the varying peak S_{N2O} concentrations before aeration (Figure 2(f)). However, as already noted, the sharp peaks in the simulated emissions due to stripping were not experimentally supported.

The overall conclusion based on the reasoning above, and several attempts to simulate the model with various parameter sets, is that the ASMN/Mampaey model may not be feasible for explaining the complete dynamics of nitrous oxide emissions from *SBR_NO2*.

It has been shown by laboratory experiments (Law *et al.* 2013) and modelling (Ni *et al.* 2014) that the high nitrite concentrations (500–600 g N m^{-3}) in combination with moderate DO concentrations (1.2–2.0 mg O_2 L^{-1} of case *SBR_NO2* would imply that the contribution of the NH_2OH pathway to the total N_2O emission is substantial. As was shown above (Figure 2) it is difficult to calibrate the Mampaey AOB denitrification model to the data without applying a very high value of the $K_{NH3,AOB,DN}$ parameter (1.0 mg NH_3-N/L or 175 mg NH_4-N/L). The NH_2OH pathway model presented by Law *et al.* (2012) could potentially

describe the data better. In that model it is assumed that the intermediates NH_2OH and NOH can accumulate if the AOB NH_3 oxidation process rate is high (e.g. at high DO and high S_{NH3}). N_2O production is then modelled following first-order kinetics as chemical decomposition of NOH. Thus if the accumulation proceeds so that the concentration of NOH is linearly proportional to S_{NH3} the NH_2OH pathway model could probably better describe the observations of case *SBR_NO2*.

MBBR anammox, case (*MBBR_AMX*)

The influent sludge liquor originated from the full-scale anaerobic digestion process at Bromma WWTP in Stockholm, Sweden. During the measurement period of 24 hours used for model calibration the ammonia load to the pilot-scale reactor was 70 g N d^{-1} or 1.7 g N·(m^2 d)$^{-1}$. This load corresponds to, compared to other periods, a low load and the amount of biomass in the system should therefore not have limited the total N removal efficiency (88%). The pH and temperature were relatively constant at 7.1 and 25 °C, respectively.

The simulated amounts of biomass in the bulk and biofilm are shown in Figure 3(a). X_{AMX} dominates and is present throughout the entire biofilm. The process is intermittently aerated 45 out of 60 minutes (Figure 3(d)) and X_{AMX} therefore has the possibility to also grow in the outer layers. X_{AOB} and a small amount of X_{NOB} are also present in the outer layers. Note that a significant amount of biomass is found in the bulk water volume (shown as dots in Figure 3(a)). In the model, and according to experimental observations, there is heterotrophic activity in the system as well due to decay and a small amount of biodegradable organic matter present in the influent.

Simulation results show that, compared to the previous case studies, the relatively low N_2O emissions of 0.5% during the studied period can be explained by heterotrophic denitrification. In the demonstrated simulations (Figure 3), the ASMN default parameters for $X_{B,H}$ were used. Approximately 3% of the influent S_{NH4} is converted via nitrification and heterotrophic denitrification and 20% out of this amount is accumulated as S_{N2O}, probably because of low S_S concentrations from hydrolysis of particulates in the biofilm. The resulting emissions of N_2O are similar to the measurements and therefore, to simplify, the AOB denitrification process equations of the model was deactivated in this case. It should, however, be noticed that higher emission rates of N_2O were measured during other periods of the

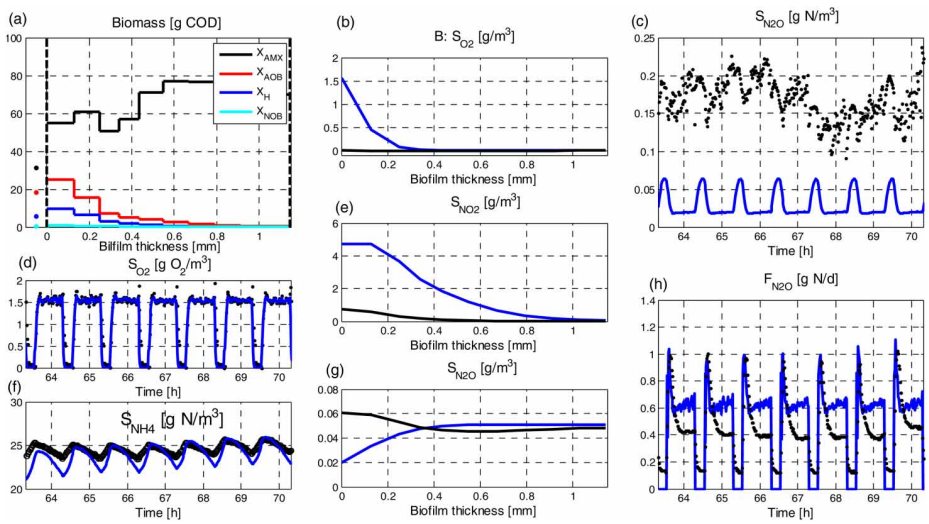

Figure 3 | Scenario *MBBR_AMX*. (a): Simulated amounts of active biomass in each of the 10 biofilm layers (lines) and bulk (dots). In total, the biofilm (40 m^2) contains 1,200 g TS (solids). (b), (e), (g): Simulated concentration profiles during the end of aerobic (blue line) and anoxic (black line) conditions. (c), (d), (f), (h): Measured (markers) and simulated (solid lines) concentrations and mass flows. (c), (d) and (f) show bulk concentrations. Please refer to the online version of this paper to see this figure in colour.

measurement campaign with higher nitrogen loads and different DO operational settings, which might indicate AOB denitrification and/or incomplete NH_2OH oxidation. The reader is referred to Yang *et al.* (2013) for further information.

Figure 3(f) shows the simulated and measured bulk S_{NH4} concentrations. S_{NO3} varies between 60 and 65 g N m^{-3} and both S_{NH4} and S_{NO3} fully penetrate the modelled biofilm. Figures 3(b), 3(e) and 3(g) show simulated concentration profiles from the bulk water through the biofilm layers on two occasions. The black line shows the profile after 15 minutes of anoxic conditions in the bulk while the grey (blue) line shows concentrations after 45 minutes of aeration. From these results it can be seen that S_{NO2} (Figure 3(e)) is produced in the outer layer during aerobic conditions and penetrates almost the entire biofilm. When aeration is turned off, S_{NO2} is consumed by X_{AMX} and $X_{B,H}$. During anoxic conditions, S_{N2O} diffuses into the biofilm where it is converted by heterotrophic denitrifiers. As aeration is turned on S_{N2O} in the bulk volume decreases due to stripping and the diffusion changes direction so that S_{N2O} moves from the biofilm to the bulk.

The simulated N_2O emissions are shown in Figure 3(h). Although much lower, emissions were also measured during non-aerated phases, a phenomenon that was not included in the model. The simulated and measured dissolved N_2O concentrations are shown as time-series in Figure 3(c). S_{N2O} accumulates during anoxic conditions, which is also seen as peaks in the N_2O emission as aeration is turned on. The measurement data do not show a clear pattern but occasionally it can be seen that S_{N2O} increases during anoxic conditions. The simulated S_{N2O} concentrations are generally lower than the measured ones. Based on the implemented model it is difficult to calibrate this effect because F_{N2O} (which is quite well predicted) is proportional to S_{N2O} and k_La_{N2O}. Thus, if the measurements are correct, either the stripping/flux model (including the diffusion coefficients) or the estimated k_La_{O2} need to be modified.

Applied parameter values

In Table 1, a summary of the parameter values for $X_{B,H}$ and X_{AOB} are shown. The table includes the values that differ from the original publications and show the major differences between the three case studies. Significant inhibition of heterotrophic denitrification was observed in *SBR_N/DN* only motivating the parameter values K_{S5}, $K_{S,EtOH,5}$ and $K_{I5,HNO2}$. The high value of $K_{NH3,AOB}$ in *SBR_NO2* is probably due to the nitritation only operation with rather high NH_3 concentrations. A plausible explanation for the lower value of μ_{AOB} in *SBR_NO2* compared to *SBR_N/DN* is inhibition due to the high HNO_2 concentrations. High concentrations of NO_2^- have been shown to have an inhibitory effect on AOB N_2O production as well (Law *et al.* 2013). However, since there are no available data with low NO_2 concentrations in the *SBR_NO2* case this cannot be validated and the potential inhibition effect is therefore lumped into the calibrated value of the $f_{DNT,A}$ parameter. AOB denitrification was not simulated in *MBBR_AMX* and therefore values of $f_{DNT,A}$, $K_{NH3,AOB,DN}$, $K_{HNO2,AOB}$ and $K_{NO,AOB}$ are not given for this case.

CONCLUSIONS

The implemented biological process model, together with physical models for the SBR- and MBBR-processes, can partly describe the N_2O emission data from the three case studies.

The AOB denitrification model, which was adopted from Mampaey *et al.* (2013), could adequately describe the behaviour of the nitrifying/denitrifying SBR (*SBR_N/DN)*. For the *nitritation only* SBR system (*SBR_NO2)* a high correlation to the ammonia concentration had to be assumed and may indicate that the implemented model is not able to fully describe the dynamics of the real system. It is possible that N_2O production by incomplete oxidation of NH_2OH, which was not included in the model, is dominating in this case.

The four-step denitrification model, which was adopted from Hiatt & Grady (2008), could be used to model accumulation of dissolved N_2O during anoxic conditions in the nitrifying/denitrifying SBR (*SBR_N/DN)*. To model the drastically decreased N_2O emission caused by addition of ethanol, an additional COD state variable had to be added.

The stripping/flux equation in the implemented model may be overly simplified. It results in sharp N_2O gas emission peaks that are not observed experimentally. For simulation of full-scale N_2O emission data in general, the retention time of the gas including the measurement devices would probably improve the conclusions that can be drawn regarding N_2O formation pathways.

The N_2O emissions from the studied MBBR anammox process (*MBBR_AMX*) data were satisfactorily simulated by assuming heterotrophic denitrification only. Results from other studies, indicate that AOB N_2O production may occur as well.

ACKNOWLEDGEMENTS

Dr Lindblom, Mr Arnell and Ms Yang acknowledge the financial support obtained through the Swedish Research Council Formas (contract no. 211-2010-141 and 211-2010-148), the Swedish Water & Wastewater Association (contracts no. 10-106, 10-107 and 11-106) and the J. Gust. Richert Memorial Fund (contract no. PIAH/11:58). Dr Flores-Alsina gratefully acknowledges the financial support provided by the People Program (Marie Curie Actions) of the European Union's Seventh Framework Programme FP7/2007–2013 under REA agreement 329349. Results based on this paper were presented at the IWA World Water Congress in Lisbon, Portugal, 21–26 September 2014.

REFERENCES

Chandran, K., Stein, L., Klotz, M. & van Loosdrecht, M. 2011 Nitrous oxide production by lithotrophic ammonia-oxidizing bacteria and implications for engineered nitrogen-removal systems. *Biochem. Soc. Trans.* **39**, 1832–1837.

DHI 2011 *WEST: Modelling Wastewater Treatment Plants – User Guide*. DHI, Hørsholm, Denmark.

Flores-Alsina, X., Gernaey, K. V. & Jeppsson, U. 2012 Benchmarking biological nutrient removal in wastewater treatment plants: influence of mathematical model assumptions. *Water Sci. Technol.* **65** (8), 1496–1505.

Flores-Alsina, X., Arnell, M., Amerlinck, Y., Corominas, Ll., Gernaey, K. V., Guo, L., Lindblom, E., Nopens, I., Porro, J., Shaw, A., Snip, L., Vanrolleghem, P. A. & Jeppsson, U. 2014 Balancing effluent quality, economic cost and greenhouse gas emissions during the evaluation of (plant-wide) control/operational strategies in WWTPs. *Sci. Total. Environ.* **466–467**, 616–624.

Foley, J., Yuan, Z., Keller, J., Senante, E., Chandran, K., Willis, J., van Loosdrecht, M. C. M. & van Voorthuizen, E. 2011 *N2O and CH4 Emission from Wastewater Collection and Treatment Systems*. Technical report, Global Water Research Coalition, London, UK.

Gernaey, K. V., Jeppsson, U., Vanrolleghem, P. A. & Copp, J. B. 2014 *Benchmarking of Control Strategies for Wastewater Treatment Plants*. Scientific and Technical Report No. 23, IWA Publishing, London, UK.

Gustavsson, D. J. I. & la Cour Jansen, J. 2011 Dynamics of nitrogen oxides emission from a full-scale sludge liquor treatment plant with nitritation. *Water Sci. Technol.* **63** (12), 2838–2845.

Hao, X. D., Heijnen, J. J. & van Loosdrecht, M. C. M. 2002 Sensitivity analysis of a biofilm model describing a one-stage completely autotrophic nitrogen removal (CANON) process. *Biotechnol. Bioeng.* **77**, 266–277.

Henze, M., Gujer, W., Mino, T. & van Loosdrecht, M. C. M. 2000 *Activated Sludge Models ASM1, ASM2, ASM2d and ASM3*. IWA Scientific and Technical Report No. 9, IWA Publishing, London, UK.

Hiatt, W. C. & Grady Jr., C. P. L. 2008 An updated process model for carbon oxidation, nitrification and denitrification. *Water Environ. Res.* **80** (11), 2145–2156.

Kampschreur, M. J., Temmink, H., Kleerebezem, R., Jetten, M. S. M. & van Loosdrecht, M. C. M. 2009 Nitrous oxide emission during wastewater treatment. *Water Res.* **43** (17), 4093–4103.

Law, Y., Ni, B. J., Lant, P. & Yuan, Z. 2012 N_2o production rate of an enriched ammonia-oxidising bacteria culture exponentially correlates to its ammonia oxidation rate. *Water Res.* **46** (10), 3409–3419.

Law, Y., Lant, P. & Yuan, Z. 2013 The confounding effect of nitrite on N_2O production by an enriched ammonia-oxidizing culture. *Environ. Sci. Technol.* **47** (13), 7186–7194.

Mampaey, K. E., Beuckels, B., Kampschreur, M. J., Kleerebezem, R., van Loosdrecht, M. C. M. & Volcke, E. I. P. 2013 Modelling nitrous and nitric oxide emissions by autotrophic ammonia-oxidizing bacteria. *Environ. Technol.* **34** (12), 1555–1566.

Ni, B. J., Yuan, Z., Chandran, K., Vanrolleghem, P. A. & Murthy, S. 2013 Evaluating four mathematical models for nitrous oxide production by autotrophic ammonia-oxidizing bacteria. *Biotechnol. Bioeng.* **110** (1), 153–163.

Ni, B. J., Peng, L., Law, Y., Guo, J. & Yuan, Z. 2014 Modeling of nitrous oxide production by autotrophic ammonia-oxidizing bacteria with multiple production pathways. *Environ. Sci. Technol.* **48** (7), 3916–3924.

Pan, Y., Ni, B. J., Lu, H., Chandran, K., Richardson, D. & Yuan, Z. 2014 Evaluating two concepts for the modelling of intermediates accumulation during biological denitrification in wastewater treatment. *Water Res.* **71**, 21–31.

Stenström, F., Tjus, K. & la Cour Jansen, J. 2014 Oxygen-induced dynamics of nitrous oxide in water and off-gas during the treatment of digester supernatant. *Water Sci. Technol.* **69** (1), 84–91.

Yang, J., Trela, J., Plaza, E. & Tjus, K. 2013 N_2o emissions from a one stage partial nitrification/anammox process in moving bed biofilm reactors. *Water Sci. Technol.* **68** (1), 144–152.

Yu, R., Kampschreur, M. J., van Loosdrecht, M. C. M. & Chandran, K. 2010 Mechanisms and specific directionality of autotrophic nitrous oxide and nitric oxide generation during transient anoxia. *Environ. Sci. Technol.* **44** (4), 1313–1319.

Zhou, Y., Pijuan, M., Zeng, R. J. & Yuan, Z. 2008 Free nitrous acid inhibition on nitrous oxide reduction by a denitrifying-enhanced biological phosphorus removal sludge. *Environ. Sci. Technol.* **42** (22), 8260–8265.

First received 12 March 2015; accepted in revised form 6 October 2015. Available online 27 October 2015

Paper III

Watermatex 2015
9th IWA Symposium on Systems Analysis and Integrated Assessment
14-17 June 2015, Gold Coast, Australia

Aeration System Modelling - Case Studies From Three Full-scale Wastewater Treatment Plants

Arnell, M.* and Jeppsson, U.***
* Division of Industrial Electrical Engineering and Automation (IEA), Department of Biomedical Engineering (BME), Lund University, Box 118, 221 00 Lund, Sweden.
** SP Urban Water Management, Gjuterigatan 1D, 582 73 Linköping, Sweden.

Keywords: aeration

Summary of key findings

The water train of three WWTPs have been modelled following the procedures of the Benchmark Simulation Model (BSM) platform (Gernaey *et al.*, 2014). Additionally the aeration system has been modelled to evaluate airflows and energy performance. The results for the airflow model are presented. The chosen airflow model is shown to be easy to apply and calibrate and robust for practical modelling cases. By simply adjusting the SOTE-polynomial, number of diffusors and airflow limitations the model replicates the real data at a level of detail suitable for most purposes where the evaluation is based on longer time averages. For peak demand evaluation the whole treatment model with influent characterization, model calibration and controllers need to be more detailed than done here. Modelling the airflow is important to allow for evaluation of air consumption, aeration energy performance and for communication of simulation results to plant staff and operators.

Background and relevance

The development of mathematical models of wastewater treatment processes has been in progress for over 30 years. Today modelling and simulation are widely accepted tools for decision-making support in wastewater management (Daigger *et al.*, 2011). The term 'model' here represents an abstract mathematical representation of a real system. The model cannot - and does not intend to - be a complete representation of the subject system. Rather, it is important to select an adequately complex model for the intended use (Olsson, 2012).

For evaluating performance and efficiency of wastewater treatment plants (WWTPs) aeration of the activated sludge unit is one of the key processes. The conventional models, i.e. the IWA activated sludge model (ASM) family, are known to well describe the oxygen consumption for most practical applications. However, these bioprocess models normally use $K_{\mathrm{L}}a$ to describe the oxygen input. $K_{\mathrm{L}}a$ input is not a practical unit measured or controlled at the WWTPs and there are several reasons for extending the model to include airflow: *i)* airflow can easily be validated against measurements; *ii)* airflow can be used for detailed modelling of power consumption for aeration; and *iii)* airflow is more communicative towards professionals at the utilities. This paper describes the implementation of an aeration model applied to three recent modelling studies of Swedish WWTPs.

Material and methods

The model developed includes the main parts of the aeration system, such as oxygen transfer in the diffusors, pressure drop over diffusors and power consumption in blowers, see Fig. 1. In this paper only the oxygen transfer model for the diffusors is presented. The oxygen transfer model is adopted from Beltran (2013). The model by Beltran (2013) was chosen prior to alternative models, such as the one by Dold and Fairlamb (2001), for its physical mechanistic approach and transparency rather than empirical equations based on parameters that are hard to estimate. The model describes a non-linear relationship between $K_{\mathrm{L}}a$ and airflow according to Equation 1:

$$K_{\mathrm{L}}a = \alpha F(1.024^{T-20})\frac{OTE_{STP}x_{O2}\rho_{g,STP}}{V_L M_G \delta S_{o,sat,STP}}Q_{air} \qquad (1)$$

where α is the process water correction factor, F is the diffusor fouling factor, T is process water temperature, OTE is the oxygen transfer efficiency, x_{O2} the fraction of oxygen in dry air, ρ_g the density

of air, V_L the reactor liquid volume, M_G the weighted molar mass of air, δ is the correction factor for liquid column pressure, $S_{o,sat}$ is the oxygen concentration in process water and Q_{air} the airflow. Index *STP* denotes standard temperature and pressure.

The oxygen transfer efficiency is a non-linear relationship specific for each diffusor type and installation, varying with submersion depth and diffusor density. In this model a polynomial fit of SOTE-data over the whole airflow range is used. SOTE-data for the three plants was retrieved and the model fitted to the data, see Fig. 2. For the three case studies no recent measurements for α values were available, and therefore values in the range of 0.6 to 0.8 were assumed.

The three WWTPs indexed 1 to 3 represent middle-sized to large WWTPs in southern Sweden. Common for all plants is that they are well equipped and controlled. The aeration control strategy for WWTP 3 is adopted from the Kruger STAR system (Rosen and Arnell, 2007) with intermittent aeration where the time periods of the aerated and not-aerated phases as well as the DO set-points are controlled based on feedback from on-line NH4-N and NO3-N measurements in the bio-reactor effluent. Basic information of the three WWTPs and their aeration systems are given in Table 1. The main purpose of modelling the three plants was to analyse future expansions plans and the evaluations were made on annual, quarterly or at most monthly basis. The water train of all three plants were modelled in Matlab/Simulink based on the BSM2 with the same selection of sub-models, except for the secondary clarifier that was modelled using the model by Burger *et al.* (2013) with 10 layers.

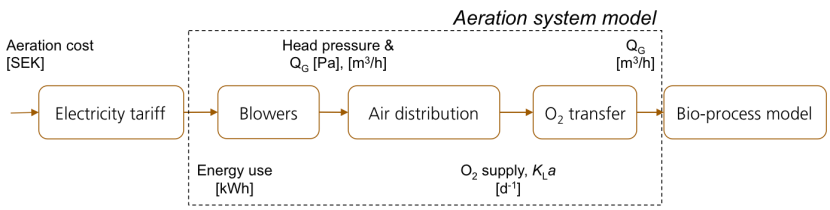

Figure 1 Schematic figure of the components included in the complete aeration model. Only the oxygen transfer over the aerators is presented here.

Table 1. Specifications of the three WWTPs in the case study.

	WWTP 1	WWTP 2	WWTP 3
Plant load [pe]	270 000	93 000	180 000
Water treatment train	Primary / MLE w precipitation / sec. clarifier / sand filters	Primary with CEPT / MLE with bio-augumentation / sec. clarifier / post precipitation & sed.	Primary with CEPT / ASP / sec. clarifier / post DN / post precipitation & sed.
ASP aerated volume	44 000	4 030	9 110
Diffusor type	Fine bubbled bottom aeration system with rubber membrane circular discs	Fine bubbled bottom aeration system with rubber membrane circular discs	Fine bubbled bottom aeration system with rubber membrane panels
Diffusor submersion depth [m]	10	3.5	3.5
Aeration control strategy	Fixed DO set-point	Fixed DO set-point	Intermittent aeration with controlled DO set-point based on NH_4-N and NO_3-N feedback

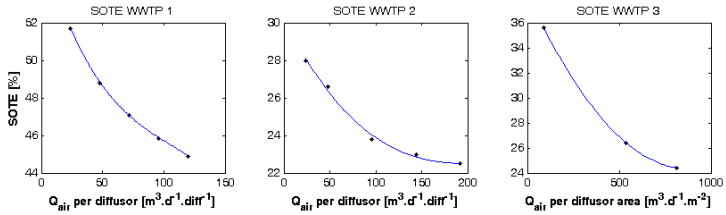

Figure 2 SOTE-data for the three WWTPs (black dot) at actual submersion depths and diffusor densities. Polynomial fit used in model (blue line).

Results

Resulting airflow curves for the three WWTP models are shown in Fig. 3 together with corresponding data. For WWTP 1 and 3 hourly average data were available but for WWTP 2 only daily averages. In Table 2 average airflows together with goodness of fit measures are presented. The goodness of fit is presented both as deviation of average airflows from averaged data and as normalised root mean squared errors evaluated with the Matlab `goodnessOfFit` function on step-wise averaged model outputs (hourly or daily) and data.

WWTP 1

In the model representing WWTP 1 four consecutive PI-controllers with four corresponding measurements were implemented. At the plant this advanced DO control set-up is only implemented for two out of five parallel lines. However, for this specific model purpose the parallel lines were modelled as one. As shown in Fig. 3, the modelled airflow is more smoothly controlled compared to the measurements but both the general air flow level and trends are captured. As for the averages and goodness of fit criteria in Table 2 the deviation is very small, only 4.4%, but the goodness of fit number not as good.

WWTP 2

As seen in Fig. 3 also the model results for the second WWTP in the study demonstrate a good fit with regard to the level and trends in airflows by only adjusting the SOTE curve and airflow limitations. Here the deviation is somewhat higher, 13%, but the goodness of fit much better. The WWTP 2 is the smallest plant and also less monitored and controlled than the other two. When calibrating the aeration model it is obvious that there are some effects not explained during the winter months (day 245 to 375). The drop in measured airflow around day 350 corresponds to a sharp peak in the ammonia concentration that the model fails to predict. Potentially the plant was exposed to some inhibitory or toxic events during this period.

WWTP 3

At the third plant the comparison is more difficult. The intermittent aeration strategy based on feedback of the treatment result makes the aeration go on-off with phases of varying length and time. At the plant the aeration phases for the 8 parallel lines are also shifted in time for practical reasons and the model simplification of reducing all the parallel lines into one cannot account for that shift. The model produces a good prediction of treatment performance. From the aeration model output in Figure 3 it can be seen that the aeration system goes on-off between 0 and the maximum air flow repeatedly and also that during some periods there are air supply limitations as the model predicts maximum airflows for the entire aerated phase. The hourly measured averages of the parallel lines are not suitable for comparison on a short time basis. However, the average values presented in Table 2 show that the deviation is only 5.3% and the goodness of fit is also adequate.

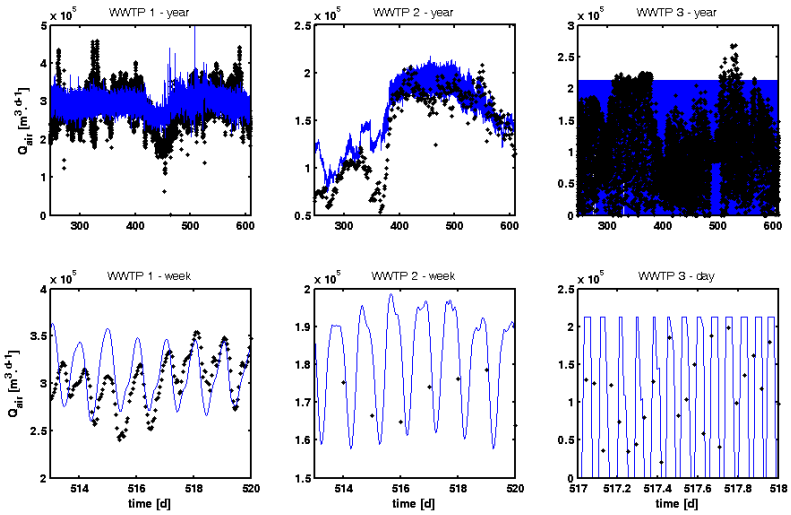

Figure 3. Total airflows from the three case studies – model (blue line) and data (black dot). Air flows over the whole evaluation period (top) and week or day selection (bottom).

Table 2. Goodness of fit of the airflow model for the three case studies. Airflow averages over the one year evaluation period for model and data, deviation between data and model averages. Goodness of fit value for the dynamic data.

	WWTP 1	WWTP 2	WWTP 3
Q_{air} model annual average [m^3/d]	2.96e+05	1.57e+05	1.10e+05
Q_{air} data annual average [m^3/d]	2.83e+05	1.39e+05	1.04e+05
Deviation [%]	4.4	13	5.3
Goodness of fit [-]	-8.6	0.032	-0.25

References

Beltrán, S., de la Sota, A., Villanueva, J.M. (2013) Model based optimization of aeration systems in WWTPs. ICA2013, 18-20 Sept., Narbonne, France.

Bürger, R., Diehl, S., Farås, S., Nopens, I., Torfs E. (2013) A consistent modelling methodology for secondary settling tanks: a reliable numerical method. *Wat. Sci. Tech.*, 68(1), 192-208.

Daigger, G. (2011) A practitioners perspective on the uses and future developments for wastewater treatment modelling. *Wat. Sci. Tech.*, 63(3), 516-526.

Dold, P., Fairlamb, M. (2001) Estimating oxygen transfer KLa, SOTE and air flow requirements in fine bubble diffused air systems. WEFTEC2001 (pp. 780-791).

Gernaey, K.V., Jeppsson, U., Vanrolleghem, P.A., Copp, J.B. (2014) Benchmarking of Control Strategies for WWTPs. STR no. 23, IWA Publ., London, UK.

Olsson, G. (2012) ICA and me - A subjective review. *Wat. Res.*, 46(6), 1585-1624.

Rosen, C., Arnell, M. (2007) Plant-wide control of WWTPs. NordIWA2007, 11-14 Nov., Hamar, Norway.

Paper IV

Parameter estimation for modelling of anaerobic co-digestion

M. Arnell*,, L. Åmand*****

* Department of Biomedical Engineering (BME), Division of Industrial Electrical Engineering and Automation (IEA), Lund University, P.O. Box 118, SE-221 00 Lund, Sweden. E-mail: magnus.arnell@iea.lth.se, Phone: +46 (0)72 727 61 40, Fax: +46 (0)46 142114.
** Urban Water Management Sweden AB, Gjuterigatan 1D, SE-582 73 Linköping, Sweden.
*** IVL Swedish Environmental Research Institute, P.O. Box 210 60, SE-100 31, Stockholm, Sweden.

Abstract: To assess the full energy recovery potential of a wastewater treatment plant, modelling and simulation of anaerobic co-digestion in a plant-wide perspective have to be further developed. A critical problem to address is the characterisation of substrates needed for proper application of the Anaerobic Digestion Model no.1, both characterisation of COD and biokinetic substrate dependent parameters, i.e. the hydrolysis rate and the maximum biogas potential. This study examines two available models for estimating the hydrolysis rate and the maximum biogas potential from biomethane potential tests and assesses the uncertainty of the models. 18 data sets from full-scale systems representing different substrates were examined and it was concluded that a first-order model was superior to a switching-type model for most of the data sets.

Keywords: Anaerobic digestion, co-digestion, hydrolysis rate, parameter estimation, substrate characterisation.

Introduction

The objective for wastewater treatment plants (WWTPs) has traditionally been effluent water quality under the constraints of technical feasibility and cost. During recent years the scope has widened to also cover energy efficiency, greenhouse gas mitigation and resource recovery from wastewater – all together increasing the focus on anaerobic digestion at WWTPs (Frijns *et al.*, 2013).

In light of the increased focus on digestion, it is important that it is possible to evaluate the performance and operation of digestion at WWTPs. Modelling and simulation is a powerful tool for evaluation provided that common applications for anaerobic digestion are included. One application that nowadays is common at WWTPs is anaerobic co-digestion of different organic wastes together with sewage sludge (Zitomer *et al.*, 2008). The Anaerobic Digestion Model no. 1 (ADM1) presented by Batstone *et al.* (2002) is a general anaerobic digestion model that have been used for different applications including modelling of co-digestion (Zaher *et al.*, 2009; Lübken *et al.*, 2007). For any modelling/simulation assignment one of the most critical tasks is to characterise the influent properly in terms of the state variables of the model. This is equally true for modelling of anaerobic co-digestion. There are studies in literature exploring methods to characterise WWTP sludges, but only a few of those studies deal with characterisation of more complex substrates (Mata-Alvarez *et al.*, 2011). The problem can be divided into two parts: i) characterisation of organic material (COD), nitrogen, charge, etc.; and, ii) determination of substrate dependent biological parameters.

This work focuses on determination of substrate dependent biological parameters and compares two published models used for the determination of the hydrolysis rate and biogas potential from bio-methane potential (BMP) tests using non-linear parameter estimation. BMP tests are controlled experiments with excess inoculum

where the methane production is monitored over time and are commonly used to estimate the extent and rate of degradation of substrates in anaerobic digestion.

This study compares two models previously published by Angelidaki *et al.* (2009) and Koch & Drewes (2014). 18 datasets from BMP tests digesting secondary sludge, mixed sludge, food waste, fat oil and grease (FOG) and vegetable waste were used for the model comparison. Separate determination of the hydrolysis coefficient of substrates for co-digestion allows for modelling of co-digestion according to Zaher *et al.* (2009). The purpose of the paper is to provide parameter estimates for a range of substrates used for anaerobic co-digestion and to assess which of the two models fit the BMP batch data the best.

Materials and Methods

A BMP test results in a data series showing the cumulative gas production over time. From this data, the first-order hydrolysis coefficient (k_{hyd}, d^{-1}) and the ultimate methane yield (P_f, $mlCH_4.gVS^{-1}$) can be estimated by fitting a model to the data with some optimisation routine. In this study, two different models previously presented in literature were compared.

Model no. 1 (eq. 1), presented by Koch & Drewes (2014), assumes that the BMP reactor is fully mixed, the volume is constant and the hydrolysis is the rate-limiting step and of first-order. The model was adapted from a continuous model for gas production published by Eastman & Fergusson (1981). Mathematically, Model 1 exhibits the same dynamics as the Monod kinetics describing growth of biomass or the Michaelis-Menten kinetics which models enzyme kinetics. Model 1 is a switching function with P_f being its highest achievable value, and the inverse of k_{hyd} being the half-saturation constant.

$$V = \frac{P_f k_{hyd} t}{1 + k_{hyd} t} \tag{1}$$

Model no. 2 (eq. 2), used by for example Angelidaki *et al.* (2009), is a first-order model derived from the first-order differential equation for growth, where k_{hyd} is the inverse time constant of the model. To be precise, P_f is in Angelidaki *et al.* (2009) referred to as B_∞ and defined as the ultimate methane production which is the cumulative methane production at the last day of the experiment. An example of the shape of Model 1 and Model 2 is found in Figure 1.

$$V = P_f\left(1 - e^{-k_{hyd}t}\right) \tag{2}$$

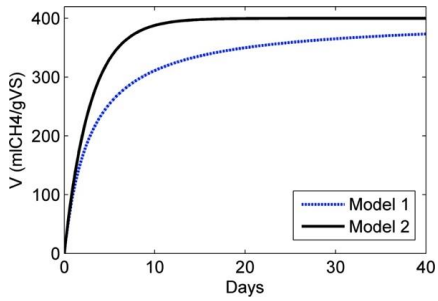

Figure 1 The dynamics of Model 1 (switch function) and Model 2 (first-order model). P_f = 400 $mlCH_4.gVS^{-1}$ and k_{hyd} = 0.35 d^{-1}.

The hydrolysis rate has different meanings in the two different models. In Model 1, the inverse of k_{hyd} is the half-saturation constant, meaning the time it takes for the test to reach 50 % of P_f. In Model 2, the inverse of k_{hyd} is the time constant, meaning the time it takes for the test to reach 67 % of P_f.

This study has involved non-linear parameter estimation to fit the two models (eq. (1), eq. (2)) to measurement data. Within parameter estimation, the cost function will be a measure of the discrepancy between the model output and the measurement data. The most commonly used cost function in parameter estimation is the sum of squared error (SSE, eq. (3)). Another alternative is to minimise the sum of absolute errors (SAE, eq. (4)), see Table 1. In this study, both SSE and SAE were used. The least squares estimate is equivalent to using SSE as a cost function, while the SAE could be referred to as the least absolute deviation. The benefit from using least absolute deviation is that the results are more robust towards outliers in the data, but compared to using least squares, least absolute deviation can result in several minima and the solution can be unstable.

Table 1 Cost functions used for non-linear parameter estimation. n is the number of data points, y is the model output and yd is the measurement data.

Name	Abbreviation	Equation	
Sum of squared error	SSE	$\sum_n (y - yd)^2$	(3)
Sum of absolute error	SAE	$\sum_n \lvert y - yd \rvert$	(4)

Modelling was made in MATLAB® (version R2012b, MathWorks). Model 1 and 2 was fitted to the BMP data using the MATLAB function *fminsearch.* Uncertainty analysis was made based on the Frequentist's approach using the Maximum Likelihood Estimate (MLE). Source code for the uncertainty analysis was provided by Technical University of Denmark (Sin, Gernaey, & Lantz, 2009). A confidence interval of 95 % was used.

Measurement data

To obtain an estimate of the values of k_{hyd} and P_f for different substrates, 18 datasets were collected from Swedish and German universities and Swedish wastewater treatment plants. The datasets are listed in Table 2. Mixed sludge is a combination of

primary and secondary sludge. Dataset 13 to 18 originates from an automatic sampling procedure, and the tests are from the same experiment where an increased fraction of food waste is added to secondary sludge. In the other tests, manual measurements were used. When applicable, average result of triplicates was used.

Results and Discussion

The results from estimating the parameters k_{hyd} and P_f from BMP data with the two models are presented in Table 1 and visualised in Figure 2. Figure 3 and 4 shows the complete results for both models with SSE as cost function. Model 2 has a better fit to the BMP data for a majority of the BMP tests, i.e. the confidence intervals on the parameters are smaller. For one data set (no. 3), Model 1 leads to a better fit than Model 2.

Model 1 results in a higher estimate of k_{hyd} and P_f than Model 2 in all but two occasions, which is expected given the difference in meaning of the hydrolysis coefficient and the ultimate gas production in the two equations. A higher k_{hyd} is expected to fit the data better in the first-order model (Model 2) since k_{hyd} is the value at 67 % of P_f, compared to 50 % of P_f in the switch function (Model 1). Also, P_f is the gas production at the end of the experiment in the first-order model, but in the switch function it is the ultimate yield of the substrate which is normally not reached during the course of a batch experiment (Koch & Drewes, 2014).

The quality of the data affects the goodness of fit. It can be seen from comparing for example Test 5 and 6 that a more scattered data series gives a wider confidence interval. Furthermore, Test 2 and 9 show an unexpected decrease in gas production at the end, rising doubts about the data quality for these tests since a cumulative gas production cannot in theory be decreased.

Both models assume a quick rise in the gas production with the maximum rate from t = 0, i.e. the second derivative is negative over the duration of the test. This does not hold for Tests 10 and 11 since they show a clear lag phase at the beginning before the rise. This lag can be due to faulty BMP tests with inappropriate inoculum etc. Since the two models do not compensate for this the fit is bad and the models cannot be recommended in this case. The uncertainty in the estimate of the ultimate gas yield is particularly high since the models do not reach a steady-state in accumulated gas production. If a test with lag is assumed to correctly describe the degradation a term compensating for the lag can be added to ether of the models. This has not been tested in this study.

There was not a large difference between the sizes of the confidence intervals resulting from using SSE or SAE as a cost function in the parameter estimation. The confidence intervals were most of the time smaller for the case of SSE and therefore only results with SSE are presented here. The most important factor which decides the size of the confidence interval is the sample size. For large sample sizes the t-distribution percentile will be smaller than for small sample sizes. This is why the confidence intervals for the automatic BMP tests with many samples (i.e. test 13 to 18) are smaller than from the manual tests. Another reason for the better fit with the automatic measurements is that the samples are smoother with fewer outliers. Still, the results from the manual sampling is believed to be qualified enough for parameter estimation.

The shape of the data influences the result of the parameter estimation. Principally the two models differs as Model 1 increases more slowly and have a longer transient phase than Model 2 for the same k_{hyd} and P_f as can be seen in Figure 3. This means that in theory, data showing similar long transient behaviour will fit better with Model 1 while data quickly reaching their maxima fit better with Model 2. However, for the selected BMP tests in this study Model 2 was better in almost all cases regarding confidence intervals (Table 1).

The hydrolysis coefficient estimated with Model 2 ranged from 0.08 to 0.70 d^{-1}. The range for P_f was 315 to 1010 $mlCH_4.gVS^{-1}$. This is in the same range as reported by other studies (Lübken *et al.*, 2007; Batstone *et al.*, 2008; Donoso-Bravo *et al.*, 2010). Batstone *et al.* (2008) does show that hydrolysis rate is much lower when estimated from batch test, compared to full-scale estimation based on gas-flow. The authors conclude that the batch estimates are not suitable for dynamic modelling. Parameter estimation of the hydrolysis coefficient from batch tests should therefore be considered as relatively rough estimates.

Table 2 Tested data sets with summary of the results for the two Models with SSE as cost function.

Test	Substrate	Model 1		Model 2	
		k_{hyd} [d^{-1}]	P_f [$mlCH_4.gVS^{-1}$]	k_{hyd} [d^{-1}]	P_f [$mlCH_4.gVS^{-1}$]
1	Secondary sludge	0.12 ± 0.029	387 ± 31.5	0.11 ± 0.017	315 ± 17
2	Mixed sludge	0.27 ± 0.068	426 ± 25.0	0.21 ± 0.036	372 ± 16
3	Mixed sludge	0.21 ± 0.011	420 ± 5.9	0.17 ± 0.034	359 ± 19
4	Mixed sludge	0.67 ± 0.14	364 ± 19.7	0.55 ± 0.069	322 ± 12
5	Mixed sludge + food waste	0.51 ± 0.30	380 ± 36.9	0.31 ± 0.064	345 ± 15
6	Mixed sludge	0.25 ± 0.17	409 ± 61.6	0.20 ± 0.092	357 ± 40
7	Mixed sludge	0.20 ± 0.19	384 ± 94.4	0.18 ± 0.10	326 ± 47
8	Food waste	0.21 ± 0.09	401 ± 39.3	0.17 ± 0.026	348 ± 13
9	Food waste	0.17 ± 0.11	508 ± 95.2	0.15 ± 0.039	422 ± 30
10	FOG	0.05 ± 0.040	1414 ± 508	0.06 ± 0.030	1010 ± 195
11	FOG	0.09 ± 0.066	859 ± 213	0.10 ± 0.037	676 ± 83
12	Vegetable waste	0.59 ± 0.10	387 ± 10.8	0.38 ± 0.099	354 ± 16
13	Secondary sludge	0.99 ± 0.033	345 ± 2.0	0.70 ± 0.012	309 ± 0.91
14	Secondary sludge + 5 % food waste	0.90 ± 0.031	355 ± 2.2	0.66 ± 0.012	315 ± 1.1
15	Secondary sludge + 15 % food waste	0.77 ± 0.039	420 ± 4.2	0.59 ± 0.010	368 ± 1.2
16	Secondary sludge + 22.5 % food waste	0.62 ± 0.038	434 ± 4.9	0.47 ± 0.011	384 ± 1.6
17	Secondary sludge + 30 % food waste	0.54 ± 0.035	439 ± 6.6	0.47 ± 0.011	371 ± 2.0
18	Food waste	0.49 ± 0.034	515 ± 8.7	0.43 ± 0.012	433 ± 2.7

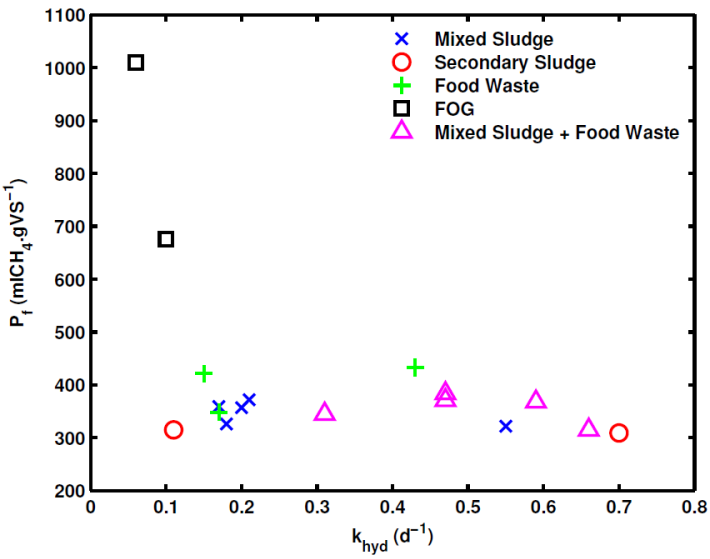

Figure 2 Resulting pairs of P_f and k_{hyd} for the 18 data sets using Model 2 and SSE.

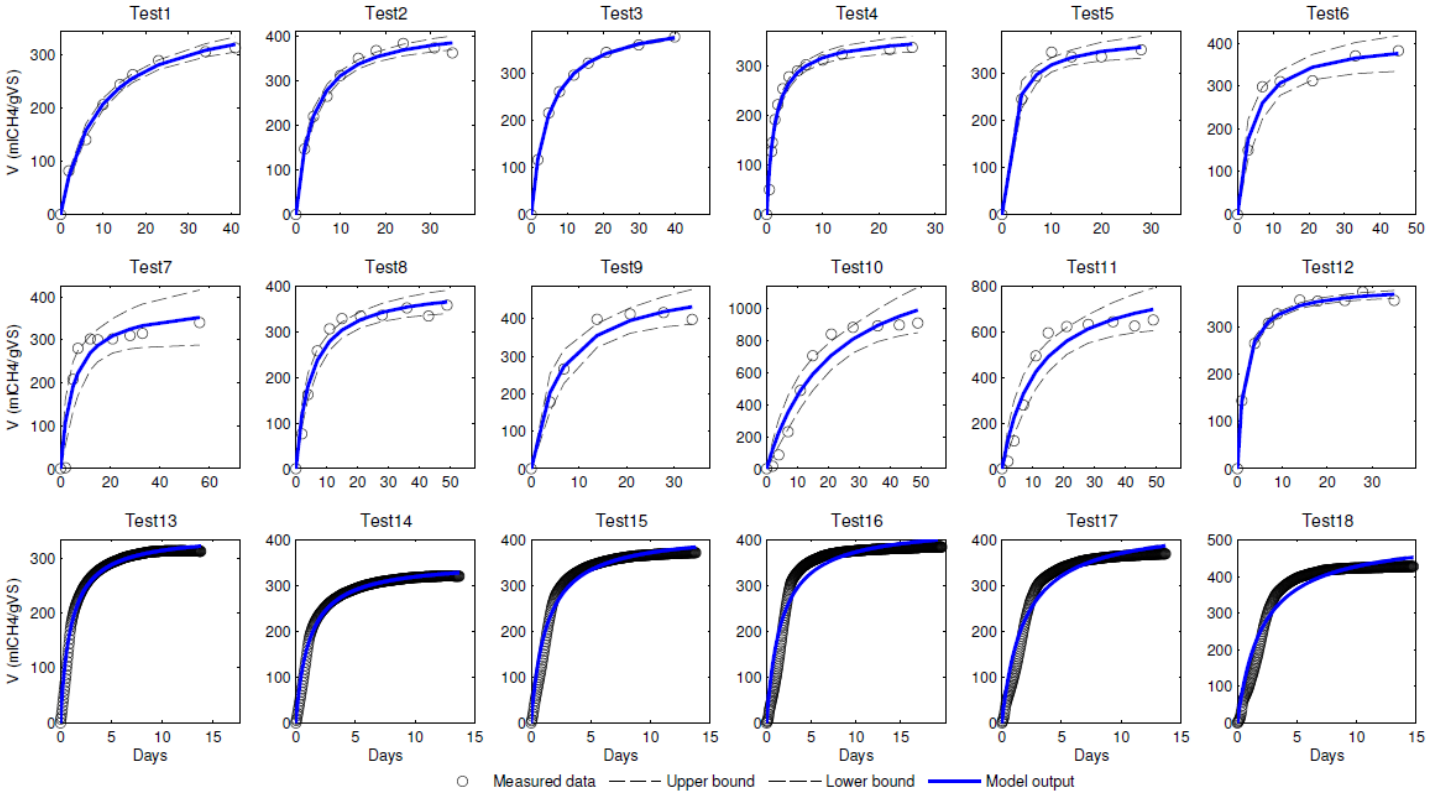

Figure 3 Model fitting results using Model 1 (Monod-type switch function).

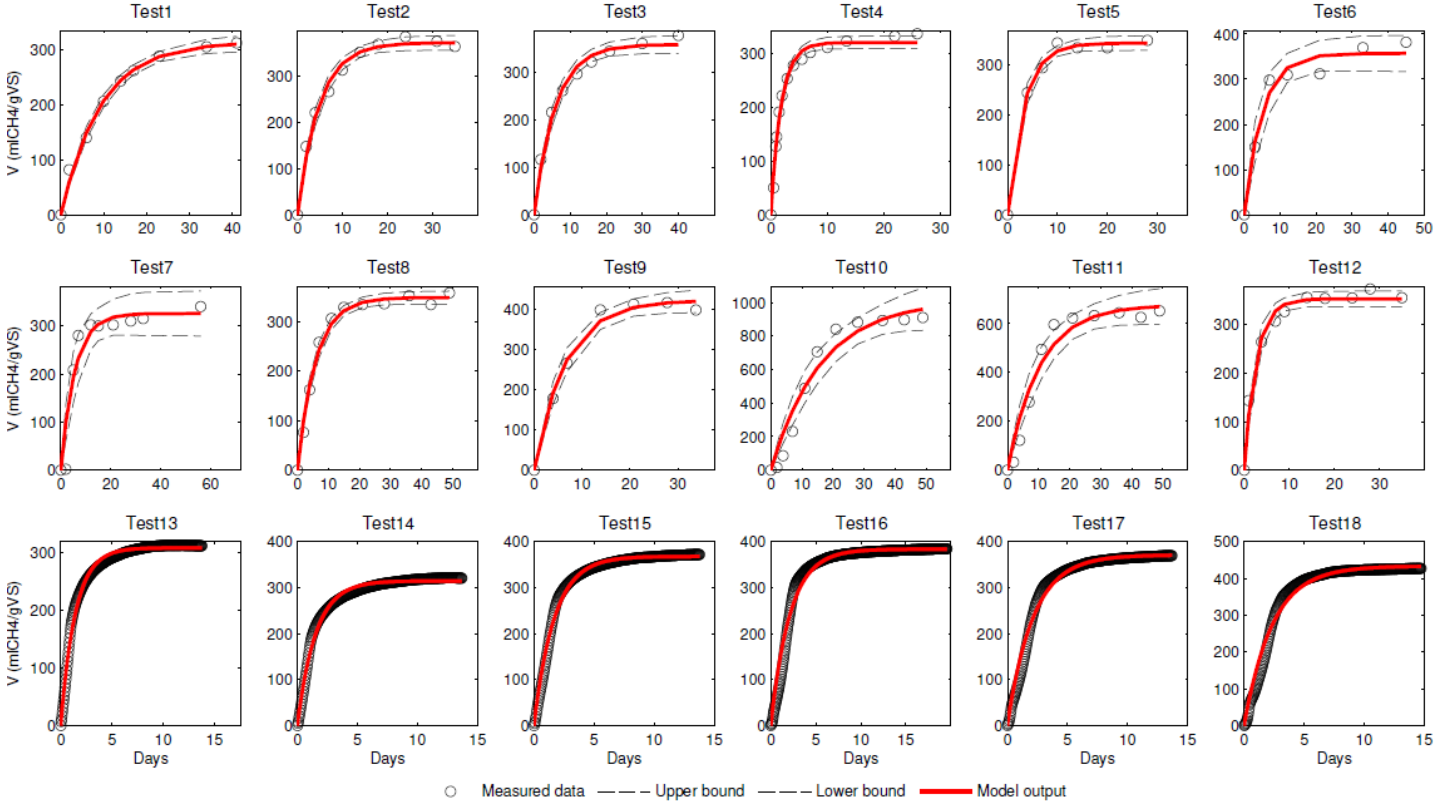

Figure 4 Model fitting results using Model 2 (first-order model).

Conclusions

Non-linear parameter estimation was used to estimate the first-order hydrolysis coefficient and the ultimate methane yield from 18 datasets with BMP batch data. The study can conclude that:

- the parameter uncertainty was lower when fitting data to a first-order model compared to a Monod-type switching function since this model could better describe the shape of the cumulative gas production in the BMP tests;
- the switching function resulted in higher estimates of the hydrolysis coefficient and the ultimate methane yield compared to the first-order model;
- the smoother the BMP curve and the more samples in the test, the smaller the confidence interval of the estimated gas production;
- the hydrolysis coefficient for the studied substrates was in the range 0.08 to 0.70 d^{-1}.

Acknowledgements

The authors fully acknowledge the support making this work possible. Dr.-Ing. Konrad Koch from Technische Universität München supported with data and valuable comments. Data were also supplied by Lund University, Stockholm Vatten AB, Tekniska Verken i Linköping AB (publ.) and Växjö kommun. The code for uncertainty analysis was provided by Associate Professor Gürkan Sin at Technical University of Denmark. Magnus Arnell was funded by the Swedish Research Council Formas (211-2010-141), the Swedish Water & Wastewater Association (10-106, 11-106). Linda Åmand acknowledges the funding from the Foundation for IVL Swedish Environmental Research Institute.

References

Angelidaki, I., Alves, M., Bolzonella, D., Borzacconi, L., Campos, J. L., Guwy, A. J., Kalyuzhnyi, S., Jenicek, P. and Van Lier, J. B. (2009). Defining the biomethane potential (BMP) of solid organic wastes and energy crops: a proposed protocol for batch assays. Water Science & Technology, 59(5), 927–934.

Batstone, D.J., Keller, J., Angelidaki, I., Kalyuzhnyi, S.V., Pavlostathis, S.G., Rozzi, A., Sanders, W.T., Siegrist, H. and Vavilin, V.A. (2002). Anaerobic Digestion Model No. 1. (ADM1). IWA Scientific and Technical Report No 13, IWA Publishing, London, UK.

Batstone, D.J., Tait, S. and Starrenburg, D. (2008). Estimation of Hydrolysis Parameters in Full-Scale Anerobic Digesters. Biotechnology and Bioengineering, 102, 1513–1520.

Donoso-Bravo, A., Pérez-Elvira, S. I. and Fdz-Polanco, F. (2010). Application of simplified models for anaerobic biodegradability tests evaluation of pre-treatment processes. Chemical Engineering Journal, 160(2), 607–614.

Eastman, J.A. and Ferguson, J.F. (1981). Solubilization of particulate organic carbon during the acid phase of anaerobic digestion. Journal of the Water Pollution Control Federation, 53(3), 352-366.

Frijns, J., Hofman, J. and Nederlof, M. (2013). The potential of (waste)water as energy carrier. Energy Conversion and Management, 65, 357–363.

Koch, K. and Drewes, J. E. (2014). Alternative approach to estimate the hydrolysis rate constant of particulate material from batch data. Applied Energy, 120, 11-15.

Lübken, M., Wichern, M., Schlattmann, M., Gronauer, A. and Horn, H. (2007). Modelling the energy bal-ance of an anaerobic digester fed with cattle manure and renewable energy crops. Water Research, 41(18), 4085-4096.

Mata-Alvarez, J., Dosta, J., Macéé, S. and Astals, S. (2011). Codigestion of solid wastes: A review of its uses and perspectives including modeling. Critical Reviews In Biotechnology, 31(2), 99-111.

Sin, G., Gernaey, K. V. and Lantz, A. (2009). Good modelling practice for PAT applications: Propagation of input uncertainty and sensitivity analysis. Biotechnology Progress, 25(4), 1043–1053.

Zaher, U., Li, R., Jeppsson, U., Steyer, J. P. and Chen, S. (2009). GISCOD: General Integrated Solid Waste Co-Digestion model. Water Research, 43(10), 2717–2727.

Zitomer, D. H., Adhikari, P., Heisel, C. and Dineen, D. (2008). Municipal anaerobic digesters for codigestion, energy recovery, and greenhouse gas reductions. Water Environment Research, 80, 229–237.

Paper v

Water Research 98 (2016) 138–146

Contents lists available at ScienceDirect

Water Research

journal homepage: www.elsevier.com/locate/watres

Modelling anaerobic co-digestion in Benchmark Simulation Model No. 2: Parameter estimation, substrate characterisation and plant-wide integration

Magnus Arnell [a, b, *], Sergi Astals [c], Linda Åmand [d], Damien J. Batstone [c], Paul D. Jensen [c], Ulf Jeppsson [a]

[a] Department of Biomedical Engineering (BME), Division of Industrial Electrical Engineering and Automation (IEA), Lund University, P.O. Box 118, SE-221 00, Lund, Sweden
[b] SP Technical Research Institute of Sweden, Gjuterigatan 1D, SE-582 73, Linköping, Sweden
[c] Advanced Water Management Centre, The University of Queensland, Brisbane, 4072, QLD, Australia
[d] IVL Swedish Environmental Research Institute, P.O. Box 210 60, SE-100 31, Stockholm, Sweden

ARTICLE INFO

Article history:
Received 5 January 2016
Received in revised form
30 March 2016
Accepted 31 March 2016
Available online 4 April 2016

Keywords:
Mathematical modelling
ADM1
Anaerobic digestion
LCFA inhibition
Waste characterisation
Codigestion

ABSTRACT

Anaerobic co-digestion is an emerging practice at wastewater treatment plants (WWTPs) to improve the energy balance and integrate waste management. Modelling of co-digestion in a plant-wide WWTP model is a powerful tool to assess the impact of co-substrate selection and dose strategy on digester performance and plant-wide effects. A feasible procedure to characterise and fractionate co-substrates COD for the Benchmark Simulation Model No. 2 (BSM2) was developed. This procedure is also applicable for the Anaerobic Digestion Model No. 1 (ADM1). Long chain fatty acid inhibition was included in the ADM1 model to allow for realistic modelling of lipid rich co-substrates. Sensitivity analysis revealed that, apart from the biodegradable fraction of COD, protein and lipid fractions are the most important fractions for methane production and digester stability, with at least two major failure modes identified through principal component analysis (PCA). The model and procedure were tested on bio-methane potential (BMP) tests on three substrates, each rich on carbohydrates, proteins or lipids with good predictive capability in all three cases. This model was then applied to a plant-wide simulation study which confirmed the positive effects of co-digestion on methane production and total operational cost. Simulations also revealed the importance of limiting the protein load to the anaerobic digester to avoid ammonia inhibition in the digester and overloading of the nitrogen removal processes in the water train. In contrast, the digester can treat relatively high loads of lipid rich substrates without prolonged disturbances.

© 2016 Elsevier Ltd. All rights reserved.

1. Introduction

The scope for wastewater treatment plants (WWTPs) has widened during recent years. Not only are the discharge limits getting stricter, also new constraints such as resource recovery, energy efficiency and mitigation of greenhouse gas emissions are being applied (Olsson, 2015). These issues increase the focus on energy recovery by anaerobic digestion (AD) at WWTPs. Many full-scale anaerobic digesters are oversized and therefore under-utilised (Lundkvist, 2005). Anaerobic co-digestion (AcoD) of organic wastes with sewage sludge allows the WWTPs to use residual digester capacity and thereby increase methane production and subsequently energy production (Batstone and Virdis, 2014; Mata-Alvarez et al., 2014). The application of AcoD at WWTPs is becoming more common and in the future is it likely that most medium to large size plants will practice AcoD. Even though the co-substrates are fed directly to the digester and not to the WWTP influent, it still produces an additional load on the WWTP water

* Corresponding author. Department of Biomedical Engineering (BME), Division of Industrial Electrical Engineering and Automation (IEA), Lund University, P.O. Box 118, Lund, SE-221 00, Sweden.
E-mail addresses: magnus.arnell@iea.lth.se (M. Arnell), s.astals@awmc.uq.edu.au (S. Astals), linda.amand@ivl.se (L. Åmand), d.batstone@awmc.uq.edu.au (D.J. Batstone), p.jensen@awmc.uq.edu.au (P.D. Jensen), ulf.jeppsson@iea.lth.se (U. Jeppsson).

http://dx.doi.org/10.1016/j.watres.2016.03.070
0043-1354/© 2016 Elsevier Ltd. All rights reserved.

Nomenclature

AcoD	Anaerobic co-digestion
AD	Anaerobic digestion
ADM1	Anaerobic Digestion Model No. 1
ASM	Activated Sludge Model
ASM1	Activated Sludge Model No. 1
ASU	Activated sludge unit
B_0	Ultimate methane potential [m^3 CH_4 ton VS^{-1}]
BMP	Biomethane potential
BOD	Biological oxygen demand [kg O_2 m^{-3}]
BSM2	Benchmark Simulation Model No. 2
C_i	Concentration of substance i [kg m^{-3}]
COD	Chemical oxygen demand [kg O_2 m^{-3}]
COD_P	Particulate fraction of chemical oxygen demand [kg O_2 m^{-3}]
COD_s	Soluble fraction of chemical oxygen demand [kg O_2 m^{-3}]
COD_t	Total chemical oxygen demand [kg O_2 m^{-3}]
DAF	Dissolved air flotation
DO	Dissolved oxygen [kg O_2 m^{-3}]
EQI	Effluent quality index
f_d	Biodegradable fraction of total chemical oxygen demand [−]
γ_i	Conversion factor to COD for substance i (kg COD kg^{-1}).
GISCOD	General Integrated Solid Waste Co-Digestion model
I_{fa}	Long chain fatty acids inhibition (ADM1) [−]
I_{NH}	Ammonia inhibition (ASM1) [−]
ISS	Inorganic suspended solids
$K_{I,50}$	50% inhibitory concentration (ADM1) [kg COD m^{-3} d^{-1}]
$K_{i,fa,low}$	Parameter in long chain fatty acid inhibition (ADM1)
$K_{i,fa,high}$	Parameter in long chain fatty acid inhibition (ADM1)
k_{hyd}	Hydrolysis parameter (ADM1) [d^{-1}]
$k_{hyd,sludge}$	Hydrolysis parameter for sludge (ADM1) [d^{-1}]
LCFA	Long chain fatty acids
M_N	Molar mass of nitrogen [g.mol^{-1}]
NOx-N	Total nitrate and nitrite nitrogen [kg N m^{-3}]
OCI	Operational cost index
OLR_{ext}	Organic loading rate for co-substrates [kg COD m^{-3} d^{-1}]
OLR_{sludge}	Organic loading rate for sludge [kg COD m^{-3} d^{-1}]
PCA	Principal component analysis
$pH_{LL,ac}$	Lower limit of pH inhibition of uptake of acetate (ADM1)
Q_{gas}	Flow of biogas [m^3.d^{-1}]
Q_{CH4}	Flow of biomethane [m^3 CH_4 d^{-1}]
S_{aa}	Amino acids (ADM1) [kg COD m^{-3}]
S_{ac}	Total acetic acid (ADM1) [kg COD m^{-3}]
S_{bu}	Total butyric acid (ADM1) [kg COD m^{-3}]
S_{fa}	Fatty acids (ADM1) [kg COD m^{-3}]
S_I	Inert soluble organics (ADM1) [kg COD m^{-3}]
S_{IN}	Inorganic nitrogen (ADM1) (kmol m^{-3})
S_{pro}	Total propionic acid (ADM1) [kg COD m^{-3}]
S_{su}	Sugars (ADM1) [kg COD m^{-3}]
S_{va}	Total valeric acid (ADM1) [kg COD m^{-3}]
TAN	Total ammonia nitrogen [kg N m^{-3}]
TKN	Total Kjeldahl nitrogen [kg N m^{-3}]
TN	Total nitrogen [kg N m^{-3}]
TS	Total solids [kg m^{-3}]
TSS	Total suspended solids [kg m^{-3}]
VFA	Volatile fatty acids [kg m^{-3}]
VFA_t	Total volatile fatty acids [kg m^{-3}]
VS	Volatile solids [kg m^{-3}]
WWTP	Wastewater treatment plant
X_c	Composite material (ADM1) [kg COD m^{-3}]
X_{ch}	Carbohydrates (ADM1) [kg COD m^{-3}]
X_i	Inert particulate organics (ADM1) [kg COD m^{-3}]
X_{li}	Lipids (ADM1) [kg COD m^{-3}]
X_{pr}	Proteins (ADM1) [kg COD m^{-3}]

train. The organic matter in the co-substrate is degraded to a certain extent in the AD process and converted to biogas; however, mineralized nutrients are mobilised and recirculated to the water train. Therefore, one of the key factors for succeeding with AcoD is to select suitable co-substrate/s and their optimal dose rate. Co-substrate characteristics and applicability have been extensively reviewed by Mata-Alvarez et al. (2014). Ideal co-substrates will have a high methane potential, high degradable fraction (and minimum impact on residual solids production) and a nutrient composition suitably balanced for the host WWTP. Generally, this means that co-substrate characteristics will differ from those of WWTP sludges in terms of composition and degradation kinetics. While there are a large number of potential co-substrates suitable for treatment at WWTP, local substrate availability and transport costs will constrain the options for individual plants. Effective modelling of AcoD is a powerful tool to assess the resource efficiency, energy balance and plant-wide effects of various co-substrate feeds at a WWTP (Razaviarani and Buchanan, 2015).

To compare the performance of different control strategies in a unified framework the Benchmark Simulation Model No. 2 (BSM2) was developed (Gernaey et al., 2014). BSM2 represents a plant-wide model including digestion of sludge with the Anaerobic Digestion Model No. 1 (ADM1, Batstone et al., 2002). In light of the increased focus on digestion, it is important that the AD process is well described and allows modelling of common and developing applications, such as AcoD. However, the current standard implementation of ADM1 in BSM2 does not allow for addition of co-substrates or dynamic hydrolysis parameters. Furthermore, some important limitations in the AD related to AcoD common practice in WWTP are missing, such as long chain fatty acid (LCFA) inhibition. The major variation in co-substrates composition poses a challenge for modelling AcoD since the model parameters have to be calibrated accordingly; and for dynamic simulations and evaluation of operational strategies, flexibility in feed composition is necessary since it also can vary over time. In the literature there are several examples of how to modify ADM1 for such purposes. The simplest approach is to characterise the actual feed mix. Derbal et al. (2009) uses the standard procedure from Batstone et al. (2002) to acquire the stoichiometric composition of composite particulate chemical oxygen demand (COD) (X_c), i.e. carbohydrates (X_{ch}), proteins (X_{pr}), lipids (X_{li}) and inerts (X_I). This approach is successful in terms of model predictions but leads to an inflexible model since the substrate mix cannot be varied without repeating the characterisation. Esposito et al. (2008) modelled AcoD of sewage sludge and food waste using a modified ADM1. For the degradation of particulate organic matter they used the standard formulation of ADM1 with disintegration and hydrolysis for all substrates and biomass decay. In order to separate the different streams they used multiple pools of composite material, i.e. X_{c1}, X_{c2}, etc. each with its individual disintegration kinetics. A more general and flexible method for

applying AcoD with ADM1 is the General Integrated Solid Waste Co-Digestion model (GISCOD) presented by Zaher et al. (2009). In the GISCOD model the particulate feed substrate is characterized as X_{ch}, X_{pr}, X_{li} and X_t, and using X_c only for internal biomass decay, i.e. X_c will only consist of dead biomass. To keep the hydrolysis for different substrates apart the GISCOD model virtually separates the hydrolysis model from the remaining processes of ADM1. This makes the model easy to expand for an arbitrary number of substrates, and flexible enough to allow for dynamic simulations with a variable mix of substrates in the digester feed. The main disadvantage is the large number of parameters and states needed where multiple complex substrates are fed, though it is common that for a given substrate, a common hydrolysis parameter for carbohydrates, lipids and proteins will be used. The interface approach used in the BSM2 (Nopens et al., 2009) also applies this approach, fractionating all particulate substrates to carbohydrates, proteins and lipids. Indeed, there is a general recommendation to avoid the use of the X_c variable for input characterisation due to inflexibility in input characterisation (Batstone et al., 2015).

One of the most important aspects for a successful modelling project is feed characterisation (including feed fractionation) and estimation of substrate dependent parameters. Several methods for feed fractionation have been suggested in literature (Kleerebezem and van Loosdrecht, 2006; Lübken et al., 2007; Zaher et al., 2009; Wichern et al., 2009; Nopens et al., 2009; Girault et al., 2012; Astals et al., 2013; Jimenez et al., 2015). While some of these methods are comprehensive and provide a detailed feed characterisation, they are also complicated and include analyses and methods not commonly performed in AD testing. The problem of input characterisation remains a major challenge as identified in a key recent review of AD modelling, particularly for mixed digesters (Batstone et al., 2015). The feasibility of a characterisation method for engineering purposes is determined by simplicity, transparency, affordability and fit for purpose accuracy. Therefore, the analyses used must be (if not already routine), common, robust, applicable on most substrates and affordable. The resulting model feed composition must at the same time be accurate enough to assure model predictive capability for relevant outputs, such as gas production, volatile solids (VS) destruction and digestate composition.

This paper investigates the influence of the substrate characteristics on model outputs and proposes a comprehensive method for implementing AcoD in a plant-wide WWTP model including:

- characterisation of substrates;
- estimation of the substrate dependent parameters;
- modifications of ADM1; and
- integration of AcoD in a plant-wide model structure, i.e. BSM2.

A simulation study is presented with three co-substrates, each rich on carbohydrates, proteins or lipids, to assess the plant-wide effects of AcoD on WWTPs.

2. Materials and methods

2.1. Input model

An input model was developed to apply AcoD in BSM2 and plant-wide models in general. The input model is divided in two steps:

Step 1 – a method to estimate the biodegradable part of COD (f_d) (or methane potential B_0 – these are fully correlated, see below), and the substrate dependent model parameters, i.e. the hydrolysis parameters (k_{hyd}) for particulate matter from biomethane potential (BMP) tests.

Step 2 – using the estimated f_d and basic physio-chemical data on the co-substrate, a scheme for fractionation of COD and total nitrogen (TN) into the classification of ADM1 state variables is proposed. The selection of important input co-substrate variables (out of the 26 default ADM1 state variables listed in the Supplementary information, Table S1) was determined by the sensitivity analysis described in Section 2.5.

In the first step the ultimate methane potential (B_0) and k_{hyd} are estimated by fitting a model to BMP data. Fitting a first-order function with a non-linear optimization routine is known to be a straight forward option (Arnell and Åmand, 2014; Jensen et al., 2011; Angelidaki et al., 2009). The full ADM1 model can also be used to model the BMP test with a similar optimization routine (but more complex model). In both cases the sum of squared errors should be used as objective function (Arnell and Åmand, 2014; Jensen et al., 2011). For this study both options were evaluated, but only results from the full ADM1 BMP model are presented below since the simple first-order model was inappropriate when inhibition was present (e.g., fatty feed). The value of f_d is determined from the B_0 estimate according to Eq. (1).

$$f_d = \frac{B_0}{350\ COD_t} VS \tag{1}$$

where:

B_0 is the ultimate methane potential [$Nm^3\ CH_4$ ton VS^{-1}];
COD_t is the total COD [kg COD m^{-3}];
f_d is the biodegradable part of COD_t [−]; and
VS is the volatile solids [kg m^{-3}].

The schematic fractionation for the second step is illustrated in Fig. 1. The particulate and soluble inert state variables are set as products of f_d and the respective particulate and soluble COD, Eqs. (2) and (3). The ADM1 does not consider inorganic suspended solids (ISS). That means that the contribution by the ash content of the substrates is not included. For modelling of substrates with high TS/VS ratio the model should be expanded with ISS as a non-reactive particulate state variable.

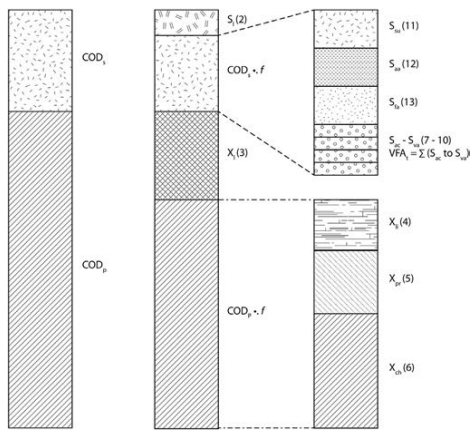

Fig. 1. Scheme for fractionation of COD into the most influential state variables of ADM1. Corresponding equation number in parenthesis.

$$S_I = COD_s(1 - f_d) \quad (2)$$

$$X_I = COD_p(1 - f_d) \quad (3)$$

where:

COD_s is the soluble COD [kg COD m^{-3}];
COD_p is the particulate COD [kg COD m^{-3}].

Secondly, the particulate biodegradable COD is considered. The variables X_{pr} and X_{li} are calculated from measurements converted to COD (conversion factors given in Supplementary information, Table S2), Eqs. (4) and (5), and the remaining part assigned to X_{ch}, Eq. (6). This strategy, previously also suggested by Galí et al. (2009), is chosen since proteins and lipids generally are easier to analyse than carbohydrates for solid substrates, and leaving enough degrees of freedom to close the mass balance. The biodegradability of the respective fractions is assumed equal to the overall degradability, f_d.

$$X_{li} = C_{li}\,\gamma_{li}\,f_d \quad (4)$$

$$X_{pr} = C_{pr}\,\gamma_{pr}\,f_d \quad (5)$$

$$X_{ch} = COD_p f_d - X_{pr} - X_{li} \quad (6)$$

where:

C_i is the concentration of substance i [kg m^{-3}];
γ_i is the conversion factor to COD for substance i [kg COD kg^{-1}]. Values given in Supplementary information, Table S2.

The four VFA state variables can be calculated directly by converting the measured values to COD, Eqs. (7)–(10). Assuming the soluble COD is small the state variables S_{su}, S_{aa} and S_{fa} can be split equal to their corresponding particulates, Eqs. (11)–(13). This assumption is better than just neglecting these state variables or splitting them in thirds as suggested by Astals et al. (2013) since it is based on available data. However, for substrates with a high proportion of COD_S, >10%, the soluble fractions need greater attention. Measurements of carbohydrate, protein and lipid contents of COD_S are then recommended.

$$S_{ac} = C_{Ac}\,\gamma_{Ac} \quad (7)$$

$$S_{pro} = C_{pro}\,\gamma_{pro} \quad (8)$$

$$S_{bu} = C_{bu}\,\gamma_{bu} \quad (9)$$

$$S_{va} = C_{va}\,\gamma_{va} \quad (10)$$

$$S_{su} = (COD_s f_d - VFA_t)\frac{X_{ch}}{COD_p f_d} \quad (11)$$

$$S_{aa} = (COD_s f_d - VFA_t)\frac{X_{pr}}{COD_p f_d} \quad (12)$$

$$S_{fa} = (COD_s f_d - VFA_t)\frac{X_{li}}{COD_p f_d} \quad (13)$$

where:

VFA_t is the sum of all VFAs [kg COD m^{-3}].

The soluble inorganic nitrogen content S_{IN} is calculated from the total ammonia nitrogen (TAN) by Eq. (14). For this study, the remaining state variables of the ADM1 were set to 0. If the substrate has a non-neutral pH the acid-base balances must be considered (Batstone et al., 2002). Furthermore, for other special substrates, for example rich on alcohols such as ethanol, methanol or glycerol, special fractionation schemes and model modifications may be needed (Garcia-Gen et al., 2013).

$$S_{IN} = \frac{TAN}{M_N 1000} \quad (14)$$

where:

TAN is the total ammonia nitrogen [g N m^{-3}];
M_N is the molar mass of nitrogen [g mol^{-1}].

The data requirements to follow the above fractionation scheme are: TS, VS, COD_t, COD_s, VFAs (i.e. Acetate, Propionate, Butyrate and Valerate), Proteins, Lipids, TAN and a BMP test.

2.2. ADM1 modifications

The initial simulations for the sensitivity analysis (see Sections 2.5 and 3.3) using the default BSM2 implementation of ADM1 showed unrealistic behaviour when co-digesting lipids, since the methane production was constant with an increasing load of X_{li} above reported LCFA inhibition thresholds (Cirne et al., 2007; Astals et al., 2014). LCFA is demonstrated to inhibit mainly uptake of S_{ac} (Zonta et al., 2013). Therefore, a function for LCFA inhibition (I_{fa}), i.e. inhibition of uptake of S_{ac} by S_{fa}, was implemented. A Gaussian function developed and tested at the University of Queensland, Eq. (15) with two parameters, $K_{I,fa,low}$ and $K_{I,fa,high}$, was identified to best fit the observed behaviour. This function has a number of advantages over existing models (Zonta et al., 2013; Palatsi et al., 2010), including non-competitive inhibition for threshold style inhibition. It has previously been used in the ADM1 for pH inhibition (Batstone et al., 2002). The structure of the inhibition function allows explicit determination of the onset of inhibition, the point at which inhibition is full, and around a 50% inhibition point ($K_{I,50}$), which is half way between the upper and lower limits. This is important when inhibition can be complete, such as for inhibition by fats.

$$I_{fa} := \begin{cases} e^{-2.77259\left((S_{fa}-K_{I,fa,low})/(K_{I,fa,high}-K_{I,fa,low})\right)^2} & \text{for } S_{fa} > K_{I,fa,low} \\ 1 & \text{for } S_{fa} \le K_{I,fa,low} \end{cases} \quad (15)$$

The simulation of the DAF sludge BMP test (Sections 2.4 and 3.1) revealed that I_{fa} led to a rapid acidification of the reactor with sequential pH inhibition. To describe a recovery in accordance with the measured data the lower limit of pH inhibition of uptake of acetate $pH_{LL,ac}$ was adjusted from 6 to 5 (Latif et al., 2015).

2.3. Plant-wide implementation of AcoD in BSM2

The GISCOD model (separate fraction/hydrolysis) was chosen for implementing AcoD in BSM2; firstly because characterisation and parameter estimation is performed independently for each substrate and secondly because it uses the same formulation of AD feed as BSM2, fractionating particulate COD as X_{ch}, X_{pr}, X_{li} and X_I rather than X_c. The later omits the disintegration step for substrates and assumes a hydrolysis of each particulate COD compound as the limiting step. The original interface by Nopens et al. (2009) from ADM1 to Activated Sludge Model No. 1 (ASM1) was kept and the

interface output was fed to a hydrolysis model for sludge. The co-substrates were characterized and fractionated using the proposed input model and fed to separate hydrolysis model blocks (Fig. 2). Due to the virtual separation of hydrolysis in GISCOD it was necessary to ensure that all processes were only active in the intended model reactor. To assure separation of hydrolysis and remaining reactions the residual particulate substrate after hydrolysis was bypassed the ADM1 reactor and put back before the ADM1 to ASM1 interface.

2.4. Case study on BMP tests and plant-wide assessment of AcoD

Three substrates were selected for a case study. For realism and diversity three fractions of slaughterhouse waste were used: paunch, blood and dissolved air flotation (DAF) sludge, each rich on carbohydrates, protein and lipids respectively. These are representative of common co-digestion feeds, and in particular, the high oil and grease content of the DAF sludge means it is representative of, and similar to other commonly used FOG wastes, such as grease trap waste. Analysis of these three substrates is provided in Astals et al. (2014), and the pure substrate curves were taken from that paper, where information about substrates, analytical methods and data is presented. The data used in this study are given in the Supplementary information, Table S3. The substrates were characterized using the proposed input model (Section 2.1) and the BMP tests of Astals et al. (2014) were simulated using the full ADM1. Machine fitting of parameters were performed with a least squares curve fitting function for non-linear problems, lscurvefit, in the Matlab software package (MATLAB 8.4, The MathWorks Inc., Natick, MA, USA, 2014). For all substrates k_{hyd} and f_{fi} were estimated and for DAF sludge also the LCFA-inhibition parameters of Eq. (15). To establish initial conditions for the BMP, the standard BSM2 was run to steady state with the AD hydrolysis rate, k_{hyd}, equal to 0.3 d^{-1} and biomass composition from this steady state used as inoculum composition. It should be noted that the actual inoculum used in this study (Luggage Pt WWTP in Brisbane, QLD Australia) has a configuration very similar to the BSM2.

A plant-wide simulation study was conducted to test the developed method for modelling AcoD at WWTPs and assess the plant-wide effects of AcoD. The WWTP in the simulation study was the standard plant set-up in BSM2. The plant contains a primary clarifier, an activated sludge unit (ASU) in a Modified Ludzack-Ettinger configuration with two anoxic tanks followed by three aerobic tanks. The last aerobic tank and the first anoxic are connected by internal recycle. A secondary clarifier with sludge recycle follows the ASU. The plant sludge train contains a thickener, an AD, a co-generation unit, a dewatering unit and a storage tank. The plant layout can be found in Supplementary information, Fig. S1. The plant was simulated with the default closed loop control strategy including dissolved oxygen (DO) control in the ASU based on feed-back control of the DO in the second aerated tank (set-point 2 g O_2 m^{-3}) and proportional airflow rate to tanks 3 and 5. The waste activated sludge flow was set constant with seasonal values of 450 m^3 d^{-1} during summer and 300 m^3 d^{-1} in winter, resulting in an average sludge age of 16 days in the ASU. In the evaluation procedure two indices are calculated: (i) effluent quality index (EQI), a weighted index of the effluent quality including total suspended solids (TSS), chemical oxygen demand (COD), biological oxygen demand (BOD), total Kjeldahl nitrogen (TKN) and total nitrate and nitrite nitrogen (NOx-N); and, (ii) operational cost index (OCI) incorporating the major operational costs for aeration, pumping, mixing, sludge production and disposal, carbon source, heating of the AD and revenue from selling produced power. Plant layout, dimensions and sub-model descriptions are detailed in Gernaey et al. (2014).

Co-digestion feed consisted of paunch, blood and DAF sludge based on characterisation from the BMPs. A $k_{hyd,sludge}$ = 0.32 d^{-1} was applied based on Arnell and Åmand (2014). The external substrate load was calculated based on the average sludge load (organic loading rate, OLR_{sludge}), OLR_{sludge} = 2.38 kg COD m^{-3} d^{-1}, such that the base organic load of co-substrate (OLR_{ext}) was about 50% of the average sludge load: 20 m^3 d^{-1} of paunch, 4 m^3 d^{-1} of blood and 1 m^3 d^{-1} of DAF sludge give an OLR_{ext} = 1.25 kg COD m^{-3} d^{-1}. On top of that two periods of further increased load were added; from day 350–410 the load of blood was increased to 15 m^3 d^{-1} giving a total co-substrate OLR_{ext} of 2.11 kg COD m^{-3} d^{-1}, and from day 500–521 the load of DAF sludge was increased to 8 m^3 d^{-1} giving a total co-substrate OLR_{ext} = 3.41 kg COD m^{-3} d^{-1}.

A full 609 days dynamic closed loop BSM2 simulation (modified with the co-digestion feed) was performed and evaluated according to the standard procedures described in Gernaey et al. (2014). During simulation nothing but the digester feed was changed in the default BSM2 closed loop strategy.

2.5. Input model sensitivity analysis

Many of the ADM1 state variables are not relevant or important for input fractionation, particularly when assessing plant-wide effects at WWTPs (Solon et al., 2015). To assess the most influential variables in co-substrate composition a sensitivity analysis was performed using Monte Carlo simulations. The simulations were designed according to Batstone (2013) with 3000 simulations of the

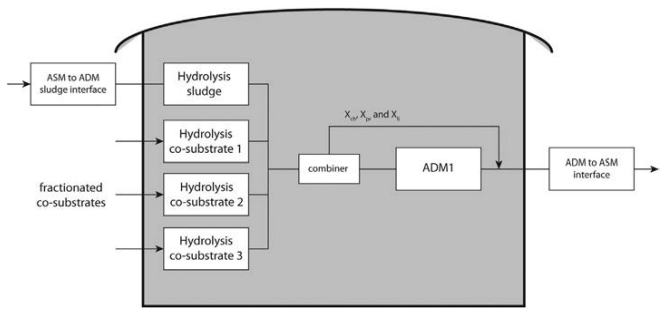

Fig. 2. Model layout in Simulink for the BSM2 AD block with integrated GISCOD model for AcoD.

BSM2 AD block. To the average sludge load of 2.4 kg COD m^{-3} d^{-1} from BSM2 an additional 8.4 kg COD m^{-3} d^{-1} of co-substrate was added with varying composition fractions (between 0 and 1) of X_{ch}, X_{pr} and X_{li} out of biodegradable COD. This high co-substrate load was intended to stress the digester stability and to reveal the sensitivity for different feed characteristics. Also the influence of f_d and the fraction of COD_s out of COD_t were investigated in this way. The results were evaluated with weighted principal component analysis (PCA) on the outputs gas flow (Q_{gas}), methane flow (Q_{CH4}), inorganic nitrogen (S_{IN}), pH and volatile fatty acids (VFA). Detailed information on the set-up of the Monte Carlo simulations is presented in the Supplementary information.

3. Results and discussion

3.1. Input model case study on BMP tests

Applying the input model to the three substrates paunch, blood and DAF sludge resulted in the state variables and parameter estimates given in Table 1. The simulated and measured BMP profiles are shown in Fig. 3. The fit to data is good for paunch and blood and. While the fit to data is less accurate for DAF sludge, the model captures the main process impacts due to LCFA inhibition The ability of the process to separately identify the two parameters in the applied for I_{fa}, and its ability to simulate the complex methane production profile justify its use over simpler models, such as non-competitive inhibition. The inhibition constants estimated from DAF sludge were also used for the simulations of the other substrates. The full list of ADM1 parameter values for the BMP model is given in the Supplementary information, Table S4.

3.2. Plant-wide assessment of AcoD

Fig. 4 shows the organic loading rate together with the resulting total methane production and relevant inhibitions. Table 2 shows the plant evaluation outputs significantly affected by AcoD as well as the default BSM2 outputs, i.e. without AcoD. The addition, the co-substrates had a positive effect on the methane production allowing a reduction in the overall Operational Cost Index (OCI) from 11 630 to 10 490. However, at the same time the effluent water quality deteriorated from the increased nitrogen load in the water train, due to AD supernatant recirculation, increasing the Effluent Quality Index (EQI) from 5330 to 5970.

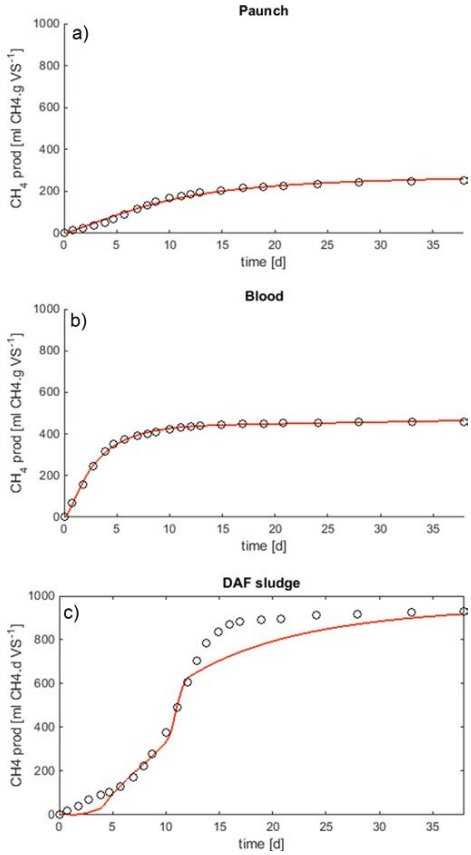

Fig. 3. BMP curves for a) paunch, b) blood and c) DAF sludge. Markers represent data and lines simulation results.

Table 1
Resulting characterisation and parameter estimation for paunch, blood and DAF sludge. State variables not listed in the table are set to 0.

	Paunch	Blood	DAF
S_I [kg COD m^{-3}]	0.366	0.0162	1.84E-05
S_{su} [kg COD m^{-3}]	0.873	0.0575	0.116
S_{aa} [kg COD.m^{-3}]	0.192	0.191	0.0490
S_{fa} [kg COD m^{-3}]	0.207	0.00540	2.83
S_{va} [kg COD m^{-3}]	0.0612	0.102	0.0408
S_{bu} [kg COD m^{-3}]	0.145	0.273	0.0182
S_{pro} [kg COD m^{-3}]	0.272	0.288	0.409
S_{ac} [kg COD m^{-3}]	0.384	1.57	0.235
S_{IN} [kmol N m^{-3}]	0.0102	0.0279	0.00350
X_I [kg COD m^{-3}]	15.2	1.70	0.00522
X_{ch} [kg COD m^{-3}]	60.7	59.4	40.7
X_{pr} [kg COD m^{-3}]	13.3	197	17.1
X_{li} [kg COD.m^{-3}]	14.4	5.58	991
k_{hyd} [d^{-1}]	0.125	0.310	0.103
B_0 [m^3 CH_4 ton VS^{-1}]	299	520	1044
f_d [−]	0.85	0.99	1.0
$K_{I,fa,low}$ [kg COD m^{-3}]	–[a]	–[a]	0.406
$K_{I,fa,high}$ [kg COD m^{-3}]	–[a]	–[a]	0.714

[a] Parameters not estimated for this co-substrate.

The reduction in OCI corresponds to a total reduction of the operational costs for the WWTP by 10%. This significant reduction was achieved because the revenue from selling co-generated power from the produced methane increased by 92%; although both the aeration energy index and the sludge production at the same time increased by 6 and 39%, respectively. Following the BSM2 evaluation procedure neither the transport cost nor gate fee revenue of the co-substrate is included in the evaluation (Malmqvist et al., 2006). In the dynamic profiles of Fig. 4 the effect of the two short-term load increases of blood and DAF sludge can be seen. The increased load of blood did not yield a proportional increase in methane production. This is because the elevated ammonia levels in the AD at the same time cause a more severe ammonia inhibition in the model. In contrast, the load peak of DAF sludge increased the methane production proportional to the load, since LCFA was minor under this scenario.

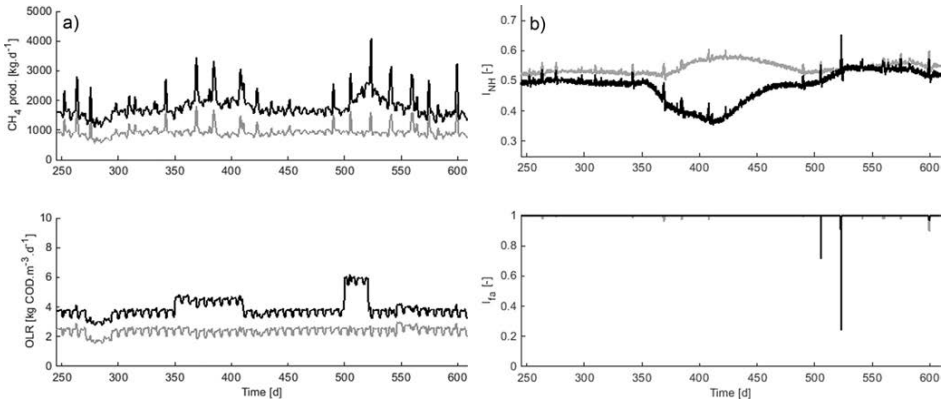

Fig. 4. Effect of AcoD on BSM2 AD process. Methane production (top left), OLR (bottom left), ammonia inhibition (I_{NH}, top right) and LCFA inhibition (I_{fa}, bottom right). Grey lines are standard BSM2 results without AcoD and black lines are the simulated scenario with AcoD (filtered values).

Table 2
Evaluation results from the simulation study compared to BSM2 default values.

	BSM2 default	BSM2 w. AcoD
Operational Cost Index [−]	11 600	10 500
Effluent Quality Index [−]	5330	5970
Average aeration energy [kWh d^{-1}]	4130	4380
Methane production [kg CH_4 d^{-1}]	935	1800
Sludge production [kg SS d^{-1}]	3480	4730
Effluent S_{NH} [g m^{-3}]	0.49	0.44
Effluent S_{NO} [g m^{-3}]	9.81	12.9
Effluent TN [g m^{-3}]	12.3	15.4
Time in violation TN [%]	0.17	15.0

The increase in EQI was mainly due to a higher effluent total nitrogen (TN), 15.4 g N m^{-3} caused by the nitrogen load from the protein rich co-substrate, which elevated the S_{NH} concentration in the returning AD supernatant; from an average of 1290 g N m^{-3} to 1610 g N m^{-3} (Fig. 5). This led to a time in violation of the effluent constrains for TN of 15% compared to 0.17% without AcoD. The violation of the effluent constrains would be an unacceptable effect of AcoD and shows the importance of selection and dose strategy for the co-substrate. The primary cause of high effluent TN was elevated effluent S_{NO} caused by insufficient carbon availability for denitrification rather than poor nitrification (Table 2, Fig. 5). The reason for this is that the default control strategy of the closed loop BSM2 has a DO control in the ASU responding to the increased ammonia load but only a fixed dosage of methanol. If the same total load of blood would have dosed over the whole period the methanol scarcity might had been less pronounced, or if it had been dosed for an even shorter period the nitrification capacity would have been exceeded as well. Effluent limit violation would have been avoided simulating an increased or controlled methanol dosage. The draw-back of the increased nitrogen load would then have manifested itself as increased methanol consumption instead of effluent violation. While being outside the scope of this publication, the strategies to cope with increased nitrogen load can easily be tested and evaluated with additional simulations (results not shown). This demonstrates how simulating AcoD in plant-wide WWTP models allows to design an optimal co-substrate composition and feed strategy and simultaneously control the effects on the water train. The presented simulation study shows the applicability of modelling and simulation to assess cost-benefit and the plant-wide effects of AcoD on WWTPs.

3.3. Influent sensitivity analysis

The simulations varying co-substrate biodegradability (f_d) confirm that the feed degradable COD fraction is very important, as previously shown (Solon et al., 2015; Galí et al., 2009). The resulting PCA of the Monte Carlo simulations from varying X_{ch}, X_{pr} and X_{li} is shown in Fig. 6 (additional figures of model outputs related to feed composition can be found in the Supplementary information, Figs. S3 and S4). The variations in the results are explained to 71.5% by Component 1 and 25.2% by Component 2. The variation in Component 1 is positively related to biogas and methane flow and negatively to VFA. Component 2 is mostly influenced by the S_{IN} concentration in the effluent digestate. Three distinctive regions can be seen marked in Fig. 6:

I. the substrate compositions positive in Component 1 and negative in Component 2 represent a well-functioning digester with low VFAs and good methane production;
II. as the protein content increases the output gradually moves from region I into II, i.e. negative in Component 1 but positive in Component 2, towards the upper-left corner. This substrate composition is at or close to digester failure as the ammonia inhibition is gradually increasing along with VFAs leading to decreasing methane production;
III. the clustered samples negative in both Components 1 and 2 are all high in X_{li} and represent the very disruptive digester failure due to LCFA inhibition where methane production totally stops and VFA increases dramatically leading to total pH inhibition. There is a relatively rapid switch from region I to region III due to the threshold nature of inhibition, specifically, when 58% of the co-substrate load of 8.4 kg COD m^{-3} d^{-1} consists of X_{li}.

This leads to the conclusion that apart from f_d, the two most important input model parameters for digester stability with co-digestion are fractions determining X_{pr} and X_{li}. The results also

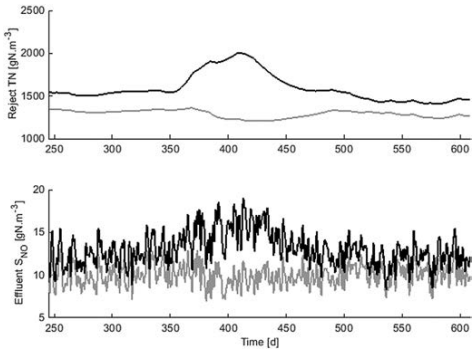

Fig. 5. Effect of AcoD on S_{NH} in dewatering supernatant (top) and S_{NO} in plant effluent (bottom). Grey lines are standard BSM2 results without AcoD and black lines are the simulated scenario with AcoD (filtered values).

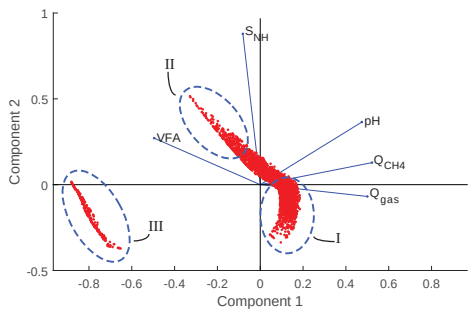

Fig. 6. Principal Component Analysis for the Monte Carlo simulations with varying AD feed composition.

show that X_{ch} is relevant for the total gas production (Fig. S3 in the Supplementary information) because a higher X_{ch} fraction leads to increased CO_2 production; which is coherent with Solon et al. (2015). Moreover, Fig. S3 reveals that high loads of carbohydrates will lead to pH inhibition subsequent to high VFA production.

4. Conclusions

Anaerobic co-digestion was for the first time implemented in BSM2, The GISCOD model was used to model AcoD complemented by a Gaussian LCFA inhibition function.

- A new input model for fractionation of COD was developed based on feasible and affordable tests. The method was proven reliable based on modelling of BMP tests of three substrates paunch, blood and DAF sludge.
- A performance assessment study of AcoD was performed with a dynamic feed mix. It revealed that the overall operational cost was reduced by 10%. However, the high nitrogen content in blood increased ammonia inhibition in the digester, leading to lower digester performance, and overloaded the denitrification capacity of the water train and deteriorated the effluent water quality.
- A sensitivity analysis on co-substrate feed characteristics found that apart from the biodegradable fraction of COD, protein and lipid fractions of particulate biodegradable COD were the two most important state variables for digester stability and methane production, and that different substrates caused different modes of failure.

Acknowledgements

The authors acknowledge the financial support obtained through the Swedish Research Council Formas (211-2010-141), the Swedish Water & Wastewater Association (10-106), SP Technical Research Institute of Sweden and the Swedish research and education consortium VA-cluster Mälardalen.

Appendix A. Supplementary data

Supplementary data related to this article can be found at http://dx.doi.org/10.1016/j.watres.2016.03.070.

References

Angelidaki, I., Alves, M., Bolzonella, D., Borzacconi, L., Campos, J.L., Guwy, A.J., Kalyuzhnyi, S., Jenicek, P., van Lier, J.B., 2009. Defining the biomethane potential (BMP) of solid organic wastes and energy crops: a proposed protocol for batch assays. Water Sci. Technol. 59 (5), 927–934.
Arnell, M., Åmand, L., 2014. Parameter estimation for modelling of anaerobic co-digestion. In: IWA 9th World Water Congress and Exhibition (IWA2014). Lisbon, Portugal, 21-26 September, 2014.
Astals, S., Batstone, D.J., Mata-Alvarez, J., Jensen, P.D., 2014. Identification of synergistic impacts during anaerobic co-digestion of organic wastes. Bioresour. Technol. 169, 421–427.
Astals, S., Esteban-Gutiérrez, M., Fernández-Arévalo, T., Aymerich, E., García-Heras, J.L., Mata-Alvarez, J., 2013. Anaerobic digestion of seven different sewage sludges: a biodegradability and modelling study. Water Res. 47 (16), 6033–6043.
Batstone, D.J., Keller, J., Angelidaki, R.I., Kalyuzhnyi, S.V., Pavlostathis, S.G., Rozzi, A., Sanders, W.T.M., Siegrist, H., Vavilin, V.A., 2002. Anaerobic Digestion Model No. 1. Scientific and Technical Report No. 13, IWA Publishing, London, UK.
Batstone, D.J., 2013. Teaching uncertainty propagation as a corecomponent in process engineering statistics. Educ. Chem. Eng. 8, 132–139.
Batstone, D.J., Virdis, B., 2014. The role of anaerobic digestion in the emerging energy economy. Curr. Opin. Biotechnol. 27, 142–149.
Batstone, D.J., Puyol, D., Flores-Alsina, X., Rodríguez, J., 2015. Mathematical modelling of anaerobic digestion processes: applications and future needs. Rev. Environ. Sci. Biotechnol. 14 (4), 595–613.
Cirne, D.G., Paloumet, X., Björnsson, L., Alves, M.M., Mattiasson, B., 2007. Anaerobic digestion of lipid-rich waste – effects of lipid concentration. Renew. Energy 32, 965–975.
Derbal, K., Bencheikh-Lehocine, M., Cecchi, F., Meniai, A.-H., Pavan, P., 2009. Application of the IWA ADM1 model to simulate anaerobic co-digestion of organic waste with waste activated sludge in mesophilic condition. Bioresour. Technol. 100, 1539–1543.
Esposito, G., Frunzo, L., Panico, A., d'Antonio, G., 2008. Mathematical modelling of disintegration-limited co-digestion of OFMSW and sewage sludge. Water Sci. Technol. 58 (7), 1513–1519.
Galí, A., Benabdallah, T., Astals, S., Mata-Alvarez, J., 2009. Modified version of ADM1 model for agro-waste application. Bioresour. Technol. 100, 2783–2790.
Garcia-Gen, S., Lema, J.M., Rodriguez, J., 2013. Generalised modelling approach for anaerobic co-digestion of fermentable substrates. Bioresour. Technol. 147, 525–533.
Gernaey, K., Jeppsson, U., Vanrolleghem, P.A., Copp, J.B., 2014. Benchmarking of Control Strategies for Wastewater Treatment Plants. IWA Scientific and Technical Report No. 23. IWA Publishing, London, UK.
Girault, R., Bridoux, G., Nauleau, F., Poullain, C., Buffet, J., Steyer, J.P., Sadowski, A.G., Béline, F., 2012. A waste characterisation procedure for ADM1 implementation based on degradation kinetics. Water Res. 46 (13), 4099–4110.
Jensen, P.D., Ge, H., Batstone, D.J., 2011. Assessing the role of biochemical methane potential tests in determining anaerobic degradability rate and extent. Water Sci. Technol. 64 (4), 880–886.
Jimenez, J., Aemig, Q., Doussiet, N., Steyer, J.P., Houot, S., Patureau, D., 2015. A new organic matter fractionation methodology for organic wastes: bioaccessibility and complexity characterization for treatment optimization. Bioresour. Technol. 194, 344–353.
Kleerebezem, R., van Loosdrecht, M.C.M., 2006. Waste characterization for

implementation in ADM1. Water Sci. Technol. 54 (4), 157–174.
Latif, M.A., Mehta, C.M., Batstone, D.J., 2015. Low pH anaerobic digestion of waste activated sludge for enhanced phosphorous release. Water Res. 81, 288–293.
Lundkvist, M., 2005. Energieffektivisering (Sweco Report 2005-01-14T) [in Swedish]. Sweco, Halmstad, Sweden.
Lübken, M., Wichern, M., Schlattmann, M., Gronauer, A., Horn, H., 2007. Modelling the energy balance of an anaerobic digester fed with cattle manure and renewable energy crops. Water Res. 41 (18), 4085–4096.
Malmqvist, P.A., Heinicke, G., Kärrman, E., Stenström, T.A., Svensson, G., 2006. Strategic Planning of Sustainable Urban Water Management. IWA Publishing, London, UK.
Mata-Alvarez, J., Dosta, J., Romero-Güiza, M.S., Fonoll, X., Peces, M., Astals, S., 2014. A critical review on anaerobic co-digestion achievements between 2010 and 2013. Renew. Sustain. Energy Rev. 36, 412–427.
Nopens, I., Batstone, D., Copp, J.B., Jeppsson, U., Volcke, E.I.P., Alex, J., Vanrolleghem, P.A., 2009. An ASM/ADM model interface for dynamic plant-wide simulation. Water Res. 43 (7), 1913–1923.
Olsson, G., 2015. Water and Energy: Threats and Opportunities – Second Edition. IWA Publishing, London, UK.
Palatsi, J., Illa, J., Prenafeta-Boldú, F.X., Laureni, M., Fernandez, B., Angelidaki, I., Flotats, X., 2010. Long-chain fatty acids inhibition and adaptation process in anaerobic thermophilic digestion: batch tests, microbial community structure and mathematical modelling. Bioresour. Technol. 101 (7), 2243–2251.
Razaviarani, V., Buchanan, I.D., 2015. Calibration of the Anaerobic Digestion Model No. 1 (ADM1) for steady-state anaerobic co-digestion of municipal wastewater sludge with restaurant grease trap waste. Chem. Eng. J. 266, 91–99.
Solon, K., Flores-Alsina, X., Gernaey, K.V., Jeppsson, U., 2015. Effects of influent fractionation, kinetics, stoichiometry and mass transfer on CH4, H2 and CO2 production for (plant-wide) modeling of anaerobic digesters. Water Sci. Technol. 71 (6), 870–877.
Wichern, M., Gehring, T., Fischer, K., Andrade, D., Lübken, M., Koch, K., Gronauer, A., Horn, H., 2009. Monofermentation of grass silage under mesophilic conditions: measurements and mathematical modelling with ADM1. Bioresour. Technol. 100 (4), 1675–1681.
Zaher, U., Li, R., Jeppsson, U., Steyer, J.P., Chen, S., 2009. GISCOD: General ntegrated Solid waste Co-Digestion model. Water Res. 43 (10), 2717–2727.
Zonta, Z., Alves, M.M., Flotats, X., Palatsi, J., 2013. Modelling inhibitory effects of long chain fatty acids in the anaerobic digestion process. Water Res. 47 (3), 1369–1380.

Supplementary information

Paper title: Modelling anaerobic co-digestion in Benchmark Simulation Model No. 2: parameter estimation, substrate characterisation and plant-wide integration

Autors: Magnus Arnell, Sergi Astals, Linda Åmand, Damien J. Batstone, Paul D. Jensen, Ulf Jeppsson

Monte Carlo simulations for sensitivity analysis

The Monte Carlo simulations were made in the Matlab/Simulink software package (MATLAB 8.4, The MathWorks Inc., Natick, MA, 2014). The model used for the sensitivity analysis was the AD-block from the Benchmark Simulation Model No. 2 (BSM2, Gernaey *et al.*, 2014) plant with a sludge feed composition equal to the steady state sludge feed from BSM2. This is a simplification since the sludge feed would be slightly affected by the changed composition of the recycled digester supernatant if anaerobic co-digestion (AcoD) is introduced. The simulations were run for 130 days with constant influent conditions.

The generation of the 3 000 co-substrate feed samples followed the description in Batstone (2013). Basic data for the feed is given in Table S.1. The co-substrate normal distributed samples with varying fractions of carbohydrates, proteins and lipids out of bio-degradable particulate COD (f_{ch}, f_{pr} and f_{li}) were generated with normalised inverted random numbers with the function call:

```
f_i = norminv(rand(n,1),f_mean,0.2);
```

the f_{ch} was generated with a mean, f_{mean} = 0.33 and out of the remaining part f_{pr} was generated with f_{mean} = 0.5 and the residual was assigned to f_{li}. Values less than 0 or greater than 1 were set to 0 and 1, respectively. The resulting influent profiles are shown in Figure S.1.

Table S.1. Basic system and feed data for the simulations.

	Co-substrate	**Sludge**
COD_t [kg.m^{-3}]	1 250	44.8
Biodegradable part of COD	0.75	0.768
Q_{feed} [m^3.d]	30	178.46
OLR [kg COD.m^{-3}.d^{-1}]	8.38	2.35

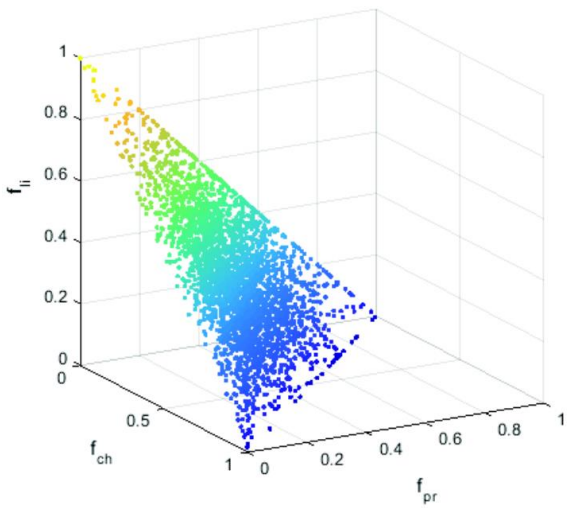

Figure S.1 Profiles of f_{ch}, f_{pr} and f_{li} for the 3 000 samples used for Monte Carlo simulations.

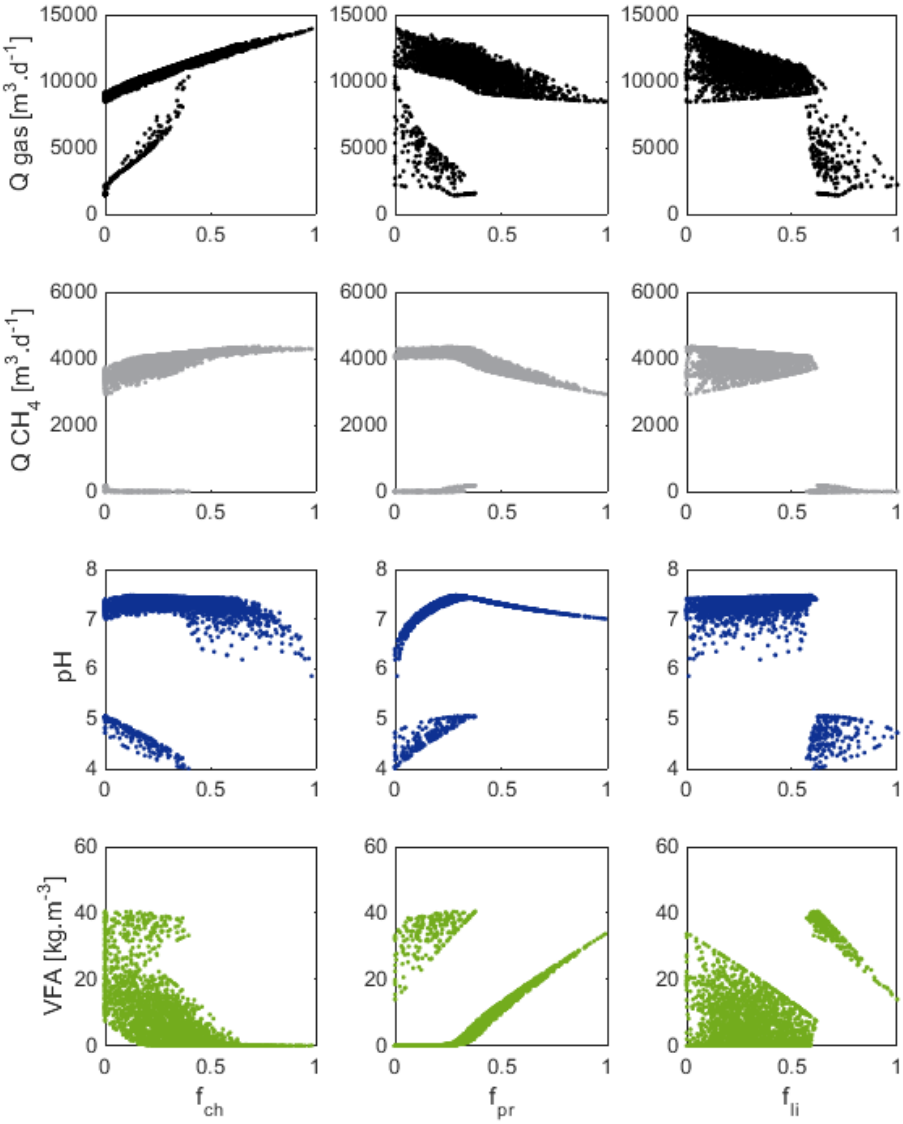

Figure S.2. Output state variables from the Monte Carlo simulations. From top to bottom the rows depict, Q_{gas}, Q_{CH4}, pH and VFA. Each state variable is plotted against the fraction of carbohydrates (f_{ch}), proteins (f_{pr}) and lipids (f_{li}), respectively, from left to right.

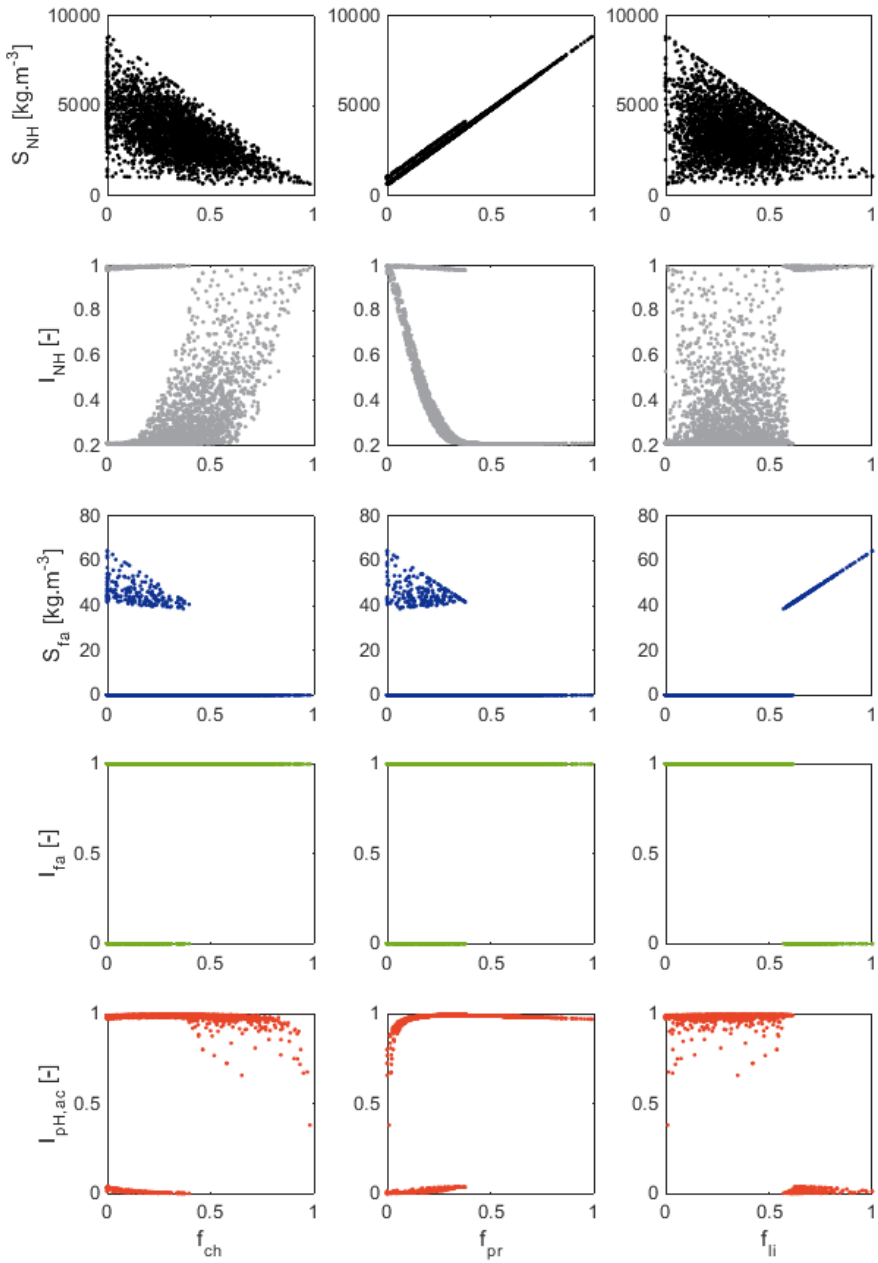

Figure S.3. AD inhibitions and corresponding inhibitory compound from the Monte Carlo simulations. From top to bottom the rows depict, S_{NH}, I_{NH}, S_{fa}, I_{fa} and $I_{pH,ac}$. Each state variable is plotted against the fraction of carbohydrates (f_{ch}), proteins (f_{pr}) and lipids (f_{li}), respectively, from left to right.

Substrate data

Table S.2. Analysis data used for substrate characterisation. From Astals *et al.* (2014) with modifications indicated.

	Paunch	Blood	DAF sludge
TS [kg.m^{-3}]	117	187	360
VS [kg.m^{-3}]	106	178	353
COD_t [kg COD.m^{-3}]	106	266	1 053
COD_s [kg COD.m^{-3}]	2.5	2.5[1]	3.7
Acetate [kg.m^{-3}]	0.36	1.47	0.22
Propionate [kg.m^{-3}]	0.18	0.19	0.27
Butyrate [kg.m^{-3}]	0.08	0.15	0.01
Valerate [kg.m^{-3}]	0.03	0.05	0.02
Proteins [kg.m^{-3}]	10.2	129.5	11.8
Lipids [kg.m^{-3}]	5.85[2]	1.95[2]	344.5[2]
TAN [g N.m^{-3}]	143	391	49

[1] measured value is higher but most COD except VFAs are assumed colloidal and therefore particulates needed to be hydrolysed;
[2] analysed values are too low due to faulty analysis and increased by 30%.

COD conversion factors

Table S.3. Conversion factors (γ) for organic fractions into COD (Grau *et al.*, 2007).

	Value
γ_{ac} [kg COD.(kg ac)$^{-1}$]	1.066667
γ_{pro} [kg COD.(kg pro)$^{-1}$]	1.513514
γ_{bu} [kg COD.(kg bu)$^{-1}$]	1.818182
γ_{va} [kg COD.(kg va)$^{-1}$]	2.039216
γ_{Pr} [kg COD.(kg Pr)$^{-1}$]	1.53
γ_{Li} [kg COD.(kg Li)$^{-1}$]	2.878

ADM1 state variables

Table S.4. State variables of ADM1 (Batstone *et al*., 2002). *S* denotes solubles and *X* particulates.

State variable	Description	State variable	Description
S_{su}	monosaccharides	X_c	composite
S_{aa}	amino acids	X_{ch}	carbohydrates
S_{fa}	total LCFA	X_{pr}	proteins
S_{va}	total valerate	X_{li}	lipids
S_{bu}	total butyrate	X_{su}	biomass
S_{pro}	total propionate	X_{aa}	biomass
S_{ac}	total acetate	X_{fa}	biomass
S_{h2}	hydrogen	X_{c4}	biomass
S_{ch4}	methane	X_{pro}	biomass
S_{ic}	inorganic carbon	X_{ac}	biomass
S_{IN}	inorganic nitrogen	X_{h2}	biomass
S_I	soluble inerts	X_I	particulate inerts
S_{cat}	cations		
S_{an}	anions		

ADM1 parameters

Table S.5. Model parameters used for ADM1 in the plant-wide simulation study. Units; N_i [kmol N.(kg COD)$^{-1}$], C_i [kmol C.(kg COD)$^{-1}$], Y_i [kg COD_X.(kg COD_S)$^{-1}$], k_i (decay rates) [d^{-1}], K_S_i [kg COD_S.m^{-3}], k_m_i [kg COD_S.(kg COD_X)$^{-1}$.d^{-1}], K_I_i [kg COD.m^{-3}], k_A_Bi [M^{-1}.d^{-1}], kLa [d^{-1}], K_A_i [M], R [bar.m^{3}.kmol^{-1}.K^{-1}].

Parameter	Value	Parameter	Value	Parameter	Value
f_sI_xc	0.1	Y_aa	0.08	pH_UL_h2	6
f_xI_xc	0.2	Y_fa	0.06	pH_LL_h2	5
f_ch_xc	0.2	Y_c4	0.06	k_dec_Xsu	0.02
f_pr_xc	0.2	Y_pro	0.04	k_dec_Xaa	0.02
f_li_xc	0.3	C_ch4	0.0156	k_dec_Xfa	0.02
N_xc	0.002685714	Y_ac	0.05	k_dec_Xc4	0.02
N_I	0.004285714	Y_h2	0.06	k_dec_Xpro	0.02
N_aa	0.007	k_dis	10	k_dec_ac	0.02
C_xc	0.02786	k_hyd_ch	0.2	k_dec_h2	0.02
C_sI	0.03	k_hyd_pr	0.3	R	0.083145
C_ch	0.0313	k_hyd_li	0.1	T_op	308.15
C_pr	0.03	K_S_IN	0.0001	pK_w_base	14
C_li	0.022	k_m_su	30	pK_a_va_base	4.86
C_xI	0.03	K_S_su	0.5	pK_a_bu_base	4.82
C_su	0.0313	pH_UL_aa	5.5	pK_a_pro_base	4.88
C_aa	0.03	pH_LL_aa	4	pK_a_ac_base	4.76
f_fa_li	0.95	k_m_aa	50	pK_a_co2_base	6.35
C_fa	0.0217	K_S_aa	0.3	pK_a_IN_base	9.25
f_h2_su	0.19	k_m_fa	6	k_A_Bva	1E+10
f_bu_su	0.13	K_S_fa	0.4	k_A_Bbu	1E+10
f_pro_su	0.27	K_Ih2_fa	0.000005	k_A_Bpro	1E+10
f_ac_su	0.41	k_m_c4	20	k_A_Bac	1E+10
N_bac	0.005714286	K_S_c4	0.2	k_A_Bco2	1E+10
C_bu	0.025	K_Ih2_c4	0.00001	k_A_BIN	1E+10
C_pro	0.0268	k_m_pro	13	kLa	200
C_ac	0.0313	K_S_pro	0.1	K_H_h2o_base	0.0313
C_bac	0.0313	K_I_h2_pro	3.5E-06	K_H_co2_base	0.035
Y_su	0.1	k_m_ac	8	K_H_ch4_base	0.0014
f_h2_aa	0.06	K_S_ac	0.15	K_H_h2_base	0.00078
f_va_aa	0.23	K_I_nh3	0.0018	k_P	50 000
f_bu_aa	0.26	pH_UL_ac	7	K_I_fa_low	0.40639
f_pro_aa	0.05	pH_LL_ac	5	K_I_fa_high	0.71421
f_ac_aa	0.4	k_m_h2	35		
C_va	0.024	K_S_h2	0.000007		

Benchmark Simulation Model No.2 plant layout

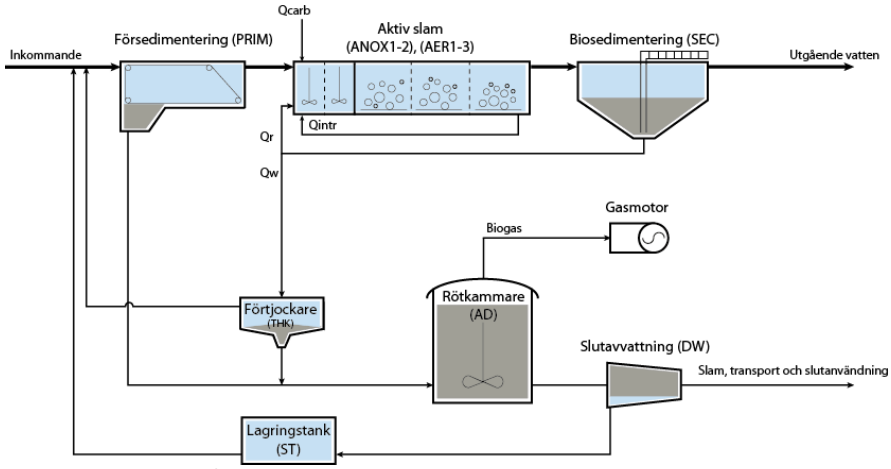

Figure S.4. Plant layout for the wastewater treatment plant in Benchmark Simulation Model No. 2 (Gernaey *et al.*, 2014).

References

Astals, S., Batstone, D.J., Mata-Alvarez, J. and Jensen, P.D. (2014) Identification of synergistic impacts during anaerobic co-digestion of organic wastes. Bioresource Technology, 169, 421-427.

Batstone, D.J., Keller, J., Angelidaki, R.I., Kalyuzhnyi, S.V., Pavlostathis, S.G., Rozzi, A., Sanders, W.T.M., Siegrist, H. and Vavilin, V.A. (2002) Anaerobic Digestion Model No. 1. Scientific and Technical Report No. 13, IWA Publishing, London, UK.

Batstone, D.J. (2013) Teaching uncertainty propagation as a core component in process engineering statistics. Education for Chemical Engineers, 8, 132-139.

Gernaey, K., Jeppsson, U., Vanrolleghem, P.A. and Copp, J.B. (2014) Benchmarking of Control Strategies for Wastewater Treatment Plants. IWA Scientific and Technical Report No. 23, IWA Publishing, London, UK.

Grau, P., de Gracia, M., Vanrolleghem, P.A. and Ayesa, E. (2007) A new plant-wide modelling methodology for WWTPs. Water Research, 41(19), 4357-4372.

Paper VI

Multi-objective Performance Assessment of Wastewater Treatment Plants Combining Plant-wide Process Models and Life Cycle Assessment

Arnell Magnus[1,2], Rahmberg Magnus[3], Oliveira Felipe[3], Jeppsson Ulf[1]

[1] Department of Biomedical Engineering (BME), Division of Industrial Electrical Engineering and Automation (IEA), Lund University, P.O. Box 118, SE-221 00 Lund, Sweden.
[2] SP Technical Research Institute of Sweden, Gjuterigatan 1D, SE-582 73 Linköping, Sweden.
[3] IVL Swedish Environmental Research Institute, P.O. Box 210 60, SE-100 31, Stockholm, Sweden.

Corresponding author: Magnus Arnell; E-mail: magnus.arnell@iea.lth.se; Phone: +46 10 516 63 33.

Abstract

Multi-objective performance assessment of operational strategies at wastewater treatment plants (WWTPs) is a challenging task. The holistic perspective applied to evaluation of modern WWTPs, including not only effluent quality but also, resource efficiency and recovery, global environmental impact and operational cost calls for assessment methods including both on and off-site effects. In this study a method combining dynamic process models – including greenhouse gas (GHG) emissions and detailed energy models – and life cycle assessment was developed. The method is applied and calibrated to a large Swedish WWTP. In a performance assessment study changing the operational strategy to chemically enhanced primary treatment was performed and evaluated. The results show that the primary objectives, to enhance bio-methane production and reduce greenhouse gas emissions were reached. Bio-methane production increased by 14% and the global warming potential (GWP) decreased by 28%. However, the LCA revealed that due to increased consumption of precipitation chemicals and additional carbon source dosing (methanol) the abiotic depletion of elements and fossil resources increased by 77 and 305%, respectively. The results emphasise the importance of using plant-wide mechanistic models and life cycle analysis to capture the dynamics of the plant – e.g. dynamics of GHG emissions – and the potential global environmental impact.

Keywords: wastewater treatment; process control; mathematical modelling; LCA; performance assessment

Nomenclature

AD	Anaerobic digester
ADM1	Anaerobic Digestion Model No 1
ADP	Abiotic depletion potential
ANOX	Anoxic model reactors
AOB	Ammonia oxidizing bacteria
ASU	Activated sludge unit
ASM1	Activated Sludge Model No 1
ASM1G	Activated Sludge Model No 1 Greenhouse Gas
BSM	Benchmark Simulation Model
BSM2G	Benchmark Simulation Model No 2 Greenhouse Gas
CEPT	Chemically enhanced primary treatment
CML	Centrum voor Milieukunde, Leiden University, The Netherlands
COD	Chemical oxygen demand [$mg.l^{-1}$]
DEOX	Non-aerated deox model reactor
DO	Dissolved oxygen [$mg.l^{-1}$]
DW	Dewatering unit
EQI	Effluent quality index
EU28	The 28 member states of the European Union
FLEX	Flexible, aerated or non-aerated model reactor
GHG	Greenhouse gas
GU	Gas upgrade unit
GWP	Global warming potential
IPCC	Intergovernmental Panel on Climate Change
ISO	International Organization for Standardization
ISS	Inert suspended solids [$mg.l^{-1}$]
LCA	Life cycle analysis
LCI	Life cycle inventory
LCIA	Life cycle impact assessment
OCI	Operational cost index
ODP	Ozone depletion potential
OX	Aerated model reactors
PRIM	Primary mechanical treatment
RAS	Return activated sludge
SF	Sand filter
STOR	Sludge storage
THK	Thickener unit
TN	Total nitrogen [$mg\ N.l^{-1}$]
TSS	Total suspended solids [$mg.l^{-1}$]
VS	Volatile solids [$mg.l^{-1}$]
WWT	Wastewater treatment
WWTP	Wastewater treatment plant

1. Introduction

The holistic view applied to modern wastewater treatment plants (WWTPs) challenges the traditional methods for performance evaluation. Today not only effluent water quality and operational cost, but also energy efficiency, resource recovery rate and global environmental impact (e.g. on climate) need to be considered when assessing plant performance (Olsson, 2015). It is well known that WWTPs can emit substantial amounts of greenhouse gases (GHGs). Apart from the mostly biotic CO_2 emissions from degraded organic matter the main direct emissions from WWTPs are typically CH_4 from the sludge treatment and N_2O from the secondary biological treatment (Foley et al. 2011; Mannina et al., 2016). Foley et al. (2011) also showed that the variations in especially the important N_2O emissions are large and dependent of process configuration and operational strategy. Since over a decade there has been a strong focus on energy efficiency and recovery at WWTPs to reduce both costs and GHG emissions (Olsson, 2015). Even if this is a commendable intention it has been shown that energy saving at the same time can lead to an overall increase in GHG emissions, for example increased N_2O emissions (Flores-Alsina et al., 2014). Altogether, this calls for better modelling tools to evaluate and compare treatment strategies. Mechanistic process models have been used for several decades to assess treatment efficiency, residual environmental load and operational costs for WWTPs. They have proven to be a valuable tool for everything from green field design of new plants to design and evaluation of detailed control strategies (Rieger et al., 2012).

However, for the global environmental impact not only the direct emissions to water, land and air of different pollutants from the plant is relevant but also the up and downstream processes need to be taken into account. That includes external processes, such as production of input goods like power and chemicals, but also impacts of the remaining effluent load in the recipient and utilisation of bio-solids and bio-methane. These types of effects have successfully been assessed for WWTPs using life cycle assessment (LCA) (Baresel et al., 2016; Svanström et al., 2016; Corominas et al., 2013a,b). LCA evaluate the potential environmental impact due to the product or service under study characterised in different categories (Baumann and Tillman, 2004). The ISO standard for LCA (ISO 14044) gives a structured procedure for performing the LCA where, after defining the study, a life cycle inventory (LCI) is done where the environmental loads from the whole system are calculated followed by a life cycle impact assessment (LCIA) where the loads are characterised by the selected impact categories to get aggregated measures of the potential environmental impacts expressed in equivalent units (Baumann and Tillman, 2004).

To capture both the dynamic performance of the WWTP and the global environmental impact the combination of mechanistic process models and LCA have

been explored on generic benchmark type WWTP layouts (Corominas et al., 2013b; Meneses et al., 2016; Bisinella de Faria et al., 2015). These studies use combinations of different WWTP models and LCA to assess control strategies, load variations and local recipient conditions. However, all of these studies are limited in their coverage of the WWTP, either just the water line is modelled mechanistically (Corominas et al., 2013b; Meneses et al., 2016) or as in Bisinella de Faria et al. (2015) where the highly dynamic GHG production is modelled using static emission factors.

This paper explores the hypothesis that it is possible to combine a plant-wide WWTP process model – with detailed energy and GHG models – and LCA study to evaluate the overall performance of operational strategies at WWTPs, capturing both the dynamic effects at the plant and the global environmental impact due to external resource use. A model framework is presented and also tested in a case study performed at a full-scale Swedish WWTP comparing two operational strategies.

2. Methods

The general method developed in the Benchmark Simulation platform (Gernaey et al., 2014) coupled to a LCA model is presented in detail. Thereafter a case study where the model is adjusted to the plant under study is described together with a simulation study on enhanced primary treatment.

2.1 Process model development

For the detailed process modelling the Benchmark Simulation Model No 2 GHG (BSM2G) presented by Flores-Alsina et al. (2014) was used as a basis. The BSM platform is a general simulation platform for benchmarking of operational and control strategies at WWTPs. It consists of: *i)* a general plant layout (see Supplementary information, Figure S.1); *ii)* a set-up of sub-models for the included processes; *iii)* models for sensors, controllers and actuators to allow implementation of various control strategies; *iv)* a specified simulation procedure including an influent profile; and, *v)* an evaluation procedure including two aggregated indices: Effluent Quality Index (EQI) and Operational Cost Index (OCI). More information about the BSM platform can be found in Gernaey et al. (2014).

The BSM2G plant consists of a primary clarifier (PRIM) modelled with a simplified model by Otterpohl and Freund (1992) followed by an activated sludge unit (ASU) in a modified Ludzak-Ettinger configuration where the initial anoxic tanks (ANOX) and last aerated tanks (OX) are connected by an internal recycle. The

bioprocess model is an extended version of the Activated Sludge Model No. 1 (ASM1) described by Guo and Vanrolleghem (2014) including greenhouse gas emissions (ASM1G); the key modifications are the two-step nitrification – with separate nitrifier biomass states: ammonia oxidizing bacteria (AOB) and nitrite oxidizing bacteria – and four-step denitrification (Hiatt and Grady, 2008) along with nitrifier denitrification by AOB proposed by Mampaey et al. (2013). The secondary settler is described by a one-dimensional 10-layer settler by Takács et al. (1991). The sludge line contains a thickener (THK), an anaerobic digester (AD) and a dewatering unit (DW). The AD is modelled using the Anaerobic Digester Model No 1 (ADM1, Batstone et al., 2002) and the THK and DW as ideal separation models. Dewatered sludge is stored for 12 months (STOR) before utilization.

The GHG emissions included in the BSM2G by Flores-Alsina et al. (2014) was supplemented with the following:

- direct emissions from digestion with 1% of the raw biogas (Avfall Sverige Utveckling, 2009);
- direct emissions from 12 months sludge storage (open storage in piles) with 8.7 kg CH_4.ton VS^{-1} (VS for volatile solids) and 0.36% of total nitrogen (TN) as N2O-N (Jönsson et al., 2015) – corresponding amounts of carbon and nitrogen are removed from the sludge;
- direct emissions from gas utilization with 1.7% of combusted raw biogas in co-generation unit (Liebetrau et al., 2010);
- indirect emissions of N_2O from the recipient due to residual effluent nitrogen with 0.005 kg N_2O-N.kg $TN_{effluent}^{-1}$, (IPCC, 2013).
- three different bio-solids utilisation alternatives included with transport (trucks), CH_4 and N_2O emissions. The organic matter (measured as chemical oxygen demand, COD) is assumed to mineralise and carbon emitted as CO_2:
    - fertilization of farm land: 38% of the bio-solids, transport 150 km, emission factor N_2O = 0.01 kg N_2O-N.kg TN^{-1} (IPCC, 2006);
    - composting; 45% of the bio-solids, transport 20 km, emission factor N_2O = 0.01 kg N_2O-N.kg TN^{-1} (IPCC, 2006), emission factor CH_4 = 0.0075 kg CH_4.kg TOC^{-1} (Kirkeby et al., 2005);
    - fertilization of forest: 17% of the bio-solids, transport 144 km, emission factor N_2O = 0.01 kg N_2O-N.kg TN^{-1} (no data available, assumed equal to farm land);

The numbers suggested are to be used together with the generic BSM2G. For specific case studies these should be updated (transport distances, % distribution) or if a coupled LCA model is used off-plant processes should be replaced by LCI data.

The model was implemented in Matlab/Simulink (MATLAB 8.4, The MathWorks Inc., Natick, MA, USA 2014) and dynamic simulations for a full year eval-

uation period were run according to the procedures in Gernaey et al. (2014). The averaged simulation results were used as input for the static LCA modelling of global environmental impact potential.

2.2 LCA model description

The LCA was performed according to the standard ISO 14044. The goal and scope of the LCA was to perform a comparative assay of the operational strategies simulated using the process model. The system boundaries for the LCA was therefore chosen to be the WWTP itself with direct emissions to water, soil and air and the production and transport of power and chemicals from resource extraction to the plant. The benefit of utilizing the produced bio-methane was accounted for with expanding the system to include the benefitting process, i.e. co-generation of heat and power (in BSM2G) or replacing diesel as vehicle fuel. For the purpose of comparing operational strategies one year of operation was considered and construction and demolition phases were excluded as it has been shown to have a limited impact for most traditional advanced WWTPs (Corominas et al., 2013a). To manage the LCI and LCIA the Gabi software tool was used (Gabi software 6.3, Thinkstep, Leinfelden-Echterdingen, Germany, 2013). The process model simulation outputs were used together with generic data from the Ecoinvent database (Weidema et al., 2013). Six impact categories were selected based on previous similar studies (Corominas et al., 2013a) and expected impacts calculated following the procedures developed by Centrum voor Milieukunde at Leiden University, The Netherlands (CML) (Guinée et al., 2002): abiotic depletion potential of elements (ADP elements) and fossil (ADP fossil) resources, eutrophication potential, acidification potential, global warming potential (GWP) and ozone depletion potential (ODP). For GWP emissions CH_4, N_2O and abiotic CO_2 were considered with GWP factors according to IPCC (2013). The procedures of CML were used also for the characterization in the LCIA.

2.3 Modelling of the Käppala WWTP

The Käppala WWTP in Lidingö outside Stockholm, Sweden receives wastewater from 11 municipalities in the northern part of the greater Stockholm area. The plant is mainly an underground facility built into the mountain close to the outer rim of the archipelago. The effluent requirements are 10 mg $N.l^{-1}$ TN and 0.3 mg $P.l^{-1}$ total phosphorous. This is achieved with a treatment process based on primary mechanical treatment, secondary biological treatment and tertiary filtration, Figure 1. The plant is built in two parallel parts where the original part has biological phosphorous removal in an A_2O process while the newer part is a pre-

denitrification configuration with simultaneous precipitation using ferrous sulphate. For the purpose of the modelling study only the new part of the plant was modelled. Where applicable the volumes and flows were reduced to correspond to the part of influent wastewater that is treated in the new part of the plant. The below description refers only to the new part of the plant if not otherwise stated. The BSM2G used as the model base and modifications are highlighted outlining the plant model below.

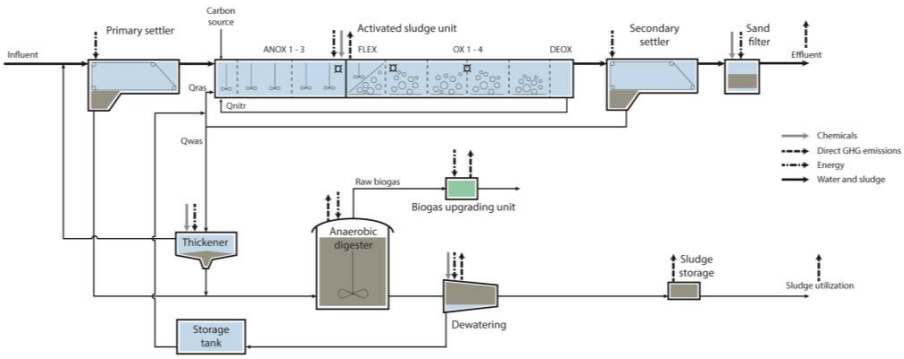

Figure 1. Process flow diagram of the modelled parts of the plant. Arrows indicate flows of water and sludge (solid black), chemical input (solid grey), direct GHG emissions (dashed black) and energy input (dot-dashed black). The measurement points for aqueous N_2O are indicated in the ASU (¤).

The treatment process in detail consists of:

Primary treatment: 3 mm bar screens followed by pre-aeration and an aerated grit chamber. Primary sedimentation in 5 parallel lines with a removal efficiency of 51% COD and a primary sludge total suspended solids (TSS) concentration of about 6%. The primary sludge is pumped to the sludge treatment. Only the primary settlers were modelled.

Biological treatment: Secondary treatment in activated sludge. 5 parallel 10 m deep reactors with a modified Ludzak-Ettinger configuration with a total anoxic volume of 34 130 m^3 utilizing influent COD as carbon source followed by aerated zones of in total 55 000 m^3 and a final non-aerated zone of 3 300 m^3 for lowering the effluent DO. The final non-aerated zone and the first denitrification zone are connected by an internal recycle. Five secondary settlers with a depth of 6.1 m separate the sludge and the return activated sludge (RAS) is pumped back in a joint RAS channel. The waste activated sludge is pumped to centrifugal thickeners. The ASU was modelled as one line – with five times the volume – with 9 zones in series (Fujie et al., 1983): three anoxic zones (ANOX 1 to 3), one swing zone (FLEX), four aerated zones (OX 1 to 4) and one final non-aerated zone (DEOX). The ASM1G model was used. To capture the effluent TSS at high flow rates the

secondary clarifiers were described using the Bürger-Diehl model (Bürger et al., 2013) implemented in Matlab by Arnell (2015). The simultaneous precipitation was not modelled as such but an addition of inorganic suspended solids (ISS) was introduced. For dissolved oxygen (DO) control the zones OX 1 to 4 have individual DO measurements and a PI regulator controls the airflow towards a DO set-point. The DO set-point in turn is controlled through ammonia feedback, i.e. a PI regulator controlling the DO set-point against a set-point of NH_4-N in the effluent of DEOX. The aeration model was extended according to the principles described in Arnell and Jeppsson (2015) for converting K_La to airflow.

Filtration: A tertiary filtration step with chemical precipitation (using ferric chloride) on two media downstream filters (SF). The filters are intermittently backwashed and the sludge is recycled to the plant influent. A simple cut-off model was constructed taking away all particulates above 5 mg TSS.l^{-1} in the filter influent to the sludge phase, which was recycled to the plant influent.

Sludge treatment: The sludge from both the old and the new part of the plant is treated in two anaerobic digesters in series, each 9 000 m^3. The primary sludge is fed to the first digester and before entering the second digester mixed with the thickened secondary sludge. The digested sludge is dewatered in centrifuges to a dry solids content of 27%, which is stored for 12 months before application. The produced biogas is up-graded to vehicle fuel quality in a gas-upgrading unit (GU) and sold to the local public transport company to be used in city busses. The bio-solids are transported and utilized for fertilization of farmland or for landscaping. The dewatering supernatant is pumped back to the joint RAS channel before entering the anoxic zones. The sludge line was modelled with default models but the reactor configuration was adjusted to the Käppala plant layout and volumes adjusted according to the modelled portion of the flow.

Consumption of resources, such as energy and chemicals, were either modelled dynamically (i.e. carbon source addition) or calculated based on specific consumption numbers. Mainly specific data were retrieved from the utility but some generic BSM2G data were used when specific data were missing. Values are tabulated in Supplementary information, Table S.1. The specific consumption factors have when possible been coupled to dynamically modelled flows and volumes but for a few energy related processes static consumptions per day were the most reliable information.

A dynamic influent profile was created from plant data for the years 2012 and 2014. The actual flow measurements were used along with a synthetic diurnal load pattern created from the averaged and normed diurnal flow rate during dry weather. For influent fractionation and calibration the procedures in Rieger et al. (2012)

were followed. The year 2012 was selected for calibration and 2014 for validation. The results from 2012 were chosen for results presentation as this was a year with several severe rain events challenging the treatment process. For calibration of the N_2O production in the bio-process model additional measurements were made in the ASU. N_2O gas concentration was measured in the ventilation channel from one of the five parallel ASU lines and at the same time the aqueous N_2O concentration was measured at three different positions (one at a time) – beginning of OX, end of ANOX and mid OX. The N_2O measurements continued for more than 100 days. During this period also grab samples were analysed for NO_2-N 11 times.

For the LCA model the WWTP was split up into the main treatment steps supplemented with extraction of resources for and production and transport of power and chemicals needed for the process. The LCA model was also extended with the use of produced bio-methane as vehicle fuel. System boundaries are illustrated in Figure 2.

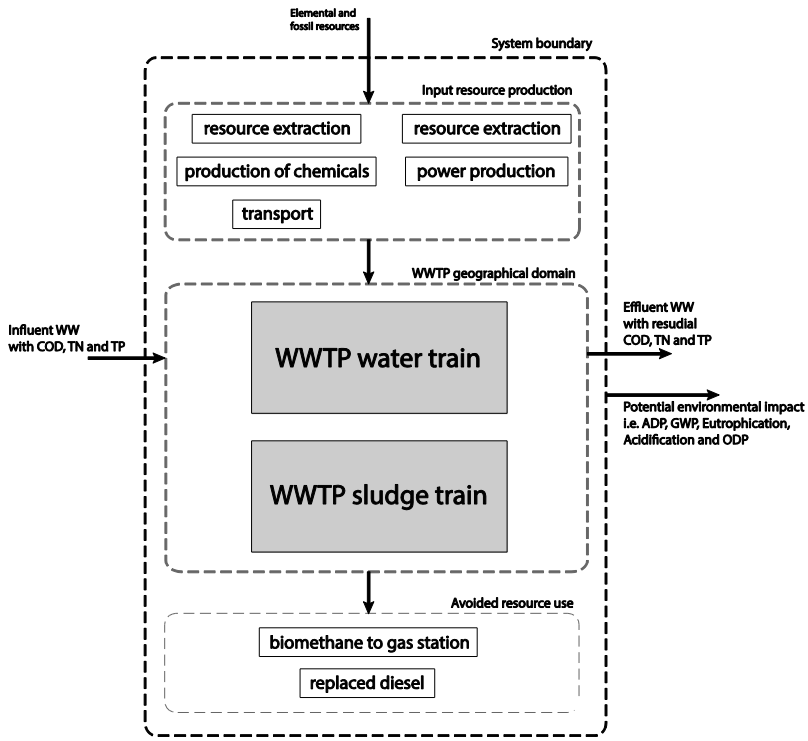

Figure 2. Schematic figure of the system boundaries and modelled activities for the LCA.

The full LCI data with references are given in Supplementary information (Table S.2) but some important assumptions were:

- for power production the average Swedish electricity grid mix was used (mainly hydro and nuclear power, about 90%);
- the methanol used in the scenario was assumed to have fossil origin;
- when used as vehicle fuel the bio-methane was assumed to replace 0.765 MJ of diesel for each MJ of bio-methane;
- for transport it was assumed with the actual transport distances (see Supplementary Information, Table S.2) with Euro 4 class trucks running on diesel containing 10 ppm of sulphur. Unloaded return trips were assumed.

For the interpretation of the LCA results the impact equivalence numbers – in functional unit, per m^3 – were normed to the base case for internal comparison and also to the total EU28 emissions (Guinée et al., 2002) (values given in Supplementary information, Table S.3) in each respective impact category for evaluation of the relative importance of the different categories.

2.4 Global performance assessment of CEPT

The interest for enhanced mechanical treatment is growing as focus is shifted towards multiple objectives for WWTPs (Bachis et al., 2015). If the reduction over the different steps of the mechanical treatment can be increased several objectives can be improved: *i)* the load on the ASU is decreased leading to lower aeration requirements and increased treatment capacity in the ASU; and, *ii)* the biogas production is increased leading to less GHG emissions if the gas is utilized to replace fossil resources. A common way to achieve this is to implement chemically enhanced primary treatment (CEPT), where pre-precipitation with metal salts are used to improve the removal efficiency over the primary clarifiers. However, there are risks with this practice; extensive pre-precipitation can easily lead to deficiency of available organic matter for denitrification and even phosphorous in the ASU. So, there is a conflicting competition for the influent organic matter, whether it is best used for denitrification in the ASU or for biogas production in the AD. For denitrification external carbon sources, such as methanol or ethanol, can be used but it comes with a cost and environmental impact from production and transport of the chemicals.

A simulation study was designed to assess the total environmental impact of this strategy using the proposed methodology. For realism and verification, the calibrated model of the Käppala WWTP was used. The base case represents the current operation of the treatment plant and the simulation results from 2012 were used as the base case. The alternative strategy with CEPT was modelled with the following model-wise simple modifications: The reduction over the PRIM was increased to 60% COD by increasing the parameter `f_corr` to 0.8 and move the

modelling of precipitation (ISS addition) to before the PRIM. A reduction over the PRIM of that magnitude is possible if the plant has effective primary settling which is the case at Käppala. The goal with the simulation study was to show the change in environmental impact from the strategy assuming the same effluent quality. Therefore, the operation was tuned to match the same effluent standards as for the base case. To achieve this it was necessary to add methanol to the anox-zones match the denitrification in the CEPT case. This was done by a 50/50 addition to ANOX 1 and 2 with a PI regulator controlling the methanol flow towards a concentration set-point of 6.7 mg $N.l^{-1}$ NO_3-N in the effluent from the DEOX.

3. Results and Discussion

3.1 Model calibration

The model calibration shows a good fit for the standard water quality variables. Priority during the calibration was to fit the sludge age in the ASU to match the nitrification. This was achieved as the sludge age in the model is 13.0 compared to data 13.4 d. The resulting effluent TN and NH_4-N differs by only 0.1 mg $N.l^{-1}$ between model output and data. To achieve this, the TSS in the ASU had to be set slightly lower than actual values, 1 700 compared to 2 100 $mg.l^{-1}$ yielding a slightly lower overall bio-solids production. Comparison between model calibration results and plant data are tabled in Supplementary information, Table S.4. Default parameter values were used in the process model.

From the measured N_2O concentration in the reactor it was evident that no N_2O production occurred in the anoxic zones, see Figure 3. The in-tank N_2O concentration was very low at the end of the last anoxic zone even if no forced stripping had occurred. However, in the aerated zones the N_2O concentration was higher and increasing along the reactor. Taking the stripping, due to aeration, into account it could be concluded that the major part of the production and emission of N_2O occurred from the aerated zones. The reason for this is assumed to be the relatively high NO_2-N concentrations measured, around 0.3 mg $N.l^{-1}$. This relationship has been reported previously in literature (Foley et al., 2011). To calibrate the NO_2-N concentrations and succeeding N_2O emissions to air two half-saturation parameters were adjusted: K_{FA} = 0.002 g $N.m^{-3}$ and K_{FNA} = 0.00035 g $N.m^{-3}$. As seen in Figure 4, the average level of the modelled emissions is in line with measured values. However, the full dynamics of the measured emissions were not well predicted by the model. The model predicts a constant base line for the emissions of about 30 kg N_2O-$N.d^{-1}$ even when the measured emissions decrease around day 425, Figure 4. The model behaviour follows from the model equations for the AOB denitrifica-

tion. However, recent publications emphasise the importance of using a two-pathway model – including both hydroxylamine oxidation and AOB denitrification – under dynamic conditions (Mannina et al., 2016; Ni and Yuan, 2015). These models predict that the N_2O production relates to the rate of nitritation rather than DO. These new two-pathway models were not available at the time when conducting this study but the present results support that additional reaction pathways need to be considered in future work. One trade-off made in favour of getting proper emissions to air was that the N_2O concentration in aqueous phase had to be calibrated to a lower than measured values for the aerated zones. The reason for this is that the modelled stripping of N_2O – as previously reported by Lindblom et al. (2015) – is too effective. A higher liquid N_2O concentration would lead to too high emissions.

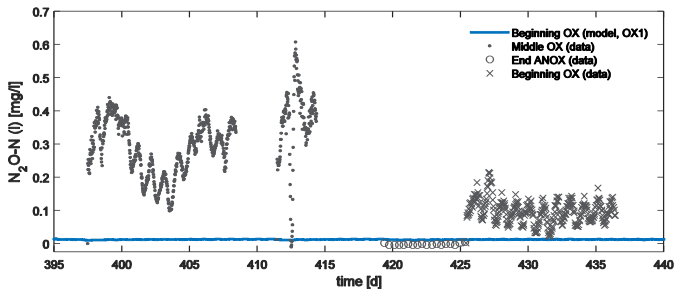

Figure 3. N_2O-N in aqueous phase. Data – grey, model – blue. The time scale represents simulation days, where 245 corresponds to 1st Jan. The three measurement points are indicated in Figure 1.

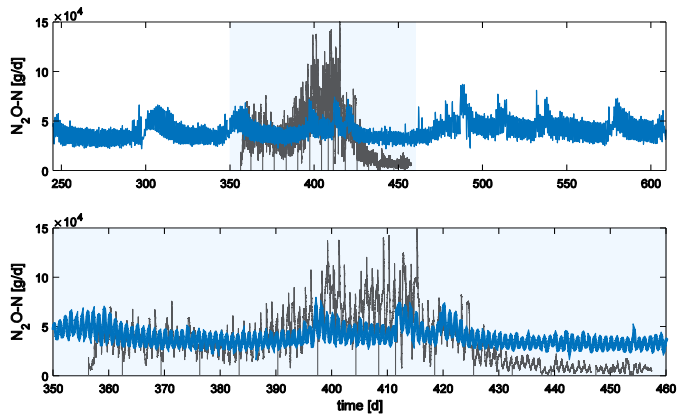

Figure 4. N_2O measurements at Käppala WWTP and model calibration result. Data – grey, model – blue. Full year simulation (top) and day 350 to 460 covering the N_2O measurement campaign (bottom).

3.2 Performance assessment of CEPT

The most relevant simulation results from the process model are presented in Table 1. The ambition that the effluent quality should be the same for the two cases was achieved and both the general Effluent Quality Index (EQI) and the specific nitrogen parameters were approximately similar for the two simulations.

The primary objective, to increase the production of bio-methane with CEPT, was reached. The bio-methane production increased by almost 14%. Along with that the energy for aeration decreased as expected. However, the change was small, due to the addition of methanol to the ANOX that kept up the total COD load on the ASU. The use of chemicals for precipitation increased substantially which was expected just as the additional methanol. The cost for operations increases with the cost of chemicals but the net operational cost could not be reported since the revenue from selling the bio-methane was not publically available.

The direct emissions of GHGs from the plant were affected by the operational strategy. The methane slip from the AD increased with CEPT due to increased gas production since it was calculated proportionally. In contrary a much larger decrease in GHG emissions were achieved as the N_2O emissions from the ASU decreased. It is hypothesised that this is due to the reduced load on the ASU with CEPT; the TN in the primary effluent was reduced and methanol was dosed which improves the C to N ratio in the ASU.

Table 1. Simulation results from the process model for the base case and CEPT.

	Unit	Base case	CEPT
Effluent Quality			
EQI	-	17 470	17 040
NH_4-N	mg $N.l^{-1}$	1.34	1.13
NO_X-N	mg $N.l^{-1}$	6.22	6.59
TN	mg $N.l^{-1}$	8.50	8.61
Sludge production	kg $TS.d^{-1}$	14 694	14 530
Resource performance			
Bio-methane production	kg $CH_4.d^{-1}$ / $kWh.d^{-1}$	4 930 / 68 400	5 610 / 77 900
Power for aeration	$kWh.d^{-1}$	6 590	6 480
Consumption precipitation chem.	kg $Fe.d^{-1}$	178	1 260
Consumption methanol	kg $COD.d^{-1}$	0	2 060
Direct GHG emissions			
N_2O ASU	kg $CO_2e.d^{-1}$	19 040	14 400
CH_4 and N_2O sludge treatment	kg $CO_2e.d^{-1}$	6 520	6 700

The LCA results based on the two simulations are presented in Table 2, Figure 5 and Figure 6. From Table 2 can it be concluded that all except ODP is within a 2 orders of magnitude related to the total emissions for 28 European countries for the year 2000; ODP is significantly smaller. Also in the LCA results the strive to keep effluent quality unchanged is evident as the difference in the impact category Eutrophication is small, Figure 5. The sought reduction in Climate impact of the operations was achieved and did decrease by 28%, Table 2. This is the result of several combined effects; a decrease of the direct plant GHG emissions, decreased power consumption as well as increased bio-methane production. The latter leads to decreased GWP as a credit is made when it substitutes fossil vehicle fuels, see Figure 6. Altogether, the Climate impact is reduced by almost a third despite the increased emissions from production and transport of methanol and precipitation chemicals.

Table 2. LCA results for the base case and modified control strategy, CEPT, for the six selected impact categories. The units only apply to absolute values, normalized values are dimensionless. The unit for ADM elements refer to antimony (Sb) equivalents and the ODP unit to equivalents of the trichlorofluoromethane R11.

		Absolute values		**Normalized values EU28 [-]**	
Impact category	**Unit**	Base case	CEPT	Base case	CEPT
ADP elements	[kg Sbe.m^{-3}]	$3.7 \cdot 10^{-8}$	$6.5 \cdot 10^{-8}$	$2{,}3 \cdot 10^{-7}$	$4{,}1 \cdot 10^{-7}$
ADP fossil	[MJ. m^{-3}]	0.29	0.90	$3{,}2 \cdot 10^{-7}$	$9{,}8 \cdot 10^{-7}$
Acidification	[kg SO_2e. m^{-3}]	$4.4 \cdot 10^{-4}$	$4.9 \cdot 10^{-4}$	$1{,}0 \cdot 10^{-6}$	$1{,}1 \cdot 10^{-6}$
Eutrophication	[kg PO_4e. m^{-3}]	$2.4 \cdot 10^{-3}$	$2.2 \cdot 10^{-3}$	$4{,}9 \cdot 10^{-6}$	$4{,}5 \cdot 10^{-6}$
GWP	[kg CO_2e. m^{-3}]	0.15	0.11	$1{,}1 \cdot 10^{-6}$	$8{,}1 \cdot 10^{-7}$
ODP	[kg R11e. m^{-3}]	$2.0 \cdot 10^{-10}$	$9.2 \cdot 10^{-10}$	$7{,}6 \cdot 10^{-10}$	$3{,}5 \cdot 10^{-9}$

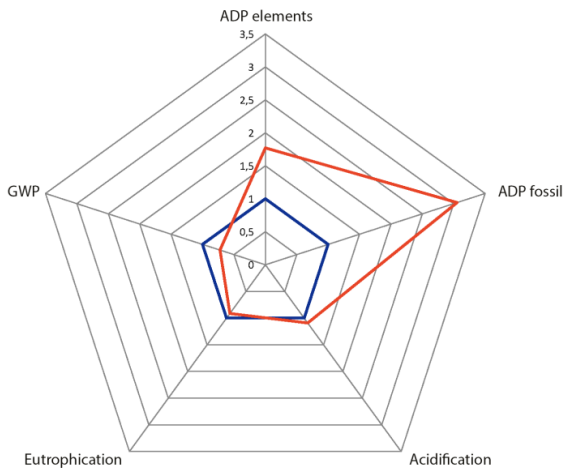

Figure 5. Comparison between the LCA results for the base case (blue) and CEPT (red). The results are normalized to the value of the base case.

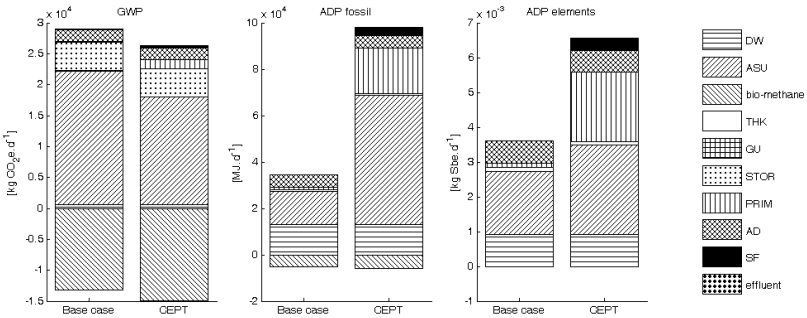

Figure 6. Bar chart over the contribution from the different plant sub-processes to the impact categories GWP (left), ADP fossil (middle) and ADP elements (right).

The improvement in Climate impact comes with a cost in terms of resource use. The elemental and fossil Abiotic Depletion potentials (ADP) are increased by 77 and 305%, respectively, see Table 2 and Figure 5. This increase is completely explained by the increased use of chemicals for precipitation and denitrification, Figure 6. The origin of the methanol was here assumed to be fossil based, which has a major impact on ADP fossil. In a parallel project using the same base model a sensitivity analysis on the origin of the carbon source was done and it showed a significant impact. The increase in fossil depletion was reduced significantly if recycled glycerol was used instead (Åmand et al., 2016).

The impact category with the largest relative change was Ozone Depletion potential (ODP); with CEPT it increased by 450%, Table 2. From the table, it is clear that the absolute values are very small and even normalized to the EU28 emissions the ODP was 2 to 4 orders of magnitude lower than that of the other categories. So, even if the increase was relatively large, it was from a low initial level.

The impact of CEPT on Acidification potential is negative but very small. The change is solely caused by production and transport of chemicals, especially methanol, which penalizes CEPT in this case.

3.3 General impact of results and limitations of method

The results above show the multidimensional, and often conflicting, impacts that arise from different operational strategies at WWTPs. When the operations are evaluated, not only based on effluent quality and cost but also on resource efficiency and global environmental impact, the evaluation grows complex. From the results it is evident that detailed process models are necessary to assess, for example N_2O production in the ASU or overall effects of return streams. This confirms findings in previous studies, i.e. Flores-Alsina et al. (2014), Guo and Vanrol-

leghem (2014) and Corominas et al. (2013b); these effects can rarely be calculated with traditional spread sheet methods (Rieger et al., 2012). At the same time the increase or decrease in resource use and recovery lead to a different environmental impact off plant that is not captured by the process model but only by LCA. To combine process modelling and LCA as in this study to describe the included processes and calculate the global environmental impact is useful for comparing alternative operational strategies at WWTPs and provides a thorough base for decision making.

The general method developed suggests also including utilization of bio-solids and expanding the system to include replacement of commercial fertilizer. This is done for completeness and consistency since effluent load is included as well as bio-methane utilization with crediting when used as vehicle fuel. In the case study there was unfortunately limited information available on the sludge utilization. Moreover, the data quality was poor for the expanded system of fertilizer replacement. Therefore, the sludge utilization was excluded. However, since the evaluated operational strategies produce very similar amounts of sludge this exclusion will have basically no impact on the conclusions.

The different impact categories in LCA measures different things expressed in different units and are not comparable per se. The standard for LCA studies, ISO 14044, states that weighted comparison of the impact categories is an optional part of the LCA conducted separately after the LCIA. This is good praxis since the subjective process of grading and weighting the results should not be mixed with the objective impact assessment. The weighting step was not performed in this study since it focuses on developing the method for impact assessment rather than decision making. However, if the results are to be used for decision making this weighting and comparison of the different impact categories' mutual importance has to be done at a later stage. This exercise can be performed by skilled decision makers involved in conducting the LCA. Principles and guidance on weighting and multicriteria analysis can be found in literature (ISO14044; Baumann and Tillman, 2004; Malmqvist et al., 2006).

4. Conclusions

- The model platform Benchmark Simulation Model No 2 Greenhouse Gas was extended to – in addition to effluent quality and operational cost – also evaluate fugitive GHG emissions, more detailed energy efficiency models and global environmental impact.
- To assess the global environmental impact the dynamic process models have been coupled with a Life Cycle Analysis (LCA) model. This novel approach to couple a detailed plant-wide model including dynamic en-

ergy and GHG calculations captures both direct emissions and off site impacts, from for example production of electricity and chemicals.

- For the first time this model concept was calibrated to a real plant, the Käppala WWTP in Lidingö, Sweden. The model calibration under current operational conditions shows that the model is suitable for this traditional municipal treatment process. However, it is not possible to capture the full dynamics in N_2O production and emission based on real data. From this fact it is concluded that a model containing N_2O production only from autotrophic and heterotrophic denitrification is not sufficient. Additional production pathways need to be considered.
- A simulation study on altering the operational strategy at the Käppala WWTP in Lidingö, Sweden was performed. The current strategy with simultaneous precipitation and pre-denitrification utilizing internal COD was compared to a strategy with extensive pre-precipitation and adding methanol in the anoxic zones. The comparative simulations show that several of the initial goals with the strategy is fulfilled, i.e. higher gas production, lower aeration energy requirement and an overall decrease in global warming potential (28%). However, at the same time the LCA reveals that the abiotic depletion of both elemental and fossil resources increases by 77% and 305%, respectively. Also the ozone layer depletion increases many fold but from a very low initial level.
- The study shows that the method is applicable for use at WWTPs. The coupled process and LCA modelling methodology captures plant-wide and global effects that would not only been hard to show with standard spread-sheet calculations but would also remain hidden using any of the models separately. The results from this type of combined study create a good basis for choosing operational strategies at WWTPs.

Acknowledgements

The authors acknowledge the financial support obtained through the Swedish Research Council Formas (211-2010-141), the Swedish Water & Wastewater Association (10-106), SP Technical Research Institute of Sweden and the Swedish WWT research and education consortium VA-cluster Mälardalen.

References

Arnell, M. (2015) Implementation of the Bürger-Diehl settler model on the Benchmark Simulation Platform. Technical report LUTEDX/(TEIE-7250)/1-48/(2015), Division of Industrial Electrical Engineering and Automation, Lund University, Sweden.

Arnell, M. and Jeppsson, U. (2015) Aeration system modelling – case studies from three full-scale wastewater treatment plants. 9th IWA Symposium on Systems Analysis and Integrated Assessment (Watermatex 2015), Gold Coast, Queensland, Australia, 14-17 June, 2015.

Avfall Sverige Utveckling (2009) Frivilligt åtagande – kartläggning av metanförluster från biogasanläggningar 2007-2008 (Voluntary commitment – survey of methane losses from biogas plants 2007-2008) (in Swedish). ISSN 1103-4092. Avfall Sverige AB, Stockholm, Sweden.

Bachis, G., Maruéjouls, T., Tik, S., Amerlinck, Y., Melcer, H., Nopens, I., Lessard, P. and Vanrolleghem, P.A. (2015) Modelling and characterization of primary settlers in view of whole plant and resource recovery modelling. Water Science and Technology, 72(12), pp 2251-2261.

Baresel, C., Dalgren, L., Almemark, M. and Lazic, A. (2016) Environmental performance of wastewater reuse systems: impact of system boundaries and external conditions. Water Science and Technology, 73(6), pp 1387-1394.

Batstone, D.J., Keller, J., Angelidaki, R.I., Kalyuzhnyi, S.V., Pavlostathis, S.G., Rozzi, A., Sanders, W.T.M., Siegrist, H. and Vavilin, V.A. (2002) Anaerobic Digestion Model No. 1. [IWA Scientific and Technical Report No. 13]. IWA Publishing, London, UK.

Baumann, H. and Tillman, A.M. (2004) The Hitch Hiker's Guide to LCA. An orientation in life cycle assessment methodology and application. Studentlitteratur, Lund, Sweden.

Bisinella de Faria, A.B., Spérandio, M., Ahmadi, A. and Tiruta-Barna, L. (2015) Evaluation of new alternatives in wastewater treatment plants based on dynamic modelling and life cycle assessment (DM-LCA), Water Research, 84, pp 99-111.

Bürger, R., Diehl, S., Farås, S., Nopens, I. and Torfs, E. (2013) A consistent modelling methodology for secondary settling tanks: a reliable numerical method. Water Science and Technology, 68(1), pp 192–208.

Corominas, Ll., Foley, J., Guest, J.S., Hospido, A., Larsen, H.F., Morera, S. and Shaw, A. (2013a) Life cycle assessment applied to wastewater treatment: State of the art. Water Research, 47(15), pp 5480-5492.

Corominas, Ll., Larsen, H.F., Flores-Alsina, X. and Vanrolleghem, P.A. (2013b) Including Life Cycle Assessment for decision-making in controlling wastewater nutrient removal systems. Journal of Environmental Management, 128, pp 759-767.

Flores-Alsina, X., Arnell, M., Amerlinck, Y., Corominas, L., Gernaey, K.V., Guo, L., Lindblom, E., Nopens, I., Porro, J., Shaw, A., Snip, L., Vanrolleghem, P.A. and Jeppsson, U. (2014) Balancing effluent quality, economic cost and greenhouse gas emissions during the evaluation of (plant-wide) control/operational strategies in WWTPs. Science of the Total Environment, 466, pp 616-624.

Foley, J., Yuan, Z., Keller, J., Senante, E., Chandran, K., Willis, J., van Loosdrecht, M.C.M. and van Voorthuizen, E. (2011) N2O and CH4 emission from wastewater collection and treatment systems. [Technical report], Global Water Research Coalition, London, UK.

Fujie, K., Sekizawa, T. and Kubota, H. (1983) Liquid mixing in activated sludge aeration tank. Journal of Fermentation Technology, 61, pp 295-304.

Gernaey, K.V., Jeppsson, U., Vanrolleghem, P.A. and Copp, J.B. (2014) Benchmarking of Control Strategies for Wastewater Treatment Plants [IWA Scientific and Technical Report No. 21]. IWA Publishing, London, UK.

Guinée, J.B., Gorrée, M., Heijungs, R., Huppes, G., Kleijn, R., de Koning, A., van Oers, L., Wegener Sleeswijk, A., Suh, S., Udo de Haes, H.A., de Bruijn, H., van Duin, R. and Huijbregts, M.A.J. (2002) Handbook on life cycle assessment. Operational guide to the ISO standards. I: LCA in perspective. IIa: Guide. IIb: Operational annex. III: Scientific background. Kluwer Academic Publishers, Dordrecht, The Netherlands.

Guo, L. and Vanrolleghem, P.A. (2014) Calibration and validation of an activated sludge model for greenhouse gases no. 1 (ASMG1): prediction of temperature-dependent N2O emission dynamics. Bioprocess and Biosystems Engineering, 37(2), pp 151-163.

Hiatt, W.C. and Grady, C.P. (2008) An updated process model for carbon oxidation, nitrification, and denitrification. Water Environment Research, 80(11), pp 2145-2156.

IPCC (2006) N2O emissions from managed soils, and CO2 emissions from lime and urea application. In: Eggleston, H.S., Buendia, L., Miwa, K., Ngara, T., Tanabe, K. (Eds.).2006 IPCC Guidelines for National Green-house Gas Inventories, vol. 5, Waste. IGES, Japan (Chapter 11).

IPCC (2013) Climate Change 2013: The Physical Science Basis. Contribution of Working Group I to the Fifth Assessment Report of the Intergovernmental Panel on Climate Change [Stocker, T.F., D. Qin, D., Plattner, G.-K., Tignor, M., Allen, S.K., Boschung, J., Nauels, A., Xia, Y., Bex, V., and Midgley, P.M. (eds.)]. Cambridge University Press, Cambridge, United Kingdom and New York, NY, USA

ISO 14044:2006. Environmental management -- Life cycle assessment -- Requirements and guidelines.

Jönsson, H., Junestedt, C., Willén, A., Yang, J., Tjus, K., Baresel, C., Rodhe, L., Trela, J., Pell, M. and Andersson, S. (2015) Minska utsläpp av växthusgaser från rening av avlopp och hantering av avloppsslam [SVU report 2015-02, in Swedish]. The Swedish Water & Wastewater Association, Stockholm, Sweden.

Kirkeby, J.T., Gabriel, S. and Christensen, T.H. (2005) Miljøvurdering af genanvendelse og slutdisponering af spildevandsslam - en livscyklus screening af fire scenarier (in Danish). Department of Environmental Engineering, Technical University of Denmark, Kgs. Lyngby, Denmark.

Liebetrau, J., Clemens, J., Cuhls, C., Hafermann, C., Friehe, J., Weiland, P. and Daniel-Gromke, J. (2010) Methane emissions from biogas-producing facilities within the agricultural sector. Engineering in Life Sciences, 10(6), pp 595-599.

Lindblom, E., Arnell, M., Flores-Alsina, X., Stenström, F., Gustavsson, D.J.I., Yang, J. and Jeppsson, U. (2015) Dynamic modelling of nitrous oxide emissions from three

Swedish sludge liquor treatment systems. Water Science and Technology, 73(4), pp 798-806.

Malmqvist, P.A., Heinicke, G., Kärrman, E., Stenström, T.A. and Svensson, G. (2006) Strategic Planning of Sustainable Urban Water Management. IWA Publishing, London, UK.

Mampaey, K.E., Beuckels, B., Kampschreur, M.J., Kleerebezem, R., van Loosdrecht, M.C.M. and Volcke, E.I.P. (2013) Modelling nitrous and nitric oxide emissions by autotrophic ammonia-oxidizing bacteria. Environmental Technology, 34(12), pp 1555-1566.

Mannina, G., Ekama, G., Caniani, D., Cosenza, A., Esposito, G., Gori, R., Garrido-Baserba, M., Rosso, D. and Olsson, G. (2016) Greenhouse gases from wastewater treatment – A review of modelling tools. Science of the Total Environment, 551–552, pp 254-270.

Meneses, M., Concepcion, H. and Vilanova, R. (2016) Joint environmental and economical analysis of wastewater treatment plants control strategies: A benchmark scenario analysis. Sustainability, 8(4), doi.10.3390/su8040360.

Ni, B.J. and Yuan, Z. (2015) Recent advances in mathematical modeling of nitrous oxides emissions from wastewater treatment processes. Water Research, 87, pp 336-346.

Olsson, G. (2015) Water and Energy: Threats and Opportunities Second Edition. IWA Publishing, London, UK.

Otterpohl, R. and Freund, M. (1992) Dynamic models for clarifiers of activated sludge plants with dry and wet weather flows. Water Science and Technology, 26(5-6), pp 1391-1400.

Rieger, L., Gillot, S., Langergraber, G., Ohtsuki, T., Shaw, A., Tak, I. and Winkler, S. (2012) Guidelines for using activated sludge models [IWA Scientific and Technical Report No. 22]. IWA Publishing, London, UK.

Svanström, M., Heimersson, S., Peters, G., Harder, R., I'Ons, D., Finnson, A. and Olsson, J. (2016) Life cycle assessment of sludge management with phosphorus utilisation and improved hygienisation in Sweden. 2nd IWA Conference on Holistic Sludge Management (HSM2016), Malmö, Sweden, June 7-9, 2016.

Takács, I., Patry, G.G. and Nolasco, D. (1991) A dynamic model of the clarification-thickening process. Water Research, 25(10), pp 1263–1271.

Weidema, B.P., Bauer, C., Hischier, R., Mutel, C., Nemecek, T., Reinhard, J., Vadenbo, C.O. and Wernet, G. (2013) The ecoinvent database: Overview and methodology, Data quality guideline for the ecoinvent database version 3. www.ecoinvent.org.

Åmand, L., Andersson, S., Arnell, M., Oliveira, F., Rahmberg, M. and Junestedt, C. (2016) Nya utsläppskrav för svenska reningsverk – effekter på reningsverkens totala miljöpåverkan (in Swedish). In press, IVL Swedish Environmental Institute, Stockholm, Sweden.

Supplementary Information

Paper title: Multi-objective Performance Assessment of Wastewater Treatment Plants Combining Plant-Wide Process Models and Life Cycle Assessment

Authors: Arnell Magnus, Rahmberg Magnus, Oliveira Felipe, Jeppsson Ulf

Life cycle inventory data

The resource consumption data used in the process modelling is presented in Table S.1. The inventory data used in the life cycle inventory (LCI) is tabulated in Table S.2. For the interpretation of the results the absolute values for the impact categories were normed to the total emissions of 28 European countries. The EU28 emissions are listed in Table S.3.

Table S.1. Data for resource consumption in the process model. For values indicated with (*), load or time de-pendent functions from Erikstam (2013) have been used.

Resource	Value	Unit	Reference
Power			
Primary mechanical treatment incl. pumping of primary sludge	1 691*	$kWh.d^{-1}$	Erikstam (2013)
Mixing of anoxic zones	0.004	$kWh.m^{-3}.d^{-1}$	Erikstam (2013)
Aeration	0.025	$kWh.m^{-3}$ air	Erikstam (2013)
Return sludge pumping	0.013	$kWh.m^{-3}$	Thunberg A. (2015) (pers. com.)
Internal recycling	0.0077	$kWh.m^{-3}$	Erikstam (2013)
Waste activated sludge pumping	0.134	$kWh.m^{-3}$	Erikstam (2013)
Thickening	1 169*	$kWh.d^{-1}$	Erikstam (2013)
Mixing of digesters	0.005	$kWh.m^{-3}.h^{-1}$	Gernaey et al. (2014)
Heating of digesters (electricity for heat pump)	3 316*	$kWh.d^{-1}$	Thunberg (2015) (pers. com.)
Dewatering	1 680*	$kWh.d^{-1}$	Erikstam (2013)
Gas upgrading unit	3 680*	$kWh.d^{-1}$	Erikstam (2013)
Chemicals			
Precipitation chem. – simultaneous	9.5	$g.m^{-3}$	Käppalaförbundet (2012)
Precipitation chem. – primary	10	$g\ Fe.m^{-3}$	Thunberg (2014)
Precipitation chem. – sand filter	3	$g\ Fe.m^{-3}$	Thunberg (2014)
Polymer – thickener	10	g polymer $.kg\ TSS^{-1}$	Käppalaförbundet (2012)
Polymer – dewatering	12	g polymer $.kg\ DM^{-1}$	Käppalaförbundet (2012)

* load or time dependent functions from Erikstam (2013).

Table S.2. Life cycle inventory data. Transport distance is given from manufacturer.

Input	Value	Transport distance	Dataset	Comment
Power	0.36 kWh.m^{-3} (base case) 0.35 kWh.m^{-3} (CEPT)	-	SE: Electricity grid mix 1 - 60 kV[1]	Swedish grid mix, 2011.
Precipitation chemical – base case		550 km, from KRONOS in Fredrikstad, Norway.	-	Assumed to be waste product $FeSO_4 \cdot 7H_2O$ from TiO_2 production.
Precipitation chemical – CEPT	0.087 kg.m^{-3}	570 km, from KEMIRA in Helsingborg, SE.	IVL – Ferric chloride 40% oxidation with oxygen[2]	Production of PIX 111 from magnetite.
Polymer	0.0017 kg.m^{-3}	570 km, from KEMIRA in Helsingborg, Sweden.	IVL – Polyelectrolyte[2]	50/50 w/w mix of acrylic acid and acrylonitrile, general model for polyelectrolytes.
Carbon source – methanol	0.013 kg.m^{-3}	870 km, from Denmark.	GLO: methanol, at plant[3]	-
Transport	-	-	GLO: Truck & trailer[1]	22 ton capacity , class Euro 4
Diesel	-	-	EU-27: Diesel mix at refinery[1]	EU-27 diesel mix. 10 ppm S.
Bio-methane combustion emissions	1 MJ bio-methane replace 0.765 MJ diesel	-	IVL – bio-methane (97% methane)[2]	Ahlvik and Brandberg (2000)
Replaced diesel (production and use)	1 MJ bio-methane replace 0.765 MJ diesel	-	IVL - Diesel, well-to-wheel[2]	Diesel production and combustion: Gode et al. (2011) Diesel combustion: Ahlvik and Brandberg (2000)

[1] Gabi software 6.3, Thinkstep, Leinfelden-Echterdingen, Germany, 2013
[2] Internal database at IVL Swedish Environmental Institute
[3] Ecoinvent database (Weidema et al., 2013)

Table S.3. Normalisation factors for EU28 year 2000 (region equivalents Apr. 2013, EU25+3 in Guinée et al., 2002). The unit for ADM elements refer to antimony (Sb) equivalents and the ODP unit to equivalents of the trichlorofluoromethane R11.

	Equivalences	Unit
Abiotic Depletion (ADP elements)	$6.04 \cdot 10^{6}$	kg Sbe
Abiotic Depletion (ADP fossil)	$3.51 \cdot 10^{13}$	MJ
Acidification Potential (AP)	$1.68 \cdot 10^{10}$	kg SO_2e
Eutrophication Potential (EP)	$1.85 \cdot 10^{10}$	kg PO_4e
Global Warming Potential (GWP 100 years), excl. biogenic carbon	$5.21 \cdot 10^{12}$	kg CO_2e

Ozone Layer Depletion Potential (ODP, steady state)	$1.02 \cdot 10^{7}$	kg R11e

Model calibration results

The adapted Käppala WWTP model was calibrated to data for the year 2012. Calibration results for some important variables are shown in Table S.4.

Table S.4. Model calibration results. Comparisons between model results and measured data for 2012. ASU is short for Activated Sludge Unit.

	Model	Data 2012	Unit
Load to plant			
COD	49 090	49 970	$kg.d^{-1}$
Total nitrogen	4 630	4 280	$kg\ N.d^{-1}$
NH_4-N	2 800	2 850	$kg\ N.d^{-1}$
Load to secondary treatment			
COD	24 304	26 100	$kg.d^{-1}$
Total nitrogen	4 550	4 370	$kg\ N.d^{-1}$
NH_4-N	3 250	3 170	$kg\ N.d^{-1}$
Effluent concentrations			
Total nitrogen	8.5	8.6	$g\ N.m^{-3}$
NO_3-N	5.9	7.1	$g\ N.m^{-3}$
NH_4-N	1.3	1.2	$g\ N.m^{-3}$
Sludge and biogas			
TSS in ASU	1 700	2 100	$g.m^{-3}$
% VS in ASU	75	69	%
WAS production	11 000	13 900	$kg\ TS.d^{-1}$
Sludge production - dewatered	5 360	4 900	$kg\ TS.d^{-1}$
Production of raw biogas	12 500	12 000	$Nm^3.d^{-1}$
Other parameters			
Sludge age	13.0	13.4	d
Air flow to ASU	269 000	278 000	$m^3.d^{-1}$

Benchmark Simulation Model No 2 plant layout

The Benchmark Simulation Model No 2 is presented in detail in Gernaey et al. (2014). The plant is designed similar to a general advanced nutrient removal wastewater treatment plant (WWTP) with high effluent requirements. The plant layout is presented in Figure S.1.

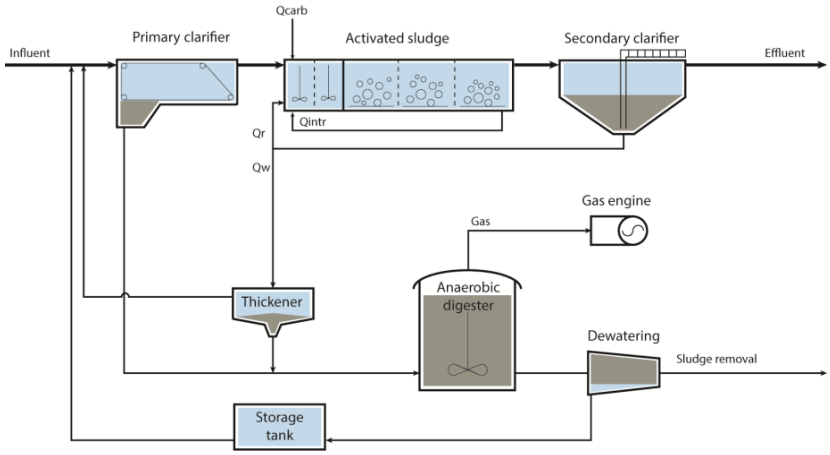

Figure S.1. Process flow diagram for the WWTP in BSM2G.

References

Ahlvik, P. and Brandberg, A.R.L. (2000) Relative Impact on Environment and Health from the Introduction of Low Emission City Buses in Sweden. SAE Technical Paper No. 2000-01-1882.

Erikstam, S. (2013) Modellering av koldioxidavtrycket för Käppalaverket med framtida processlösning utformad för skärpta reningskrav (in Swedish). MSc thesis (UPTEC W 13 008), Uppsala University, Sweden.

Gernaey, K.V., Jeppsson, U., Vanrolleghem, P.A. and Copp, J.B. (2014) Benchmarking of Control Strategies for Wastewater Treatment Plants [IWA Scientific and Technical Report No. 21]. IWA Publishing, London, UK.

Gode, J., Martinsson, F., Hagberg, L., Öman, A., Höglund, J. and Palm, D. (2011) Miljöfaktaboken 201,1Estimated emission factors for fuels, electricity, heat and transport in Sweden (in Swedish). Värmeforsk Service AB, Stockholm, Sweden

Guinée, J.B., Gorrée, M., Heijungs, R., Huppes, G., Kleijn, R., de Koning, A., van Oers, L., Wegener Sleeswijk, A., Suh, S., Udo de Haes, H.A., de Bruijn, H., van Duin, R. and Huijbregts, M.A.J. (2002) Handbook on life cycle assessment. Operational guide to the ISO standards. I: LCA in perspective. IIa: Guide. IIb: Operational annex. III: Scientific background. Kluwer Academic Publishers, Dordrecht, The Netherlands.

Käppalaförbundet (2012) Miljörapport 2012 (in Swedish). Käppalaförbundet. Lidingö, Sweden.

Thunberg, A. (2014) Processdimensionering för nya utsläppsvillkor beräkningsunderlag, 2014-08-06 (in Swedish). Käppalaförbundet, Lidingö, Sweden.

Weidema, B.P., Bauer, C., Hischier, R., Mutel, C., Nemecek, T., Reinhard, J., Vadenbo, C.O. and Wernet, G. (2013) The ecoinvent database: Overview and methodology, Data quality guideline for the ecoinvent database version 3. www.ecoinvent.org.